ISAPP-Baikal Summer School 2018

TRACER balloon experiment

10^9 - 10^{14} eV

LOFAR

10^{16} - 10^{18} eV

KASCADE(-Grande) air shower experiment

10^{13} - 10^{18} eV

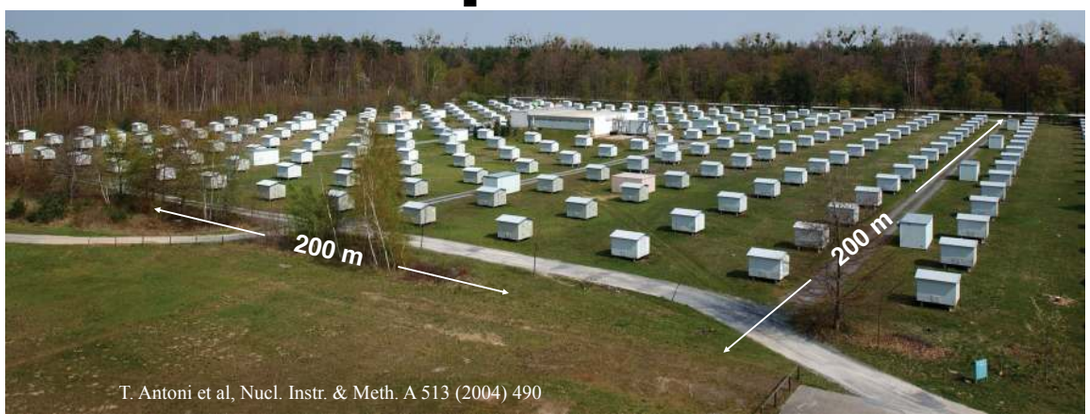

Pierre Auger Observatory

$>10^{17}$ eV

task leader radio at Pierre Auger Observatory
PI LOFAR key science project Cosmic Rays

Jörg R. Hörandel RU Nijmegen, Nikhef, VU Brussel http://particle.astro.ru.nl

ISAPP-Baikal Summer School 2018

Radio detection of extensive air showers

Precision measurements of the properties of cosmic rays

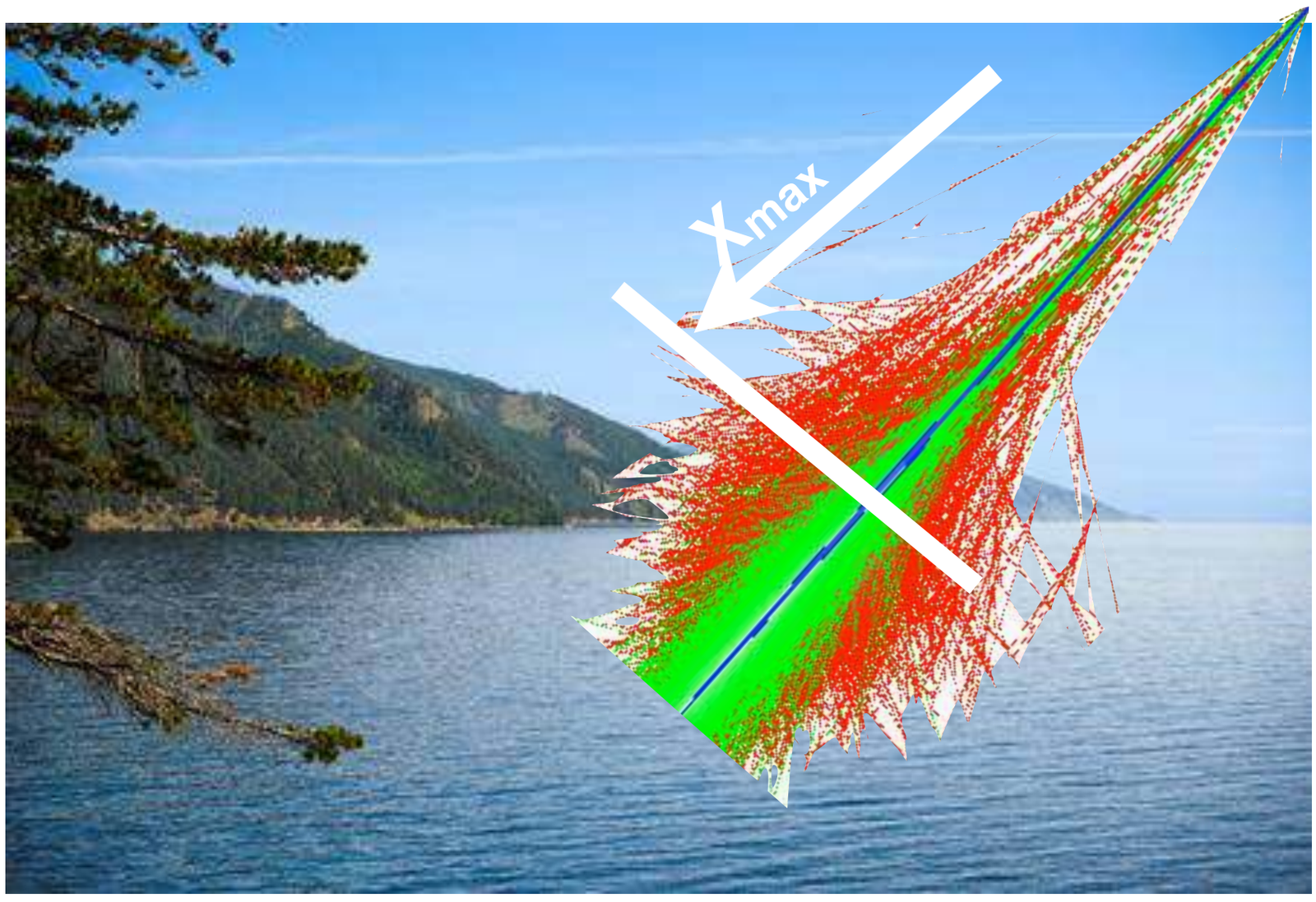

characterize cosmic rays:
-direction
-energy
-mass
@100% duty cycle

task leader radio at Pierre Auger Observatory
PI LOFAR key science project Cosmic Rays

Jörg R. Hörandel **RU Nijmegen, Nikhef, VU Brussel** **http://particle.astro.ru.nl**

ISAPP-Baikal Summer School 2018

Radio detection of extensive air showers

Precision measurements of the properties of cosmic rays

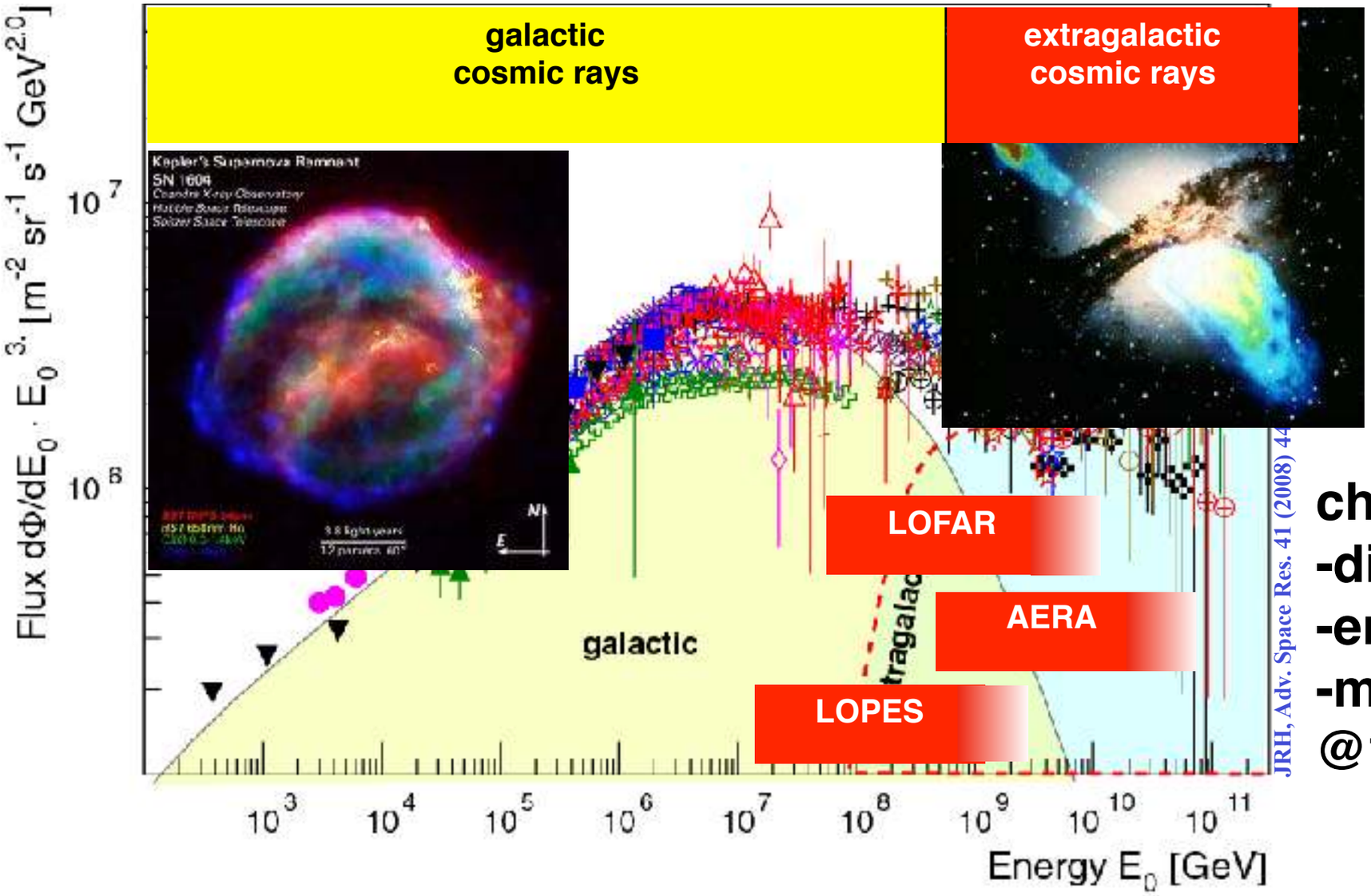

characterize cosmic rays:
-direction
-energy
-mass
@100% duty cycle

Jörg R. Hörandel **RU Nijmegen, Nikhef, VU Brussel** **http://particle.astro.ru.nl**

Jodrell Bank 1946

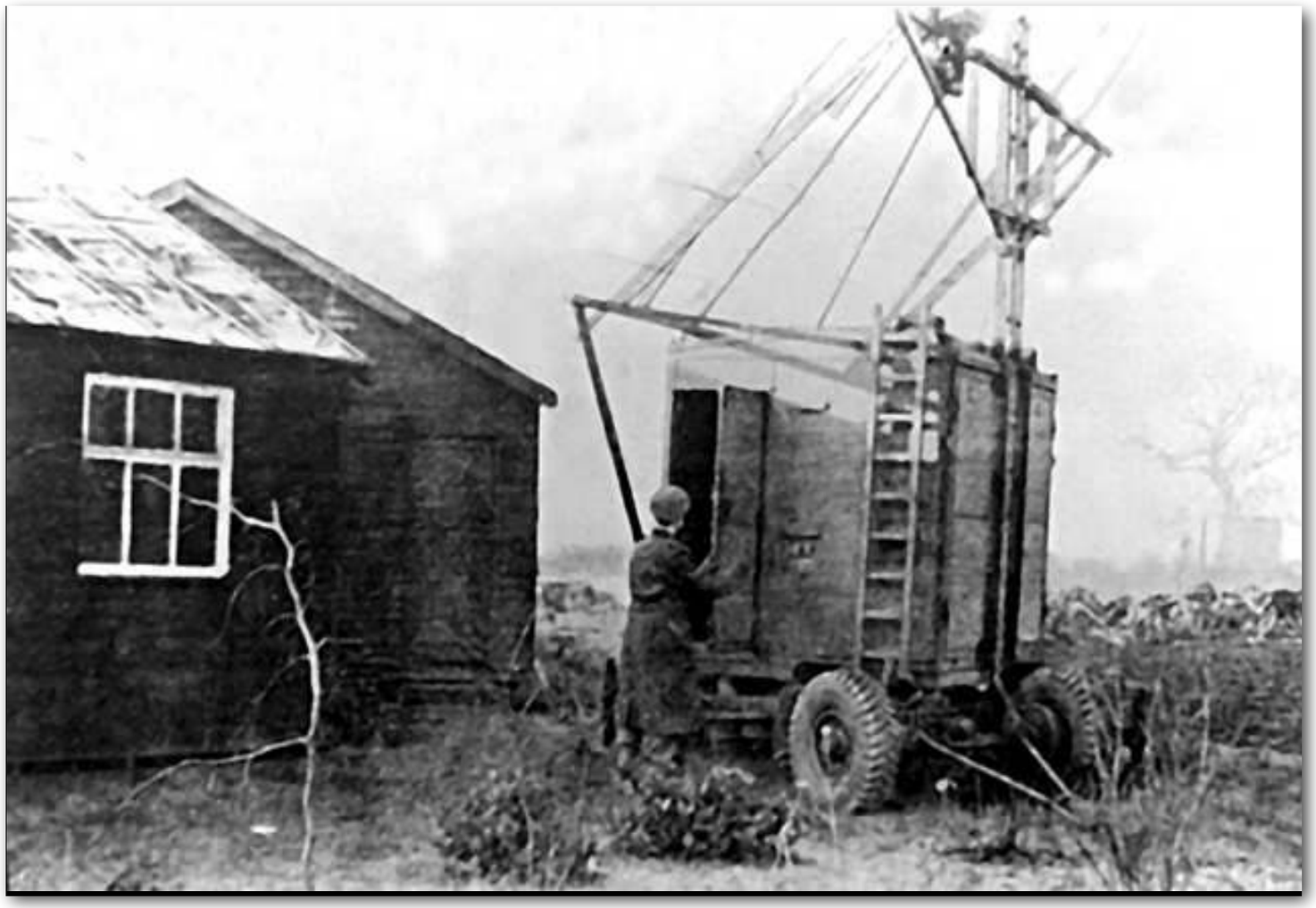

No luck due to rapid attachment time (ns) of free electrons in the lower atmosphere (damping factor)

$$O_2 + e \rightarrow O_2^-$$

No air showers detected

Echos from meteor trails
Radio emission from M31 → **radio astronomy**

First radio detection of air showers 1965

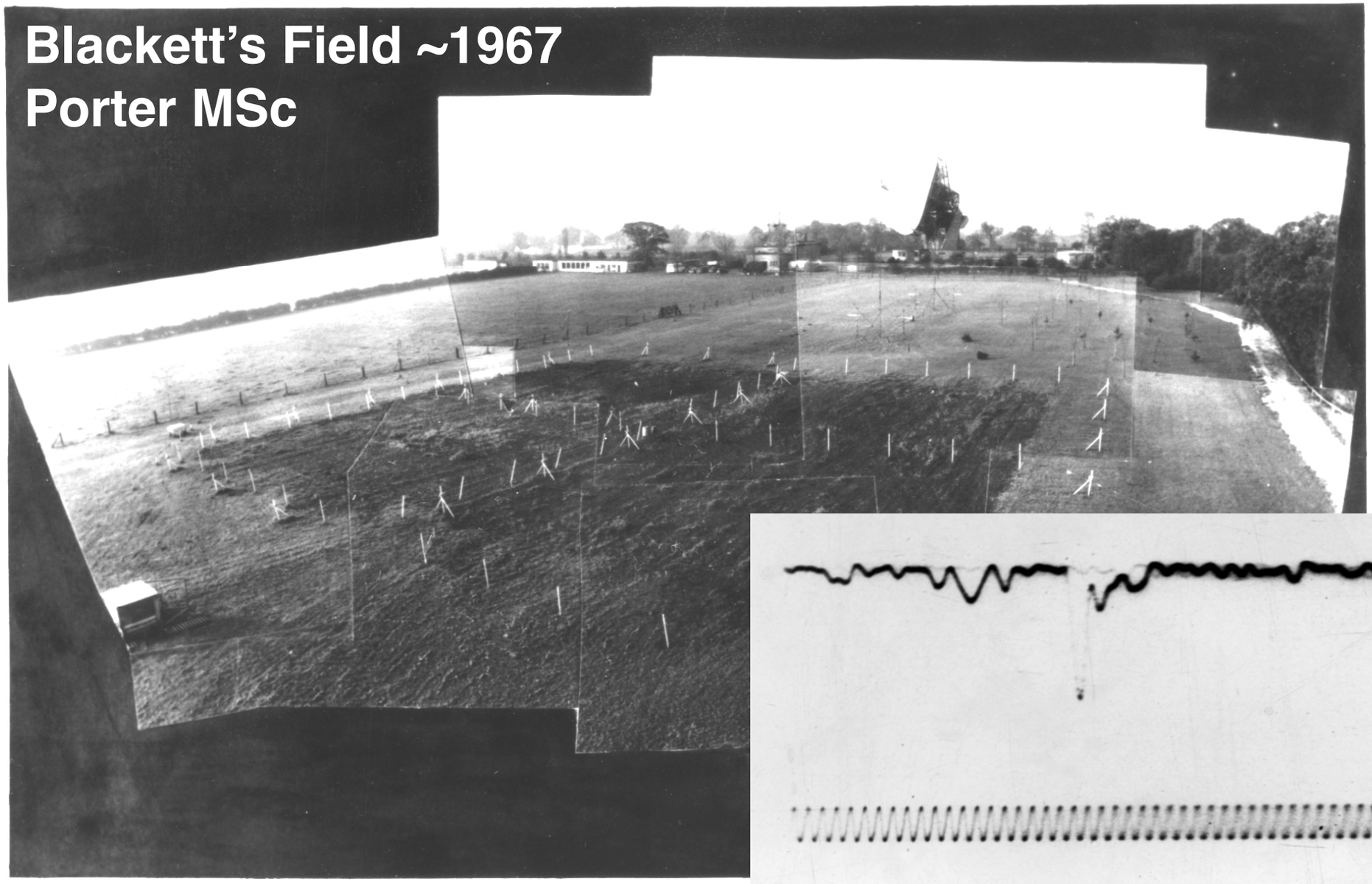

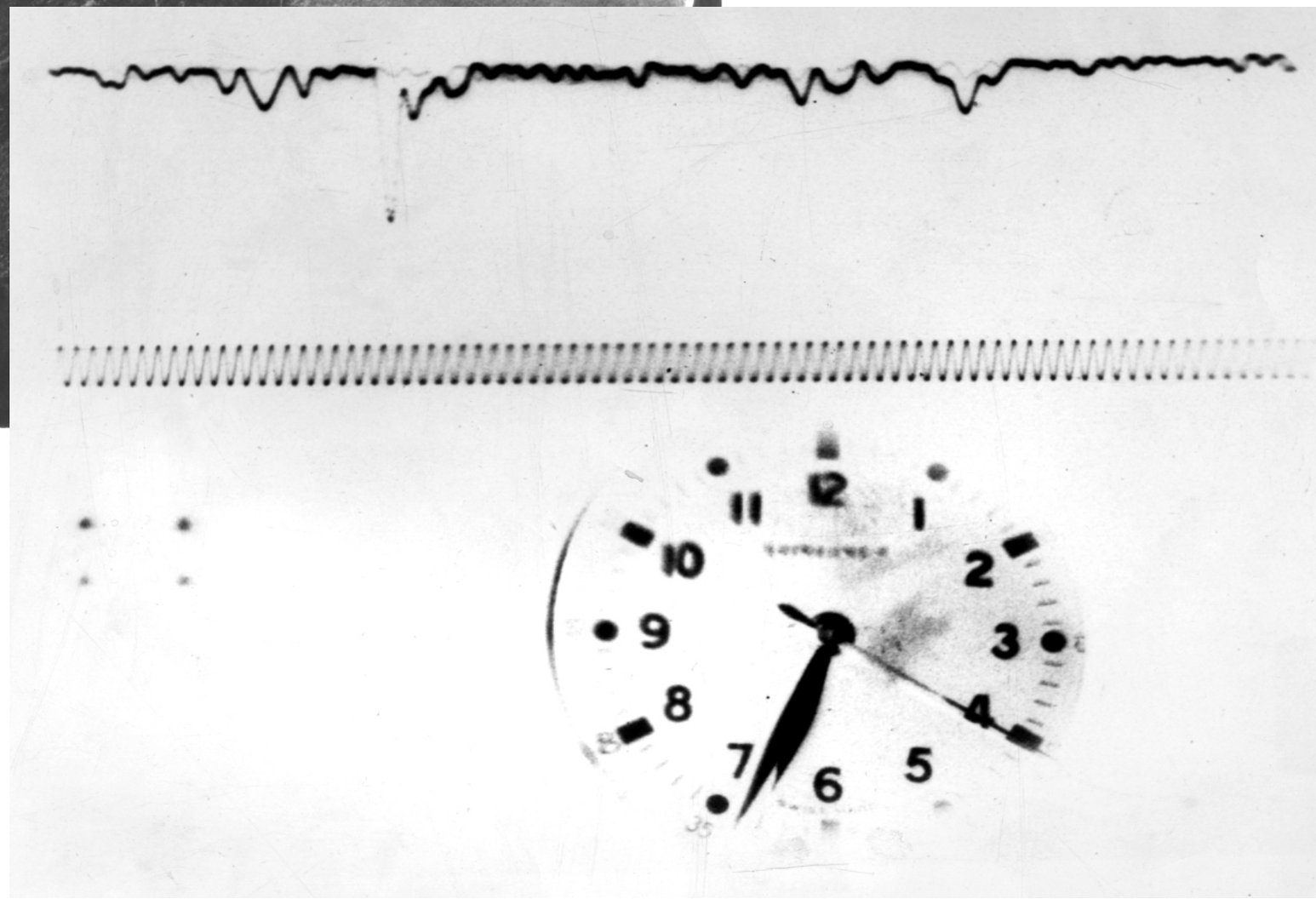

Jelley et al Nature 1965
R. A. Porter MSc Thesis 1967

Haverah Park (Leeds)

Allan 1971

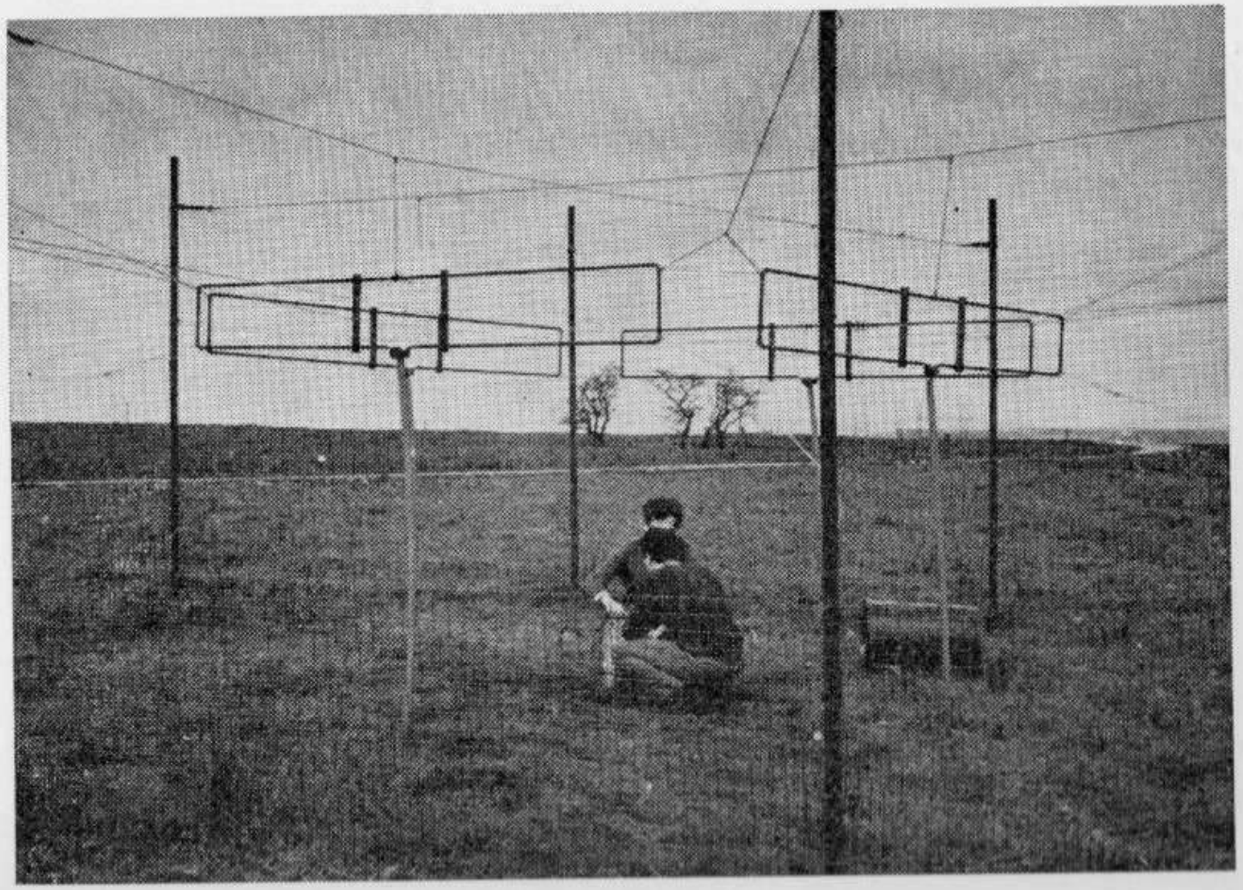

Recent receiving antennas (44 MHz) forming part of the Haverah Park Extensive Air Shower Array.

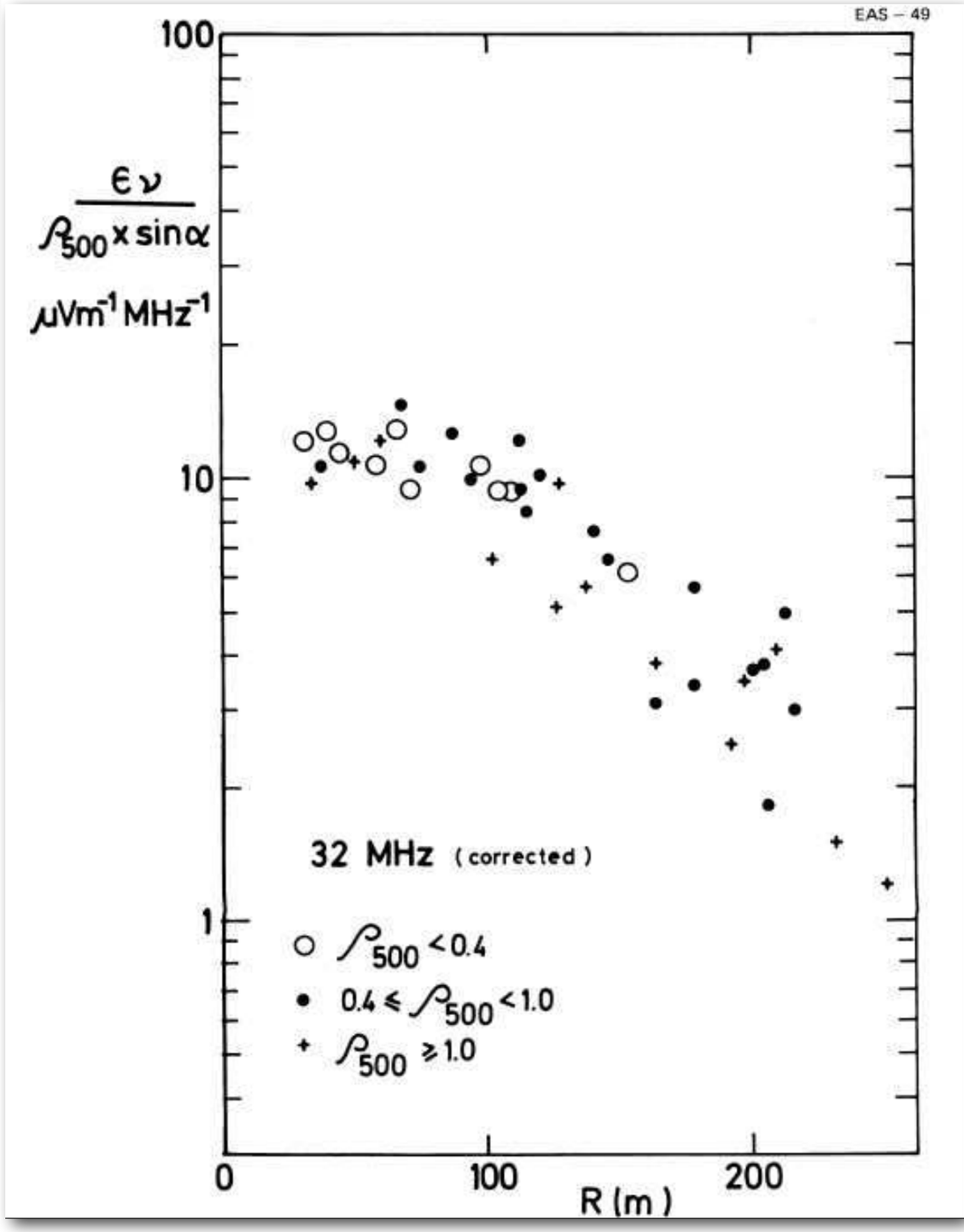

$$\varepsilon_\nu = 2\left(\frac{E_p}{10^{17}}\right)\left(\frac{\sin\alpha\cos\theta}{\sin 45\cos 30}\right)\exp\left(\frac{-r}{r_0}\right)\left(\frac{\nu}{50}\right)^{-1} \quad \mu\text{V/m/MHz}$$

$r_0 = 110$ m at ν=55 MHz. α=angle to B, θ=Zenith angle

H.R. Allan, Prog. Element. Part. Cosmic Ray Phys (1971) 169

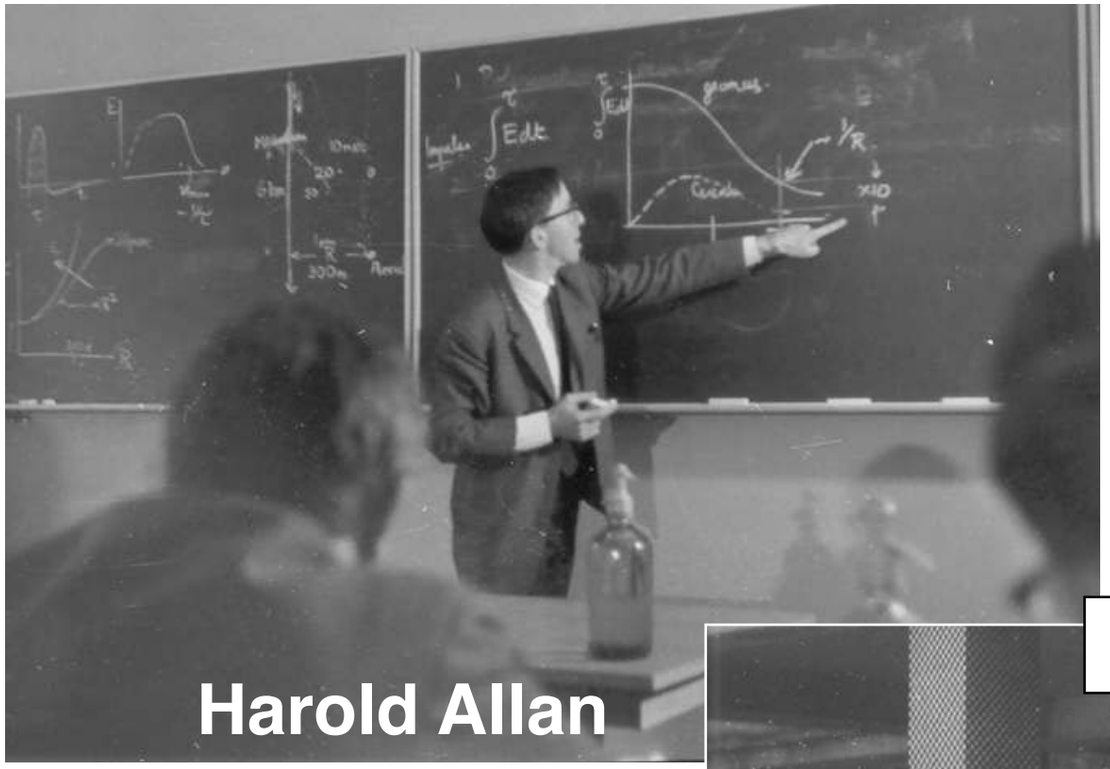

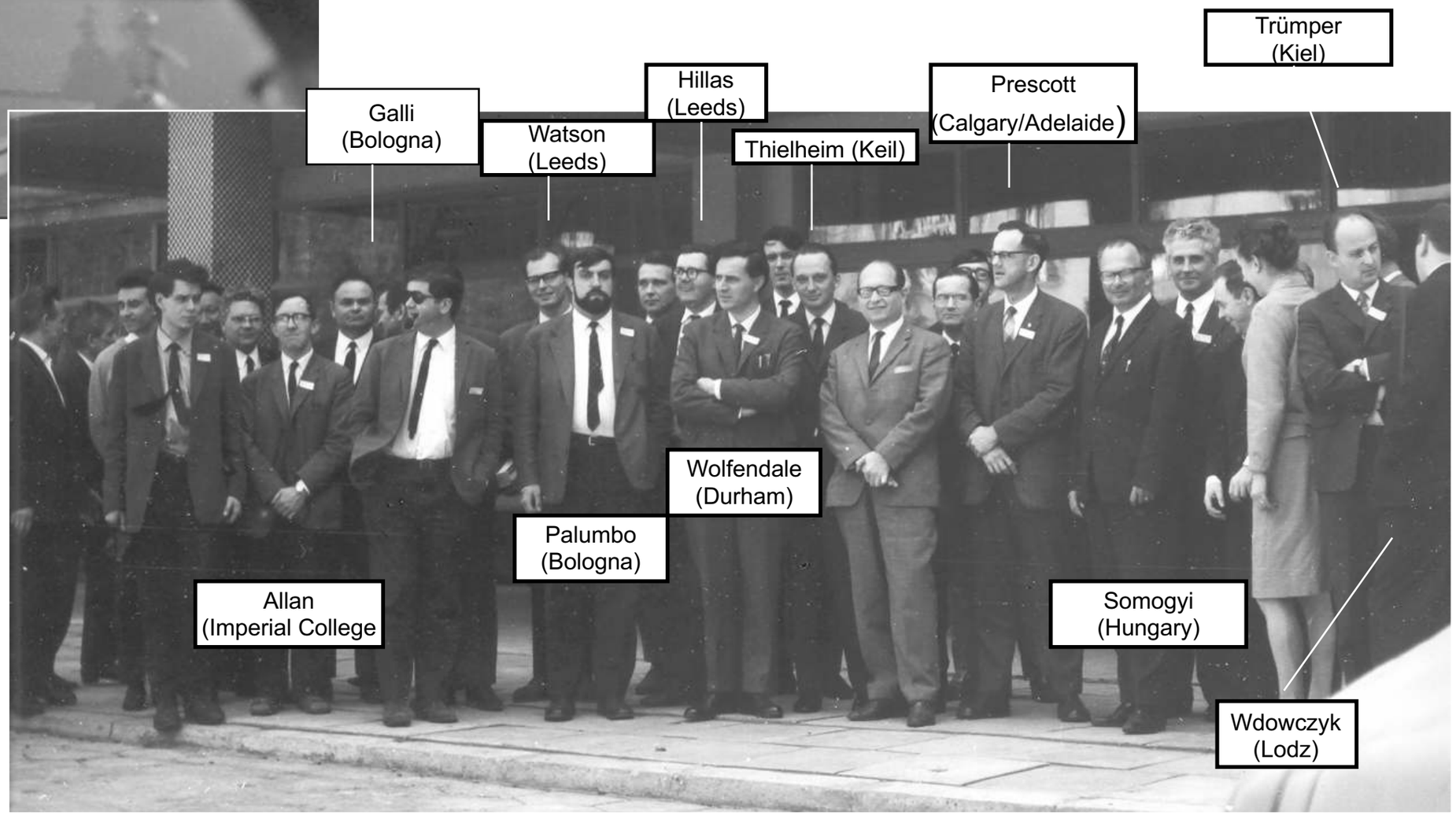

First European Symposium on High Energy Interactions and Extensive Air Shower: Lodz, Poland April 1968

33RD INTERNATIONAL COSMIC RAY CONFERENCE, RIO DE JANEIRO 2013
THE ASTROPARTICLE PHYSICS CONFERENCE

ICRC 2013

The renaissance of radio detection of cosmic rays

TIM HUEGE[1]

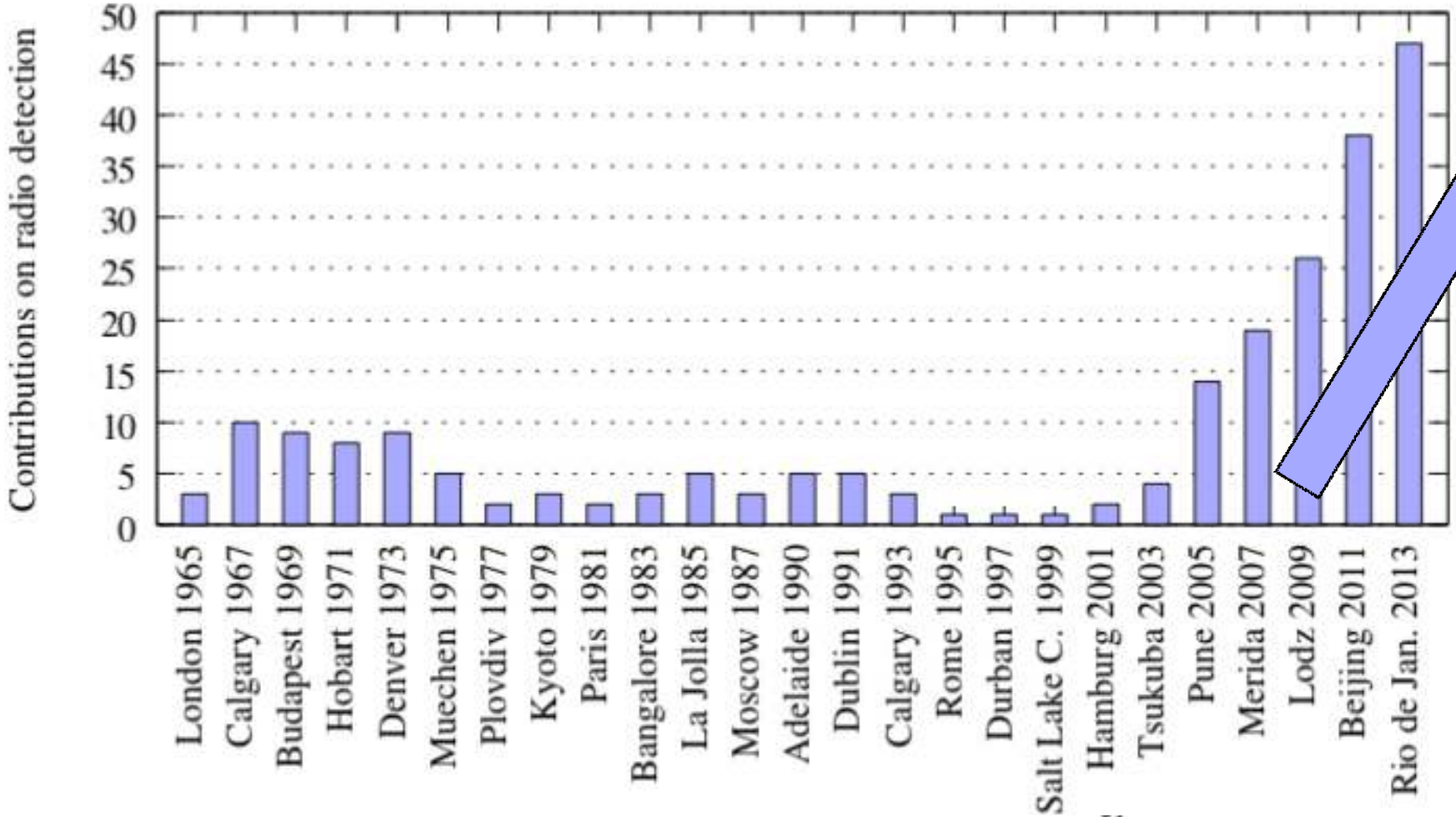

Figure 1: Number of contributions related to radio detection of cosmic rays or neutrinos to the ICRCs since 1965. The field has grown very impressively since the modern activities started around 2003. Data up to 2007 were taken from [11].

2018: **beyond capabilities of standard installations**

2016: **radio technique mature: properties of cosmic rays**

2014: **understanding the emission processes**

2005: understanding the signal

Radio Detectors

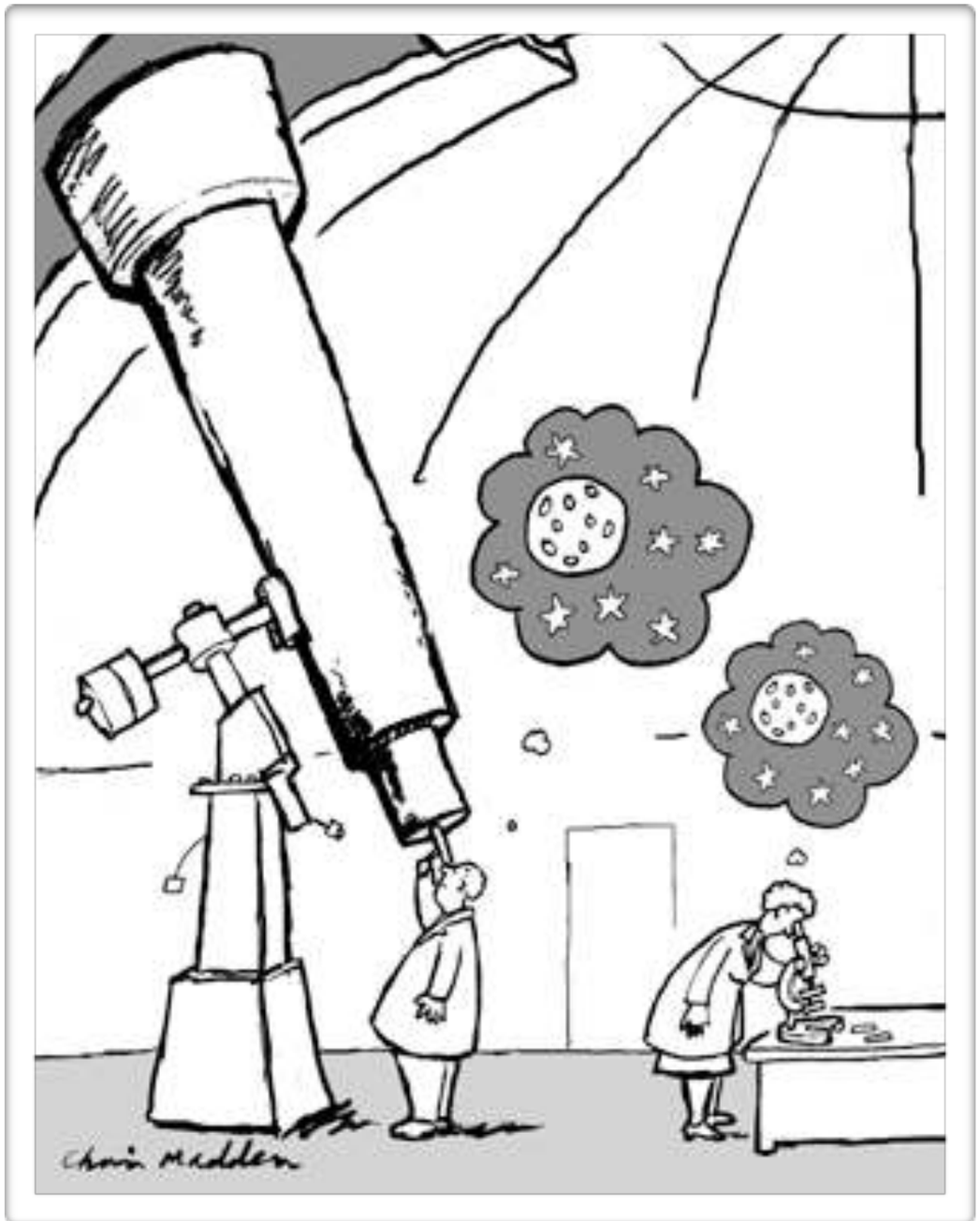

Radio detection of extensive air showers around the world

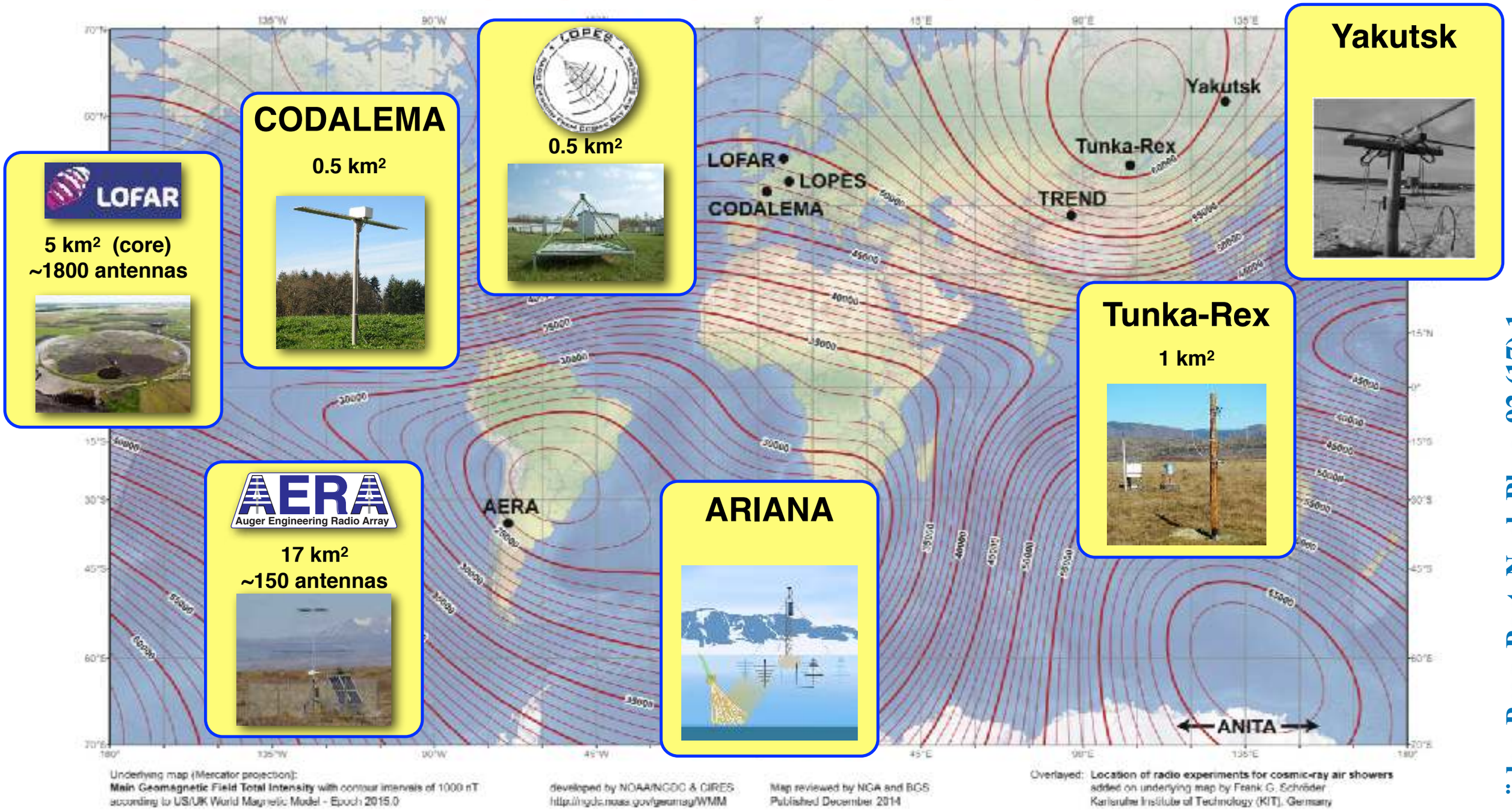

Fig. 21. Map of the total geomagnetic field strengths (world magnetic model [207]) and the location of various radio experiments detecting cosmic-ray air showers.

F.G. Schröder, Prog. Part. Nucl. Phys. 92 (17) 1

LOPES

Lofar Prototype Station

30 antennas operating at KASCADE-Grande

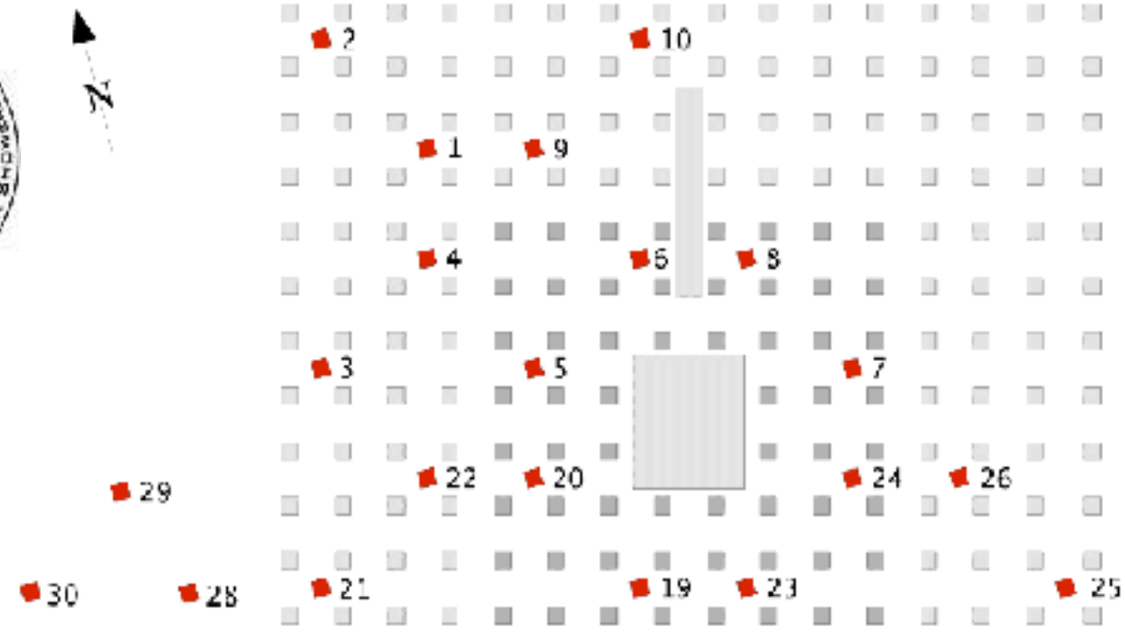

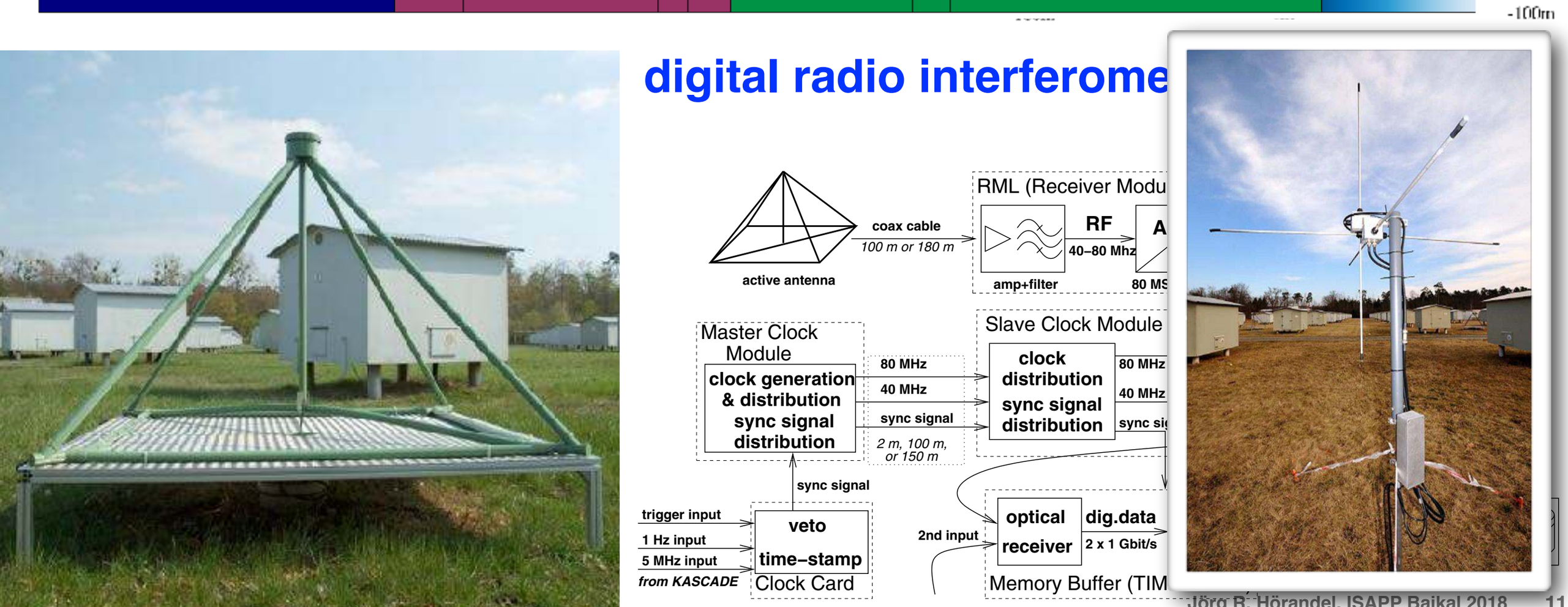

digital radio interferome

LOFAR

core
23 stations ~5 km²

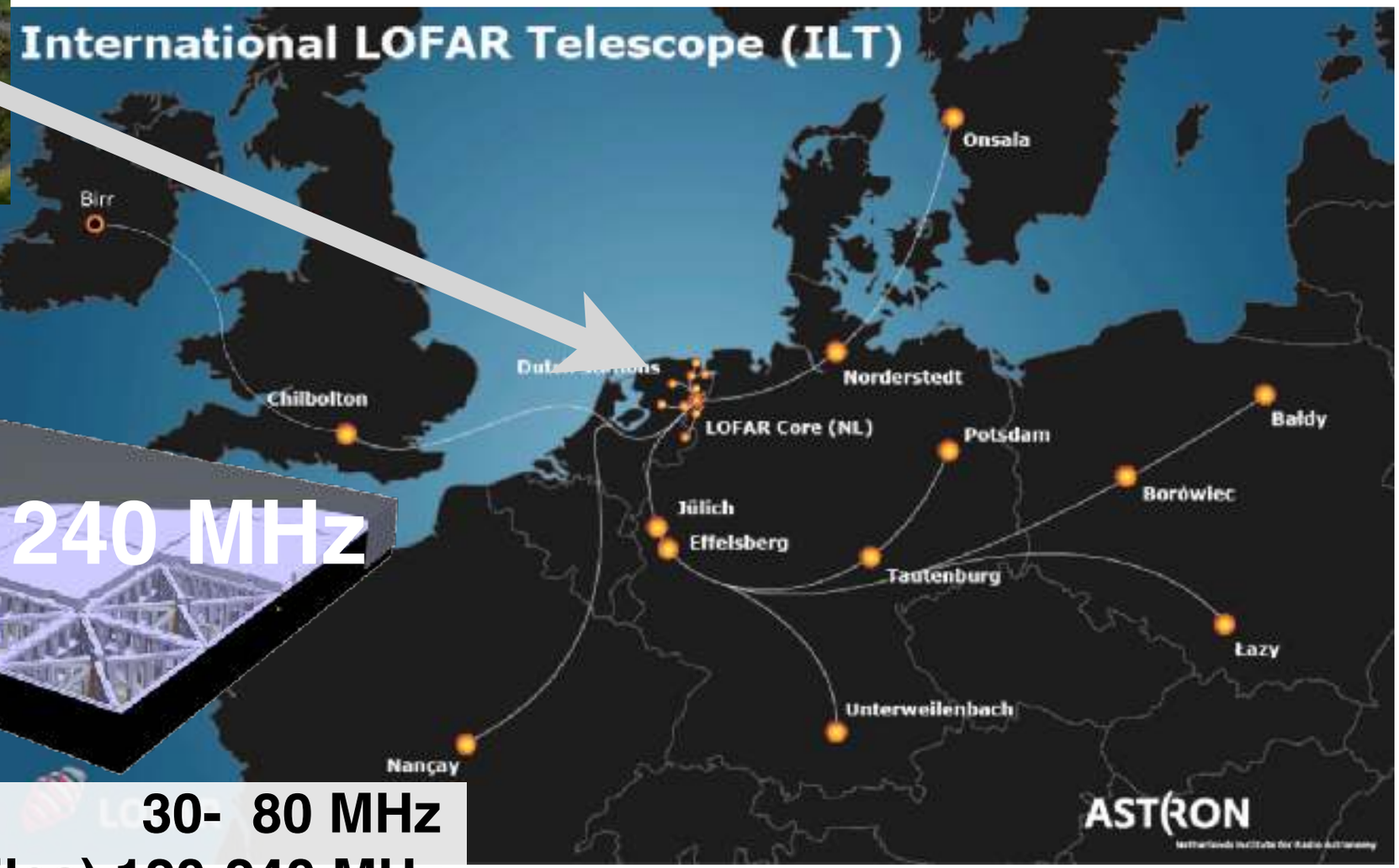

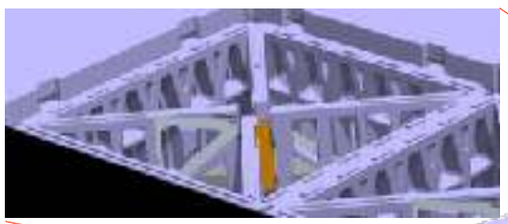

each (dutch) station:
96 low-band antennas 30- 80 MHz
high-band antennas (2x24 tiles) 120-240 MHz

M. van Haarlem et al., A&A 556 (2013) A2

S. Thoudam et al., Nucl. Instr. Meth. A 767 (2014) 339

LOFAR Radboud Air Shower Array - LORA

20 scintillator units (~1 m² each) in LOFAR core

provide

- properties of EAS
- and trigger

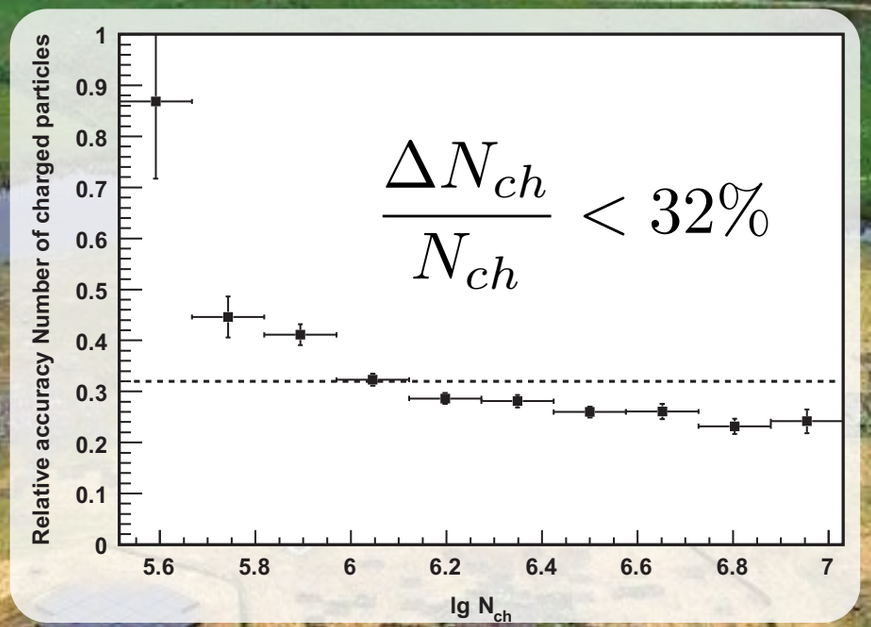

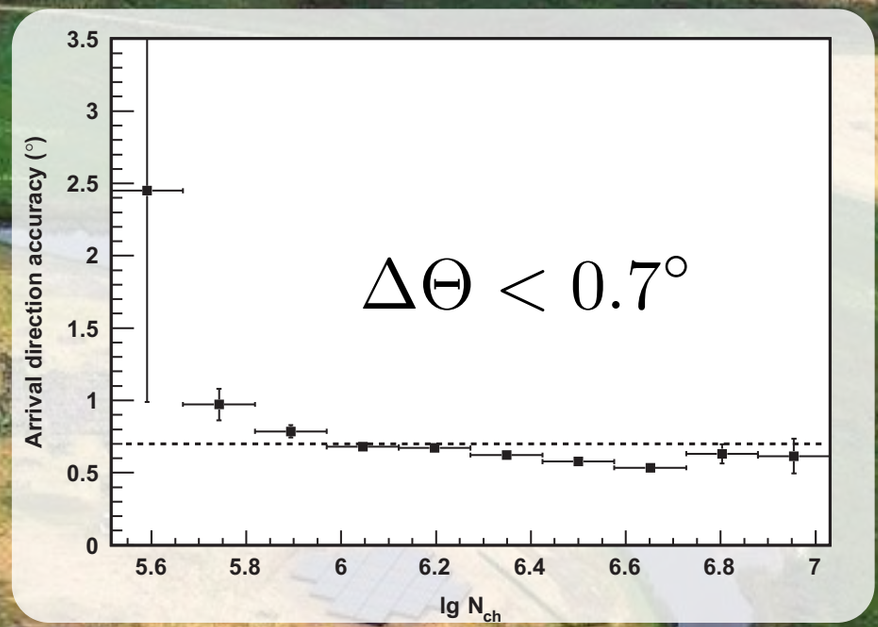

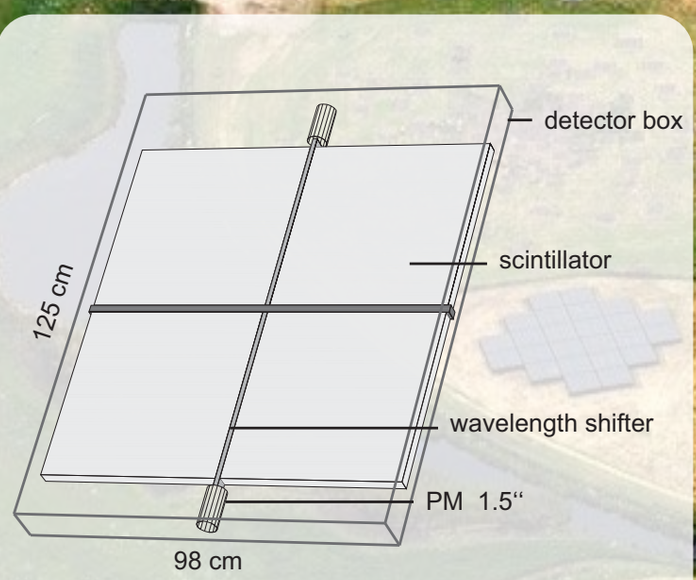

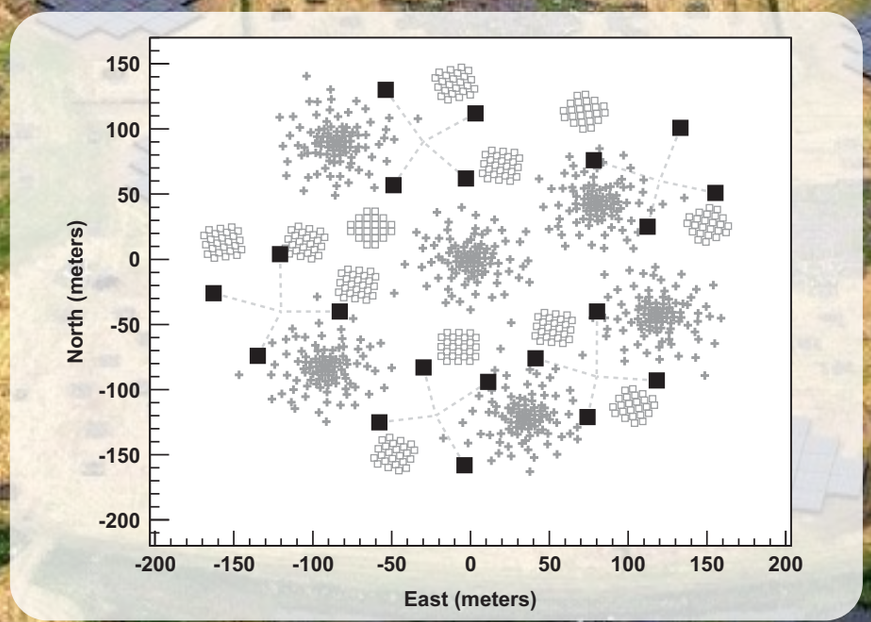

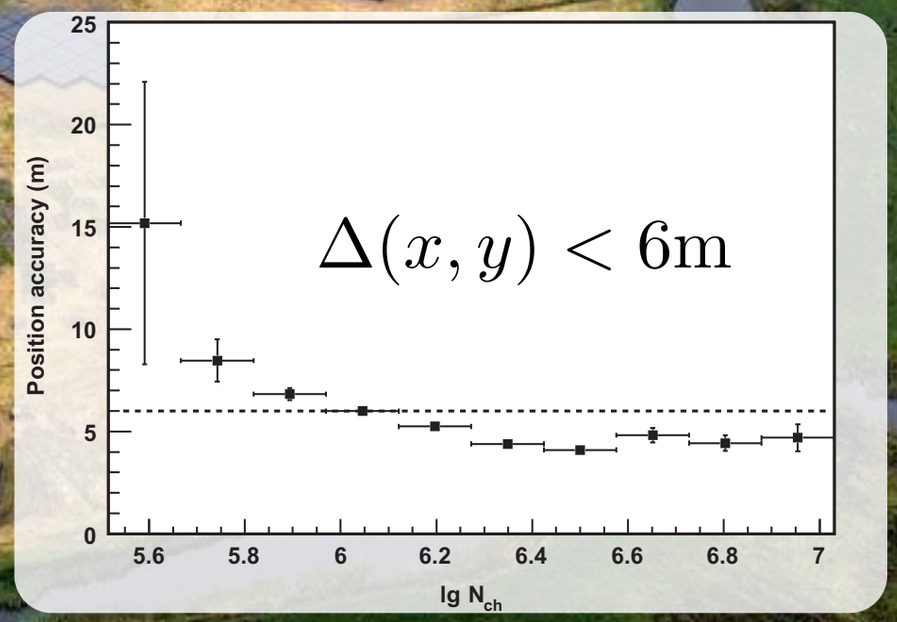

S. Thoudam et al, Nucl. Instr. Meth. A 767 (2014)

LORA
LOFAR Radboud Array
scintillator detectors

Superterp:
* diameter ~ 300 m
* 20 LORA detectors
* 6 LBA stations
  (= 6 x 48 antennas)

* more LBA stations
around superterp

trigger: 13 of 20
detectors

offline analysis
P. Schellart et al., A&A 560, 98 (2013)

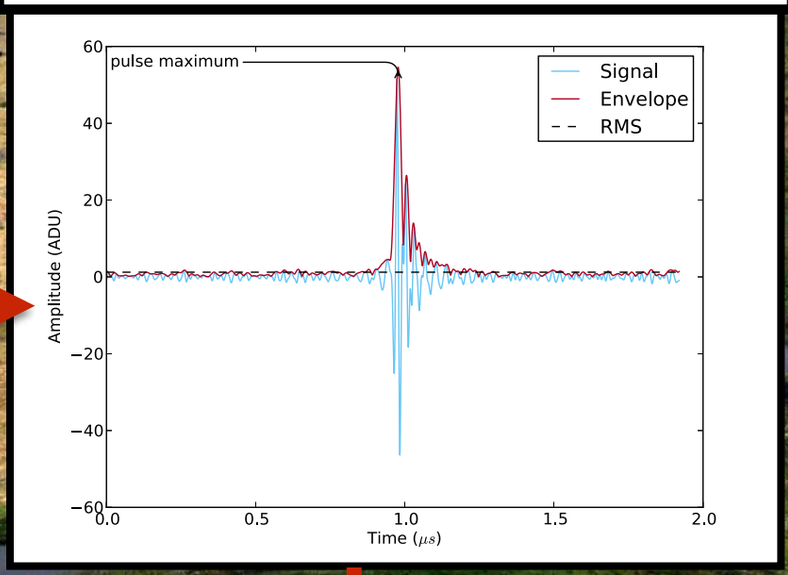

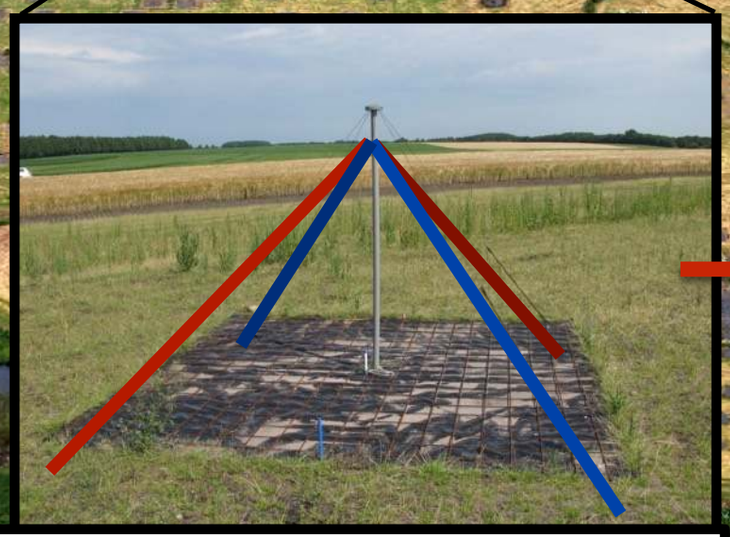

buffer
2 ms read-out

Low Band Antennas (LBA)
30 - 80 MHz

Selection this analysis:
4+ LBA stations

PIERRE AUGER OBSERVATORY

AERA
Auger Engineering Radio Array

~150 antennas
~17 km²
30-80 MHz

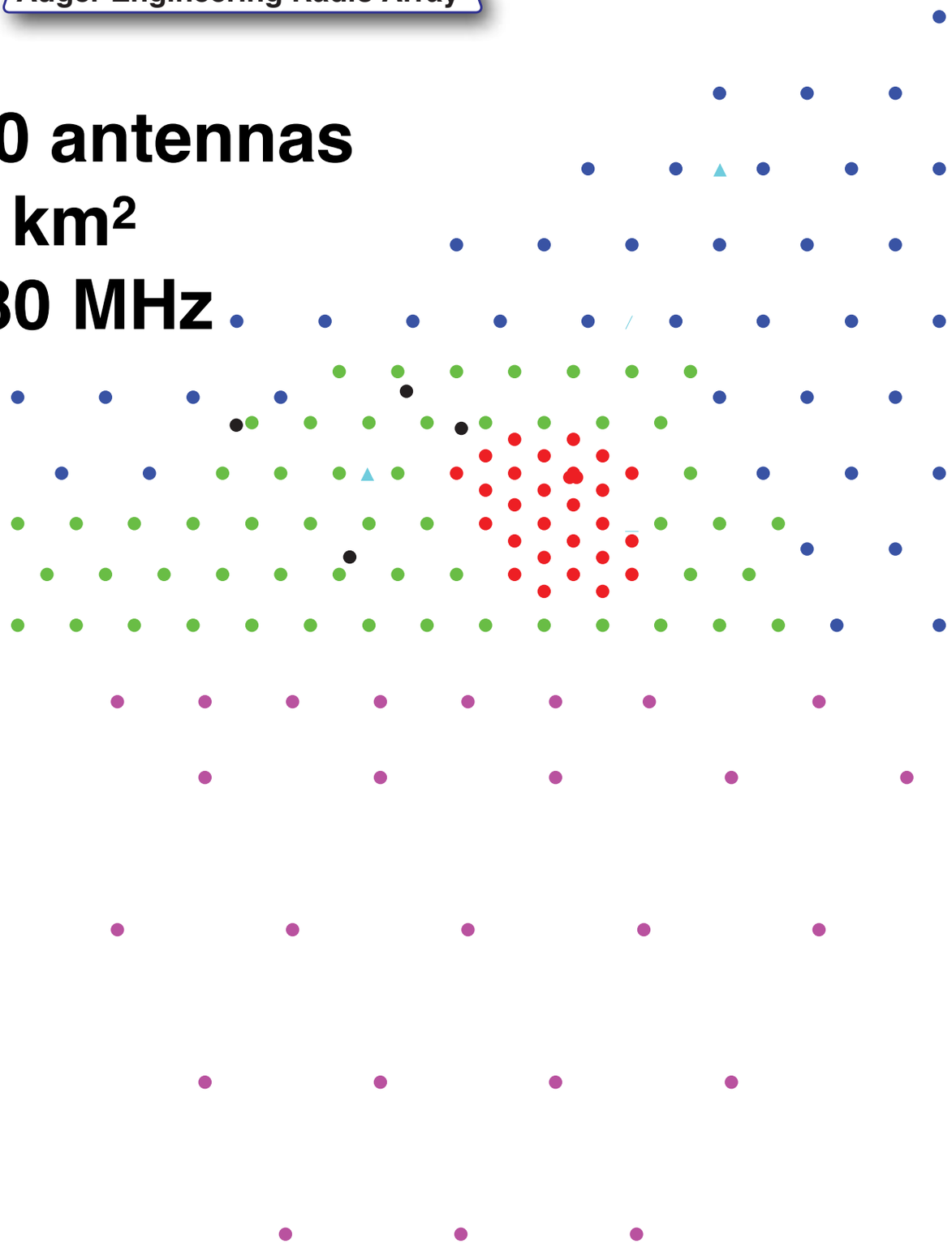

LOFAR core
23 stations ~5 km²

>2000 antennas

1 km

PIERRE AUGER OBSERVATORY

AERA
Auger Engineering Radio Array

~150 antennas
~17 km²
30-80 MHz

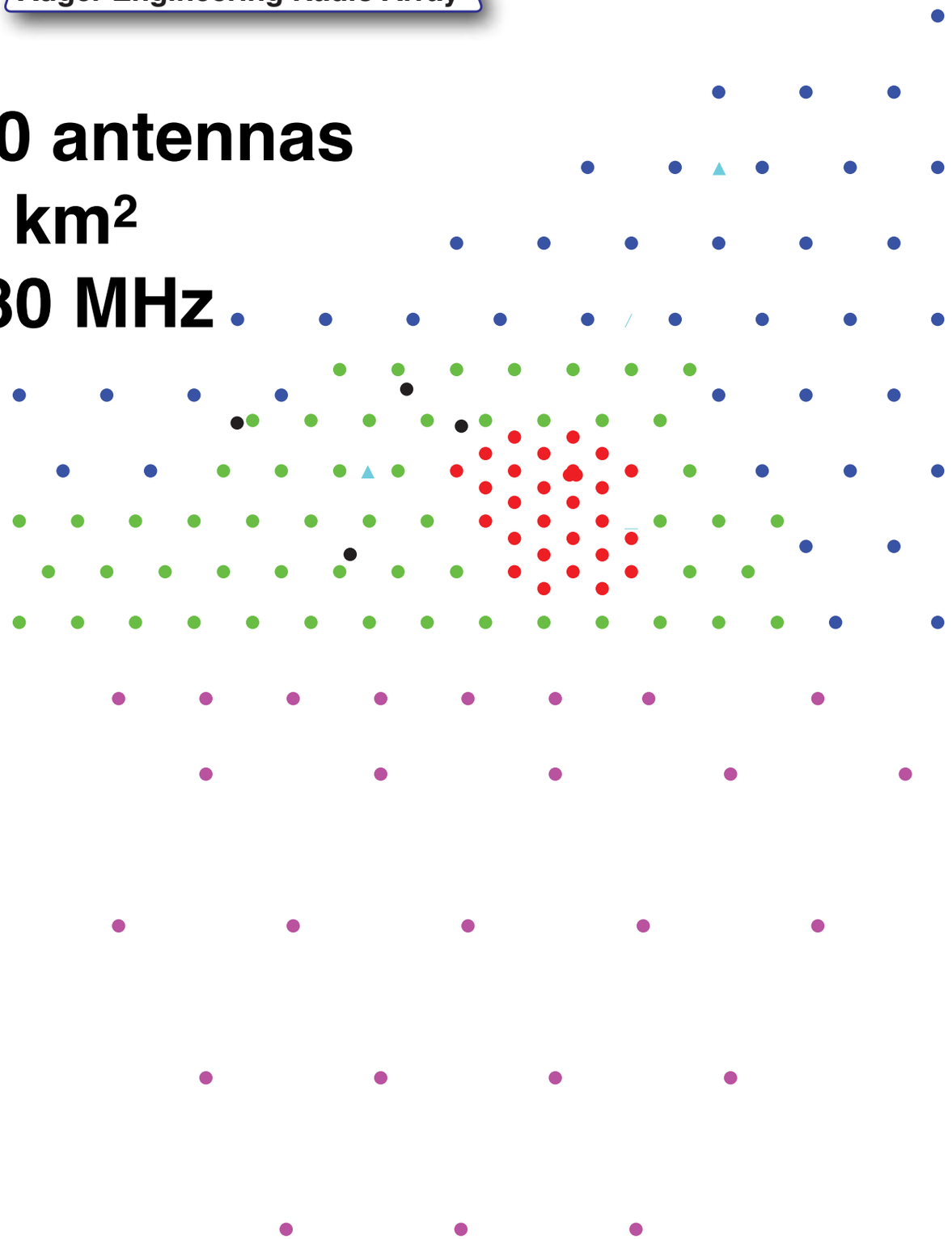

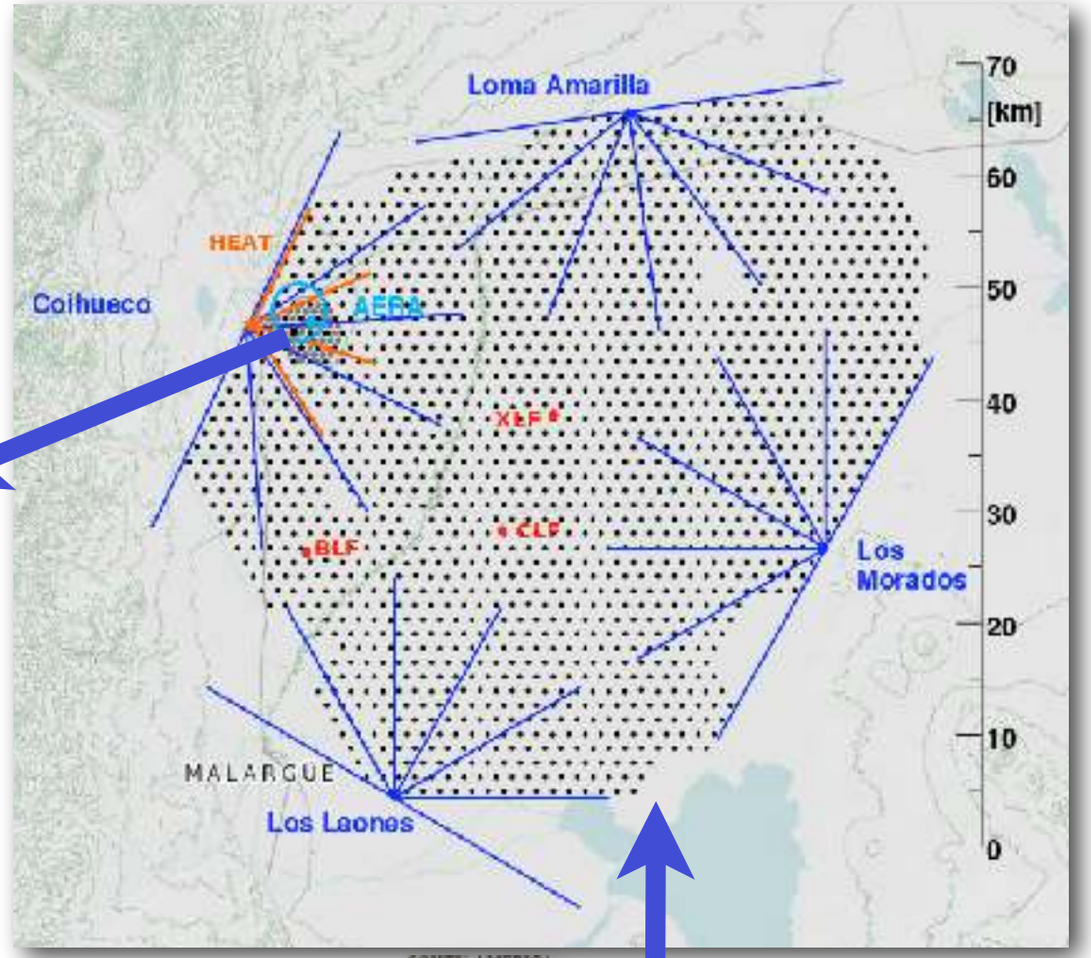

PIERRE AUGER OBSERVATORY

AERA
Auger Engineering Radio Array

~150 antennas
~17 km²
30-80 MHz

AERA basic idea

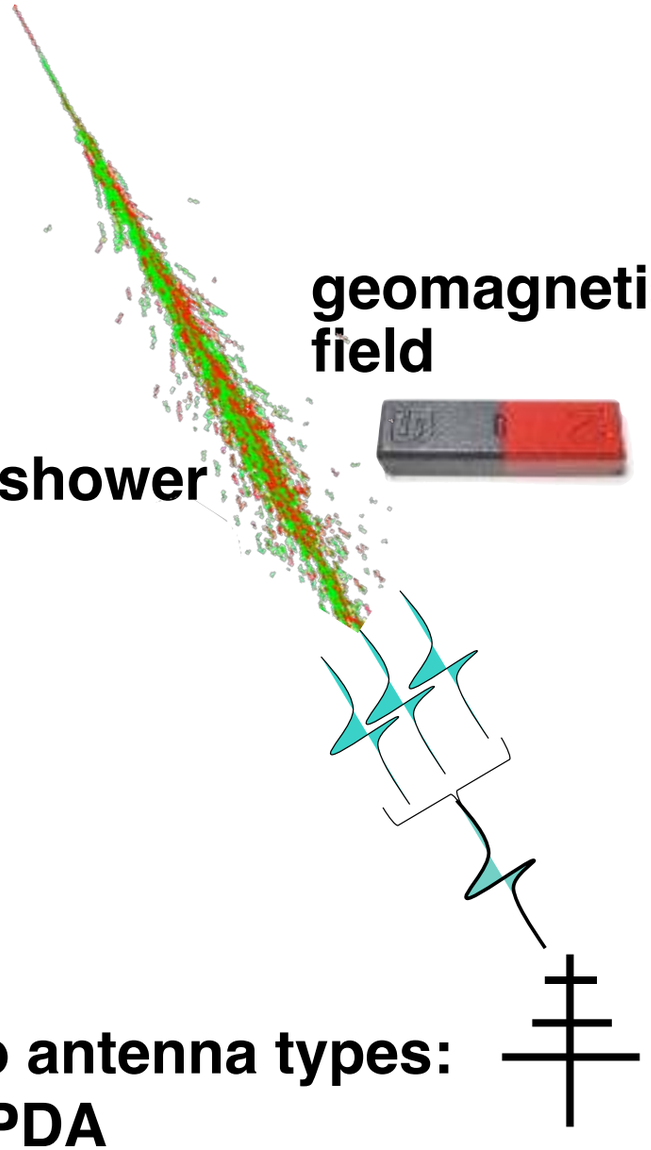

two antenna types:
- **LPDA**
- **butterfly**

data taking:
- **trigger through SD (CDAS), radio self trigger, int. scint. trigger**
- **all AERA data are combined in DAQ at Co**

DAQ (@CO)
Co comms tower

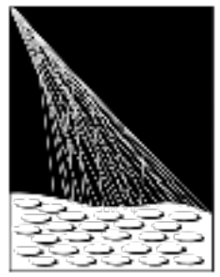

PIERRE AUGER OBSERVATORY

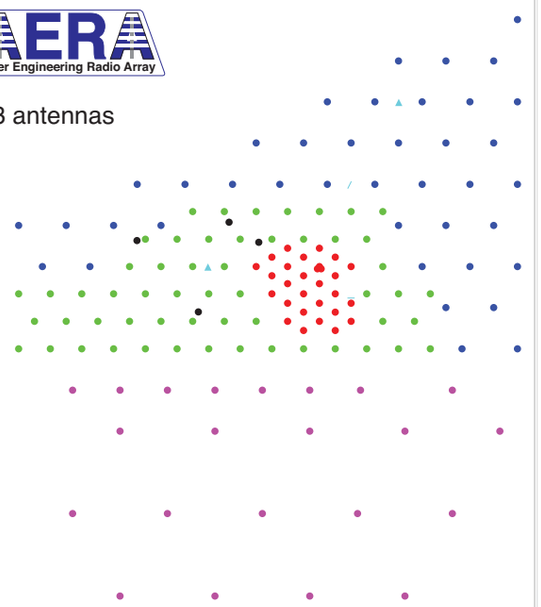

autarcic system:
- **solar power**
- **battery buffer**
- **GPS -> time**
- **wireless comms (fiber in 1st phase)**

measure electric fields in NS and EW directions
two digitizer types:
- **ring buffer + external trigger (SD) (Ger)**
- **selftrigger + internal scintillator trigger (NL)**

AERA
Auger Engineering Radio Array

station layout

24 LPDA
dense core with fiber read-out

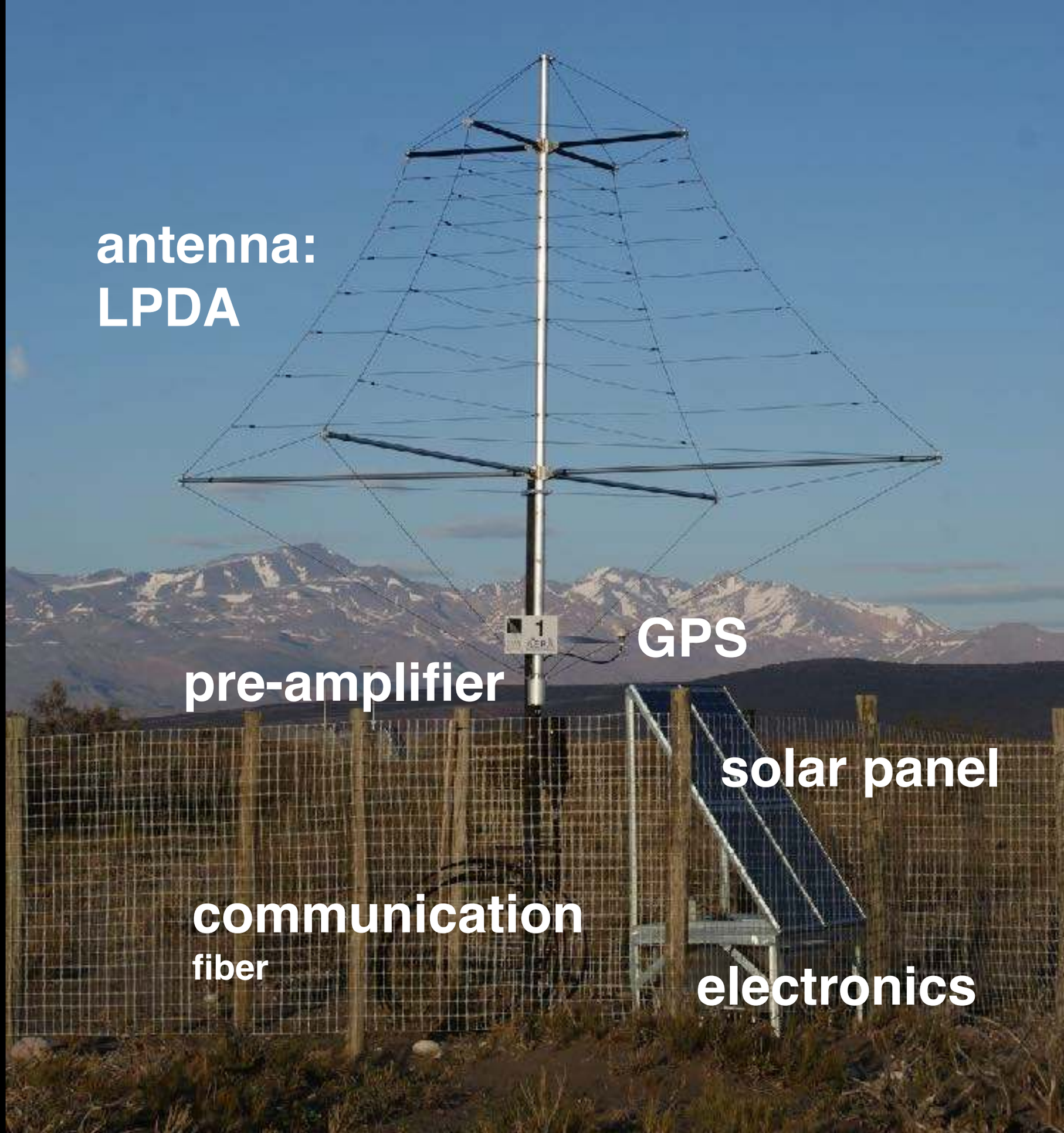

Problem:

sensitivity
30 MHz - 80 MHz

$$\frac{\lambda}{4}$$

how long are antenna arms at 30 MHz? and 80 MHz?

antenna:
LPDA

AERA
Auger Engineering Radio Array

geomagnetic field

air shower

comms antenna

GPS antenna

radio pulses

physics antenna: butterfly 30 - 80 MHz

68

solar panel

electronics & battery

A measured air shower

angular difference particles - radio

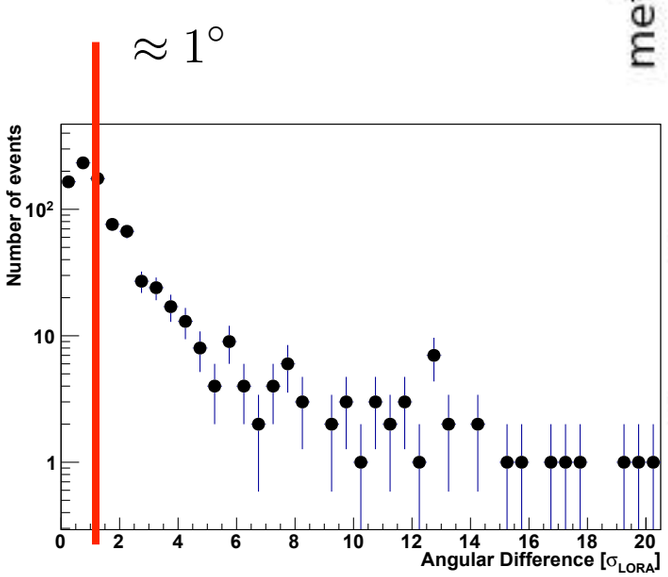

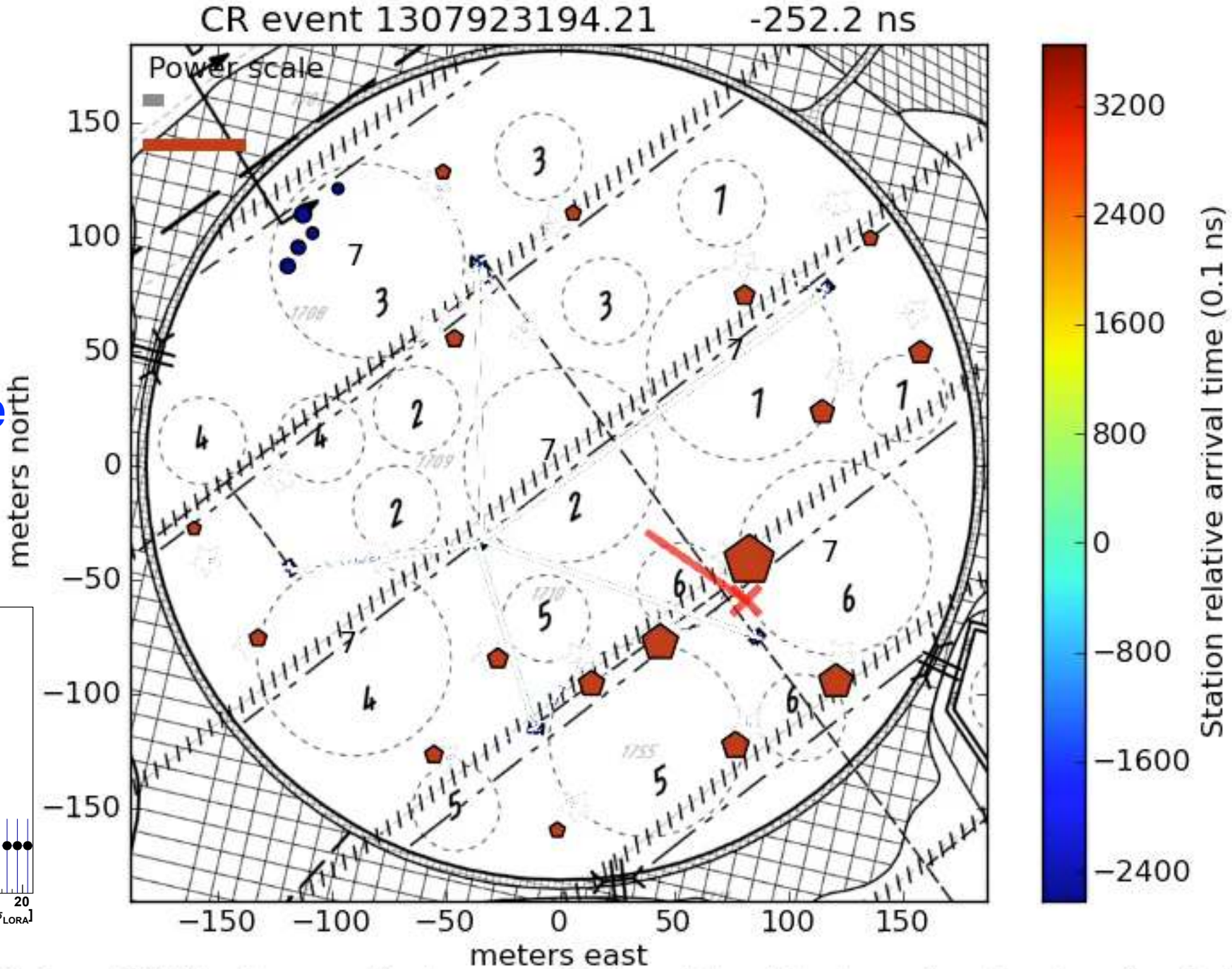

Circles: LOFAR antennas, Pentagons: LORA particle detectors, size denotes signal strength

Problem:

diameter ~300 m

assume a horizontal air shower

what is the time difference between the first and the last detector being hit?

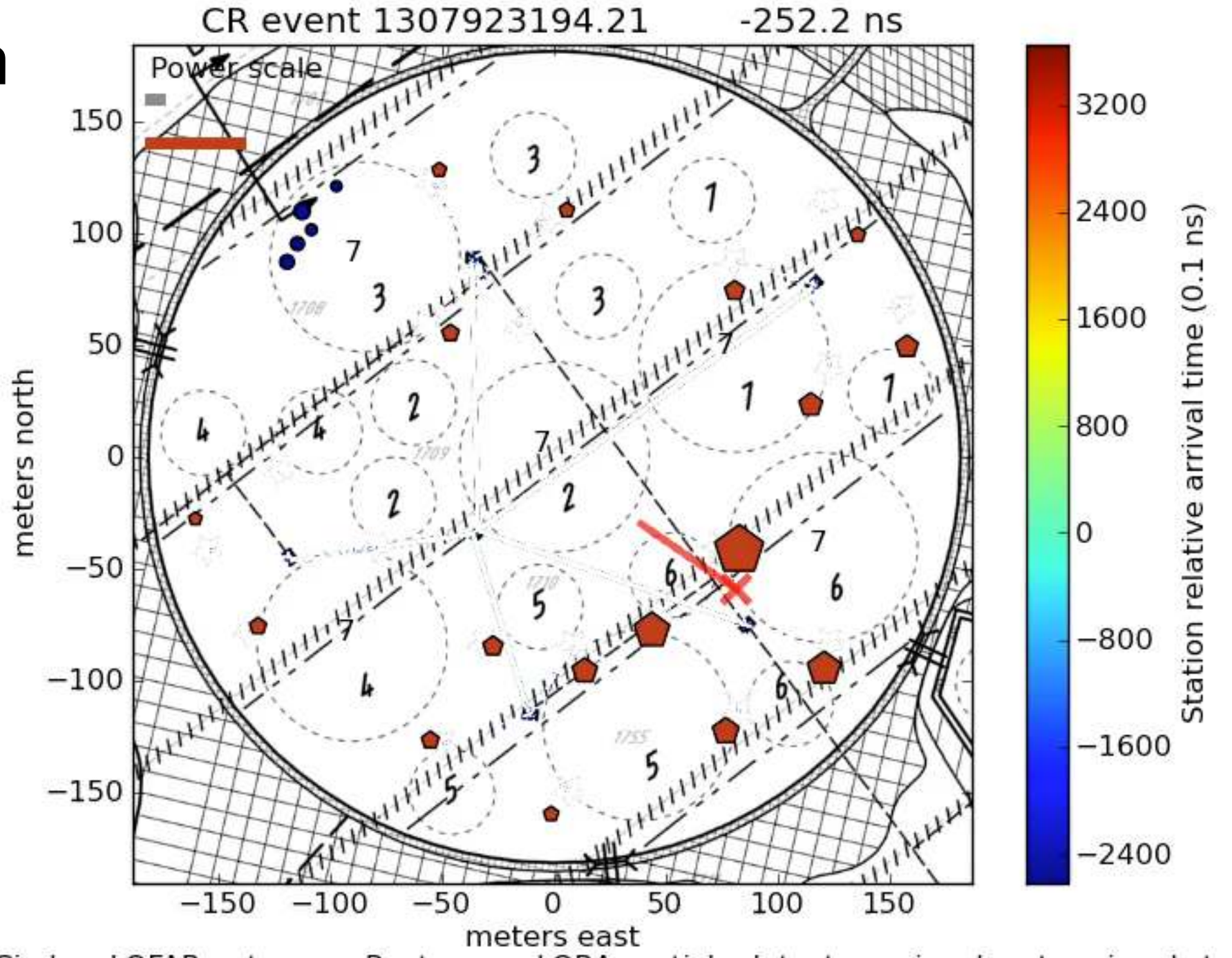

Circles: LOFAR antennas, Pentagons: LORA particle detectors, size denotes signal stre

An air shower measured simultaneously with ...

PIERRE AUGER OBSERVATORY

the Surface Detectors

the Fluorescence Telescopes

the Radio Detectors

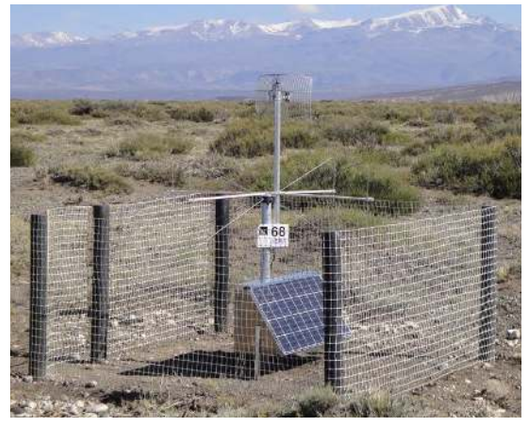

footprint

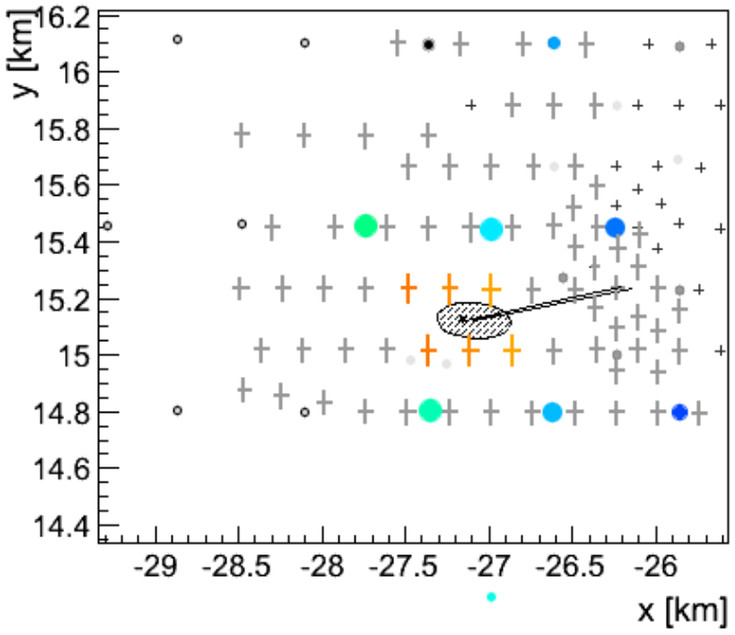

longitudinal shower profile

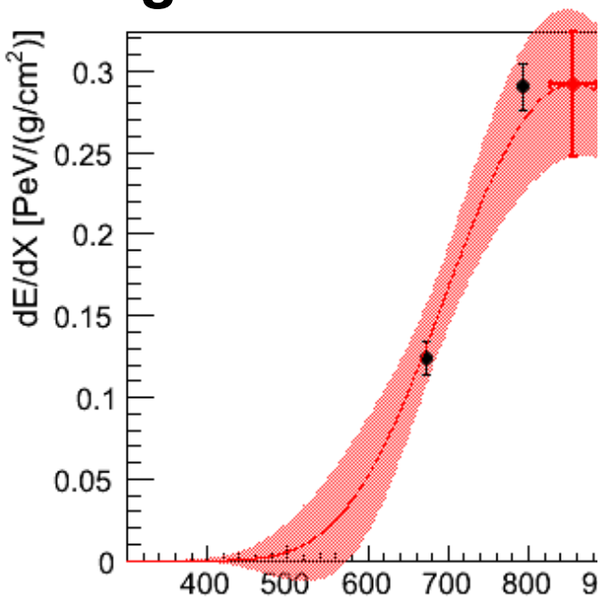

radio pulse

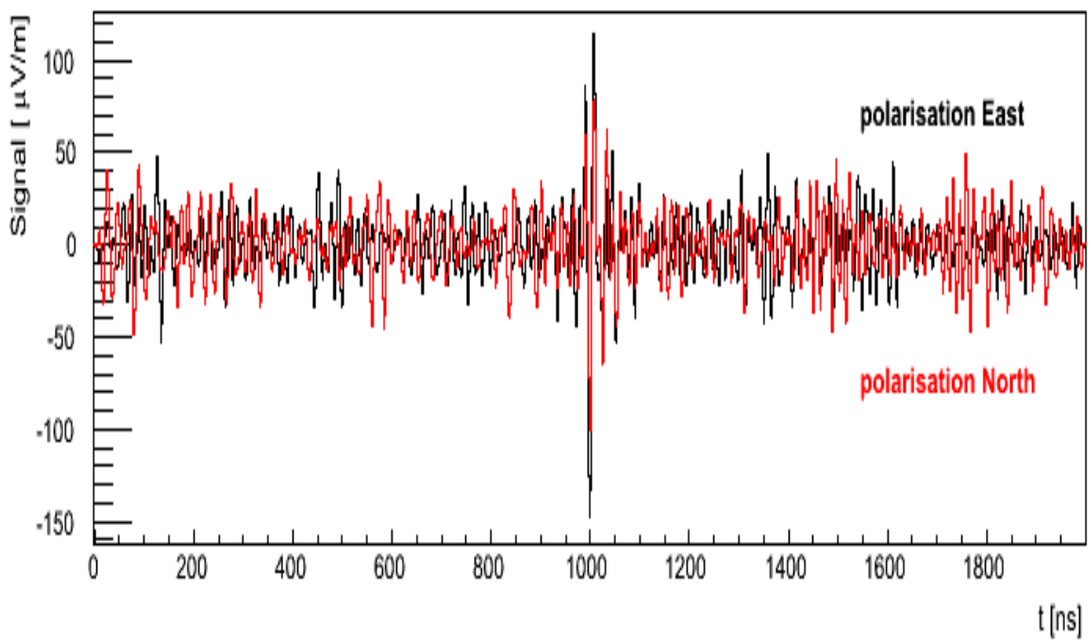

E ~ 2*10^{17} eV X_{max} ~ 860 g/cm^2 zenith angle ~ 75° azimuth angle ~ 8°

An air shower measured simultaneously with ...

PIERRE AUGER OBSERVATORY

the Surface Detectors

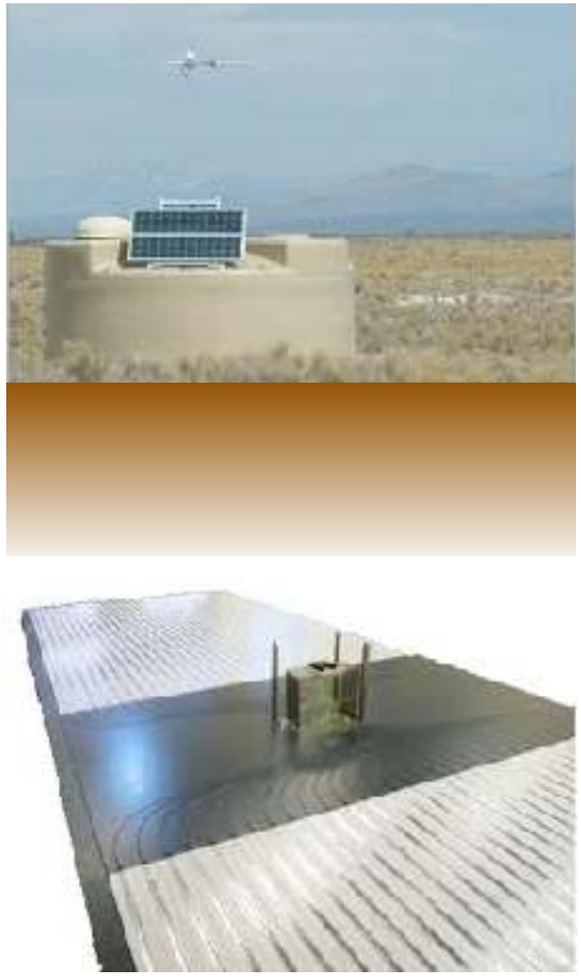

the Muon Detectors

lateral shower profile

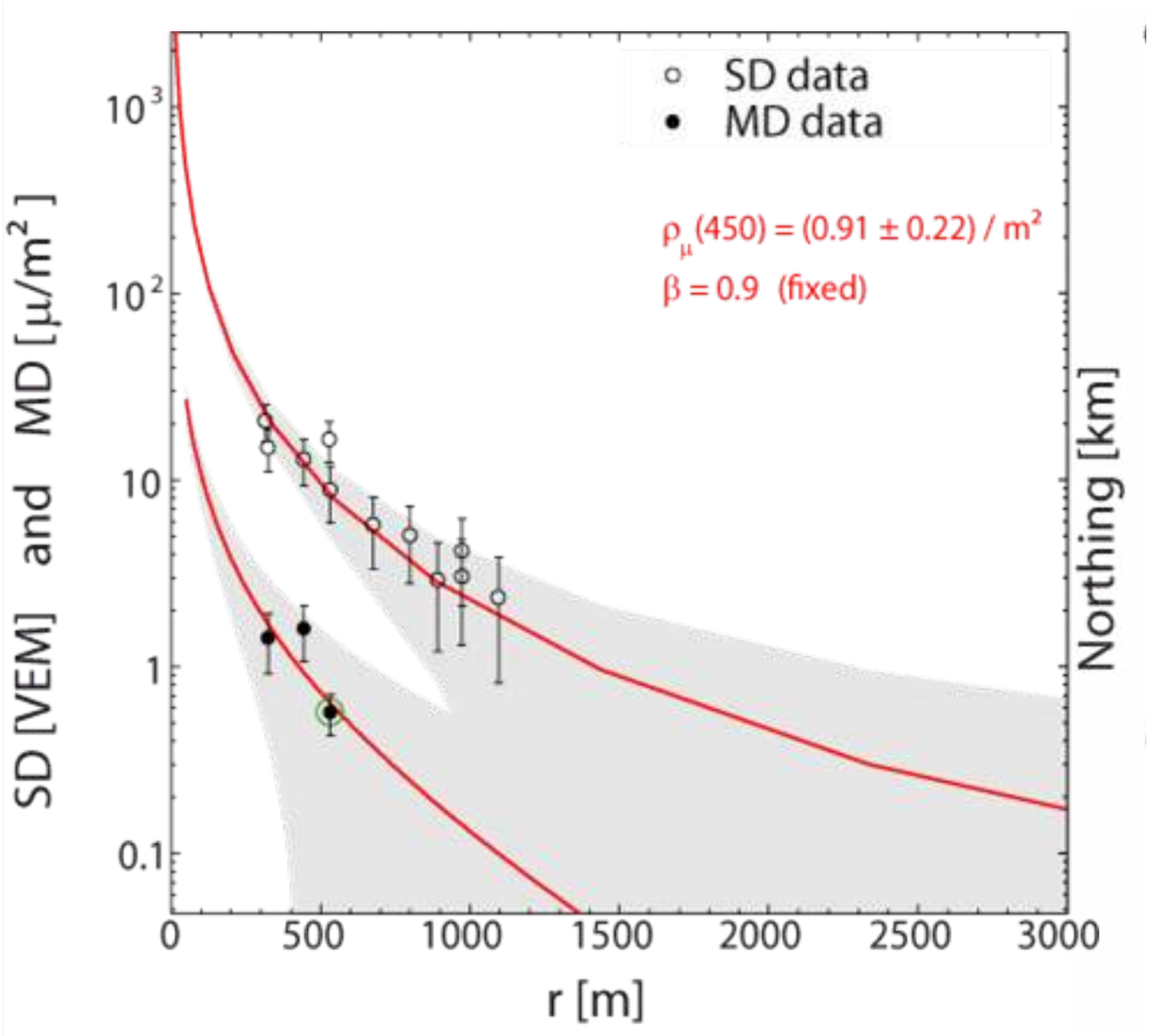

E ~ $2*10^{17}$ eV X_{max} ~ 860 g/cm² zenith angle ~ 75° azimuth angle ~ 8°

Tunka-Rex

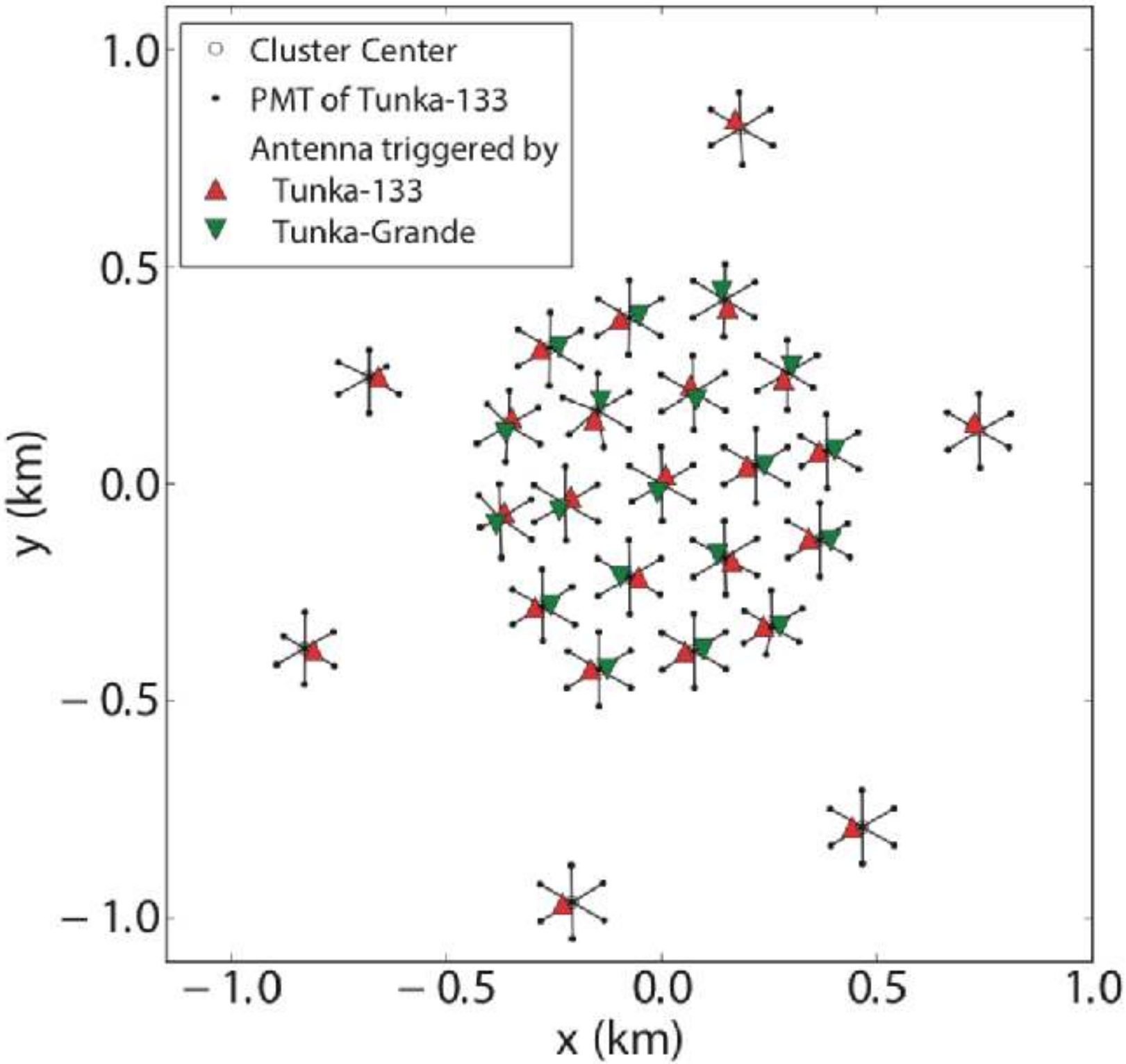
Cluster Center
PMT of Tunka-133
Antenna triggered by
Tunka-133
Tunka-Grande
1.0
0.5
0.0
− 0.5
− 1.0
y (km)
− 1.0
− 0.5
0.0
0.5
1.0
x (km)

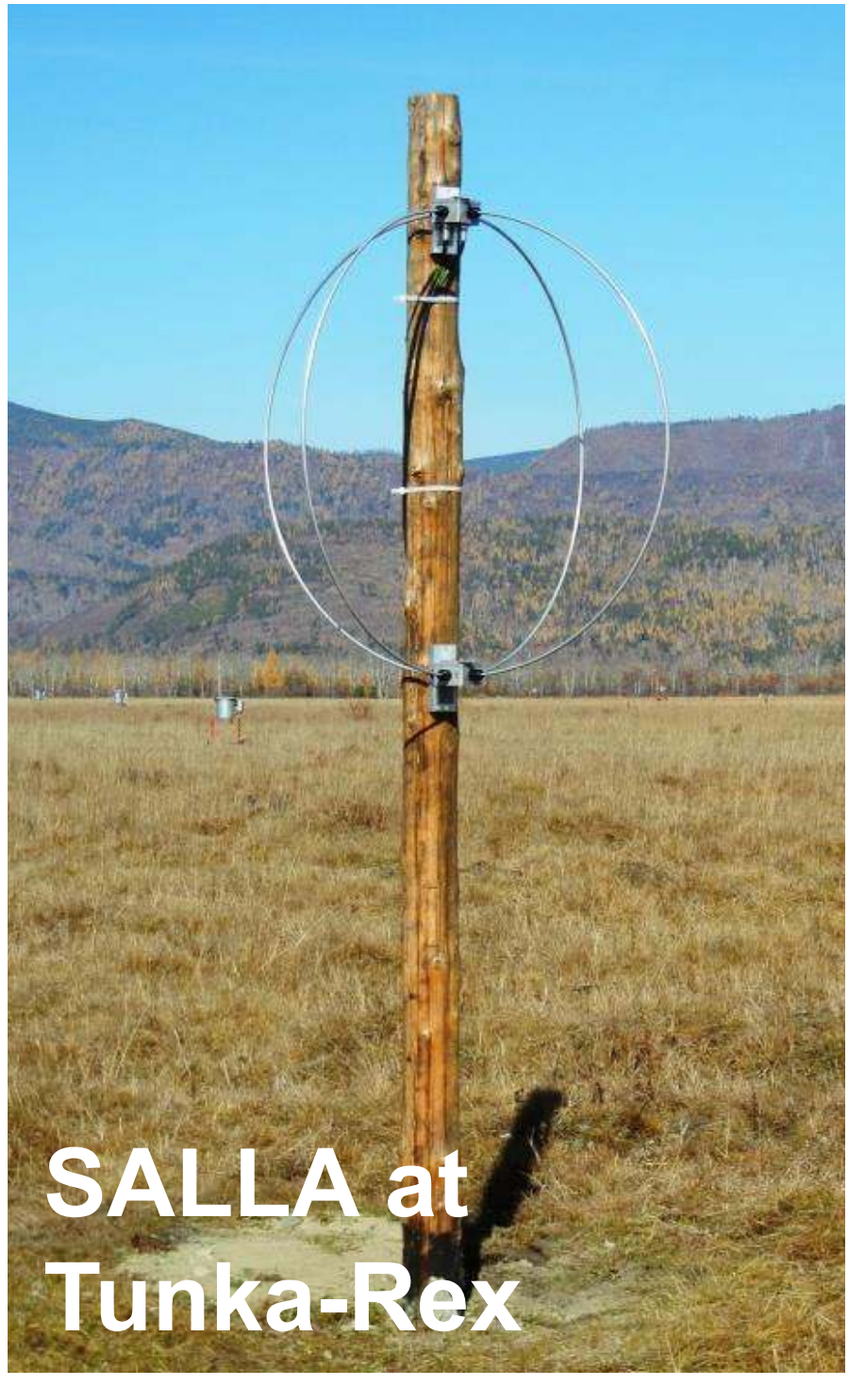
SALLA at
Tunka-Rex

Radiation Processes

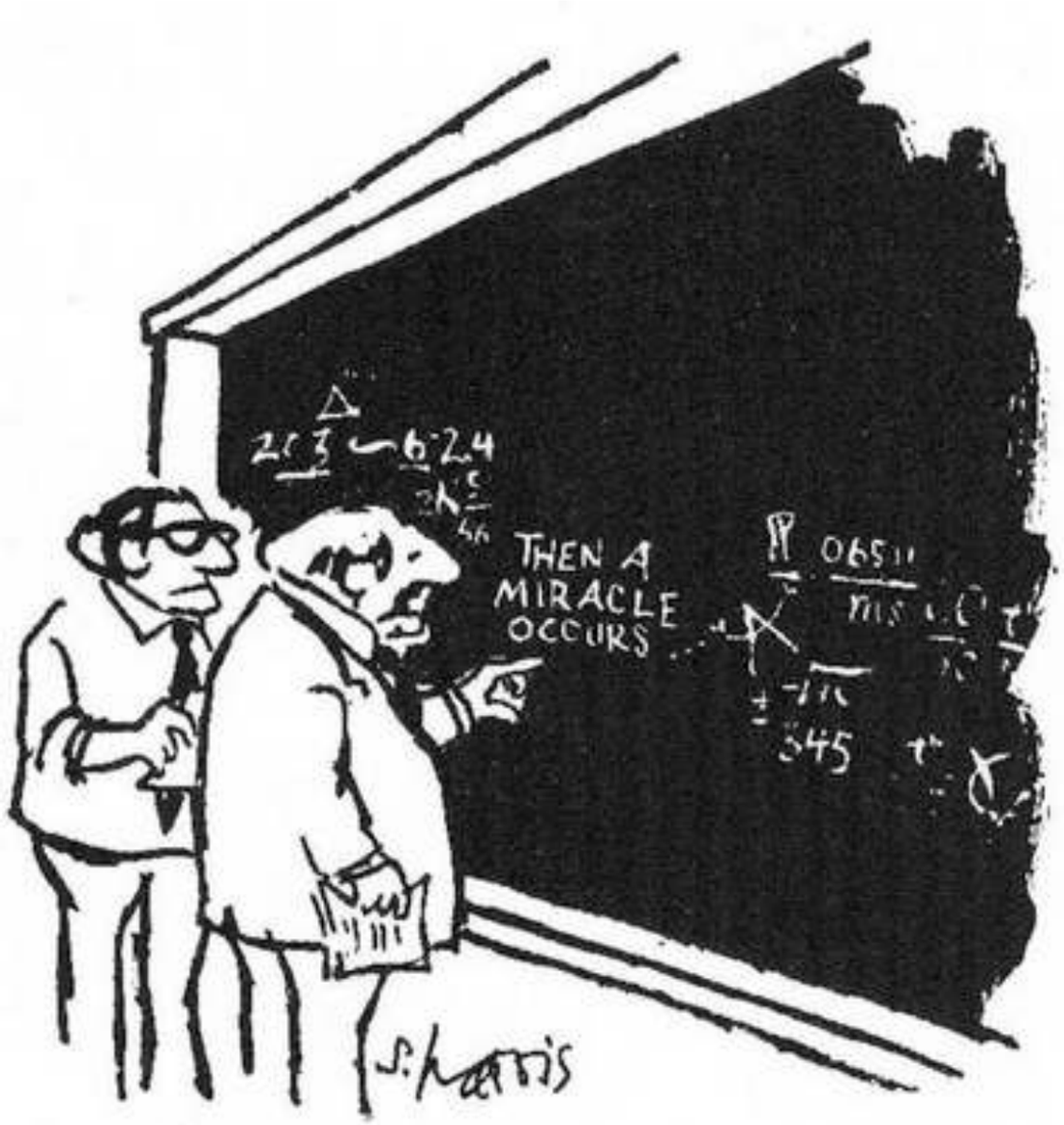

"I think you should be more explicit here in step two."

Radio Emission in Air Showers

Mainly: Charge separation in geomagnetic field

$$\vec{E} \propto \vec{v} \times \vec{B}$$

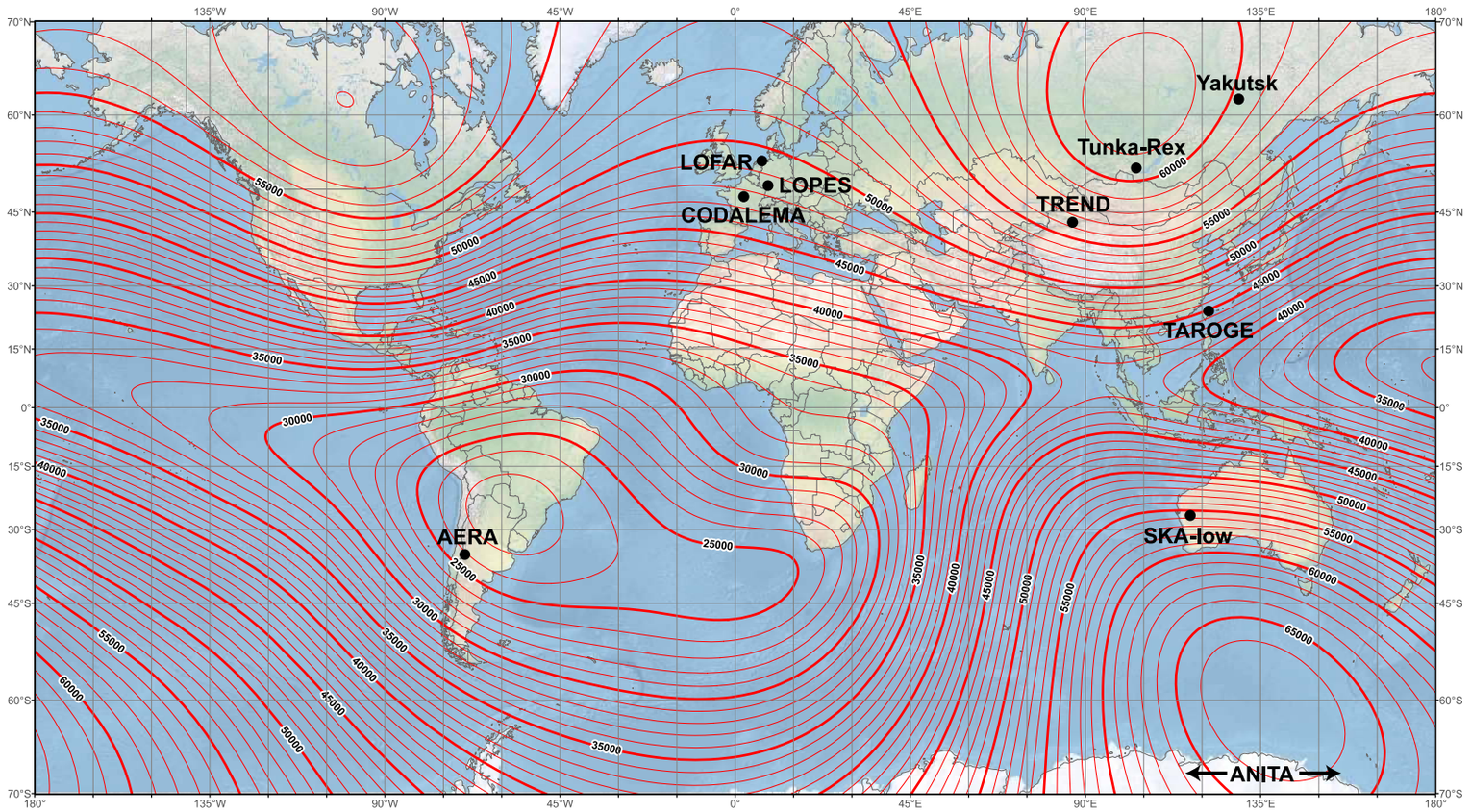

Underlying map (Mercator projection):
Main Geomagnetic Field Total Intensity with contour intervals of 1000 nT
according to US/UK World Magnetic Model - Epoch 2015.0

developed by NOAA/NGDC & CIRES
http://ngdc.noaa.gov/geomag/WMM

Map reviewed by NGA and BGS
Published December 2014

Overlayed: **Location of radio experiments for cosmic-ray air showers**
added on underlying map by Frank G. Schröder
Karlsruhe Institute of Technology (KIT), Germany

F. Schröder, Prog. Part. Nucl. Phys. 93 (2017) 1

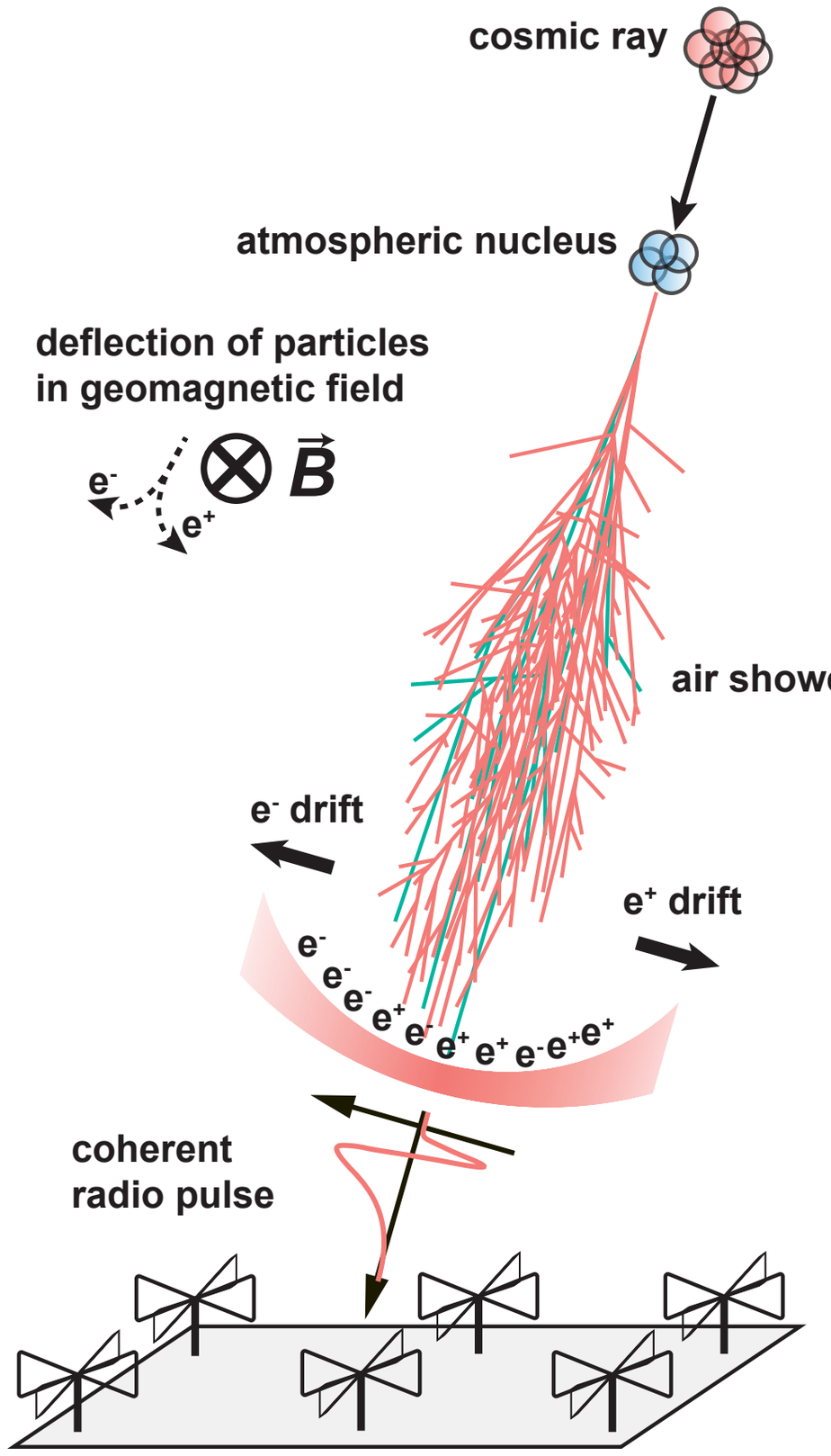

Arrival direction of showers with strong radio signals

north-south asymmetry
v x B effect

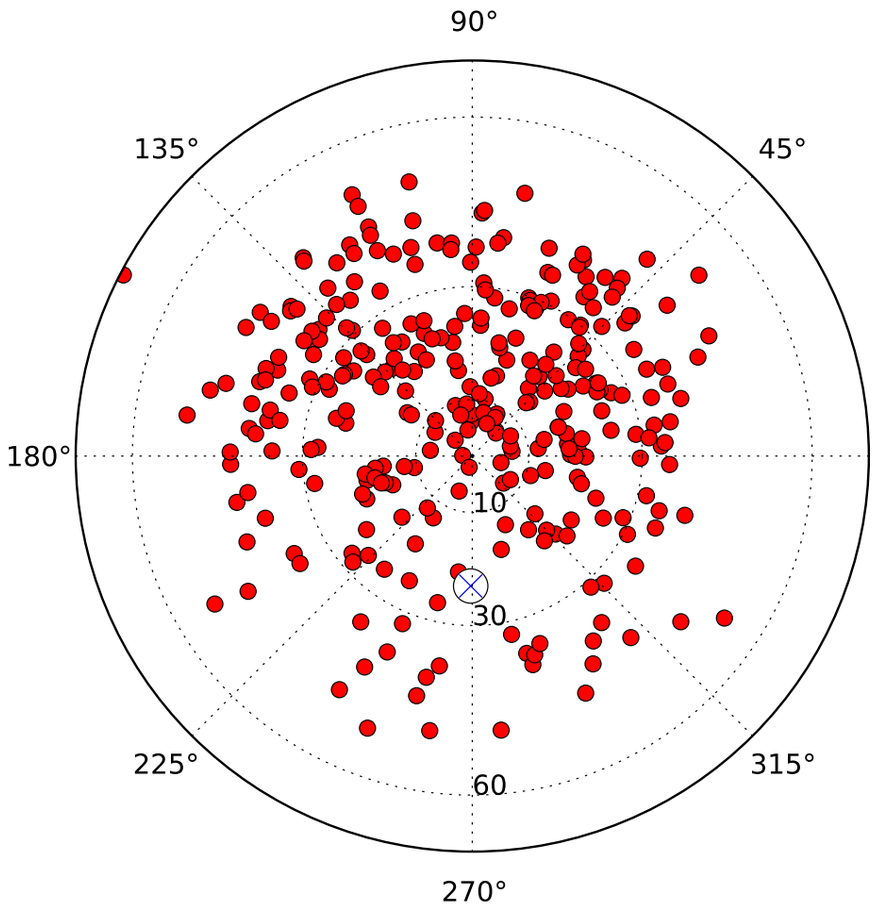

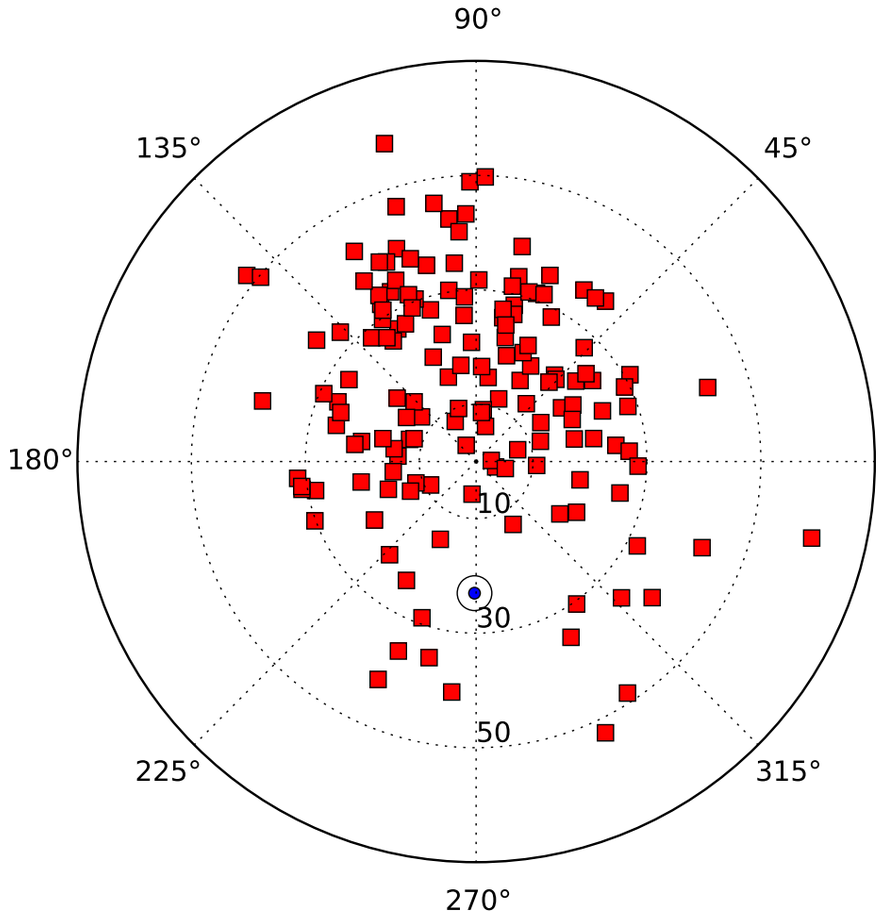

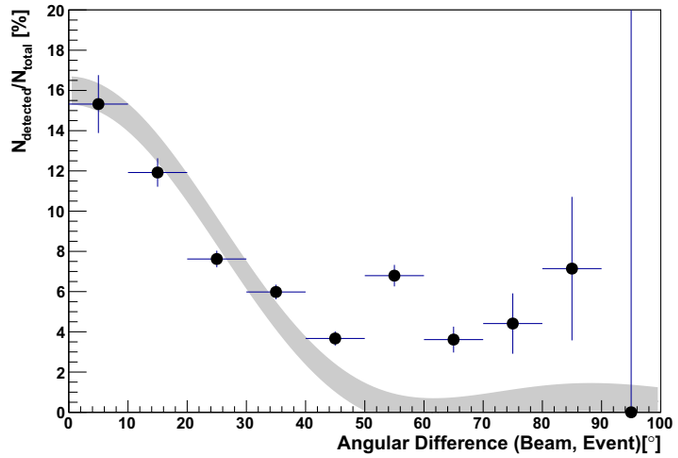

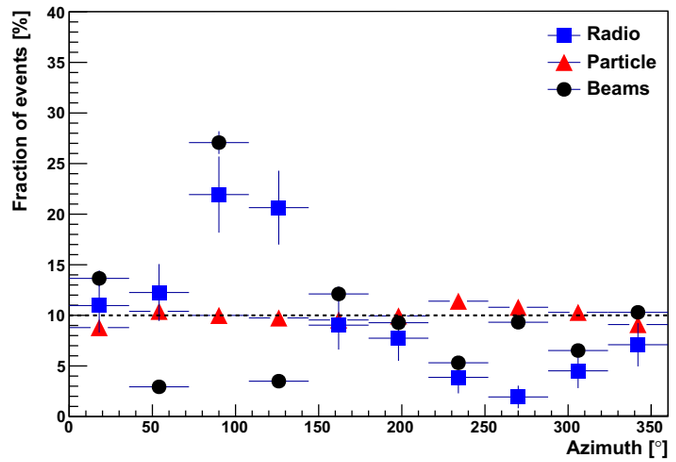

LOFAR

30 - 80 MHz

110 - 190 MHz

A. Nelles et al., Astroparticle Physics 65 (2015) 11

P. Schellart et al., A&A 560 (2013) A98

Arrival direction of showers with strong radio signals

north-south asymmetry
v x B effect

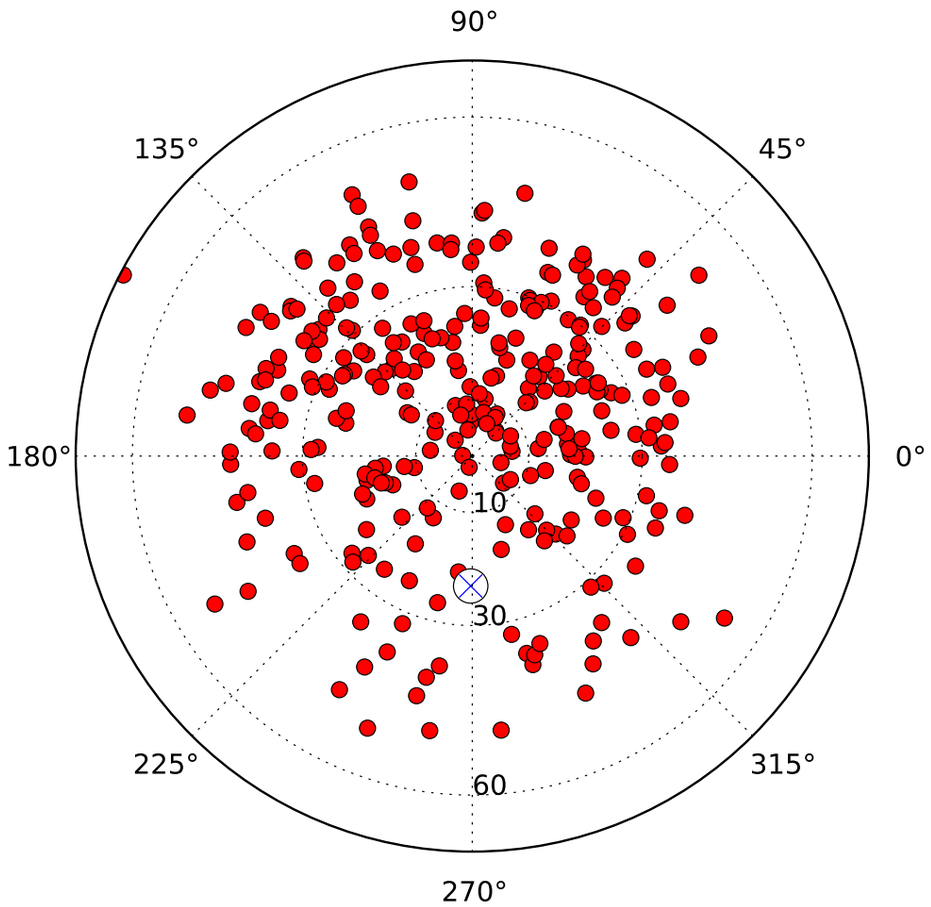

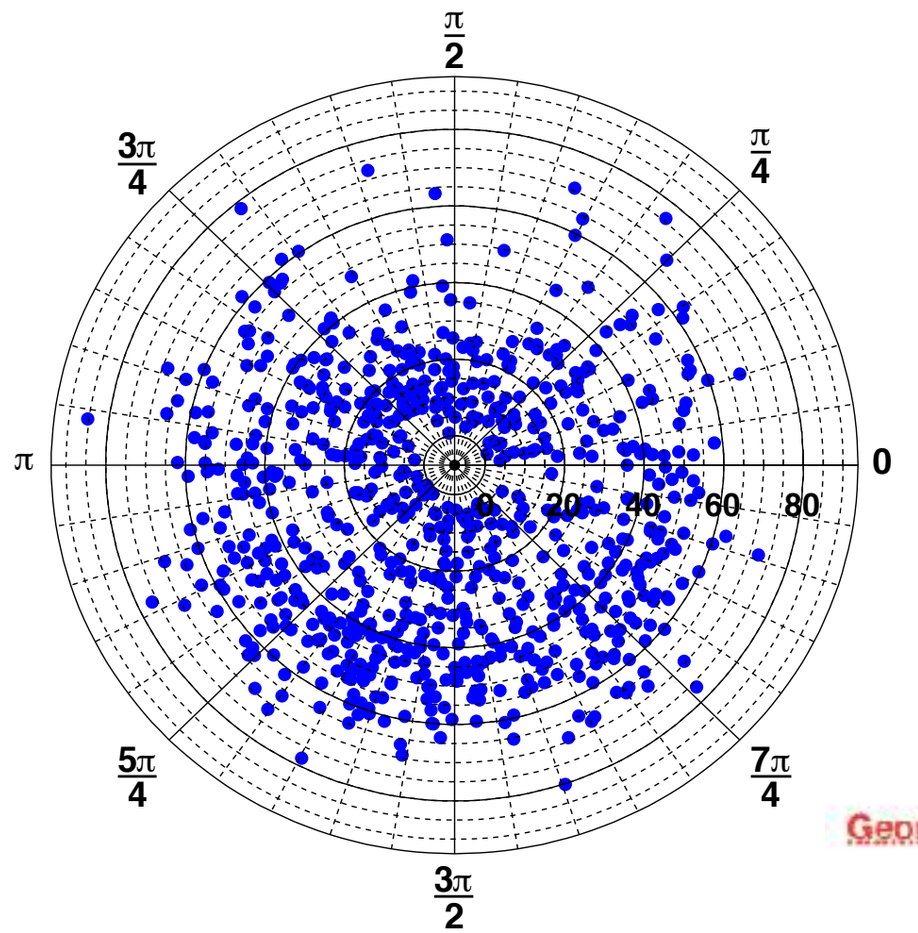

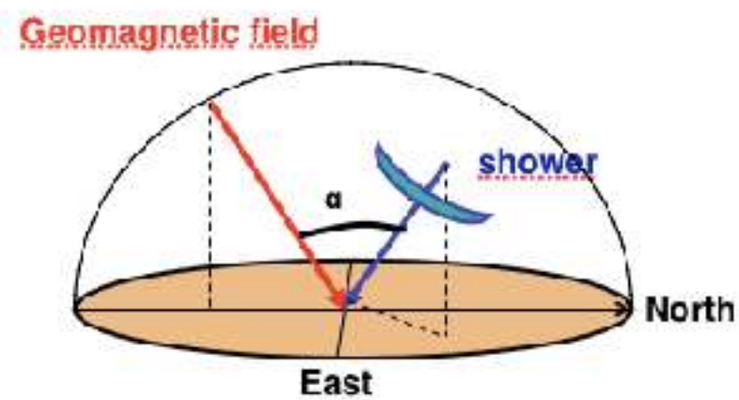

LOFAR

AERA
Auger Engineering Radio Array

30 - 80 MHz

P. Schellart et al., A&A 560 (2013) A98

Astroparticle Physics 31 (2009) 192–200

Contents lists available at ScienceDirect

Astroparticle Physics

journal homepage: www.elsevier.com/locate/astropart

Geomagnetic origin of the radio emission from cosmic ray induced air showers observed by CODALEMA

D. Ardouin [a], A. Belletoile [a,c]
S. Dagoret-Campagne [d], R. I
N. Gautherot [f], T. Gousset [a],
F. Lefeuvre [g], L. Martin [a,*], E
K. Payet [c], G. Plantier [e], O. R
S. Valcares [a]

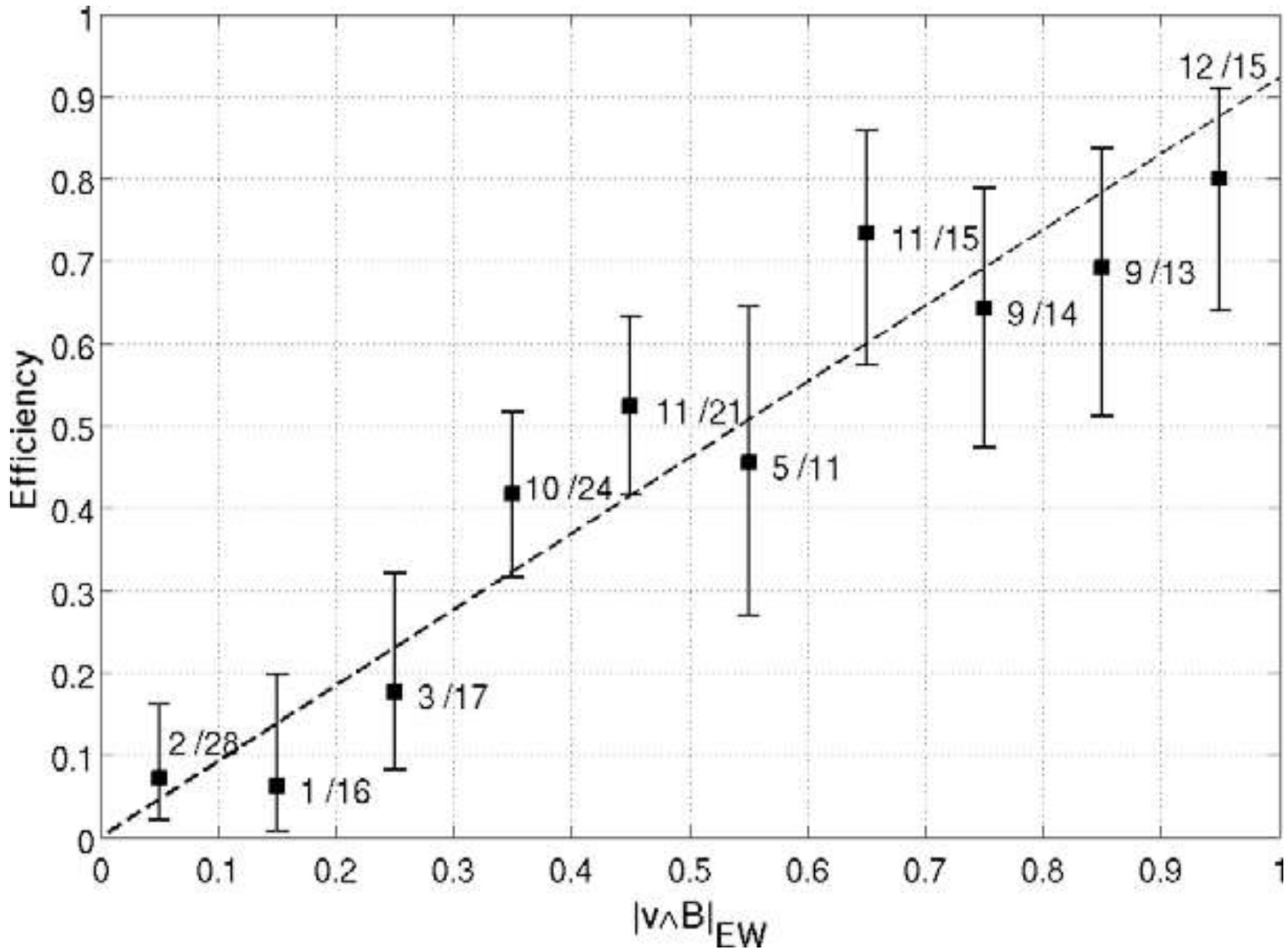

Fig. 11. Number of radio events relative to the number of scintillator events ($E > 10^{17}$ eV) with respect to $|(\mathbf{v} \wedge \mathbf{B})_{EW}|/(vB)$.

Geomagnetic effect

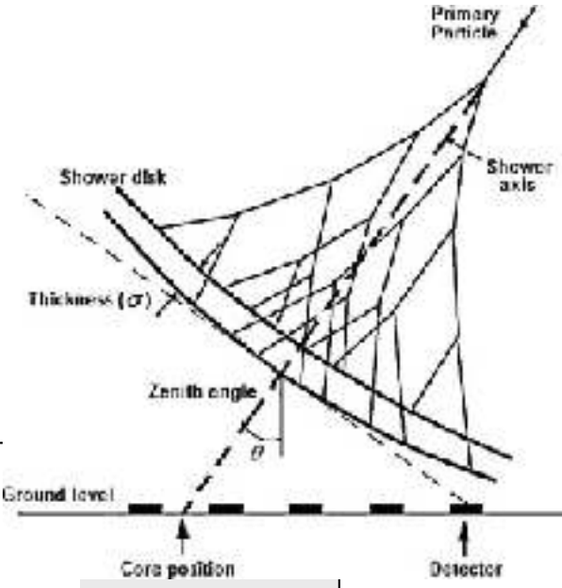

T. Huege / Physics Reports 620 (2016) 1–52

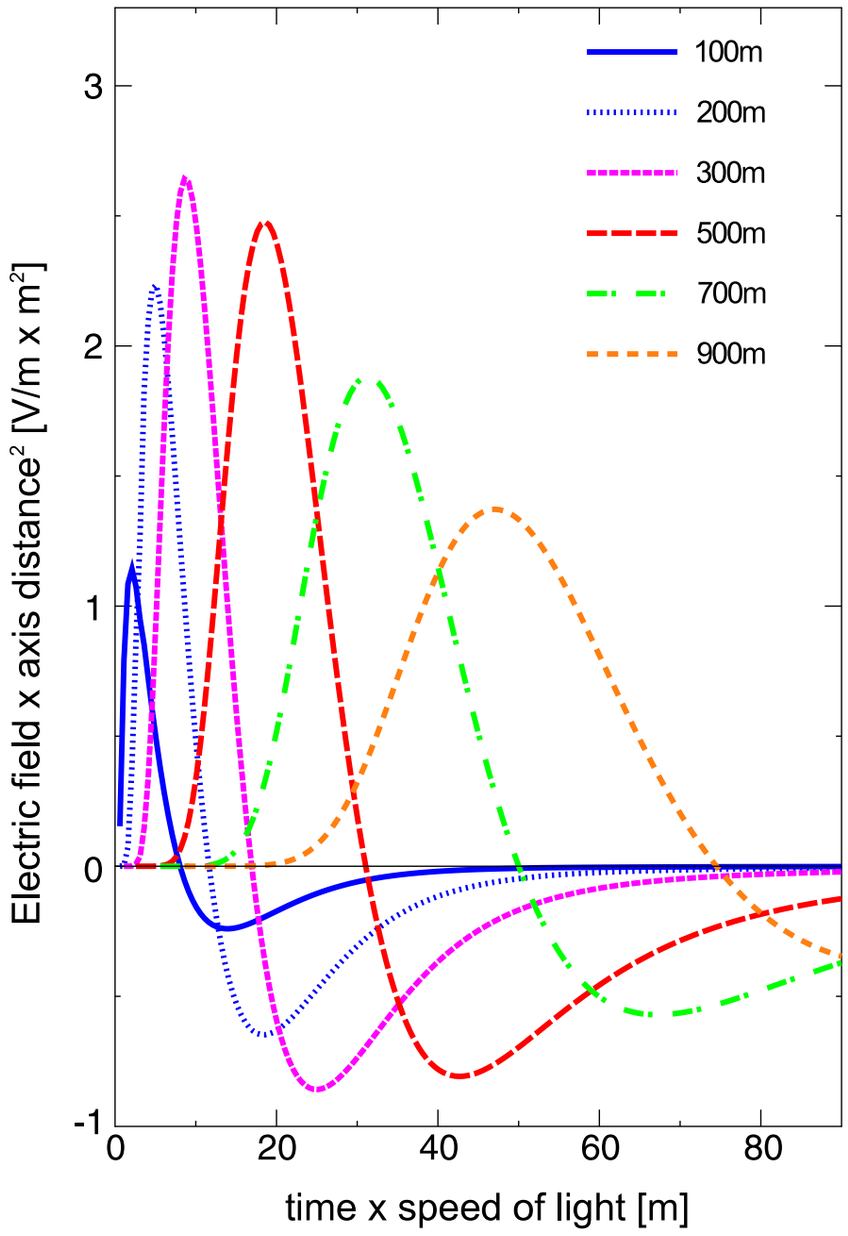

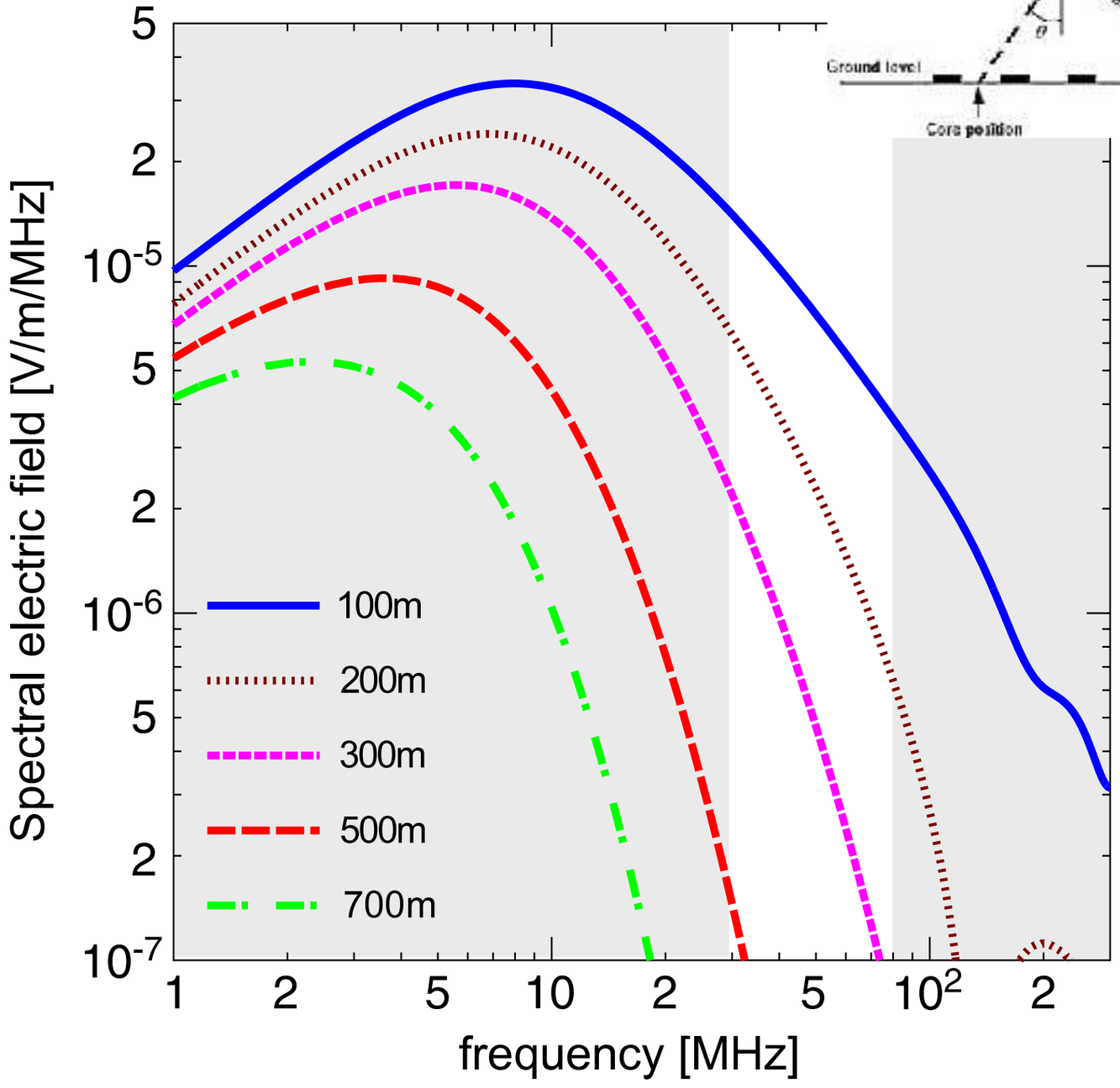

Fig. 4. Radio pulses (top) arising from the time-variation of the geomagnetically induced transverse currents in a 10^{17} eV air shower as observed at various observer distances from the shower axis and their corresponding frequency spectra (bottom). Refractive index effects are not included.
Source: Adapted from [18].

Radio Emission in Air Showers

- **Mainly: Charge separation in geomagnetic field**

$$\vec{E} \propto \vec{v} \times \vec{B}$$

Theory predicts additional mechanisms:

- **excess of electrons in shower: charge excess**
- **superposition of emission due to Cherenkov effects in atmosphere**

polarization of radio signal

geomagnetic **Askaryan**

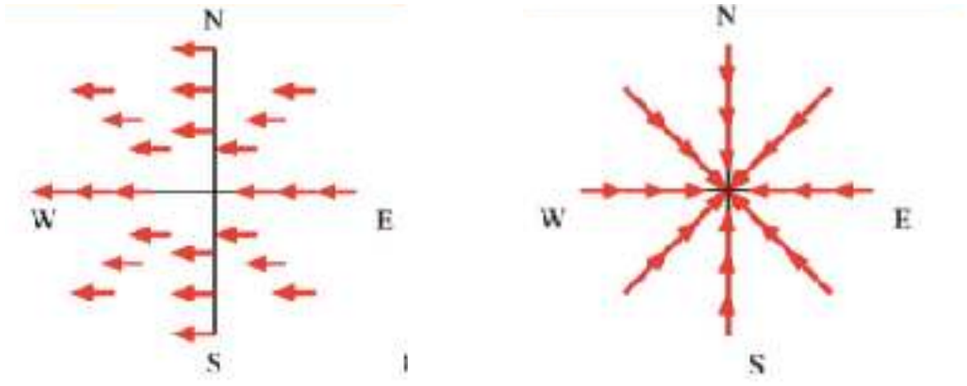

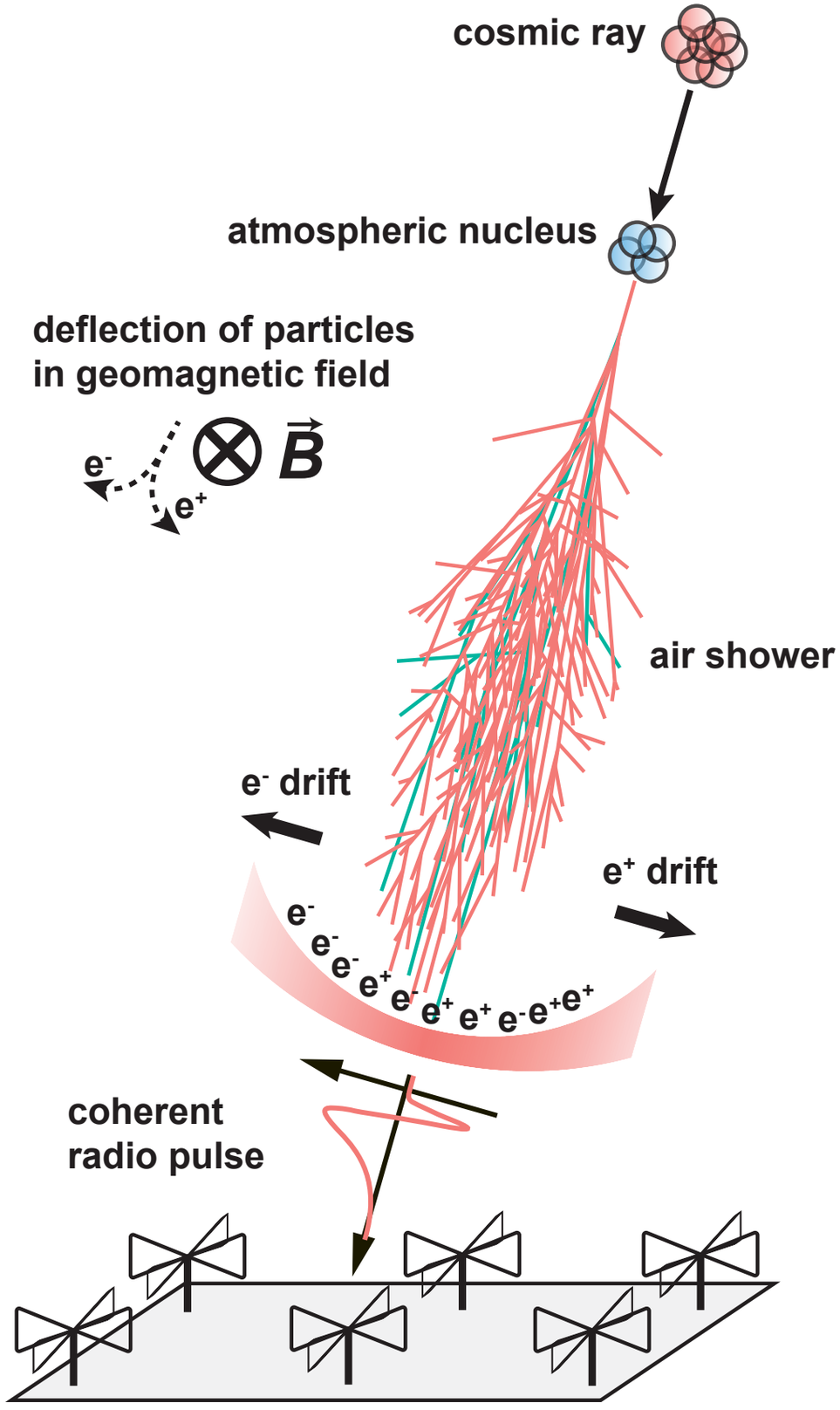

Polarization footprint

of an individual air shower

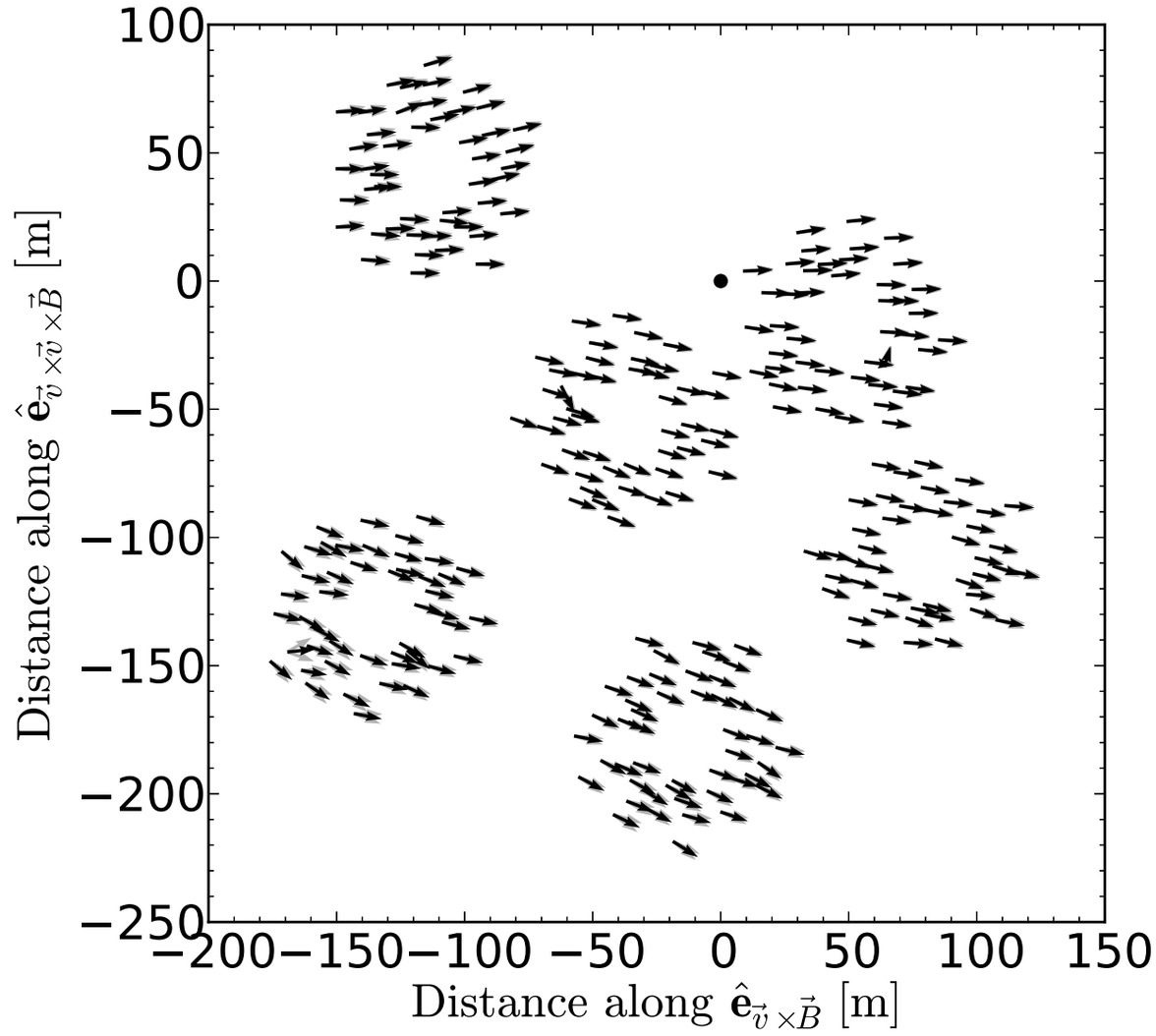

geomagnetic

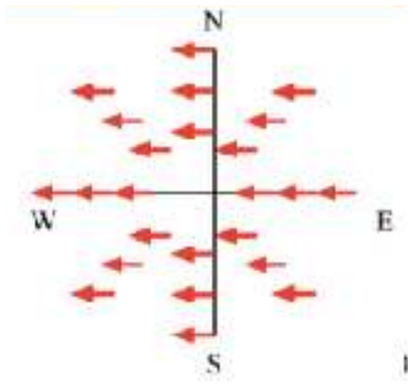

Askaryan

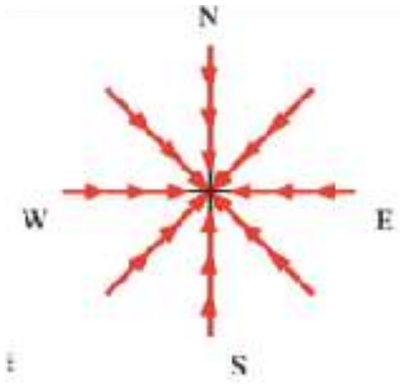

LOFAR

P. Schellart et al., JCAP 10 (2014) 014

Charge excess fraction

Askaryan

geomagnetic

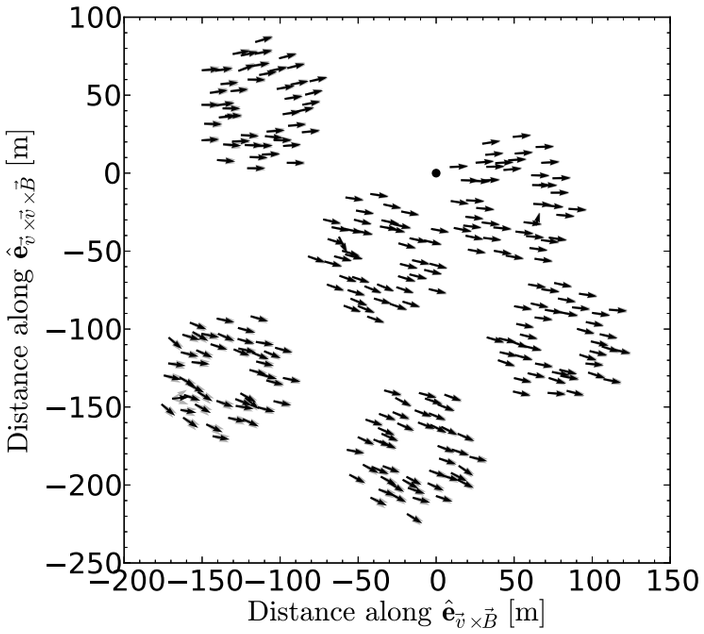

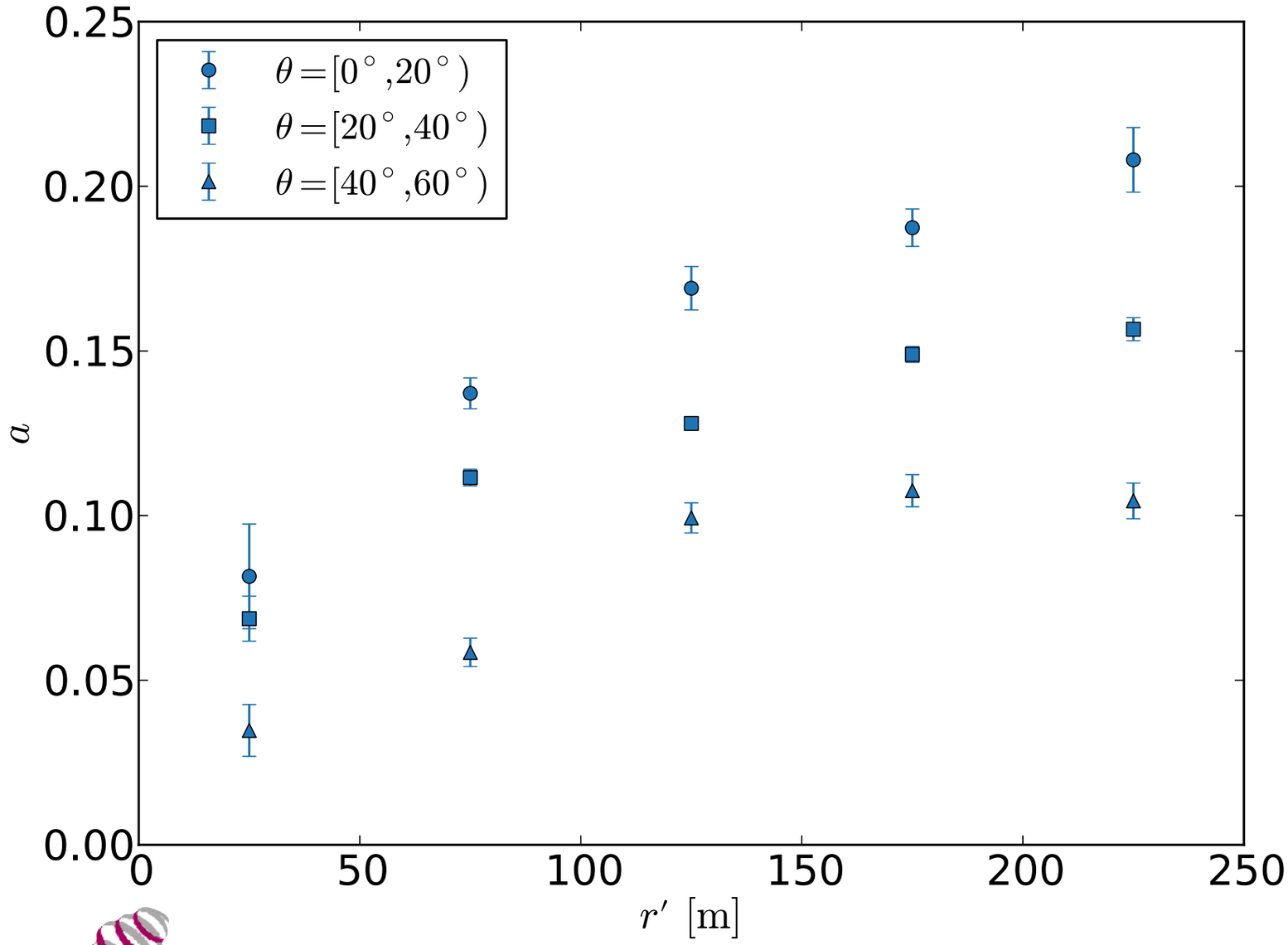

geomagnetic **Askaryan**

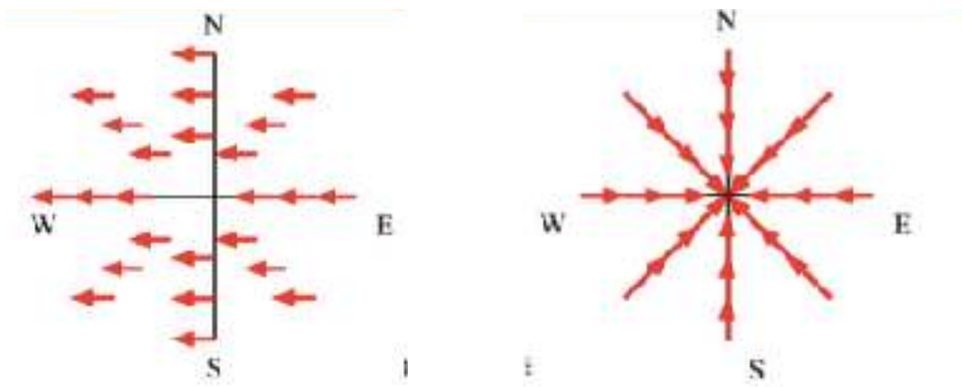

LOFAR

P. Schellart et al., JCAP 10 (2014) 014

Charge excess fraction

Auger Engineering Radio Array

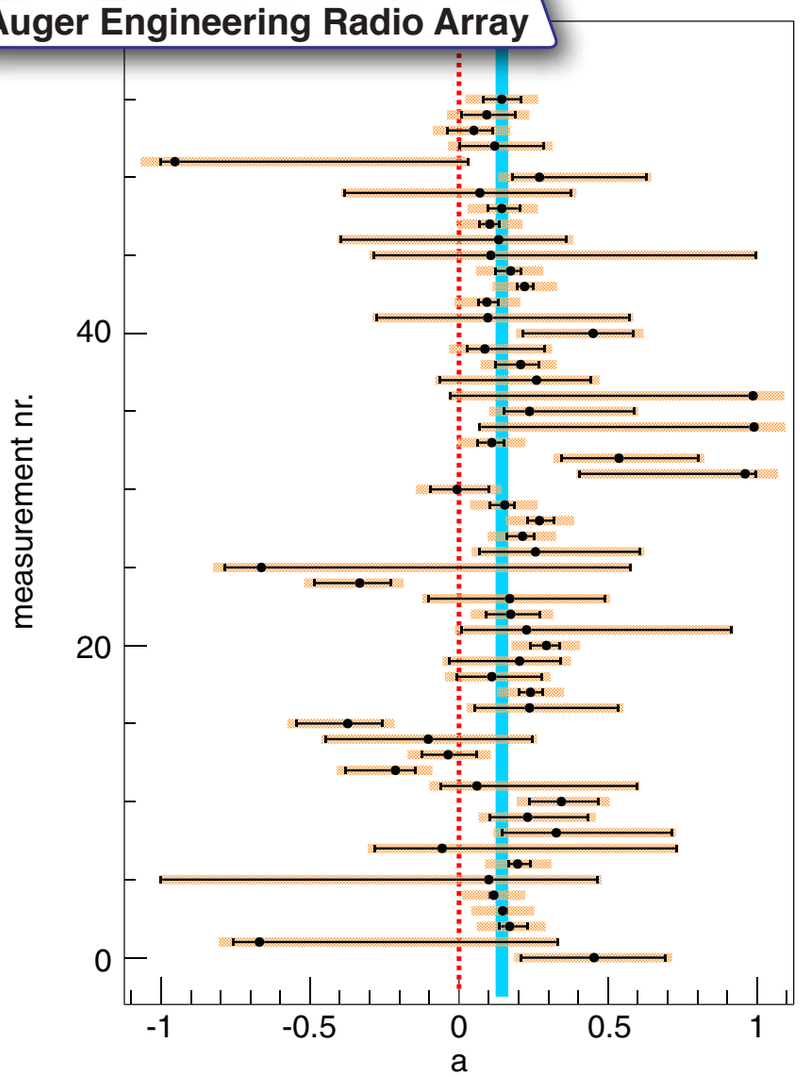

Askaryan

geomagnetic

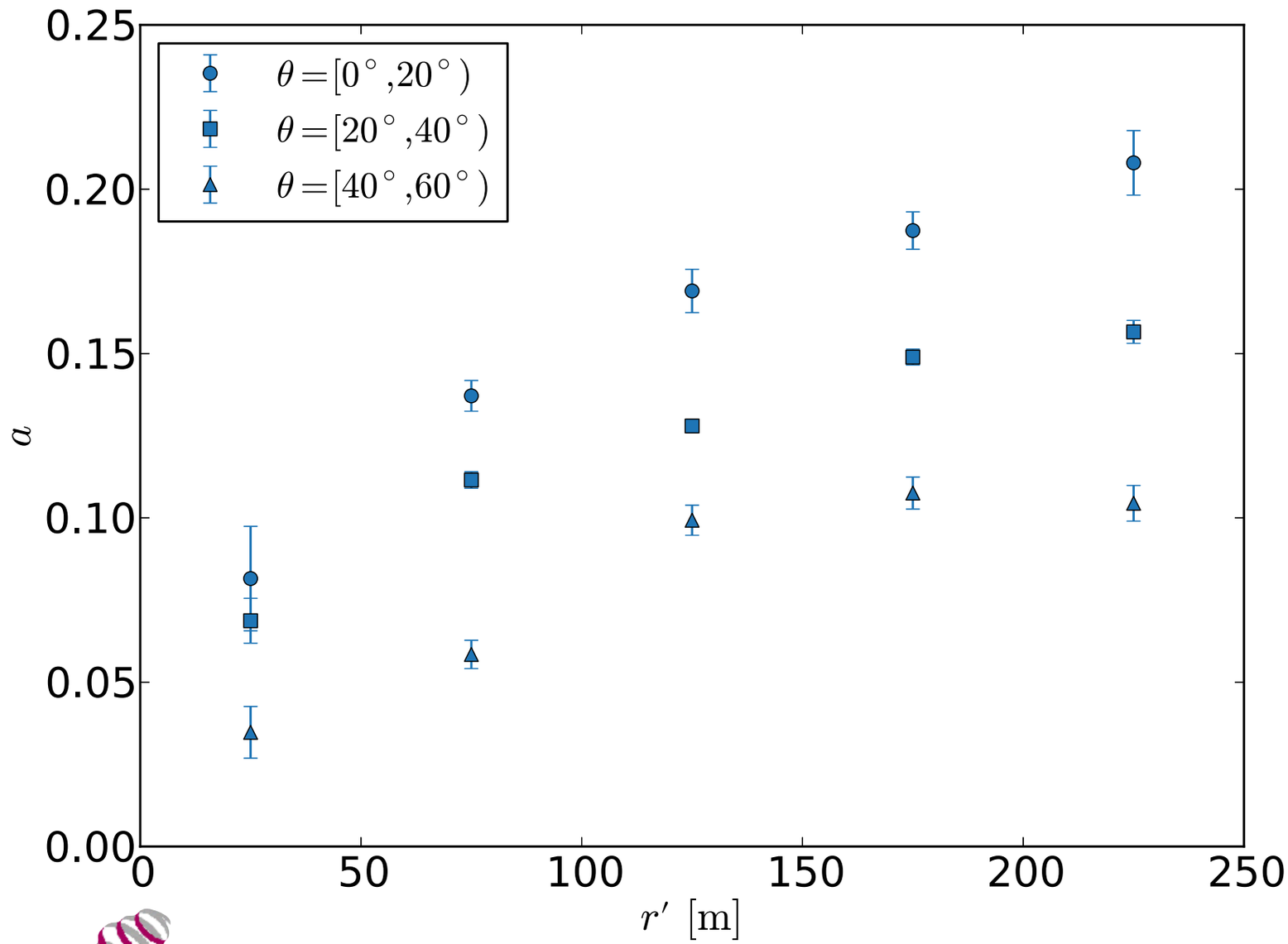

LOFAR

A. Aab, PRD 89 (2014) 052002

P. Schellart et al., JCAP 10 (2014) 014

Charge excess signature in the CODALEMA data. Interpretation with SELFAS2.

VINCENT MARIN[1], FOR THE CODALEMA COLLABORATION[1,2,3,4,5,6,7]
[1]*SUBATECH, Université de Nantes/Ecole des Mines de Nantes/IN2P3-CNRS, Nantes France.* [2]*LESIA, USN de Nançay, Observatoire de Paris-Meudon/INSU-CNRS, Meudon France.* [3]*LPSC, Université Joseph Fourier/INPG/IN2P3-CNRS, Grenoble France.* [4]*LAL, Université Paris-Sud/IN2P3-CNRS, Orsay France.* [5]*GSII, ESEO, Angers France.* [6]*LAOB, Université de Besançon/INSU-CNRS, Besançon France.* [7]*LPCE, Université d'Orléans/INSU-CNRS, Orléans France.*
vincent.marin@subatech.in2p3.fr DOI: 10.7529/ICRC2011/V01/0942

Abstract: The systematic shift between the shower core estimation using the particle array data and the shower core estimation using the radio array data of the CODALEMA experiment is discussed. Using the simulation code SELFAS2 we show that the consideration of the charge excess contribution in the total radio emission of air showers generates a shift of the apparent ground radio core along the east-west axis. This radio core shift is then characterized for the CODALEMA statistic and compared with the experimental data. The good agreement between data and simulation suggests that this behavior can be considered as an experimental signature of the charge excess contribution.

Keywords: CODALEMA, SELFAS, radio detection, charge excess

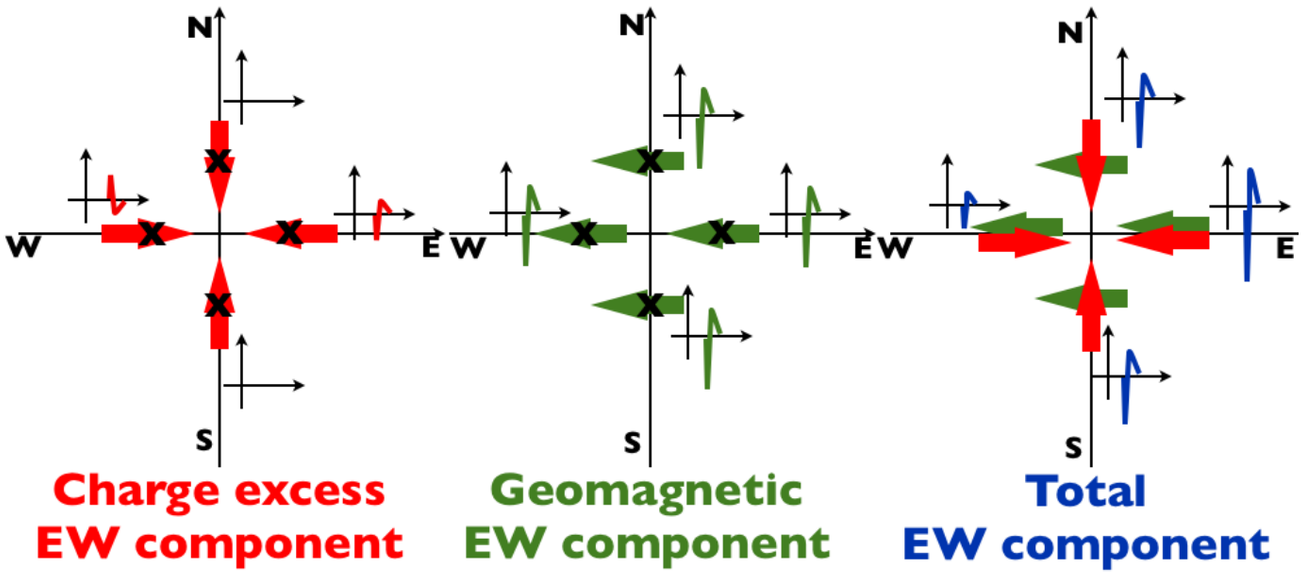

FIGURE 2 – Polarization vectors of the charge excess and transverse current contributions in the plane perpendicular to the shower axis. Due to the fact that the polarization vectors of these two contributions are not always oriented in the same direction, their combination can be constructive or destructive following the antenna position.

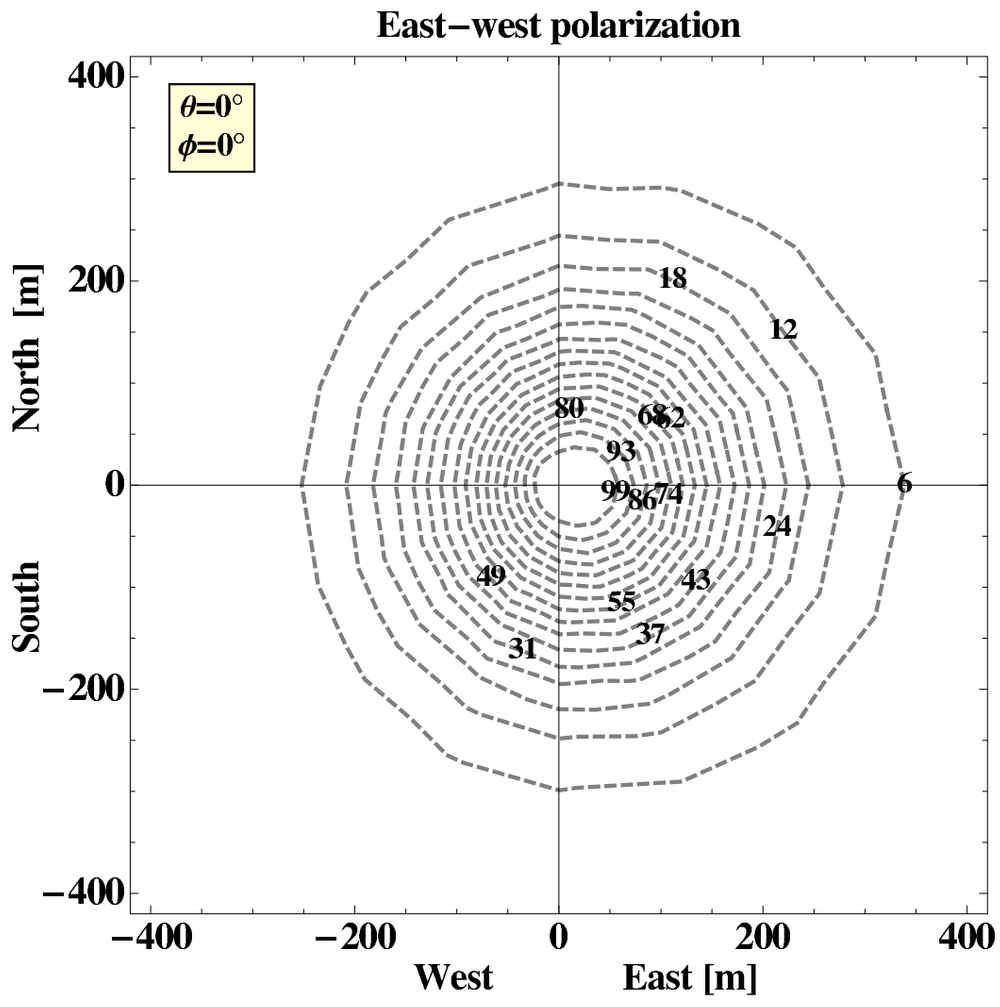

FIGURE 1 – Ground footprint of the signal deposited (absolute value) by a 10^{17} eV vertical EAS in the east-west polarization simulated with SELFAS2. The origin of the frame corresponds to the simulated ground particles shower core. The contour lines are in μV.m^{-1}, a 23-83 MHz numerical passband filter is applied on signal. The ground radio core is toward the east.

Footprint of radio emission on the ground

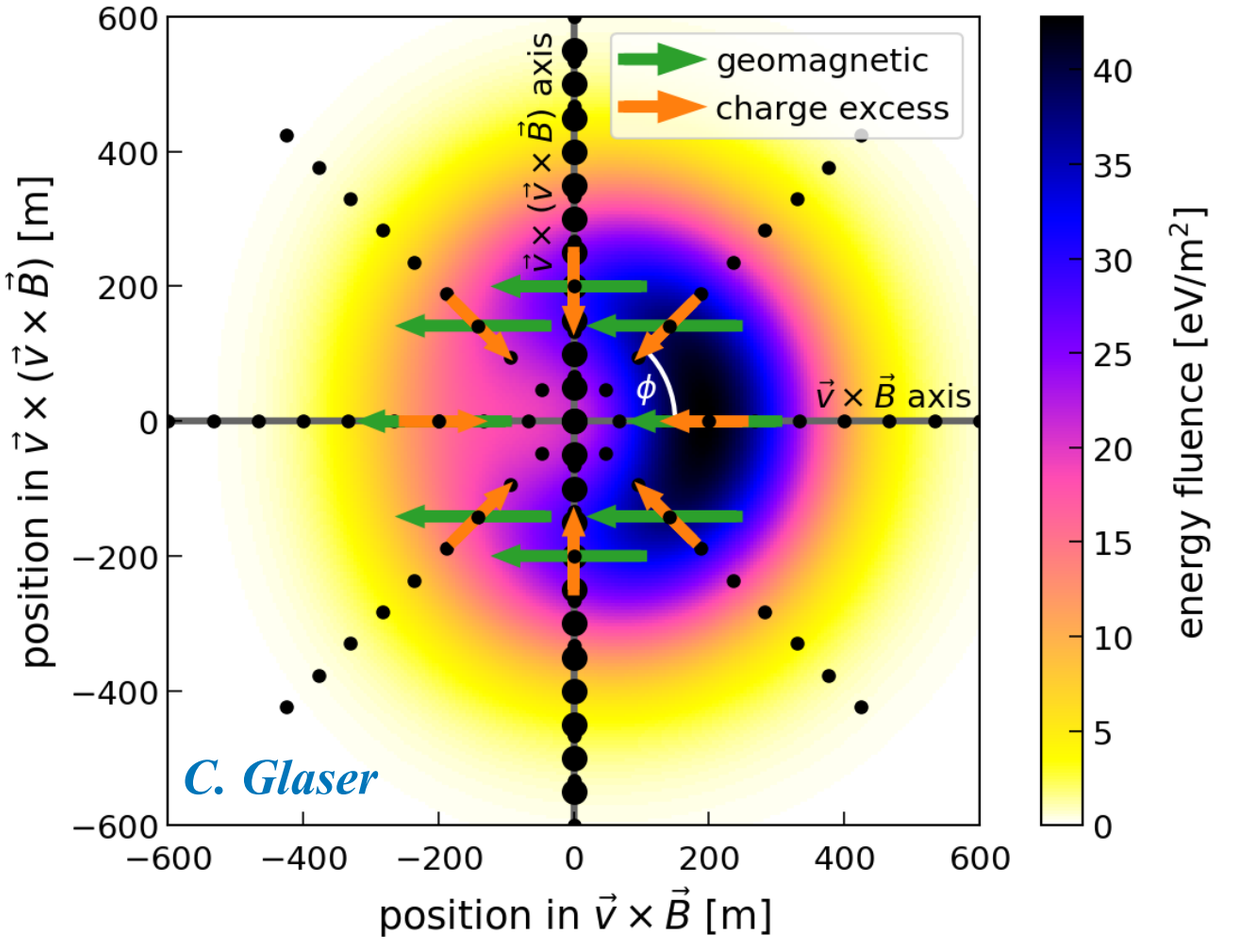

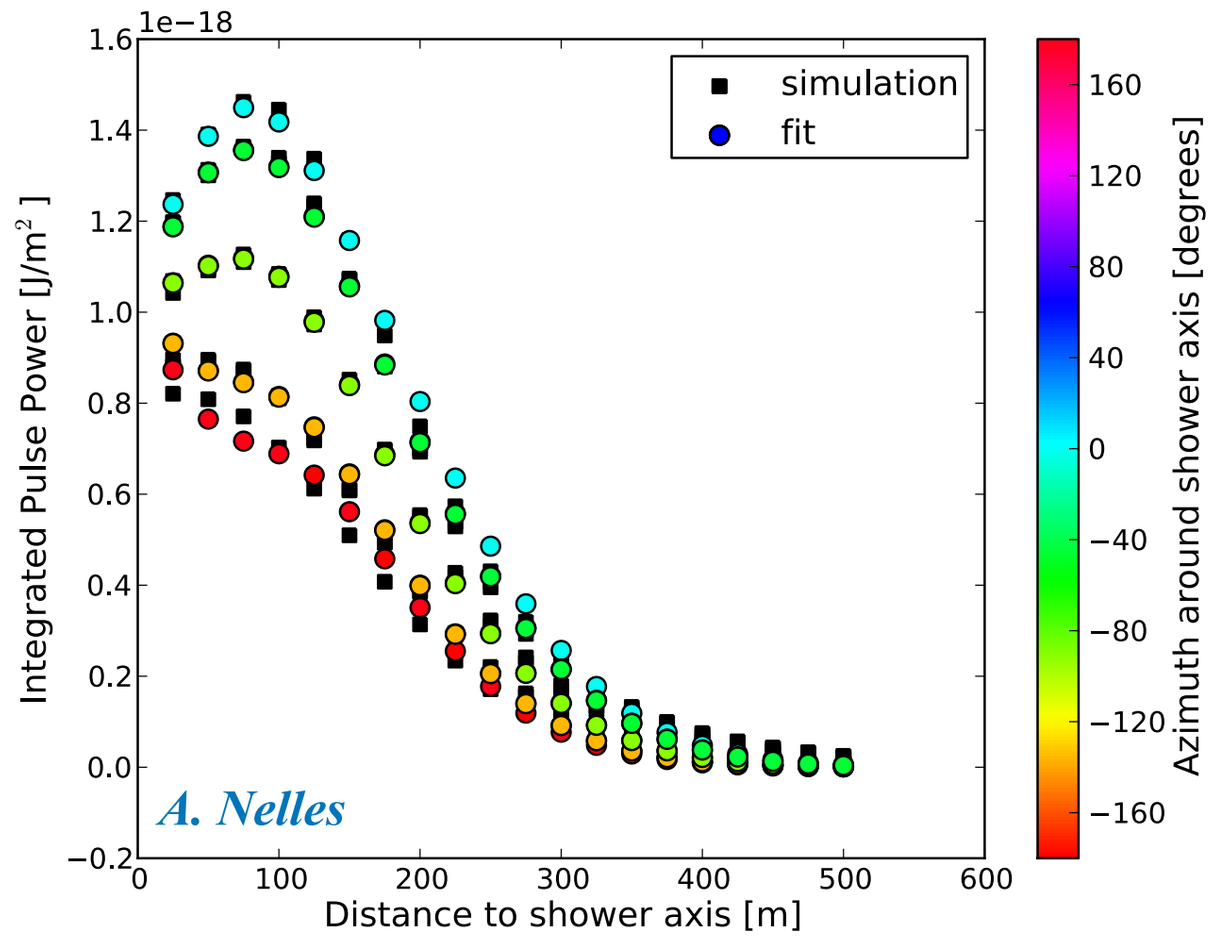

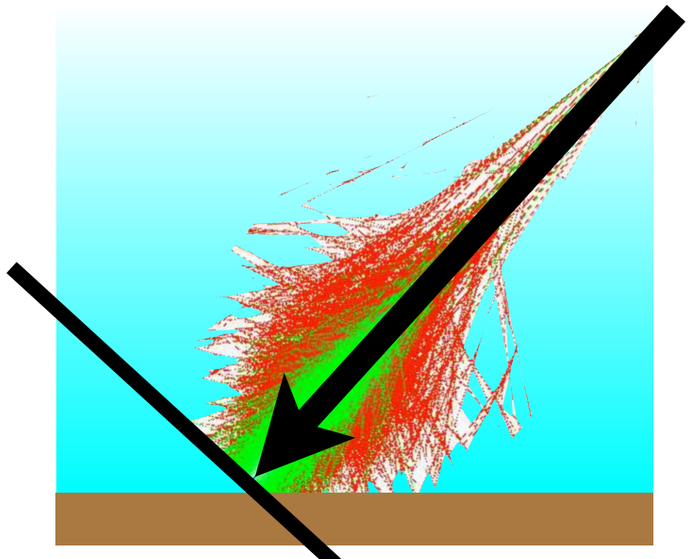

Footprint of radio emission on the ground

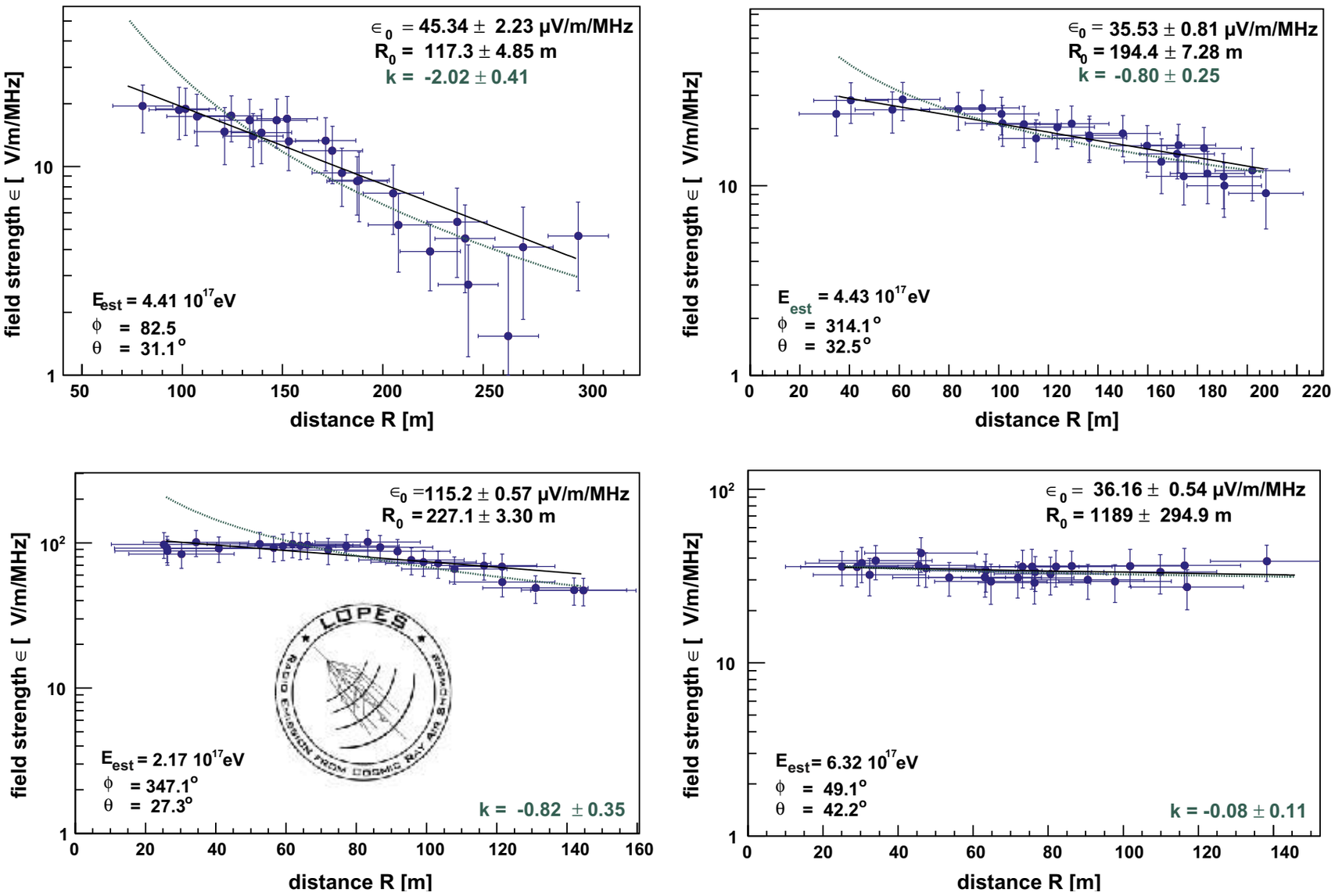

Fig. 6. Same as Fig. 5, but for four lateral distributions with unusual shapes. Discussion see text.

W.D. Apel et al., Astroparticle Physics 32 (2010) 294–303

Footprint of radio emission on the ground

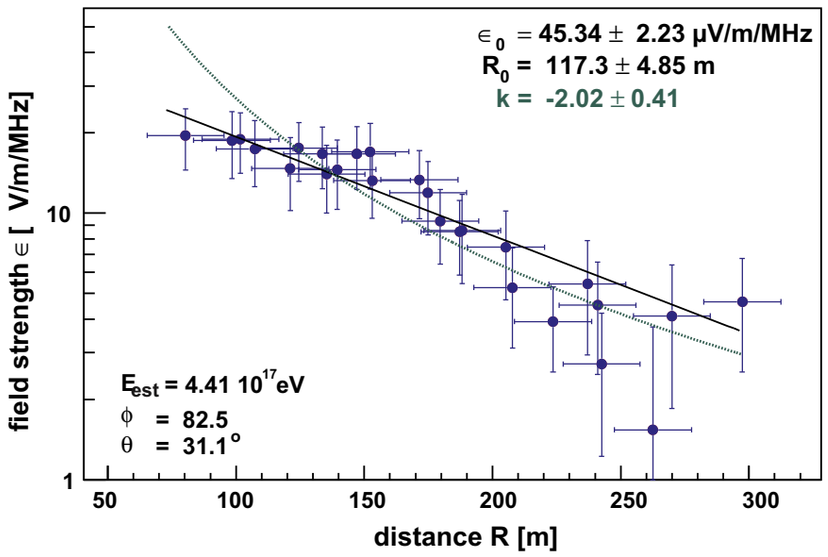

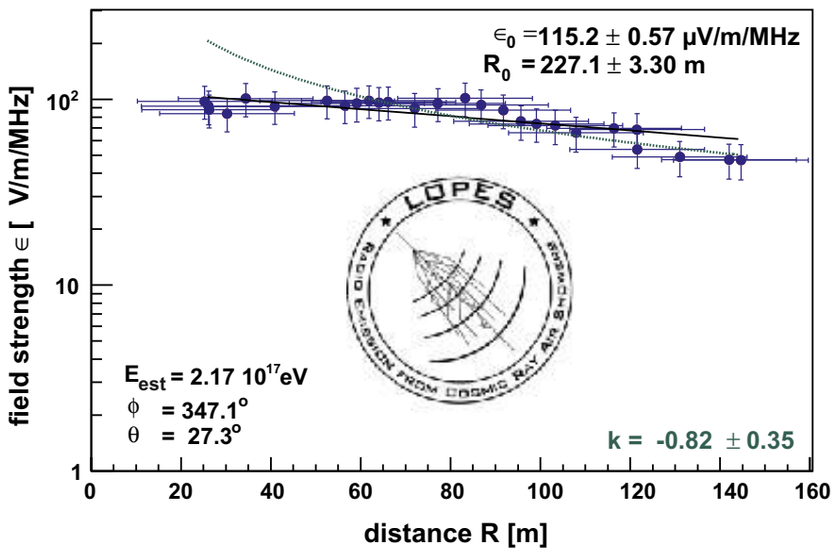

LOFAR

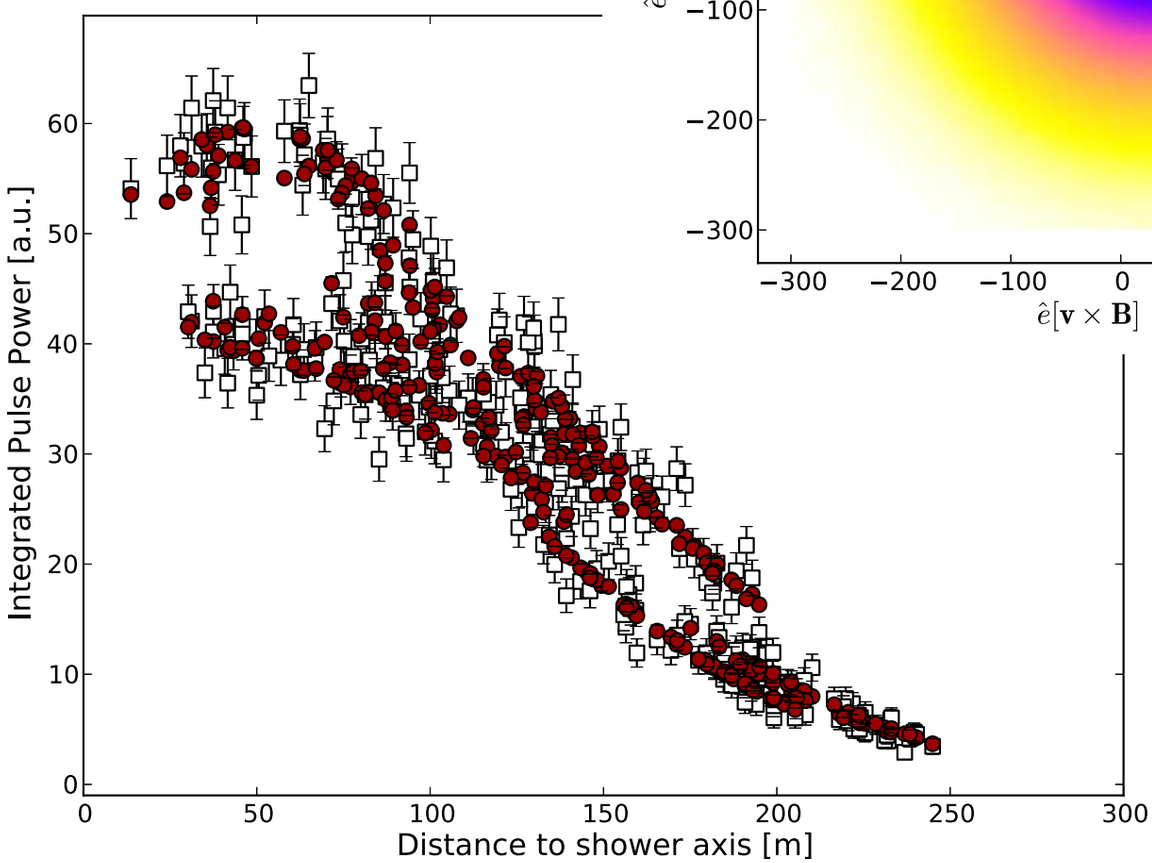

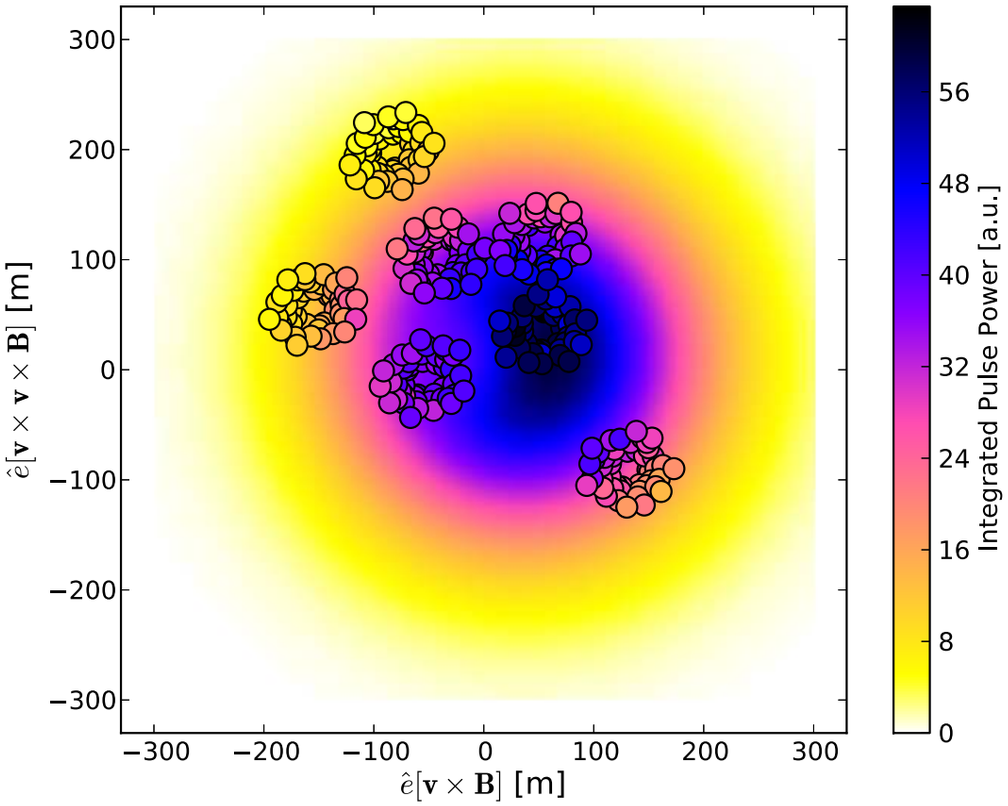

A. Nelles et al., Astropart. Phys. 60 (2015) 13

W.D. Apel et al., Astroparticle Physics 32 (2010) 294–303

Lateral distribution of radio signals

not rotationally symmetric —> fit two Gaussian functions

v x (v x B)

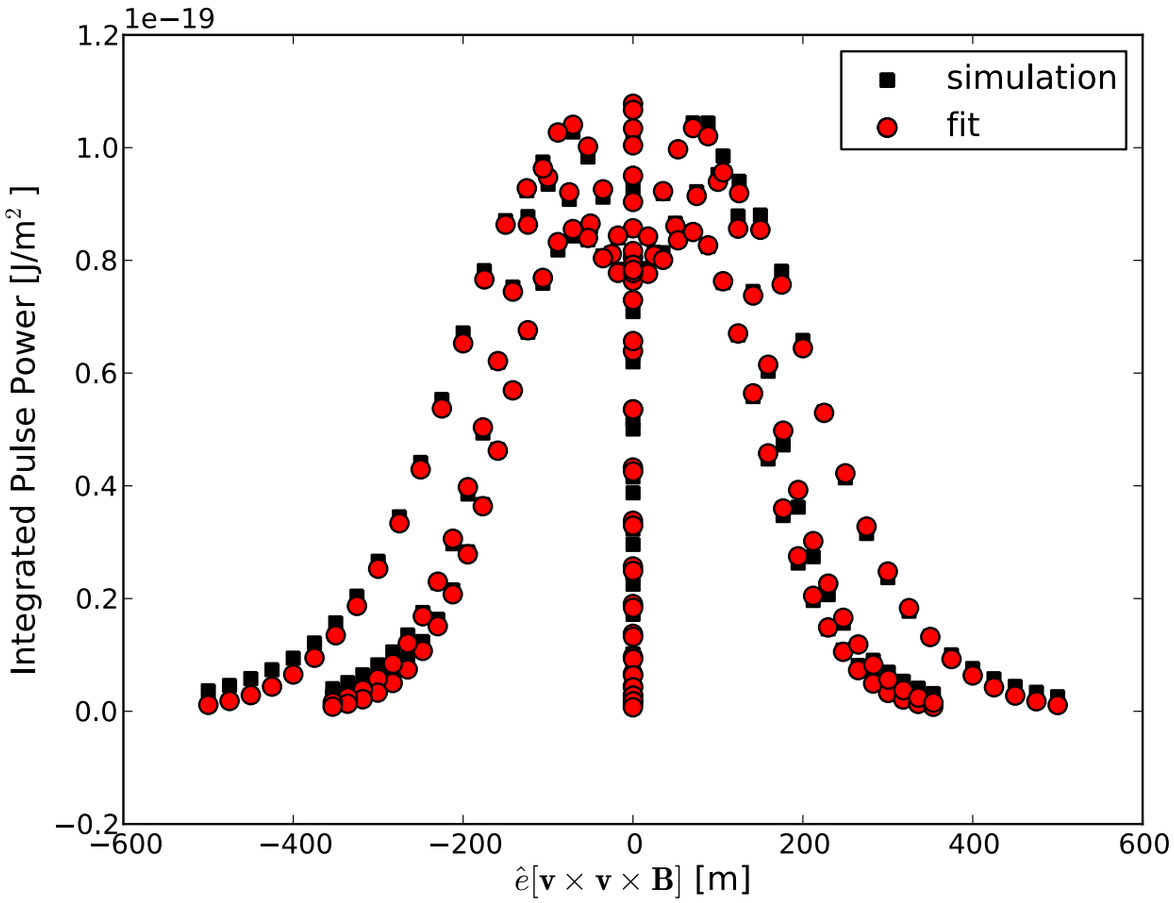

v x B

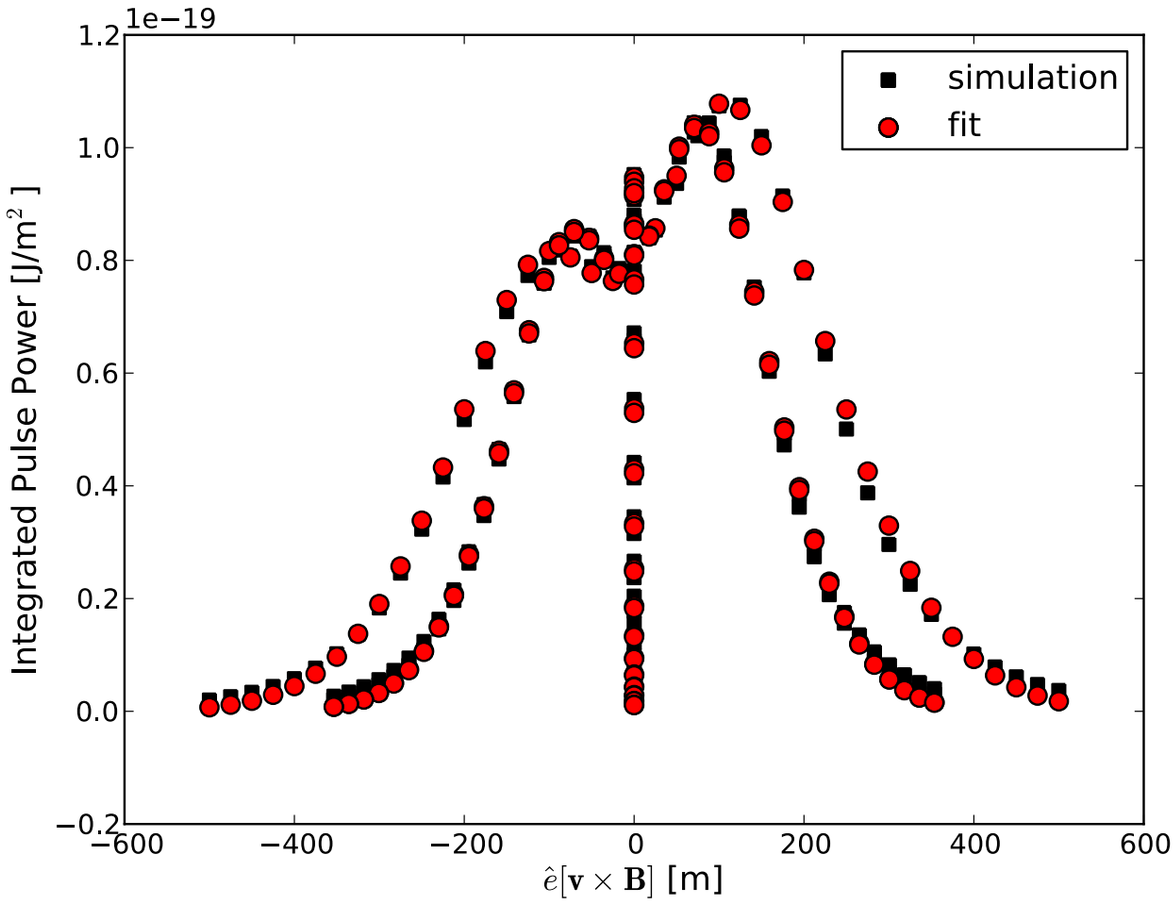

$$P(x', y') = A_+ \cdot \exp\left(\frac{-[(x' - X_+)^2 + (y' - Y_+)^2]}{\sigma_+^2}\right) - A_- \cdot \exp\left(\frac{-[(x' - X_-)^2 + (y' - Y_-)^2]}{\sigma_-^2}\right) + O$$

A. Nelles et al., Astropart. Phys. 60 (2015) 13

LBA 10-90 MHz

Simulations & Measurements

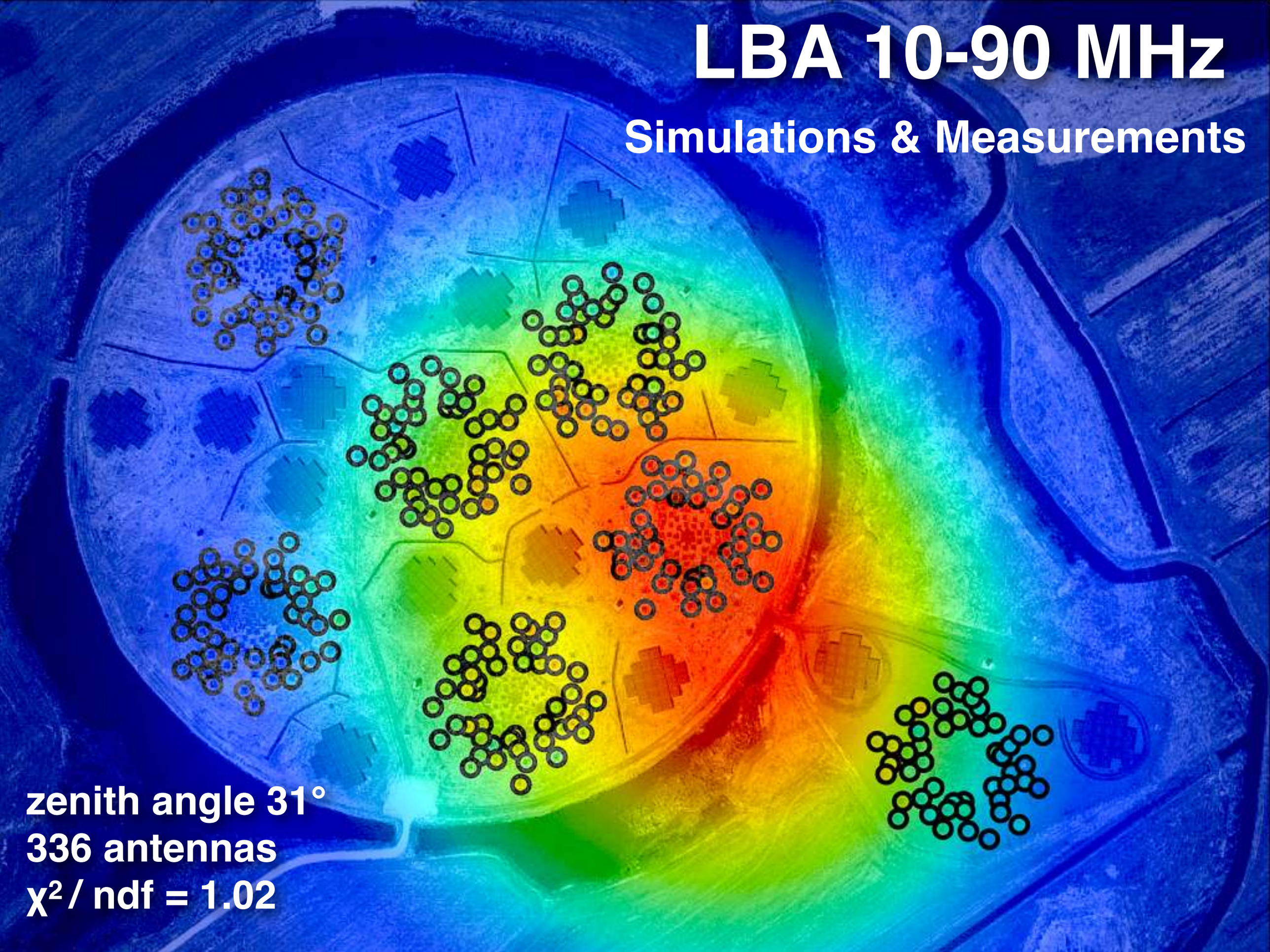

zenith angle 31°
336 antennas
χ^2 / ndf = 1.02

HBA 110-240 MHz

Simulations & Measurements

A. Nelles et al., Astroparticle Physics 65 (2015) 11

Relativistic time compression gives a Cherenkov ring

Measuring Cherenkov Rings

110 - 190 MHz

- **LOFAR is the only dedicated experiment with high-band antennas**
- **higher frequency-range: dominance of relativistic time-compression**
- **signals expected to be on a ring of emission**
- **first experiment to observe these in single showers**

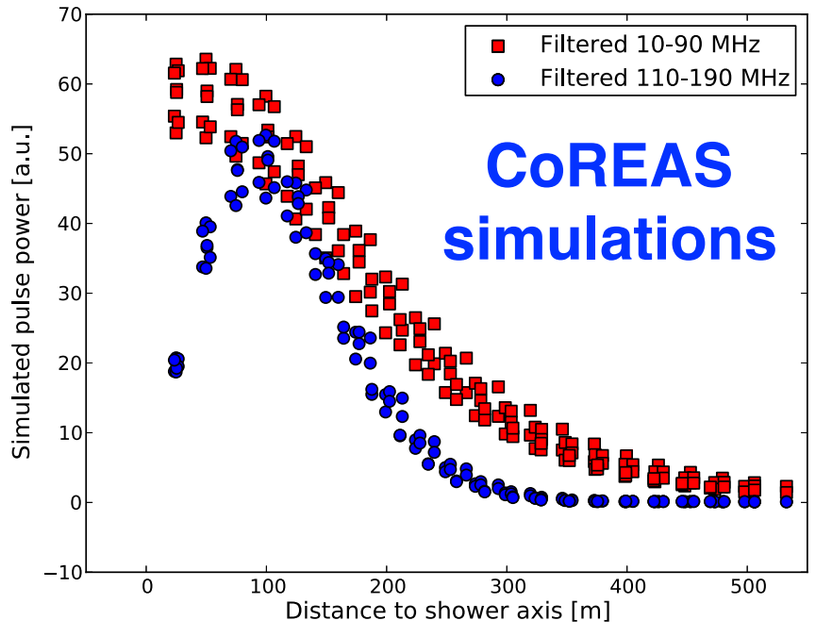

A. Nelles et al., Astroparticle Physics 65 (2015) 11

Measuring Cherenkov Rings

110 - 190 MHz

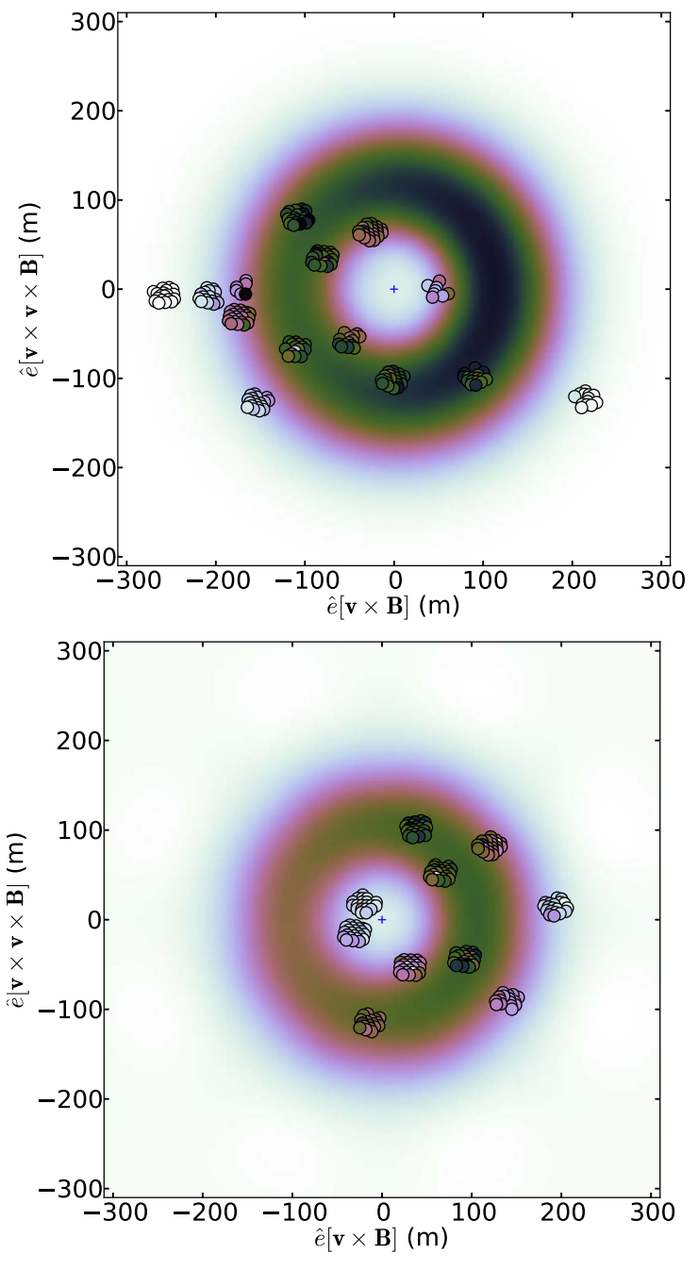

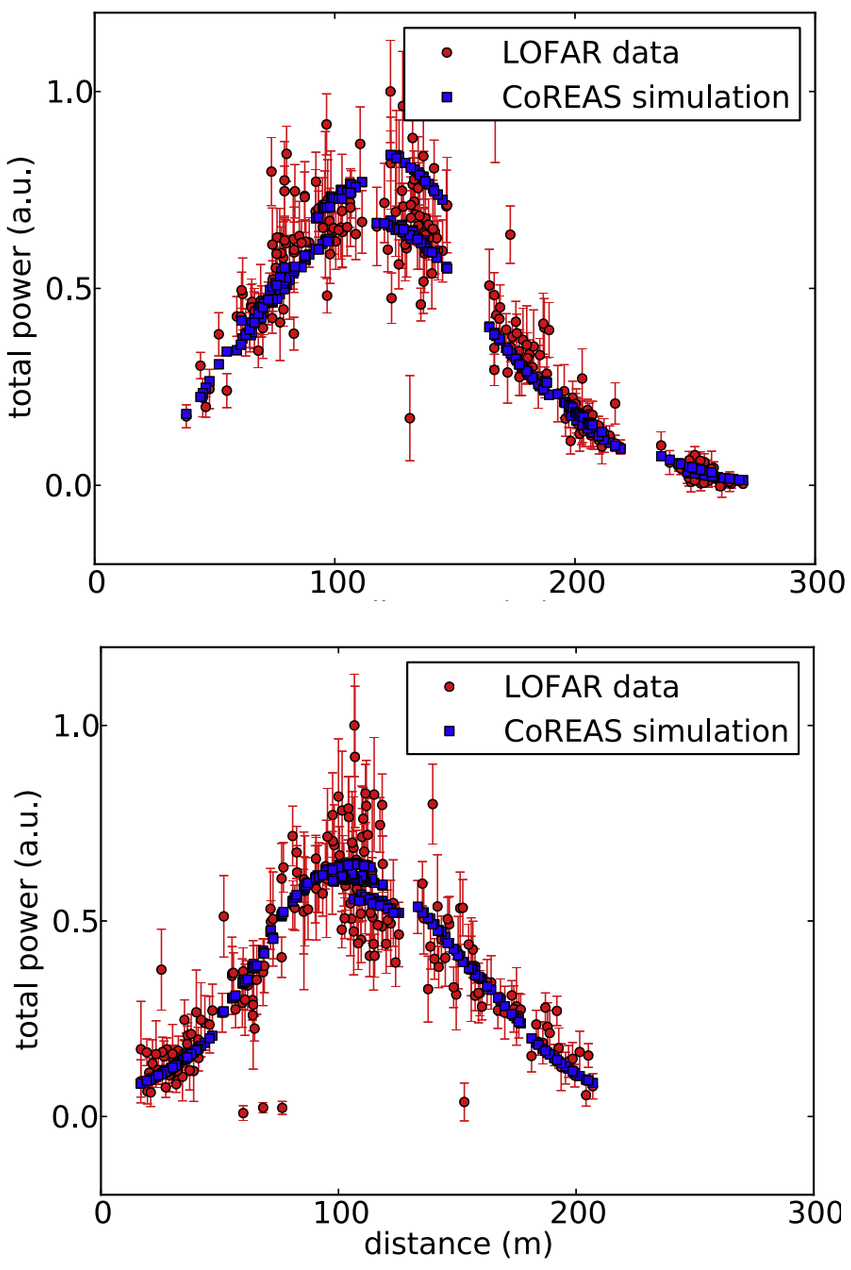

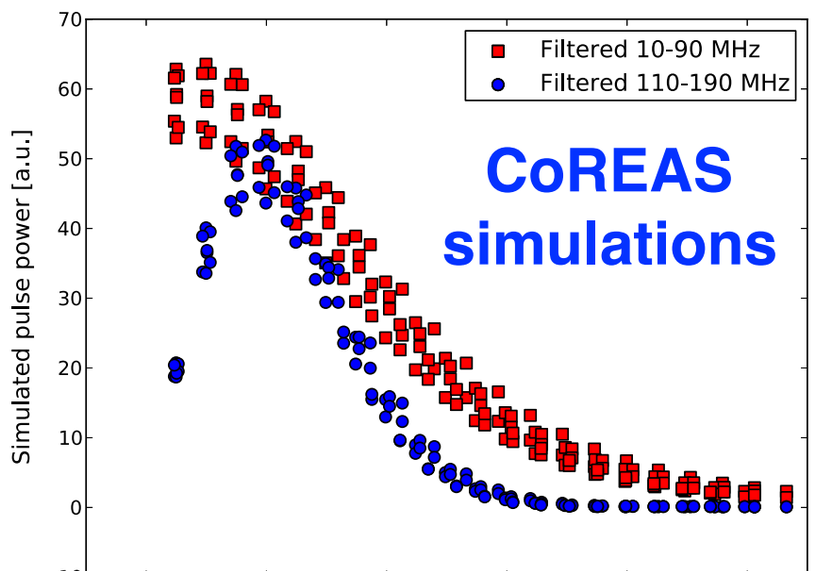

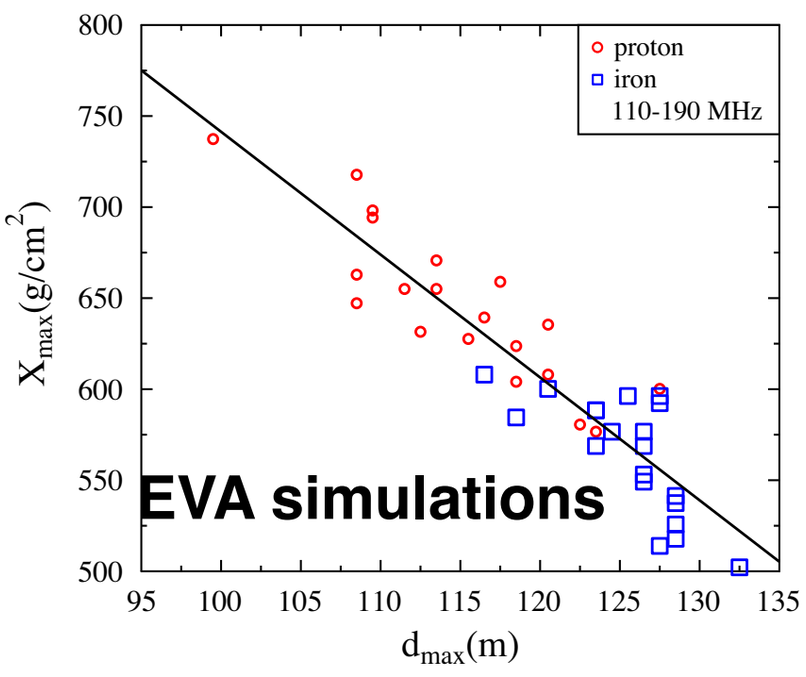

ring size sensitive to Xmax

A. Nelles et al., Astroparticle Physics 65 (2015) 11

Effect of refractive index

emission angle

$$\cos\alpha = \frac{1}{\beta n}, \quad \alpha \approx \sqrt{2\,\beta\,(n-1)},$$

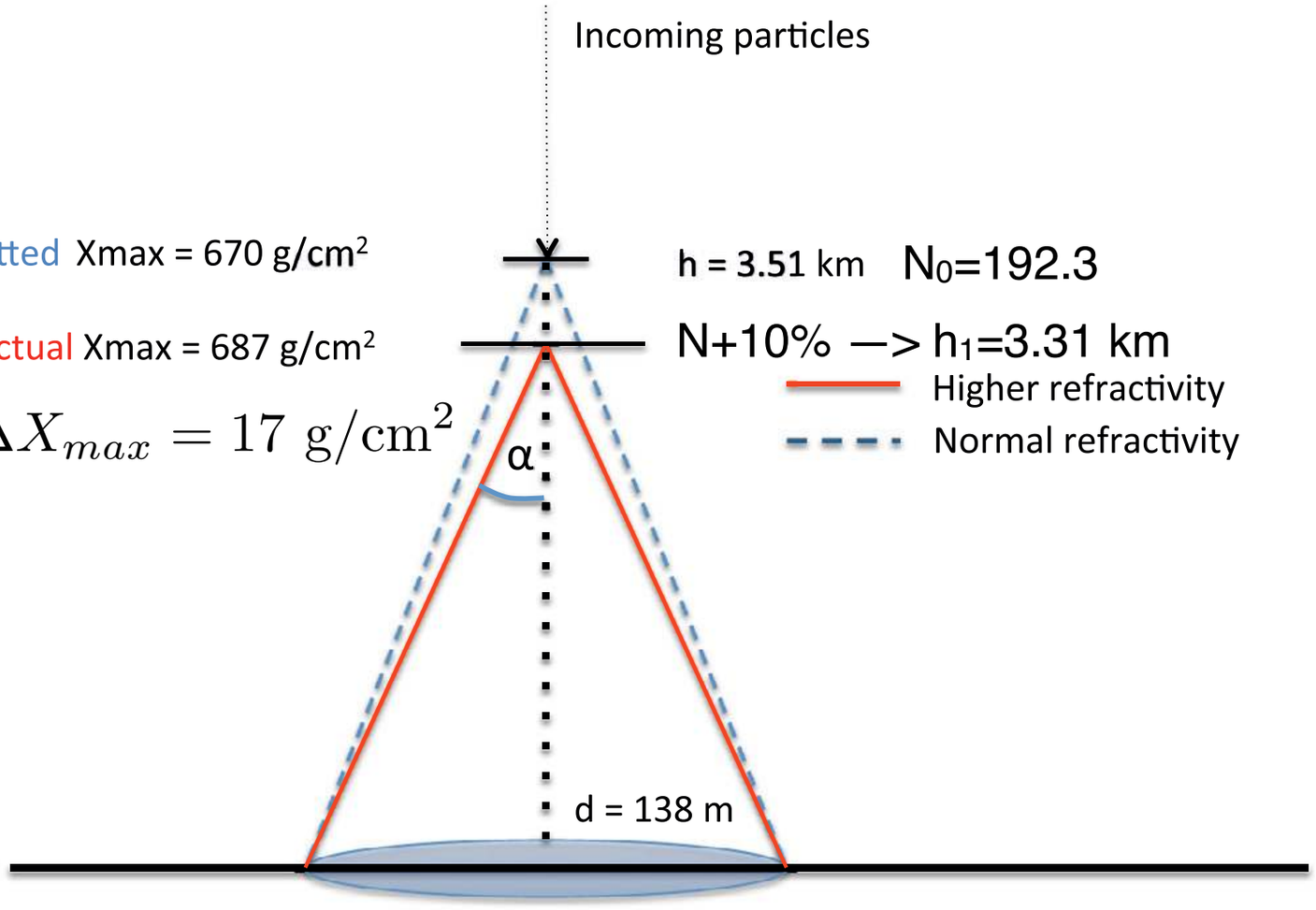

Fig. 1. Schematic picture (stretched horizontally) of the effect of a higher refractivity on the estimate of $X_{\max}$. This model uses the Cherenkov angle α, and the fact that the radio emission is maximal around $X_{\max}$. (For interpretation of the references to colour in this figure legend, the reader is referred to the web version of this article.)

depth of shower maximum [g/cm2]

$$X_{\max} \equiv X(h_0) = \frac{1}{\cos\theta}\int_{h_0}^{\infty} \rho(h)\,\mathrm{d}h,$$

column density [g/cm2]

$$X(h_0) = \frac{10}{g}\,\frac{p(h_0)}{\cos\theta},$$

g **gravitational acceleration**

refractivity

$$N = 10^6\,(n-1)$$

impact on Xmax measurement

$$\sqrt{N_1/N_0}\,h_1\,\alpha(h_1) = h_0\,\alpha(h_0),$$

$$\Rightarrow h_1 = h_0\,\frac{\alpha(h_0)}{\alpha(h_1)}\sqrt{\frac{N_0}{N_1}}$$

A. Corstanje et al., Astroparticle Physics 89 (2017) 23

Implementation of GDAS to CORSIKA/CoREAS

New program(python):
Gdastool
(inputs:UTCtimestamp,coordinates etc)

creates

File: Atmosphere.dat

Atmosphere layer definitions | Tabulated RI

reads

CORSIKA:
New: option in input file:

ATMF: atmosphere.dat

calls

CoREAS:
Replaces on-the-fly calculation of RI with look up table

Implementation of GDAS to CORSIKA/CoREAS

New program(python):
Gdastool
(inputs:UTCtimestamp,coordinates etc)

creates

File: Atmosphere.dat

Atmosphere layer definitions | Tabulated RI

reads

Released in CORSIKA v-76300

Calibration

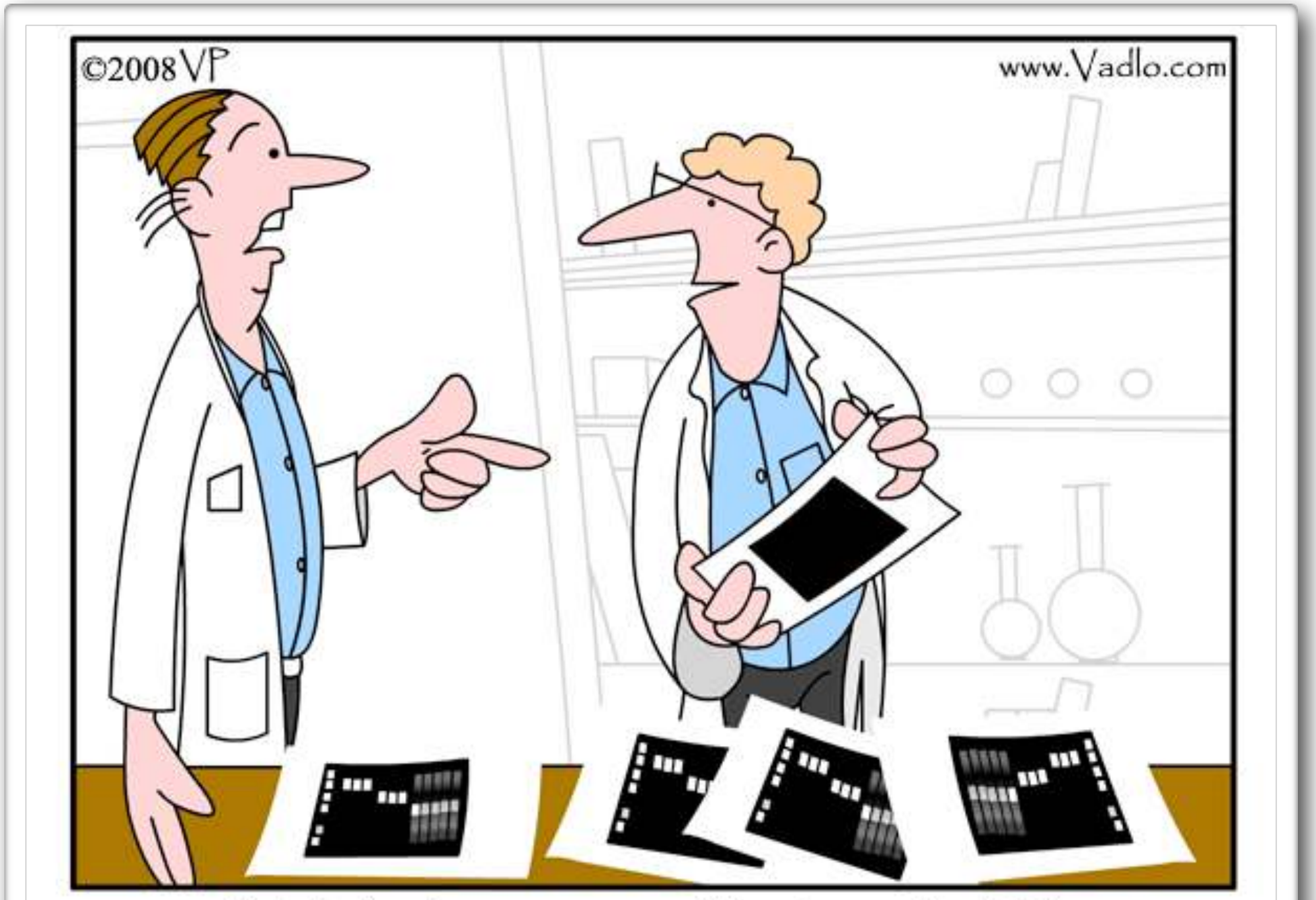

Data don't make any sense, we will have to resort to ***statistics****.*

LOFAR LBA Calibration

measured signal recorded in ADC counts (P_m)

voltage received at the antenna (P_e)

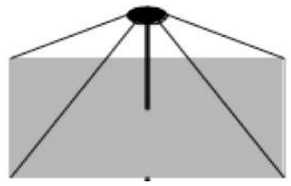

2 independent methods

Nelles, A. et al. 2015,Journal of Instrumentation, 10, P11005

1. Reference Source

+ Angular response
- Relies on conflicting manufacturer data sheets
- Not easily repeatable

2. Galactic Emission

- Average over whole sky
+ Can be done anytime
- Large error bars due to electronic noise

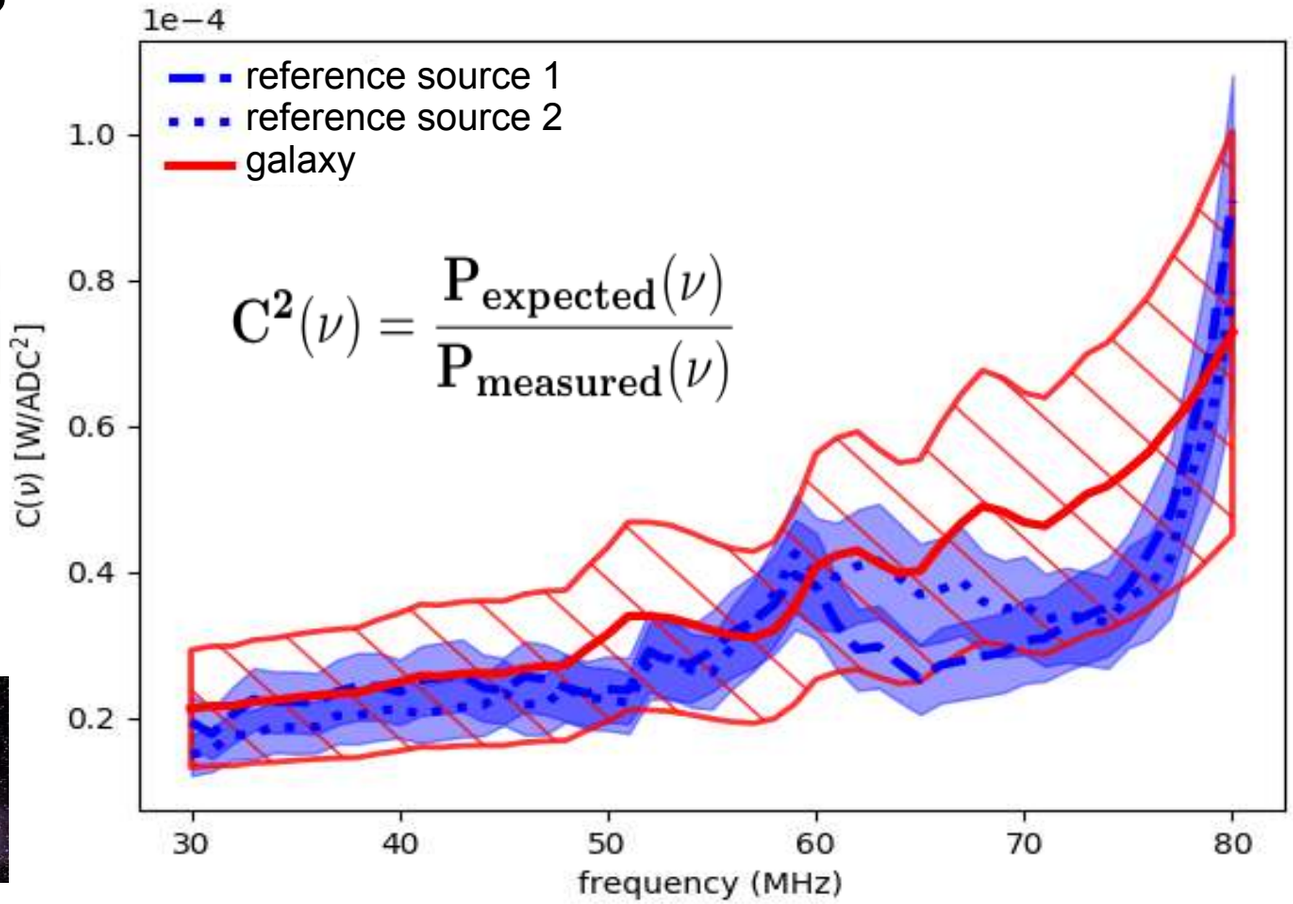

1

Galactic Calibration

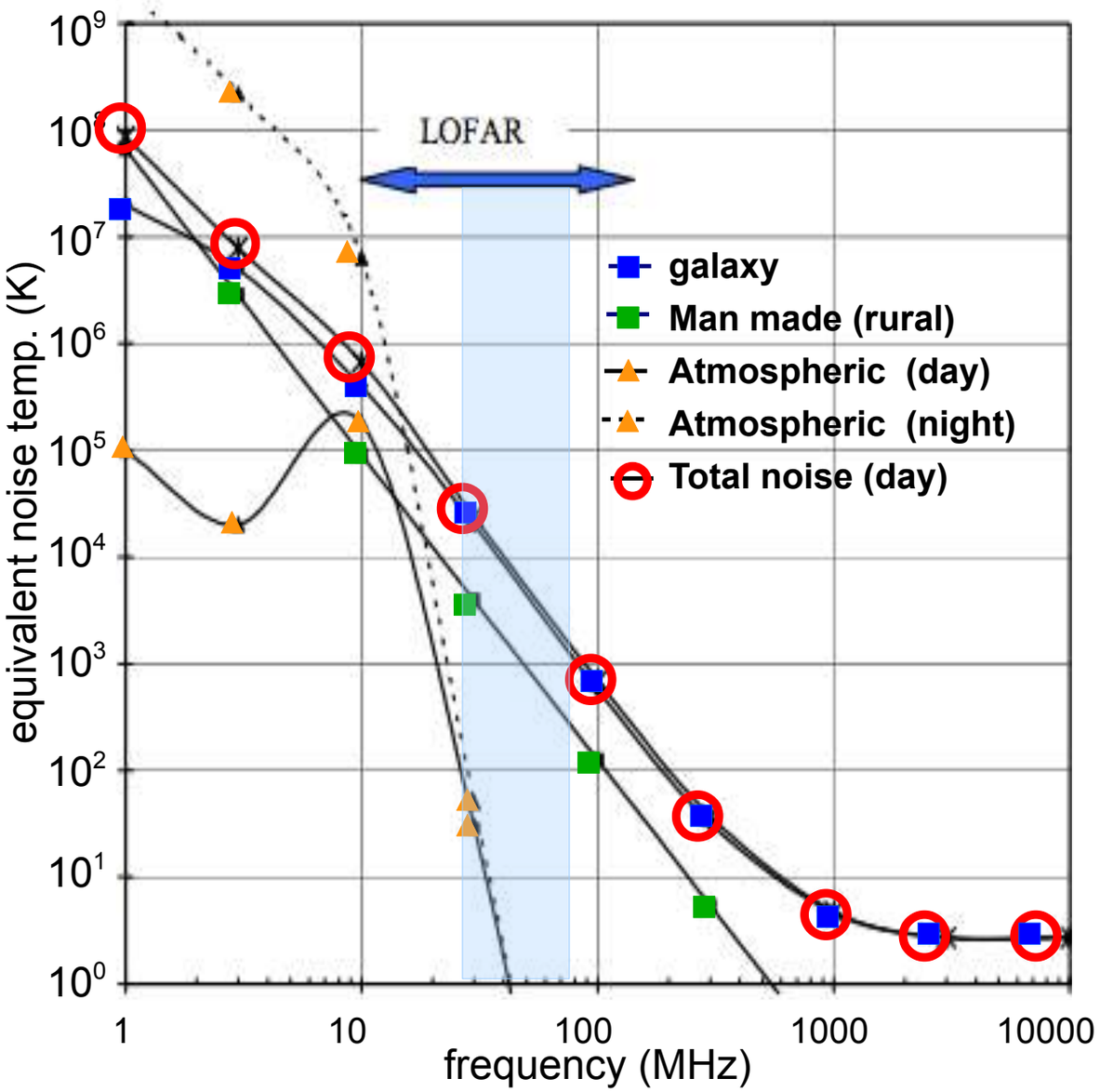

$$C^2(\nu) = \frac{P_{sky+elec.noise}(\nu)}{P_{measured}(\nu)}$$

- Galaxy noise is primary external source of noise in LBA frequency range

  Galaxy noise + electronic noise = recorded signal

- **Lfmap** software provides frequency dependent galactic noise temperature

$$T_{sky}(\nu, \alpha, \delta) = T_{CMB} + T_{Iso}(\nu) + T_{gal}(\nu, \alpha, \delta)$$

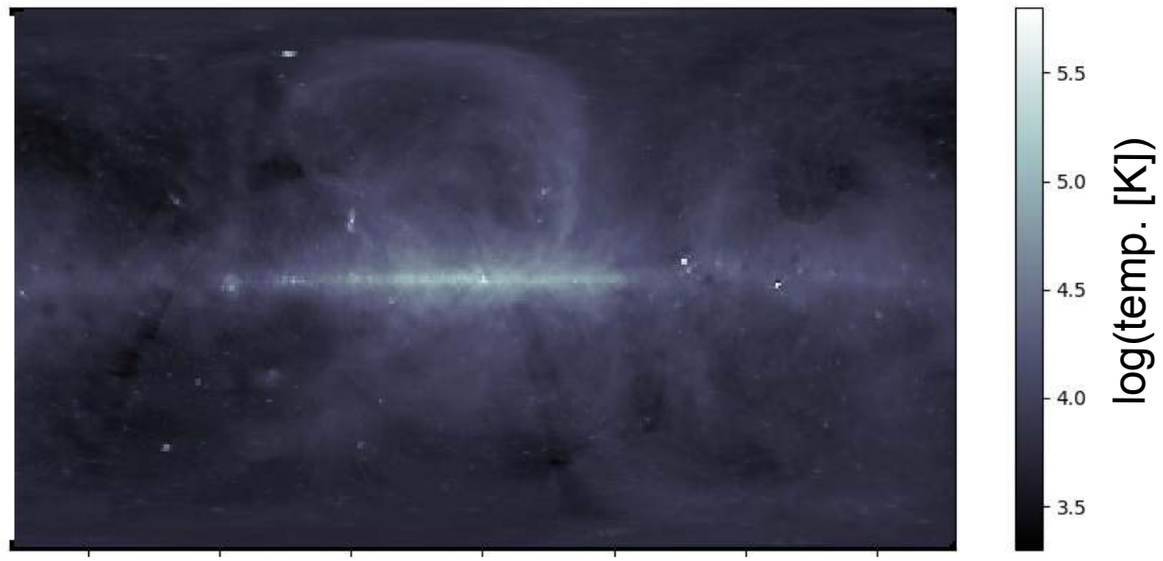

E. Polisensky, LFmap: A Low Frequency Sky Map Generating Program. , Long Wavelength Array (LWA) Memo Series 111 (2007).

3

K. Mulrey, ARENA 2018

Simulating Galaxy Noise

LOFAR

Visible galaxy at 00.00,6:00,12:00,18:00 Local Sidereal Time

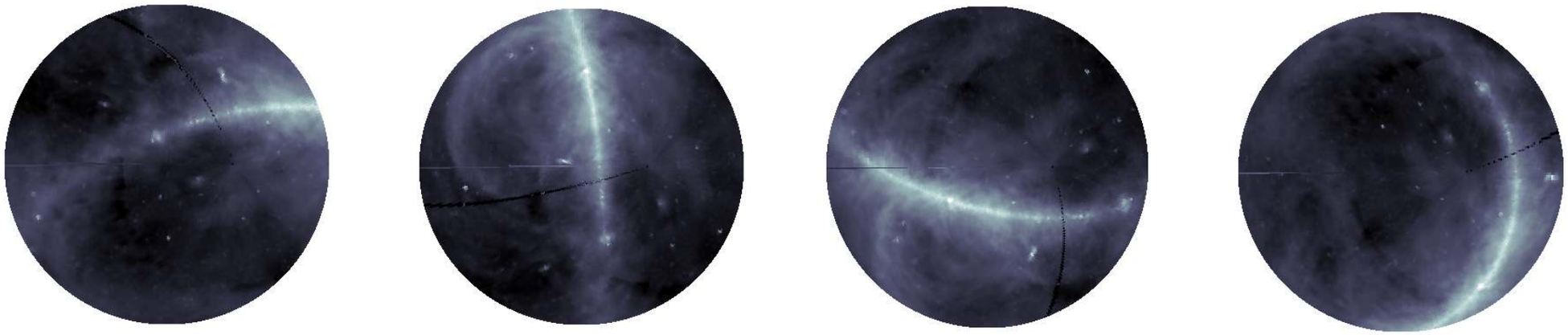

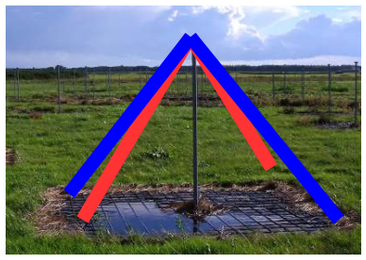

$$\mathbf{P}(\nu) = \frac{\mathbf{2k_B}}{\mathbf{c^2}}\nu^2 \int \mathbf{T_{sky}}(\nu,\theta,\phi)\frac{|\vec{\mathbf{H}}(\nu,\theta,\phi)|^2\mathbf{Z_0}}{\mathbf{2Z_a}}\mathbf{d\Omega} \quad \mathbf{WHz^{-1}}$$

Average antenna response at 55 MHz

$$< |\vec{\mathbf{H}}(\nu,\theta,\phi)|^2 >$$

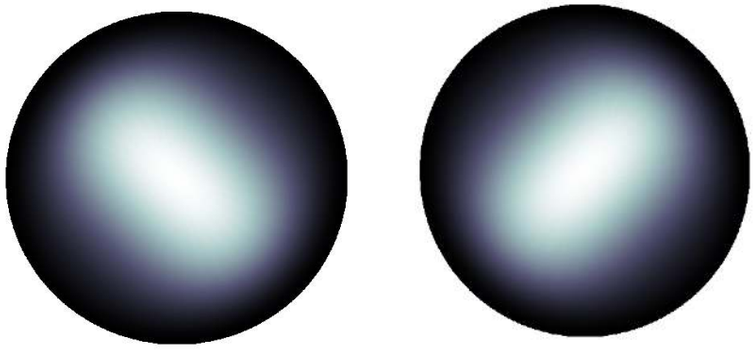

pol 0 pol 1

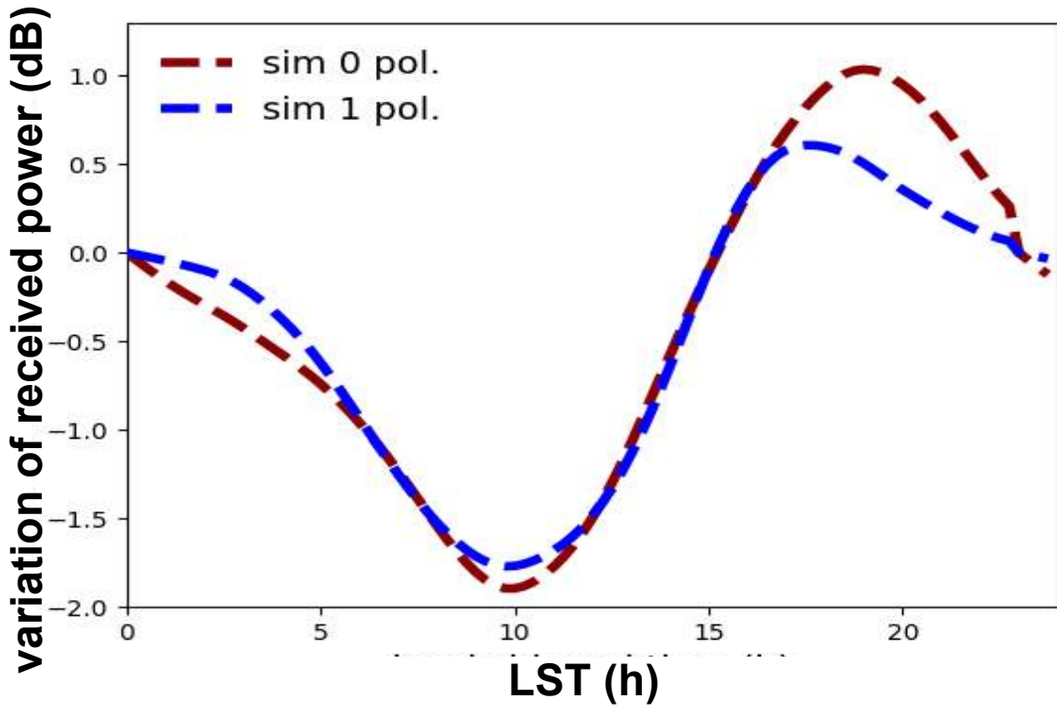

LOFAR Signal Chain

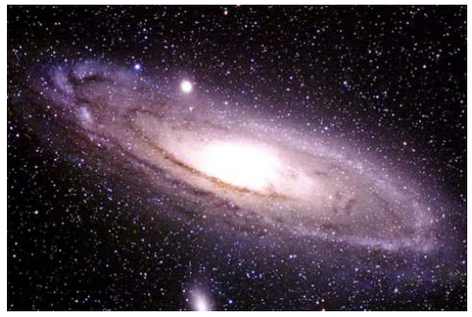

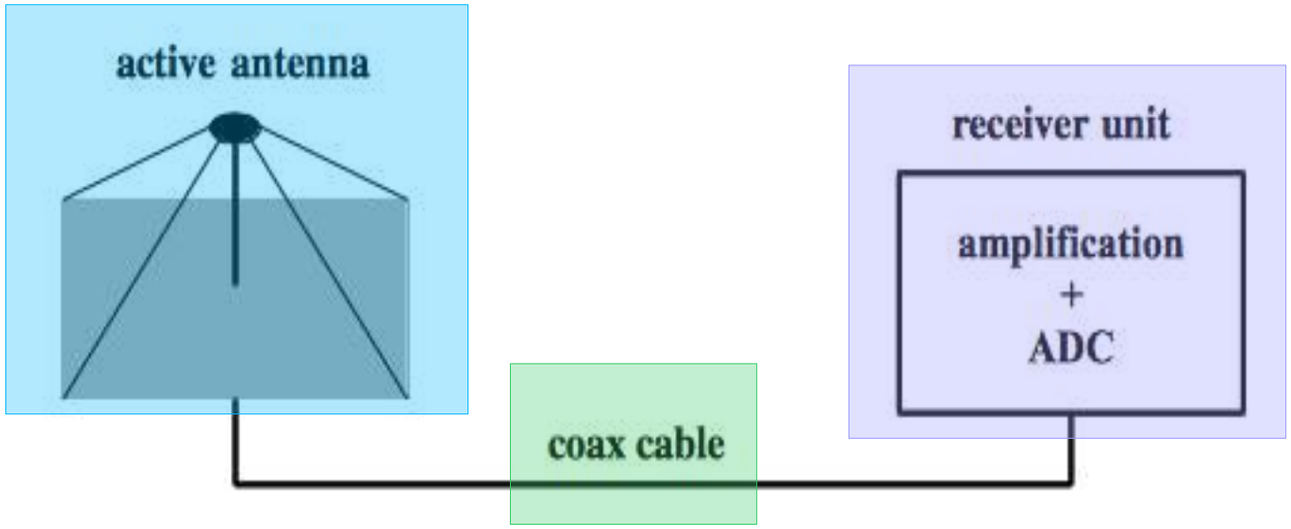

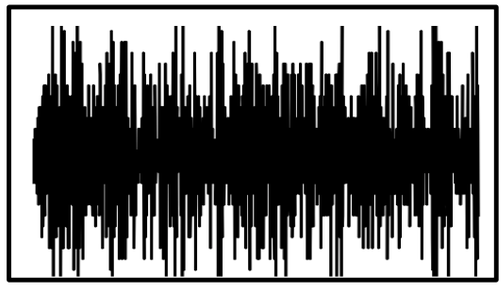

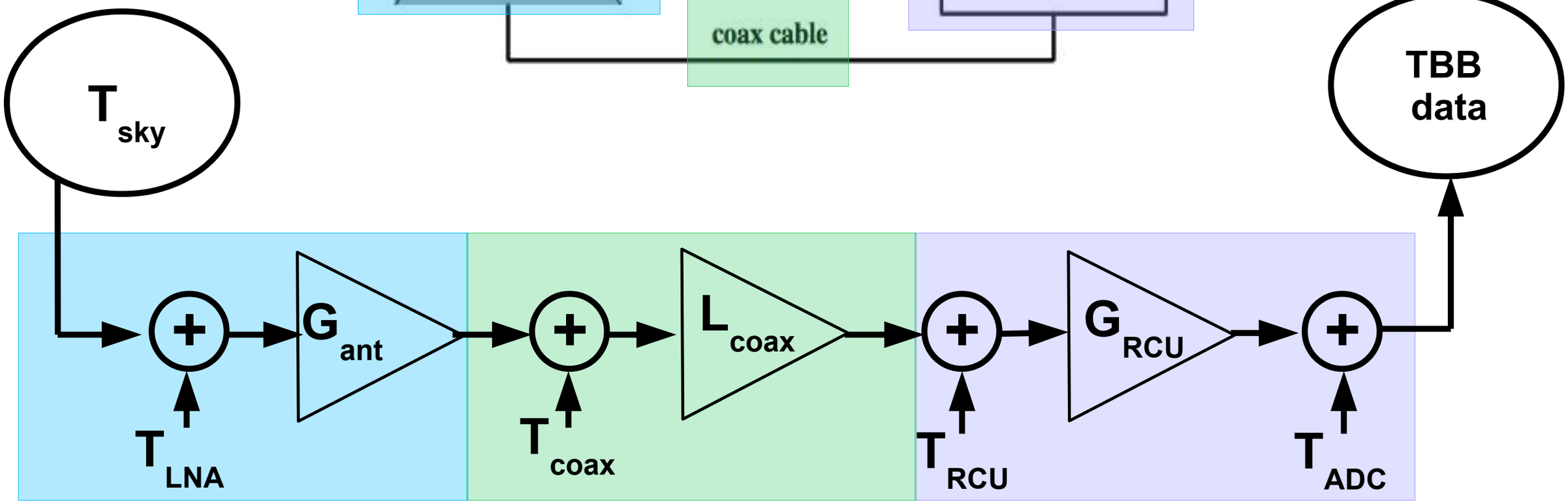

G_{ant} , L_{coax}, G_{RCU} → Freq. Dependent losses and gains

T_{LNA} , T_{coax} , T_{RCU} , T_{ADC} → Constant noise values

7

LOFAR Signal Chain

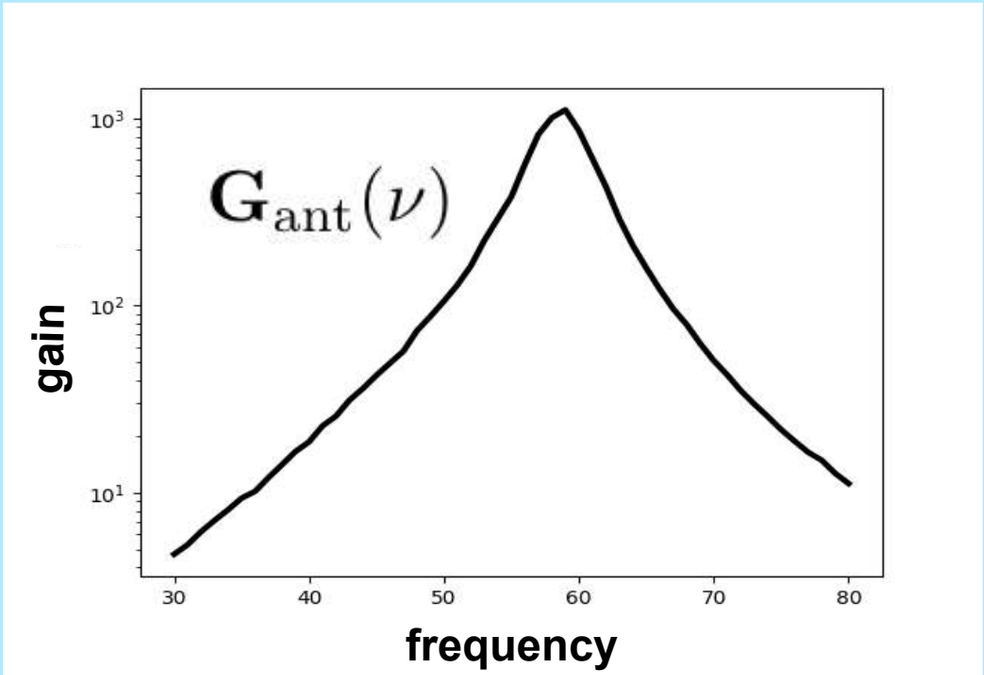

$$\left(\mathbf{P}_{\mathrm{sky}}(\nu, \mathbf{t}) + \mathbf{T}_{\mathrm{LNA}}\right)\mathbf{G}_{\mathrm{ant}}(\nu)\mathbf{A}(\nu)$$

$\mathbf{G}_{\mathrm{ant}}(\nu)$ Antenna gain, simulated with WIPL-D software, with known misaligned resonance frequency

$\mathbf{A}(\nu)$ correction to antenna model

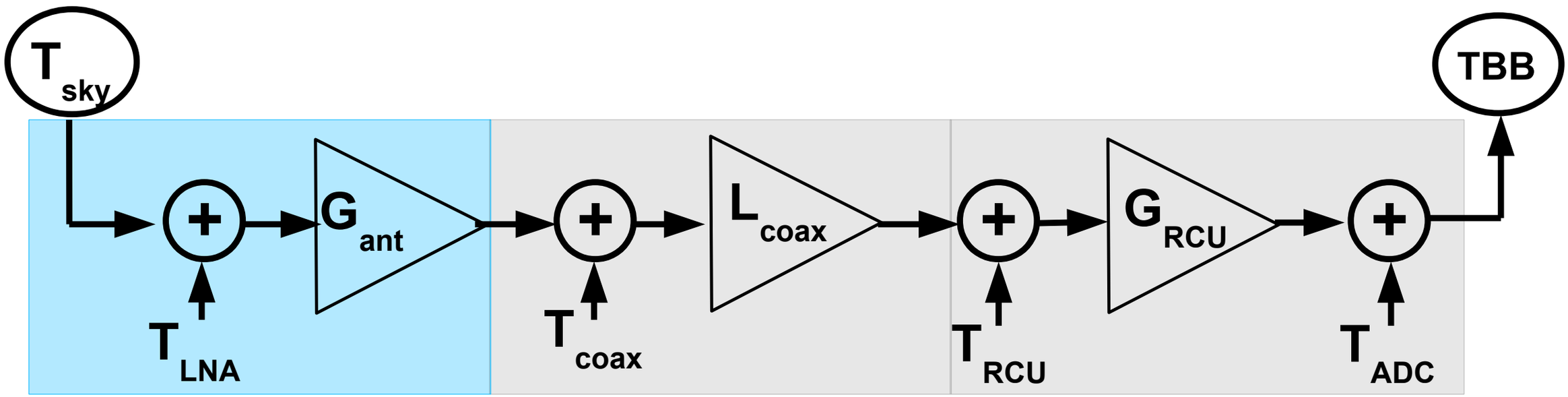

LOFAR Signal Chain

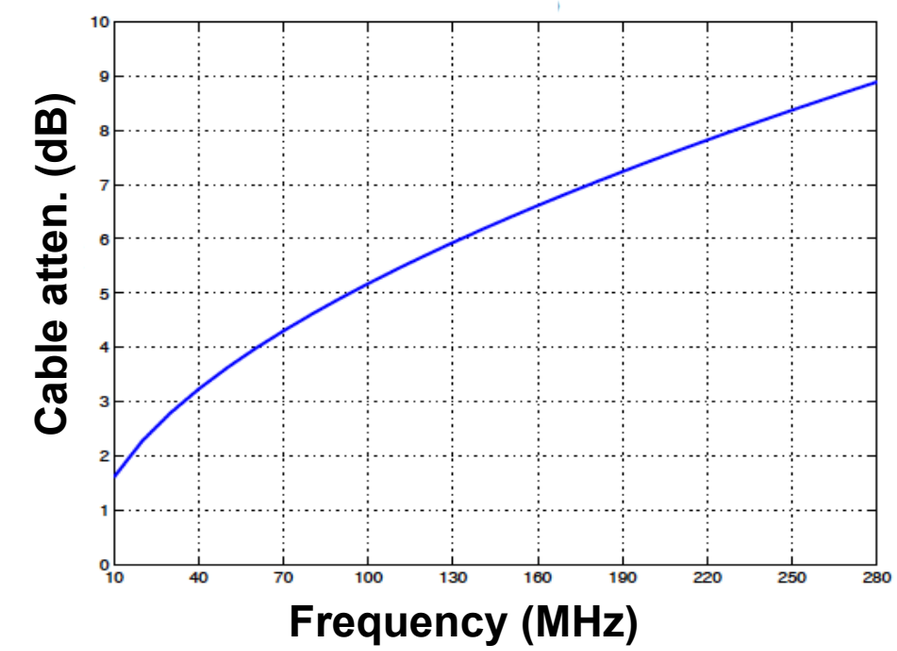

$$\left(\mathbf{P}_{\mathrm{sky}}(\nu,\mathbf{t})+\mathbf{T}_{\mathrm{LNA}}\right)\mathbf{G}_{\mathrm{ant}}(\nu)\mathbf{A}(\nu)\mathbf{L}_{\mathrm{coax}}(\nu)$$

$\mathbf{L}_{\mathrm{coax}}(\nu)$ Cable attenuation (50m, 80m ,115m)

$$\mathbf{T_{coax}} << \mathbf{T_{LNA}}, \mathbf{T_{RCU}}, \mathbf{T_{ADC}}$$

(not included in model)

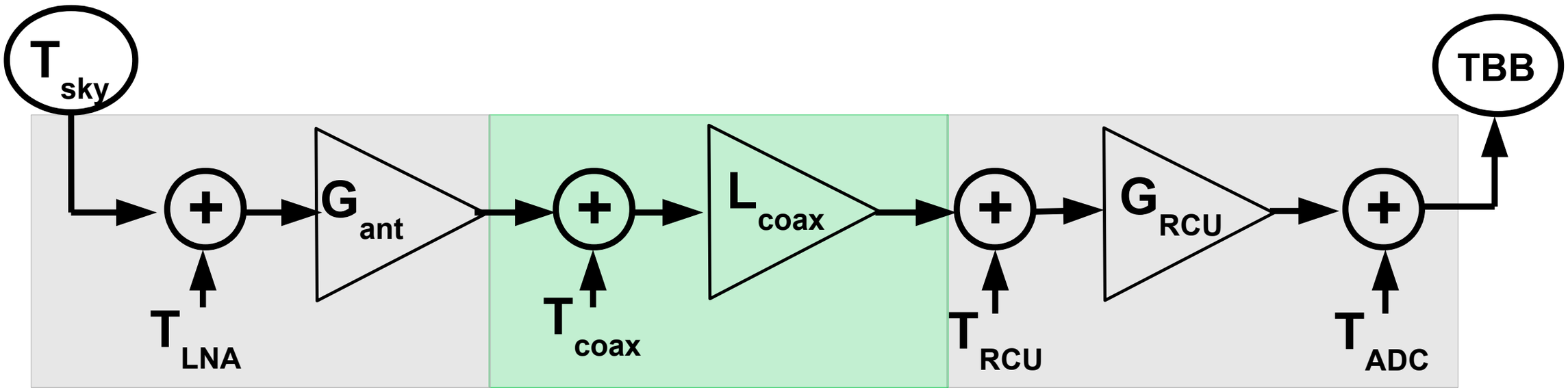

9

LOFAR Signal Chain

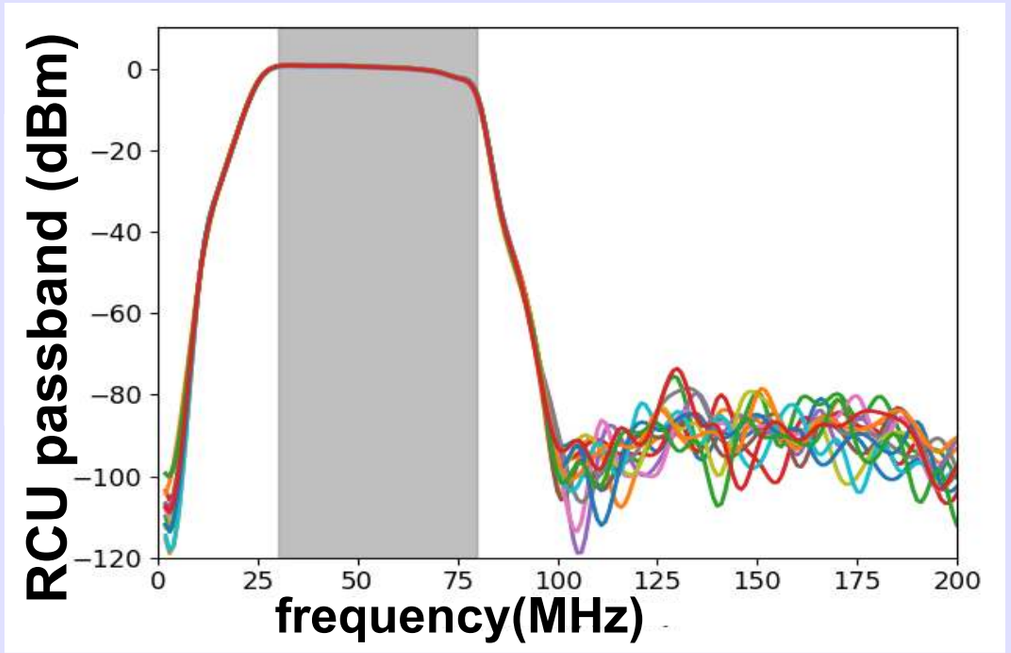

$\mathbf{T_{RCU}}$ Noise from amplification in RCU

$\mathbf{G_{RCU}}(\nu)$ RCU passband filter

$\mathbf{S}$ scale factor between voltage and ADC units

$\mathbf{T_{ADC}}$ time jitter noise from digitization

$$\left(\left(\mathbf{P}_{\mathrm{sky}}(\nu,\mathrm{t})+\mathbf{T}_{\mathrm{LNA}}\right)\mathbf{G}_{\mathrm{ant}}(\nu)\mathbf{A}(\nu)\mathbf{L}_{\mathrm{coax}}(\nu)+\mathbf{T_{RCU}}\right)\mathbf{G}_{\mathrm{RCU}}(\nu)\mathbf{S}+\mathbf{T}_{\mathrm{ADC}}=\mathbf{P}_{\mathrm{sim}}(\nu,\mathrm{t})$$

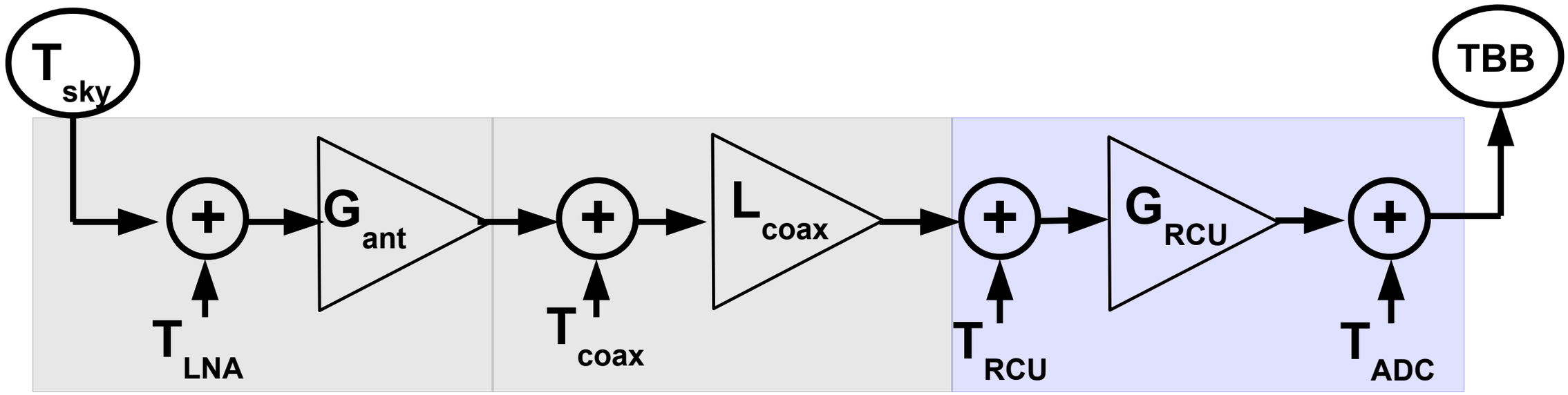

10

LOFAR Signal Chain

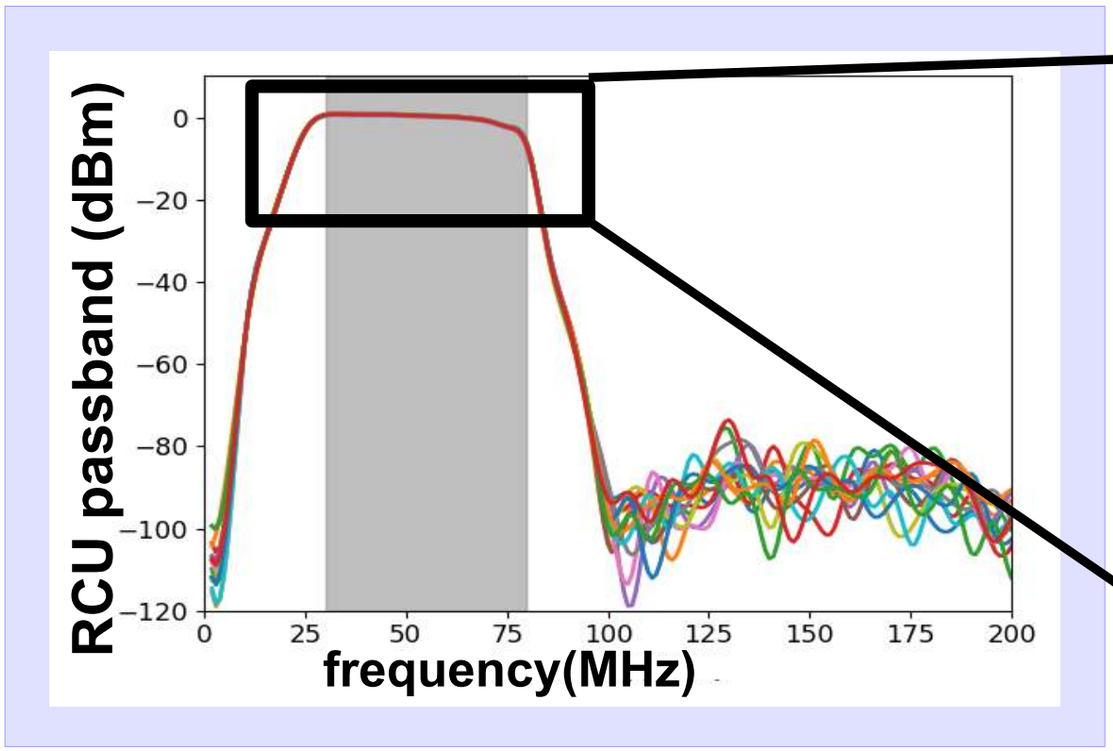

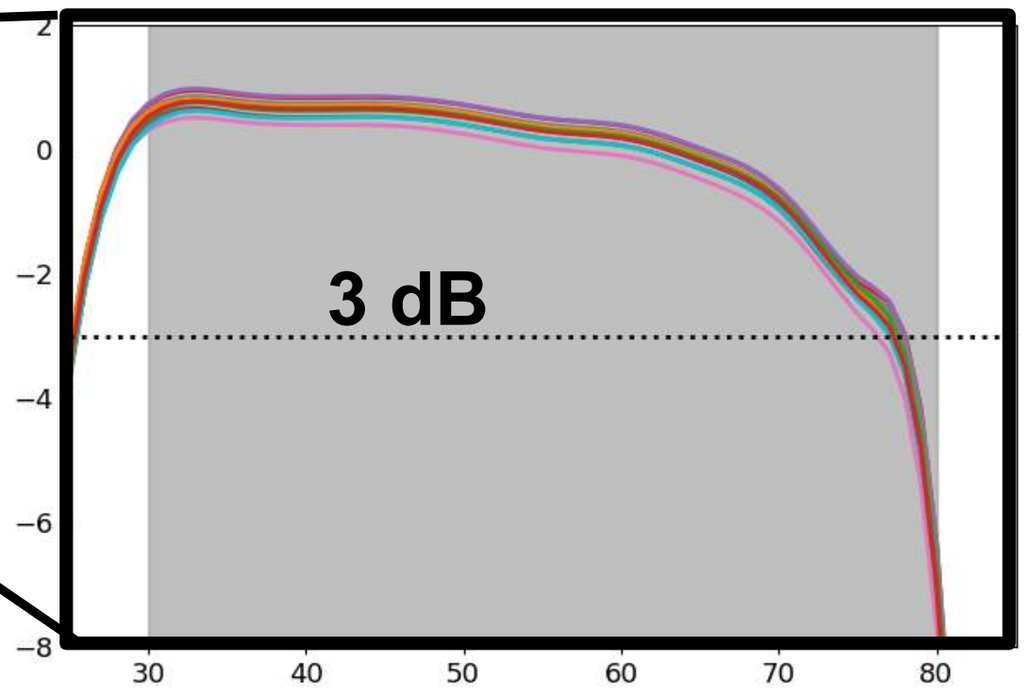

$$\left(\left(\mathbf{P}_{\mathrm{sky}}(\nu,\mathrm{t})+\mathbf{T}_{\mathrm{LNA}}\right)\mathbf{G}_{\mathrm{ant}}(\nu)\mathbf{A}(\nu)\mathbf{L}_{\mathrm{coax}}(\nu)+\mathbf{T}_{\mathbf{RCU}}\right)\mathbf{G}_{\mathrm{RCU}}(\nu)\mathbf{S}+\mathbf{T}_{\mathrm{ADC}}=\mathbf{P}_{\mathrm{sim}}(\nu,\mathrm{t})$$

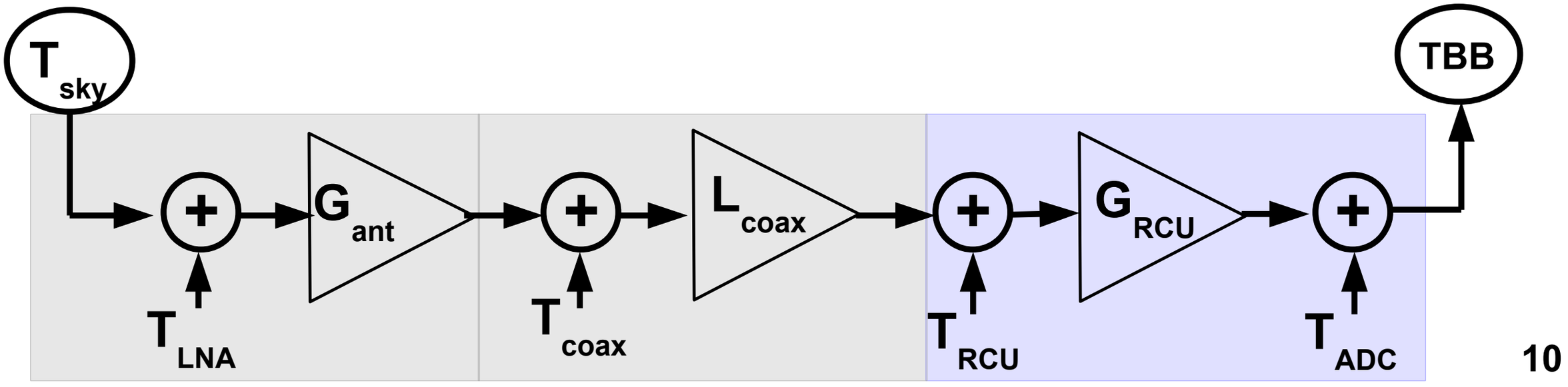

10

Fitting for Electronic Noise

$$\left(\left(\mathbf{P}_{\rm sky}(\nu,\mathbf{t}) + \mathbf{T}_{\rm LNA}\right)\mathbf{G}_{\rm ant}(\nu)\mathbf{A}(\nu)\mathbf{L}_{\rm coax}(\nu) + \mathbf{T}_{\rm RCU}\right)\mathbf{G}_{\rm RCU}(\nu)\mathbf{S} + \mathbf{T}_{\rm ADC} = \mathbf{P}_{\rm sim}(\nu,\mathbf{t})$$

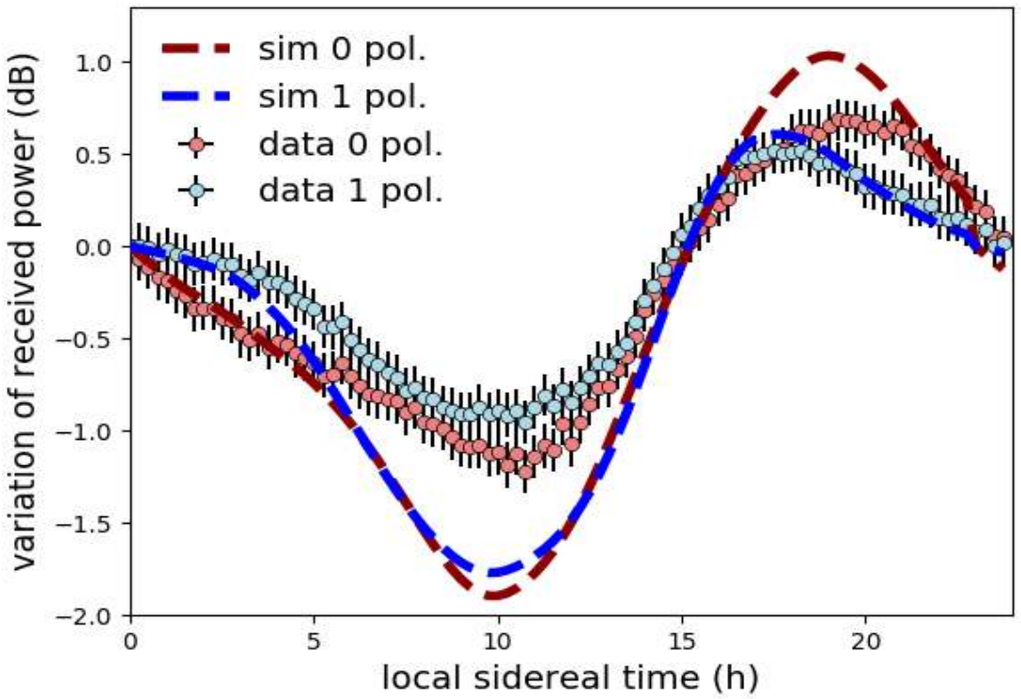

known, frequency dependent quantity

unknown, constant quantity

Fitted noise values at ADC

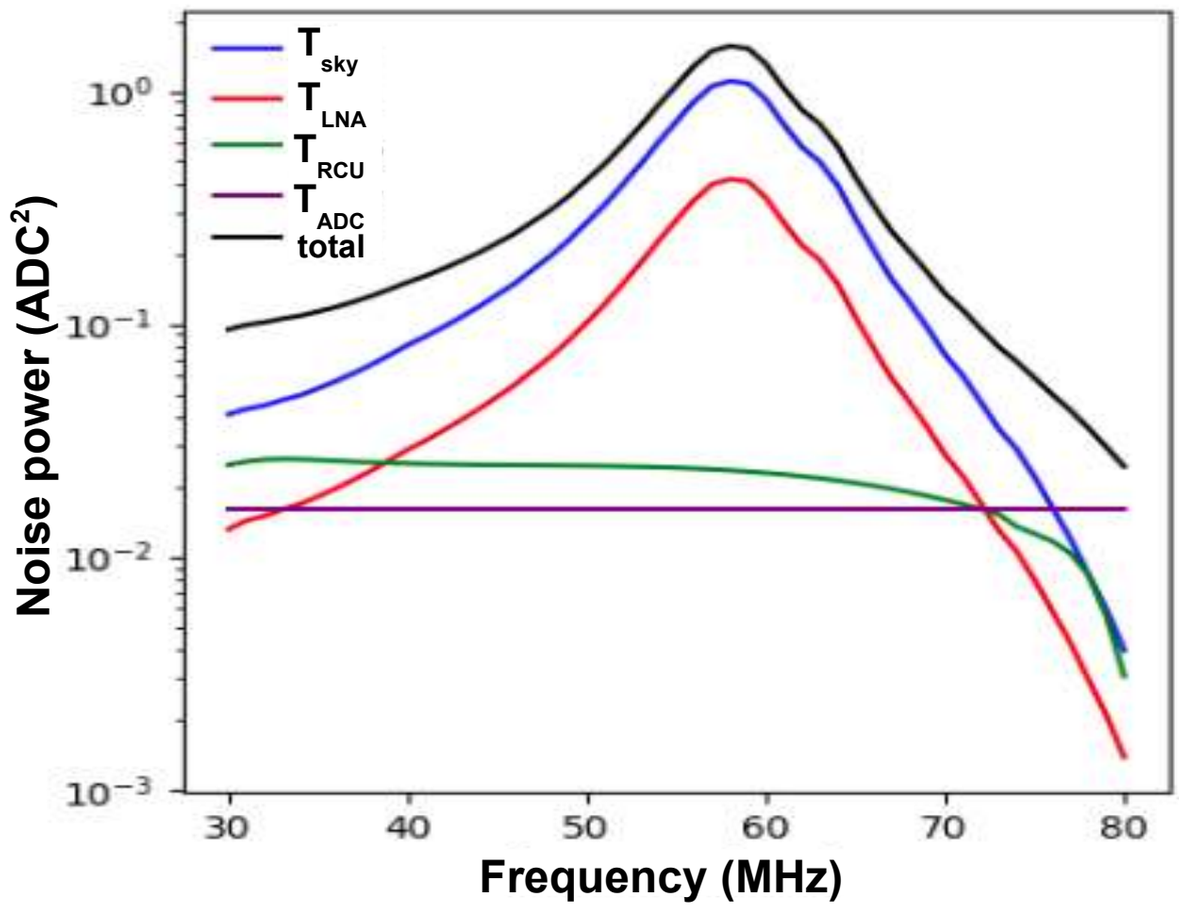

$$X^2 = \sum \frac{(\mathrm{P}(\nu,\mathrm{t})_{\rm data} - \mathrm{P}(\nu,\mathrm{t})_{\rm sim})^2}{\sigma(\nu,\mathrm{t})_{\rm data}}$$

★ All noise contributions are required to fit simulation to data at all frequencies

11

Calibration Results

$$\mathbf{C^2}(\nu) = \mathbf{A}(\nu)\mathbf{L}_{\mathrm{coax}}(\nu)\mathbf{G}_{\mathrm{RCU}}(\nu)\mathbf{S}$$

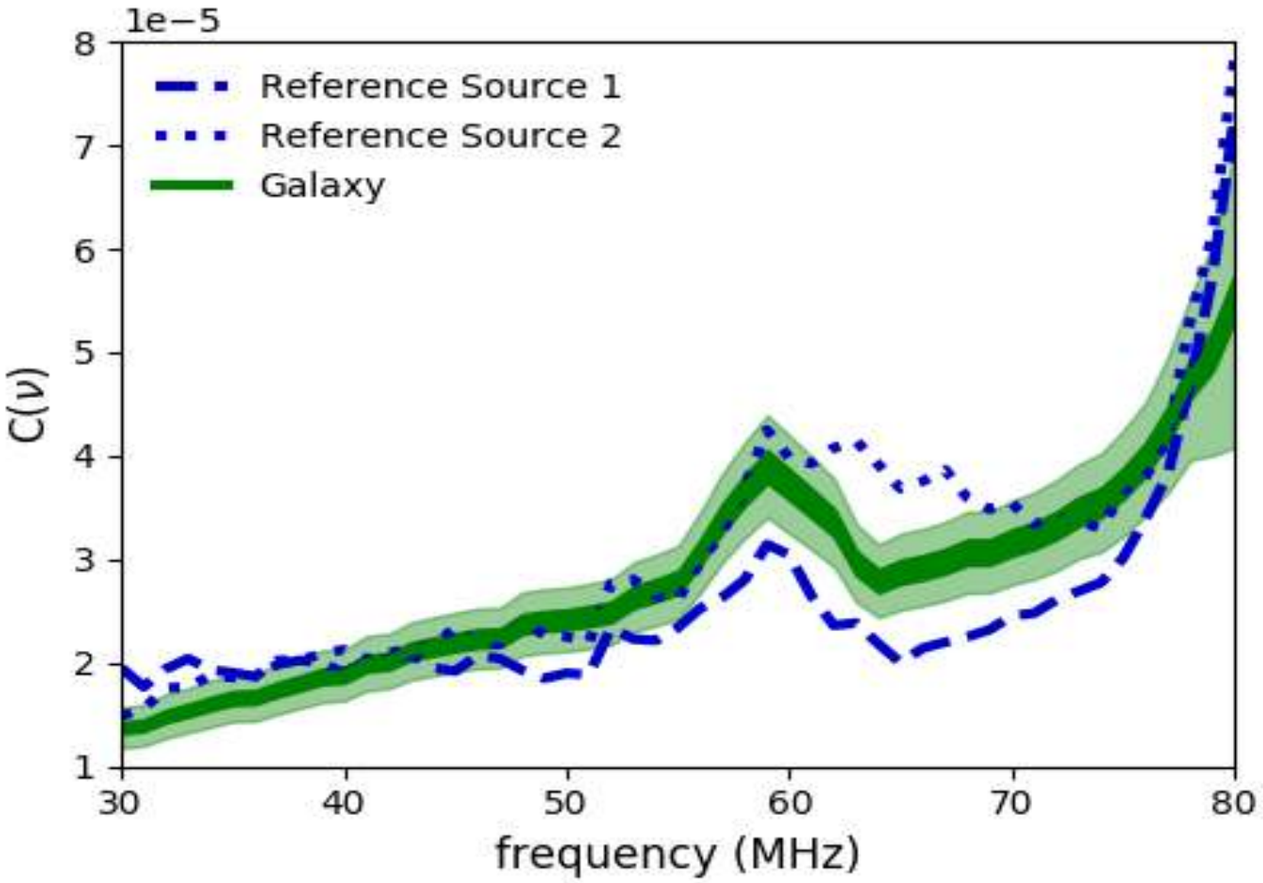

Uncertainty	Percentage
event-to-event fluctuation	4
galaxy model	12
electronic noise < 77 MHz	5-6
electronic noise > 77 MHz	10-20
total < 77 MHz	**14**

- Galaxy model now limits systematic uncertainties
- Uncertainties from electronic noise are found by comparing resulting calibration constants for different antennas

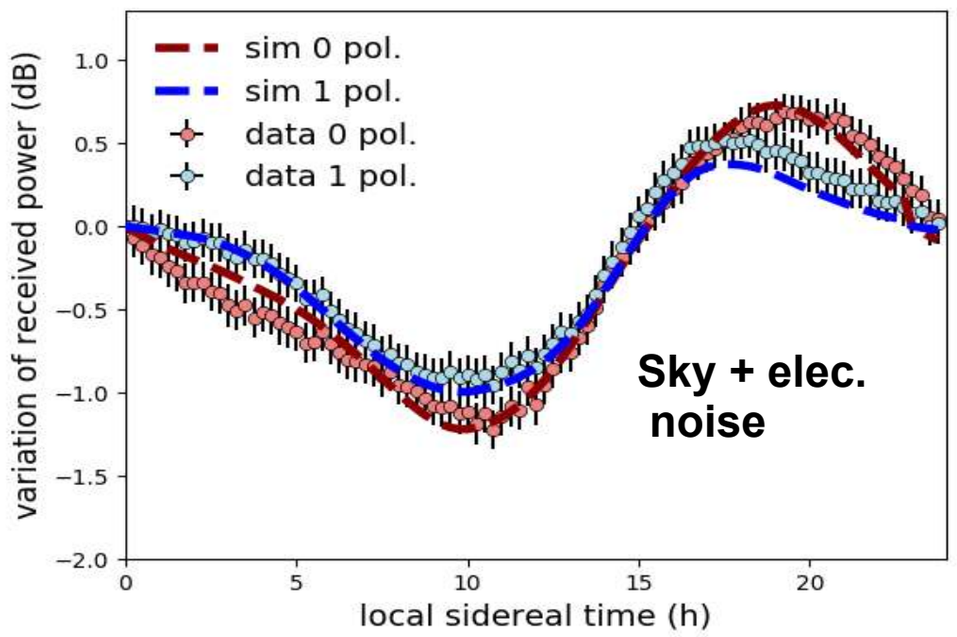

12

Comparison to CoREAS

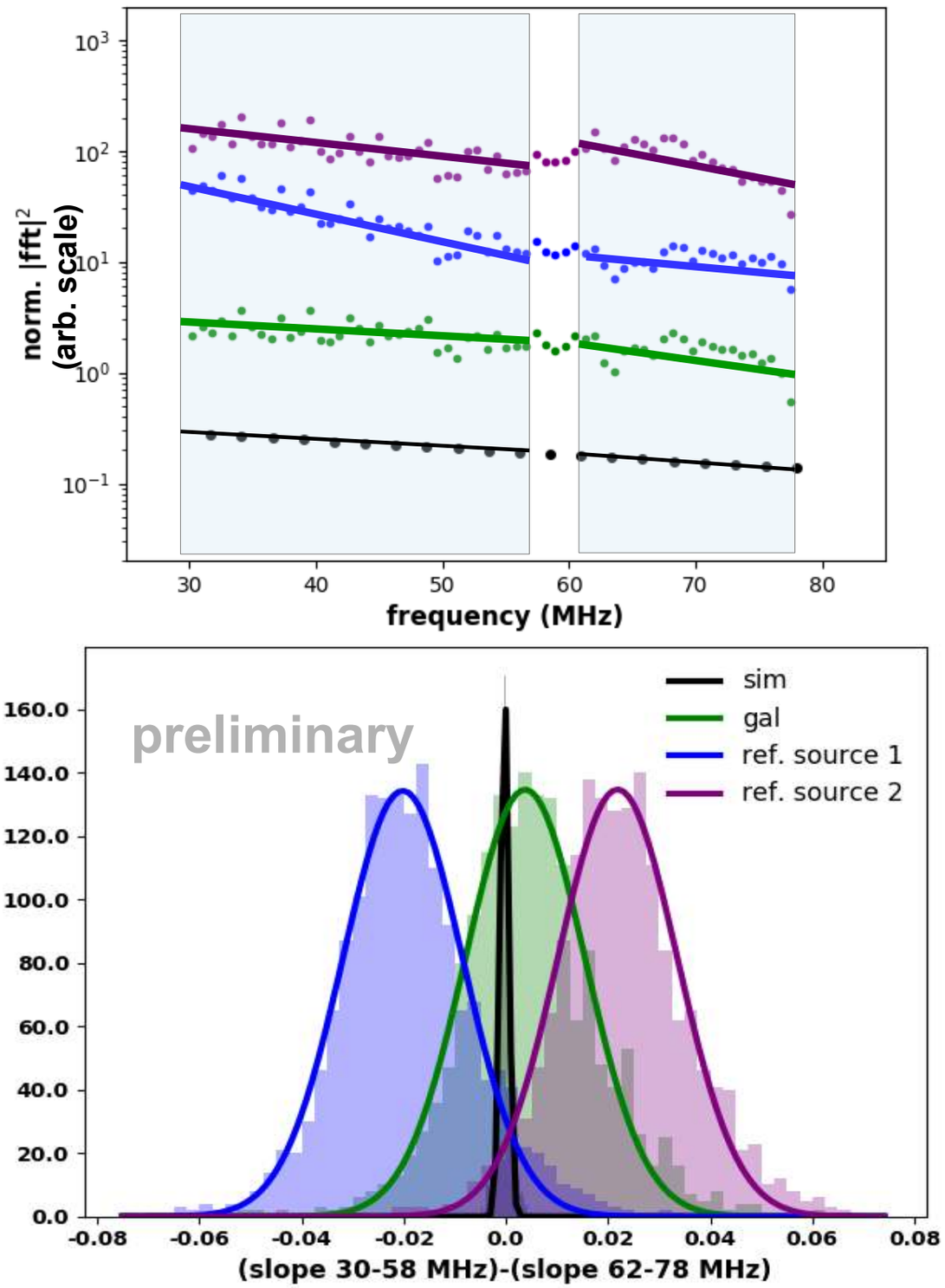

For ~20 strong events (x 3 stations x 48 antennas), compare slope on either side of resonance frequency

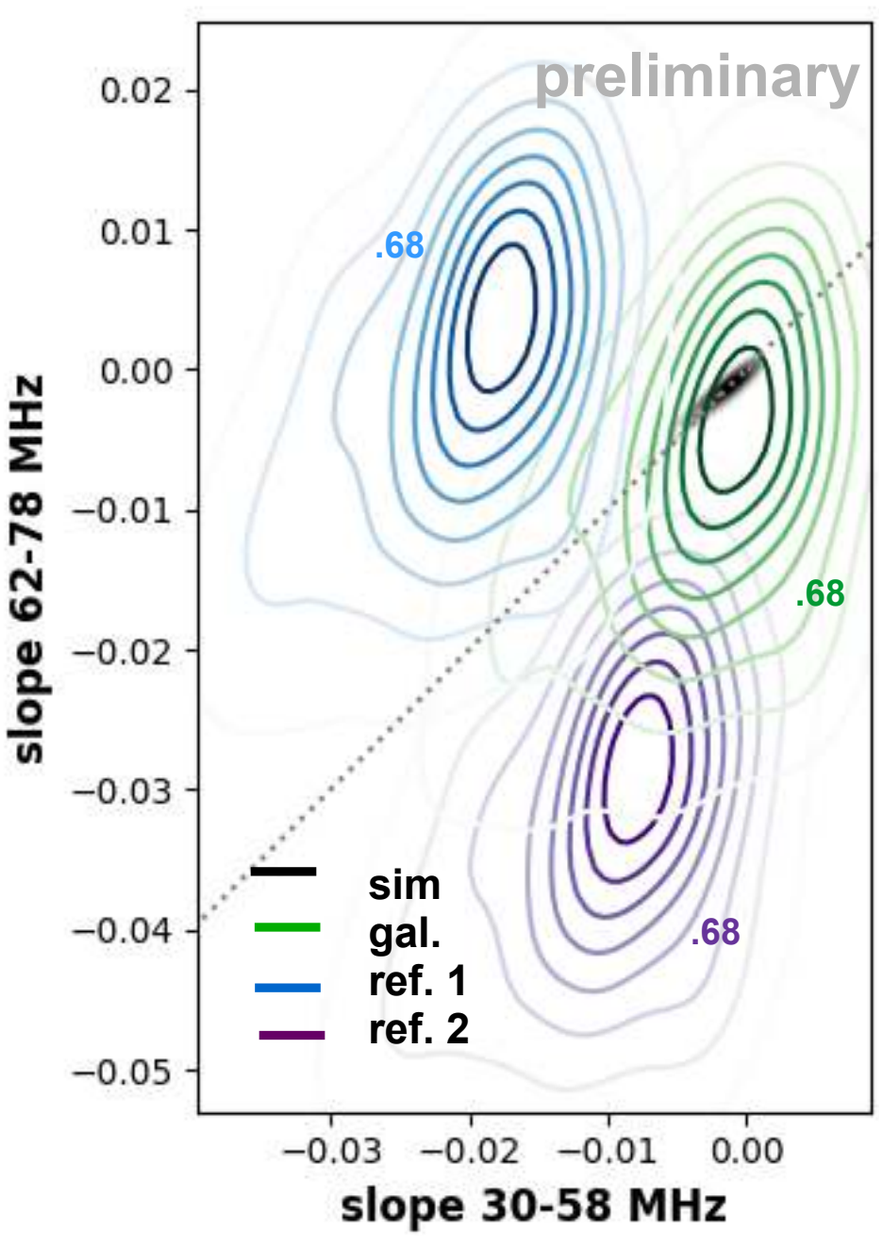

13

Timing calibration

Use beacon broadcasting at 4 different frequencies to measure relative time shifts

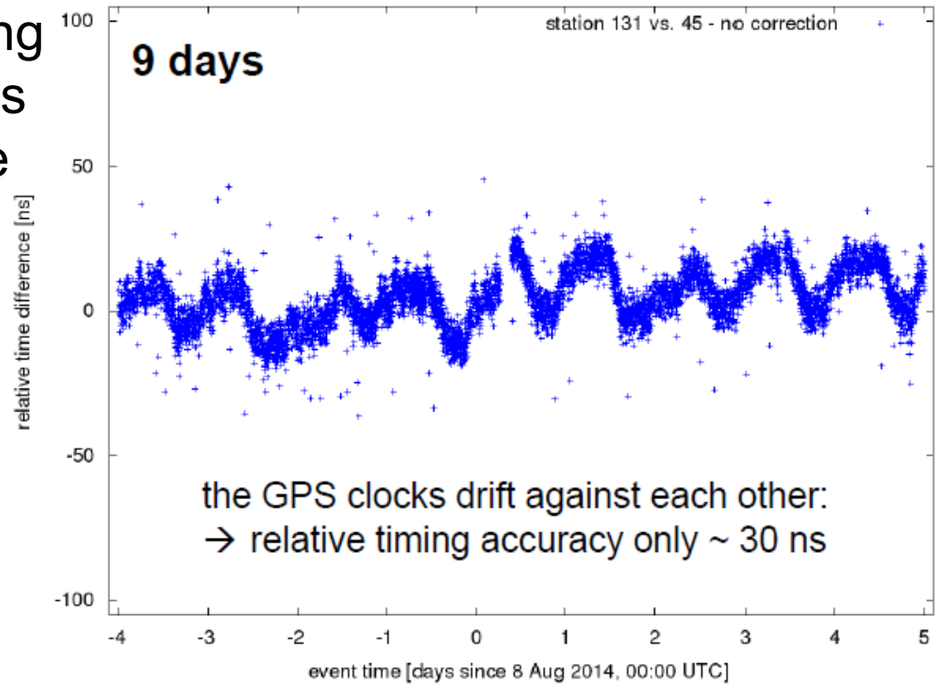

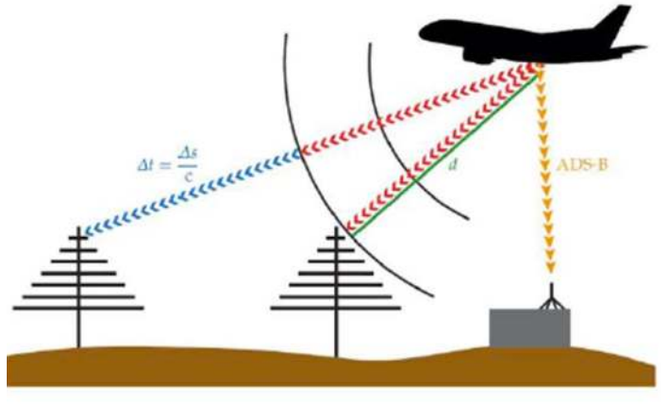

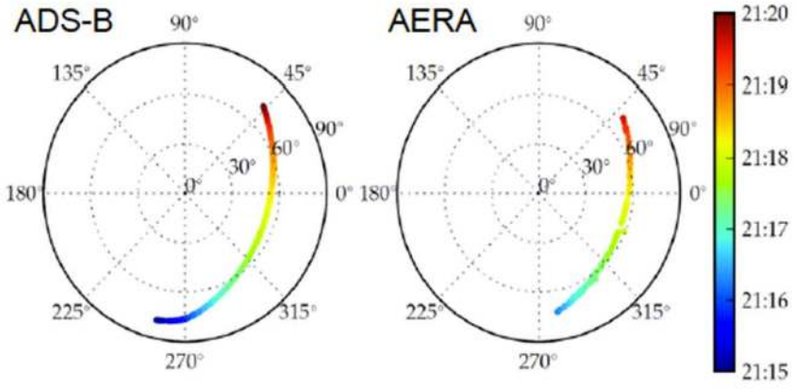

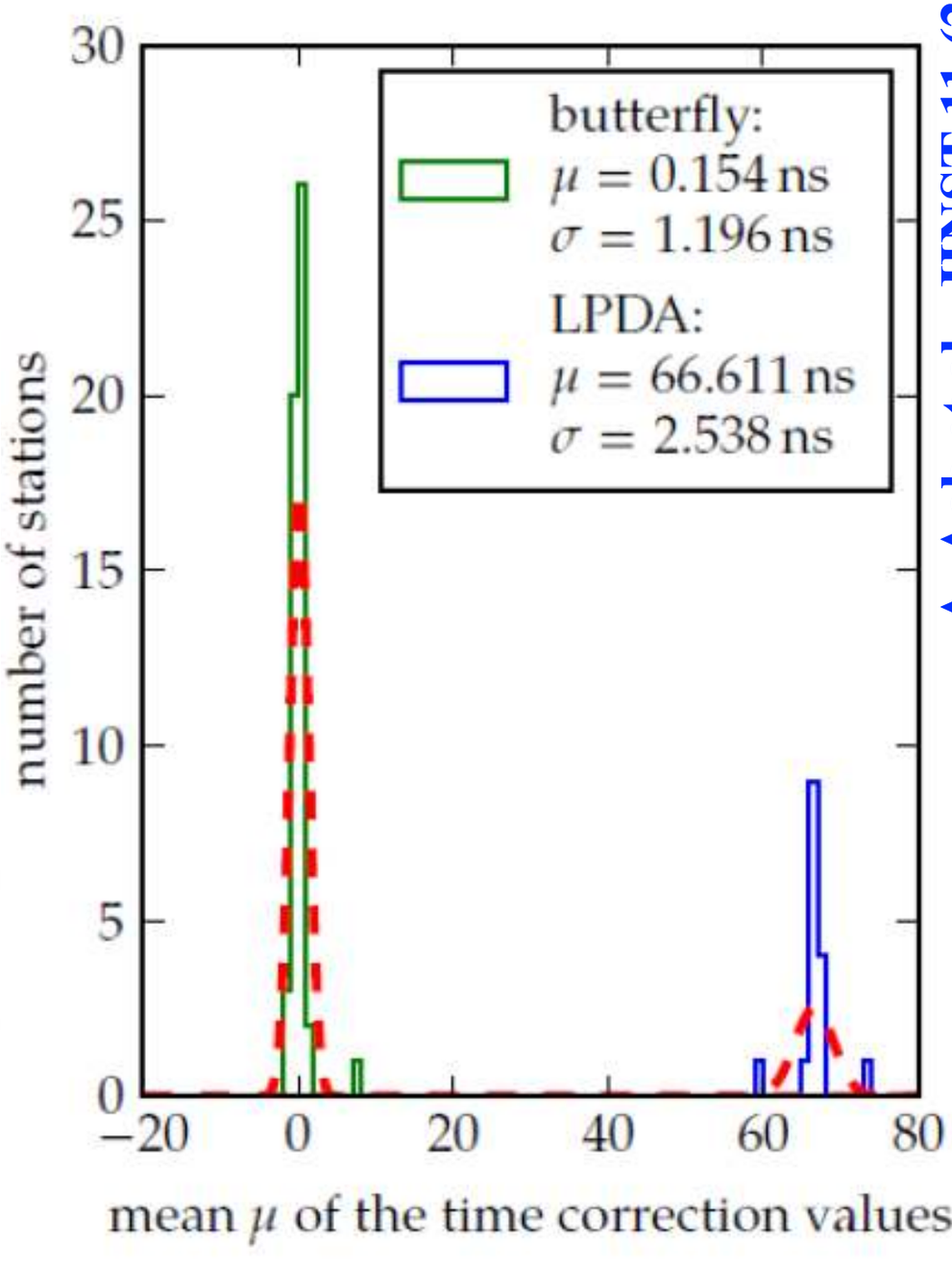

A. Aab et al., JINST 11 (2016) no.01, P01018

ISAPP-Baikal Summer School 2018

Radio detection of extensive air showers

Precision measurements of the properties of cosmic rays

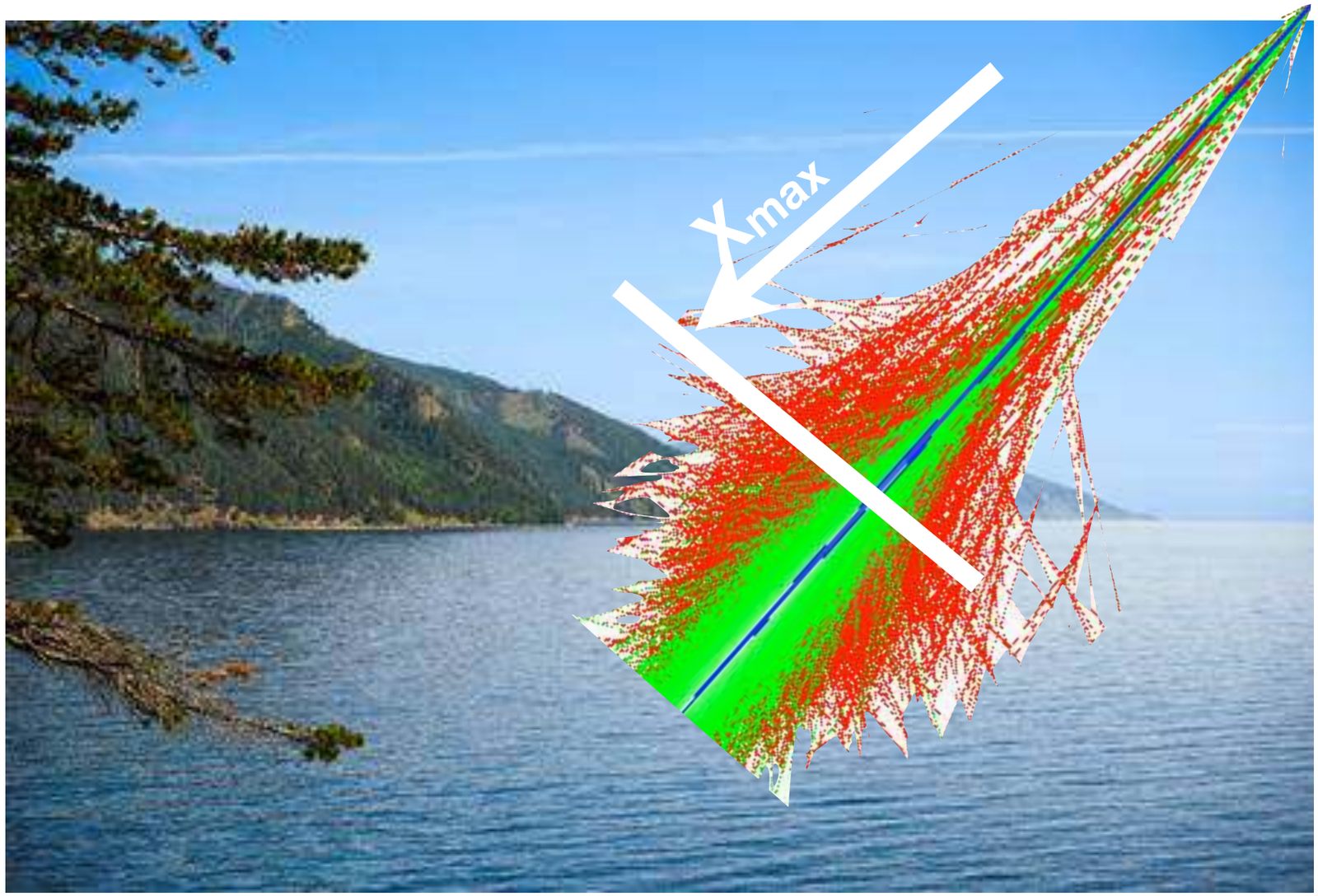

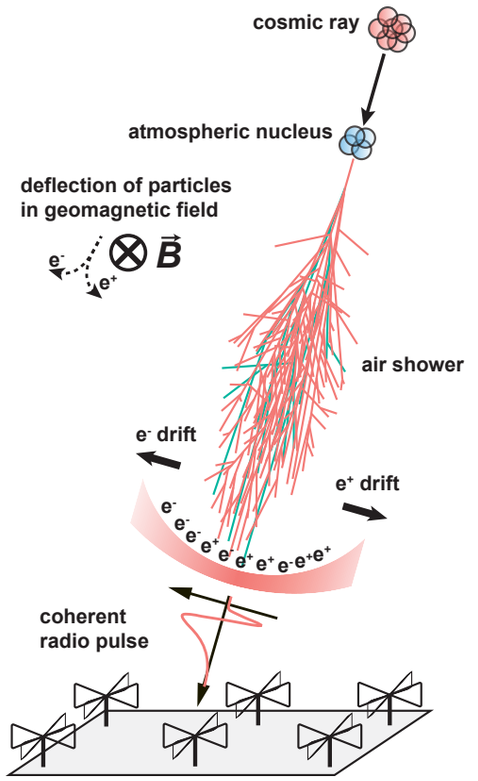

characterize cosmic rays:
-direction
-energy
-mass
@100% duty cycle

task leader radio at Pierre Auger Observatory
PI LOFAR key science project Cosmic Rays

Jörg R. Hörandel **RU Nijmegen, Nikhef, VU Brussel** **http://particle.astro.ru.nl**

Properties of incoming cosmic ray

- direction
- energy
- type

Direction

Arrival time of radio signals

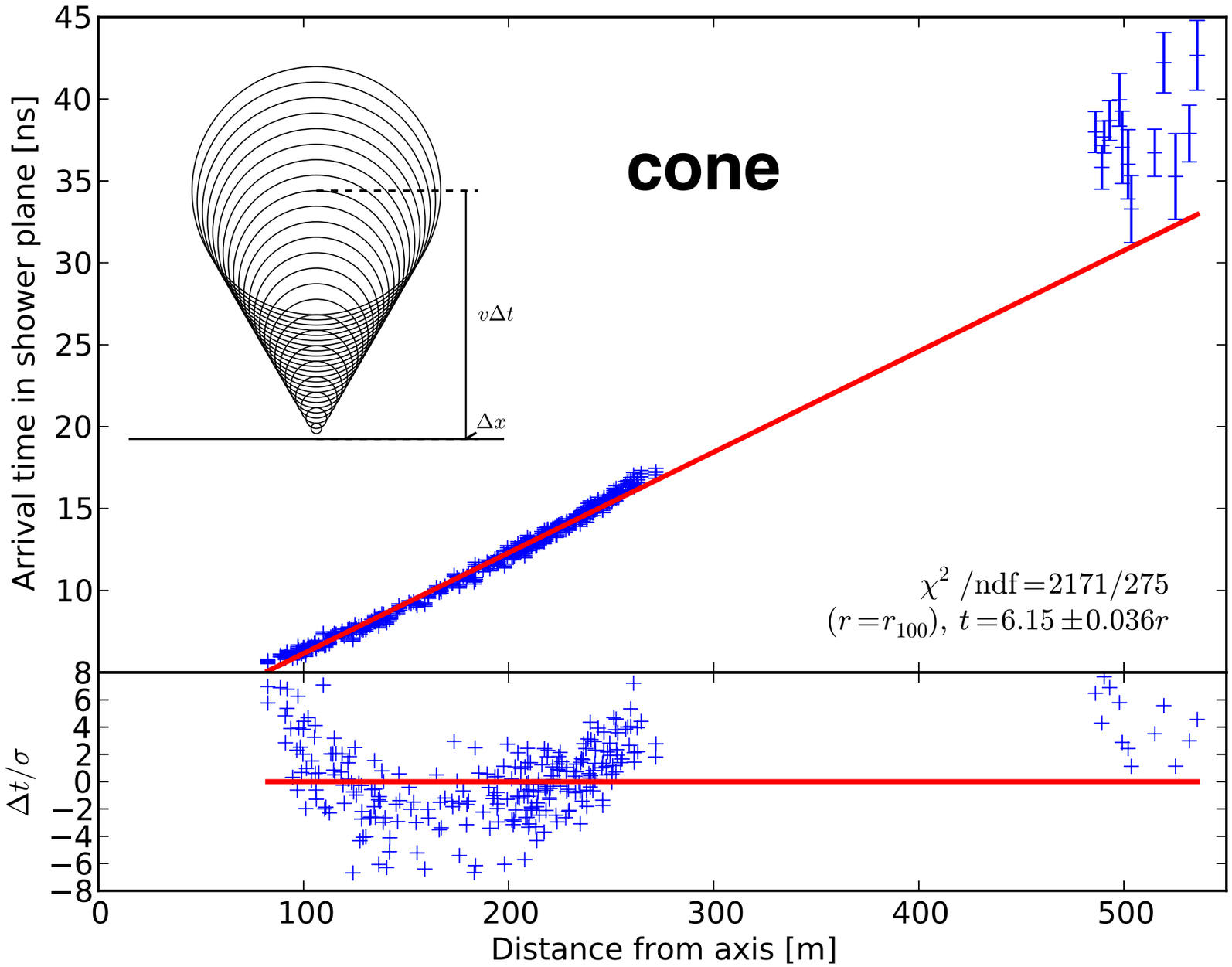

A. Corstanje et al., Astropart. Phys. 61 (2015) 22

Arrival time of radio signals

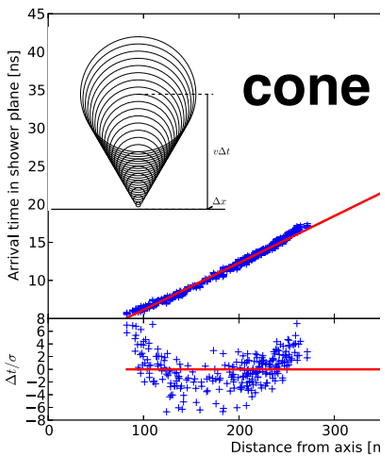

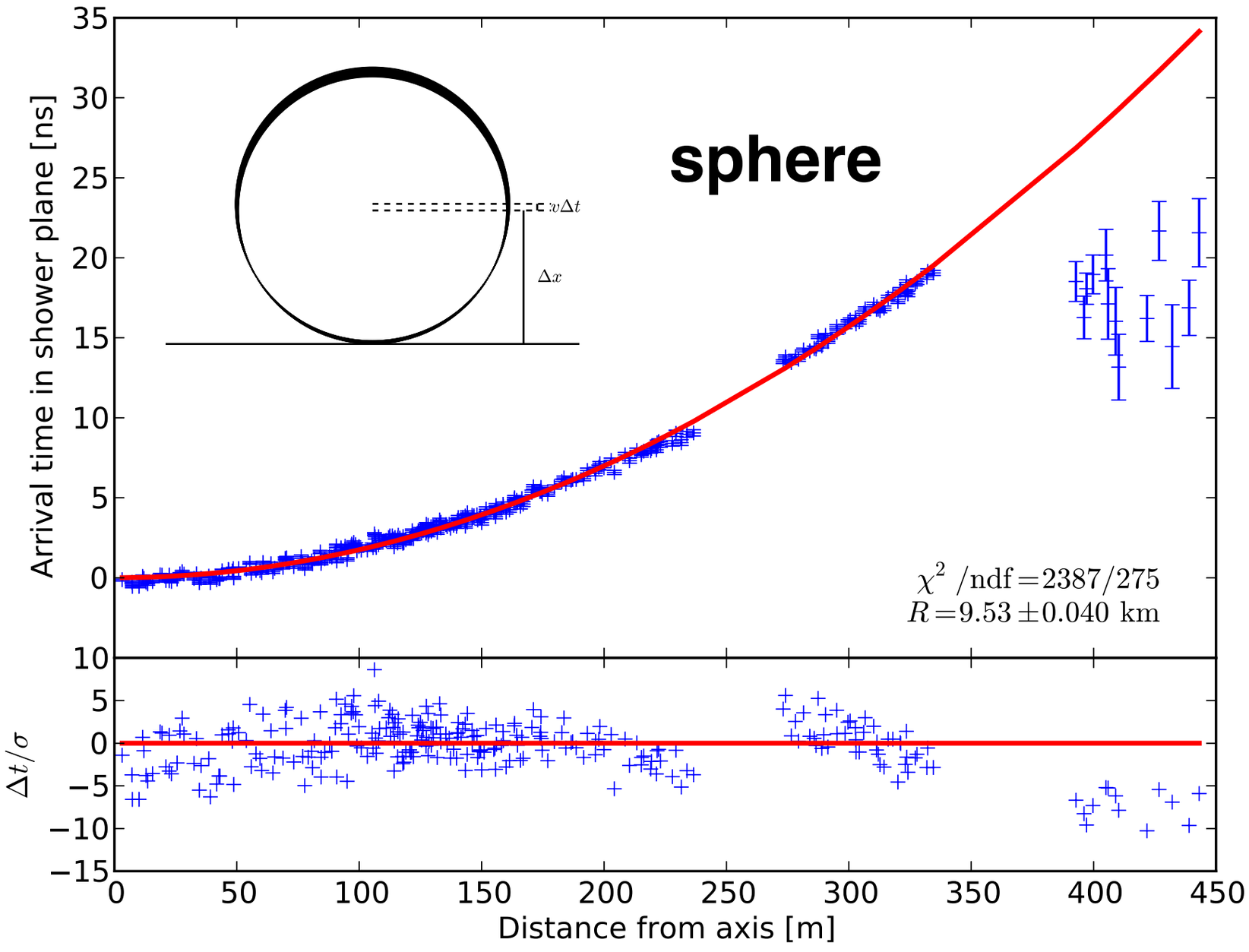

A. Corstanje et al., Astropart. Phys. 61 (2015) 22

Arrival time of radio signals

LOFAR

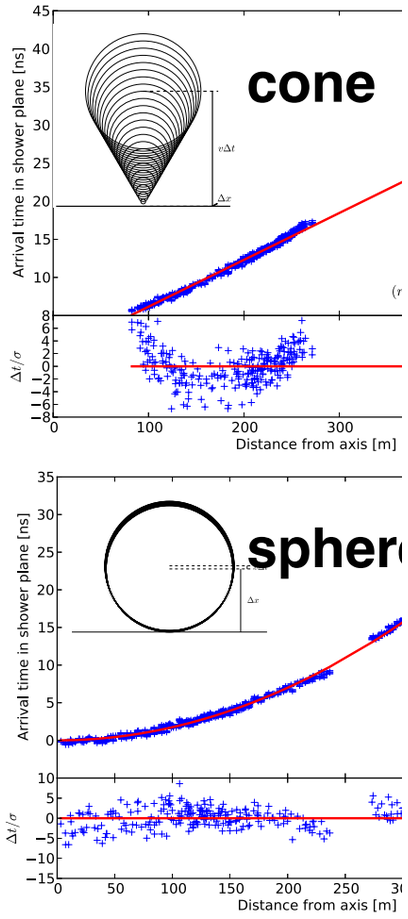

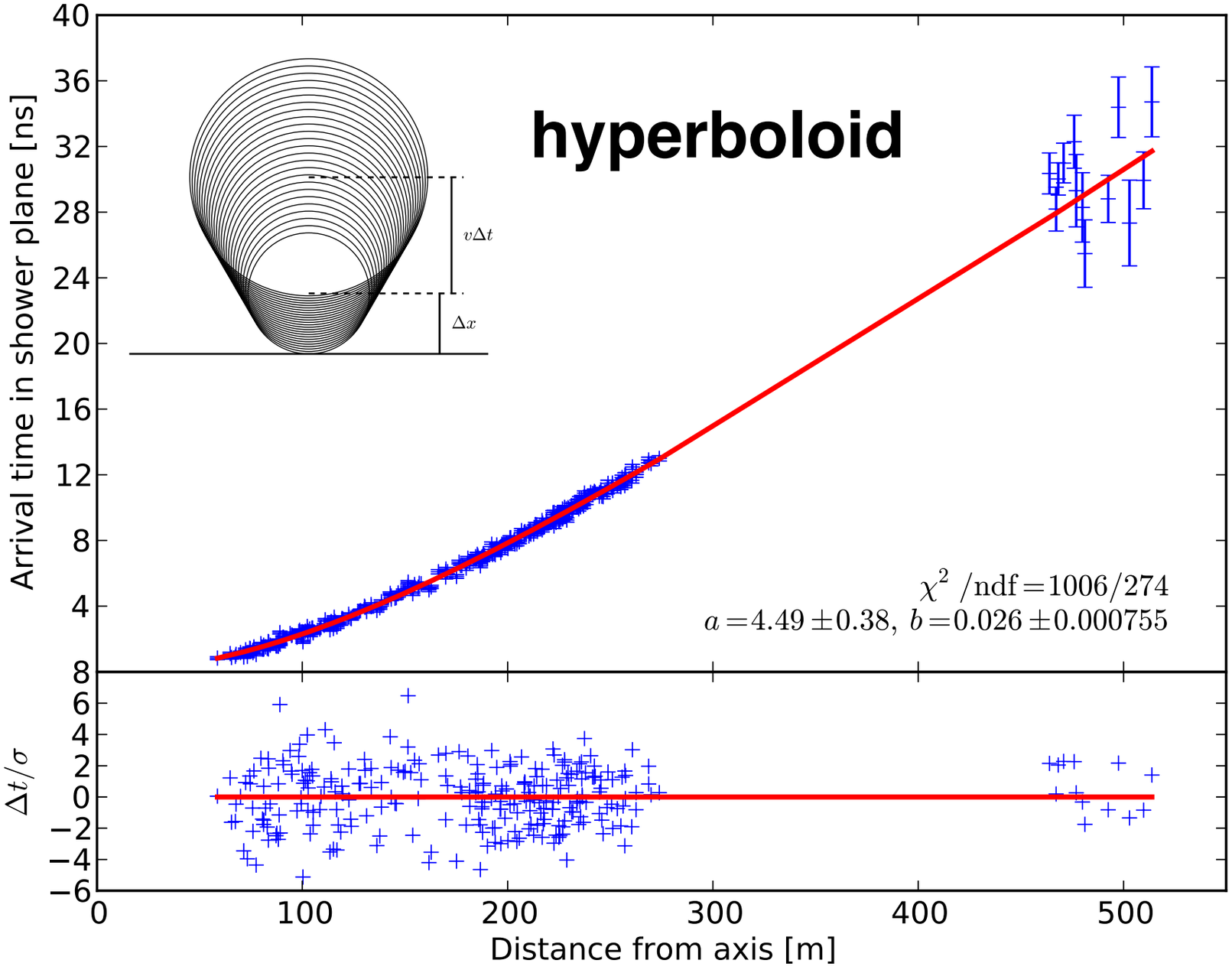

A. Corstanje et al., Astropart. Phys. 61 (2015) 22

Shape of Shower Front

LOFAR

fit quality

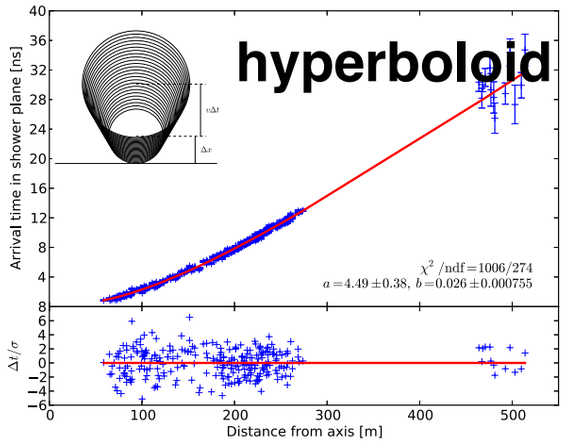

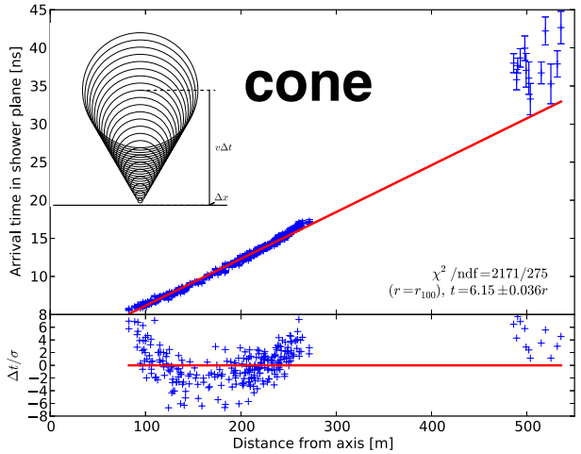

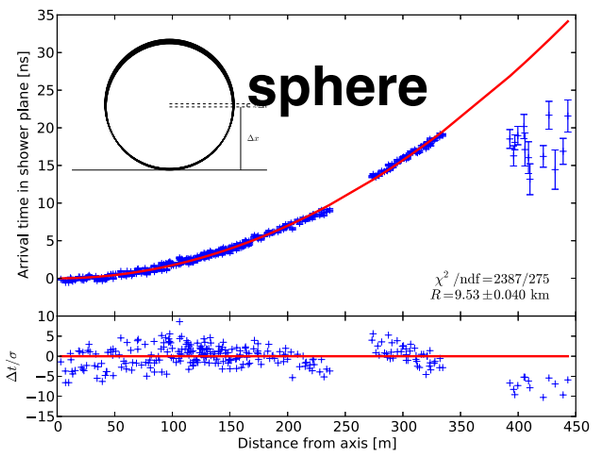

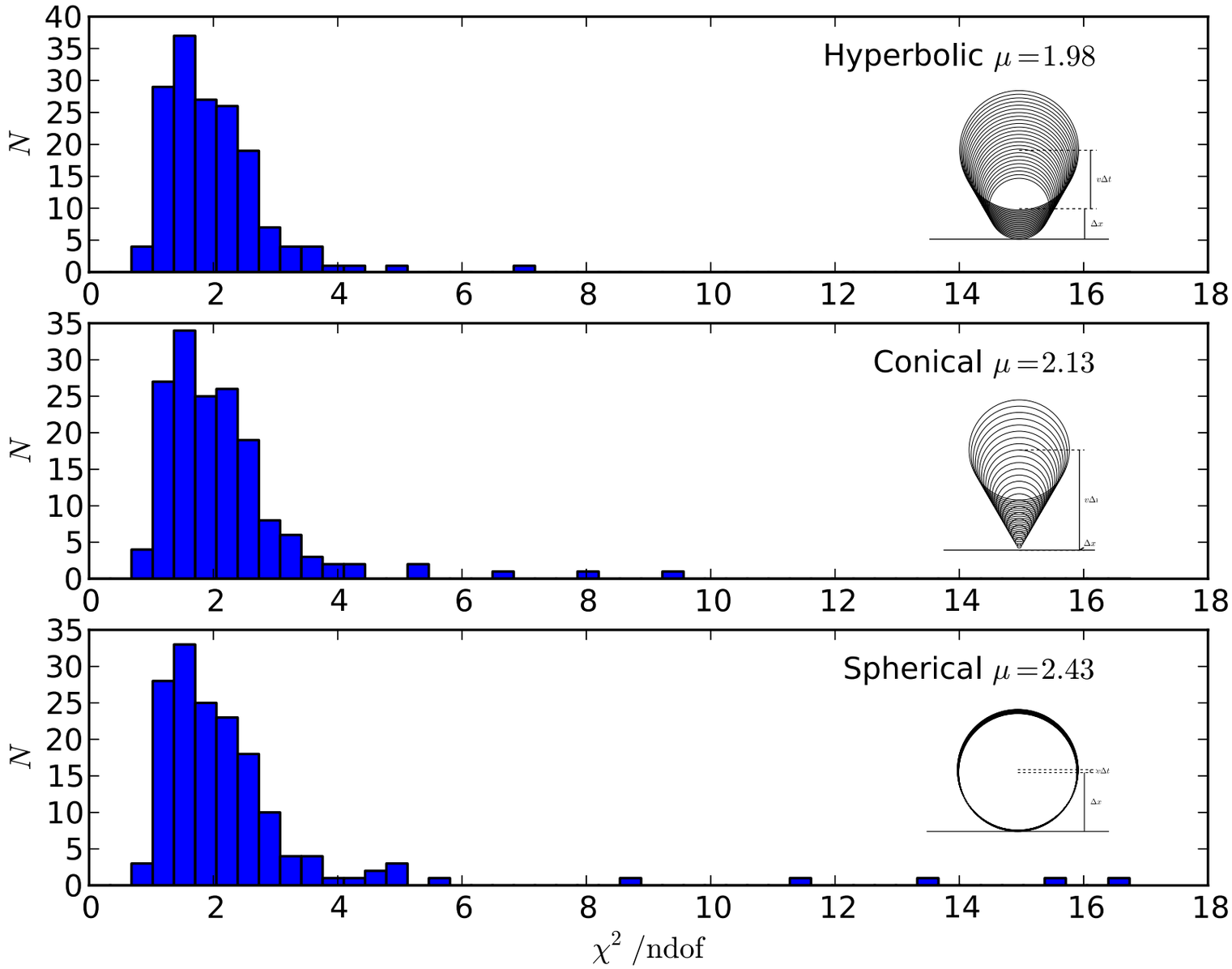

A. Corstanje et al., Astropart. Phys. 61 (2015) 22

Shape of Shower Front

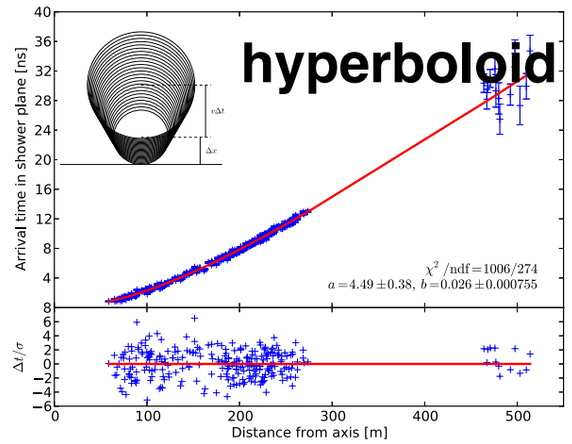

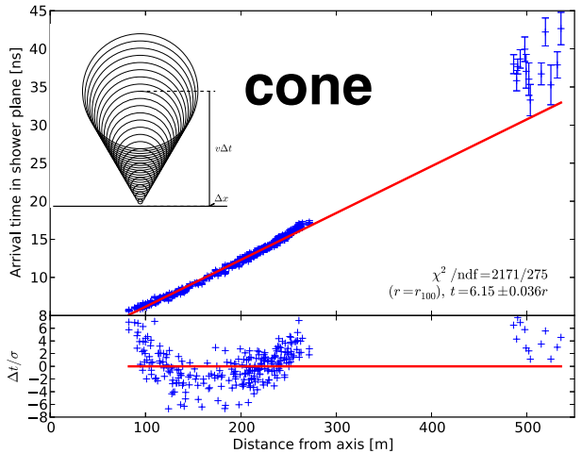

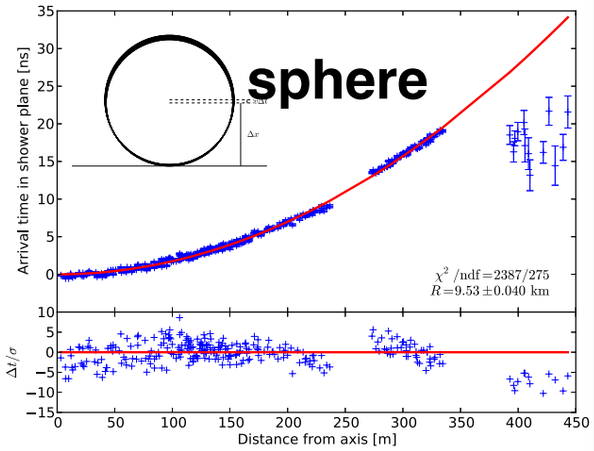

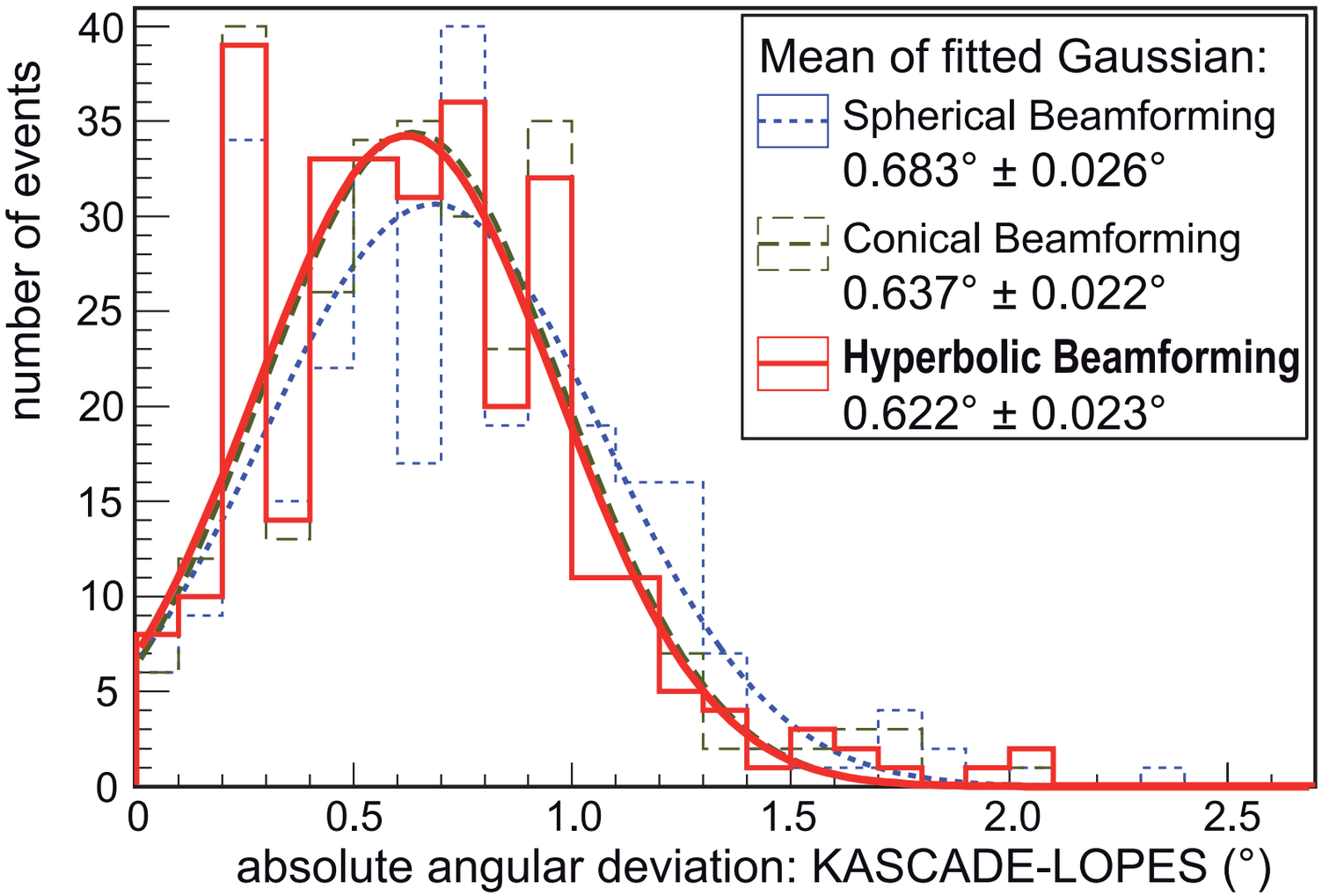

W.D. Apel et al., JCAP 1409 (2014) no.09, 025

A. Corstanje et al., Astropart. Phys. 61 (2015) 22

Accuracy of Shower Direction

angular difference between..

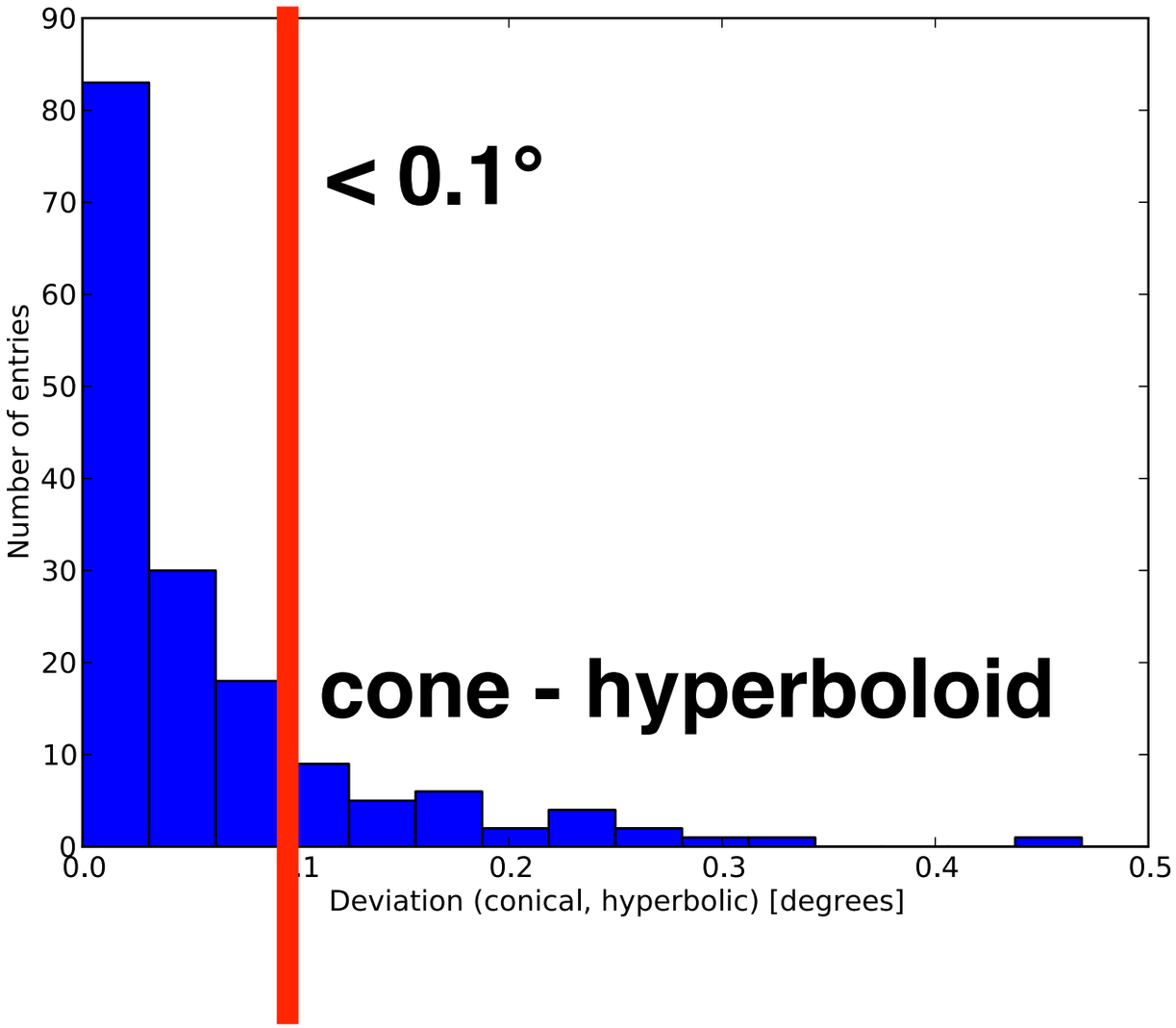

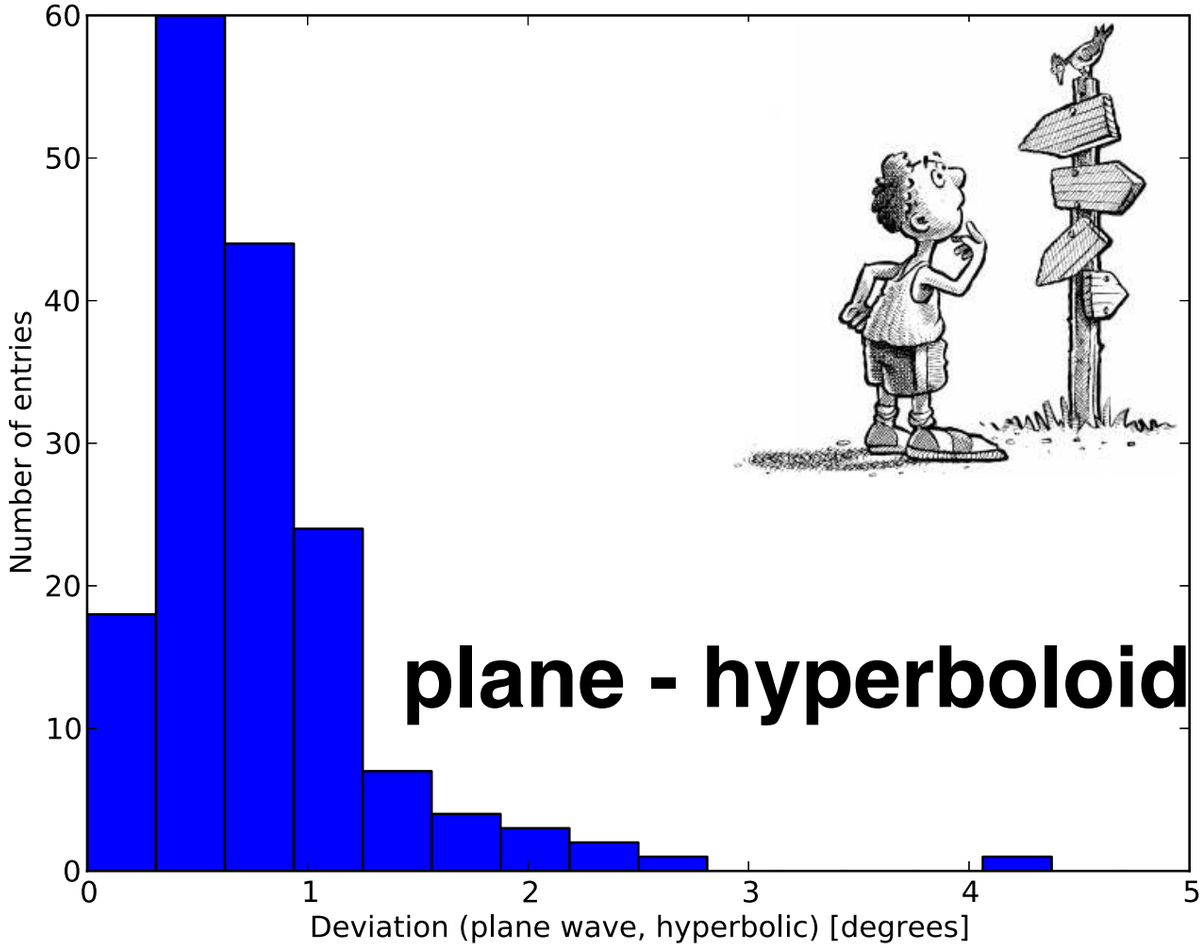

A. Corstanje et al., Astropart. Phys. 61 (2015) 22

Energy

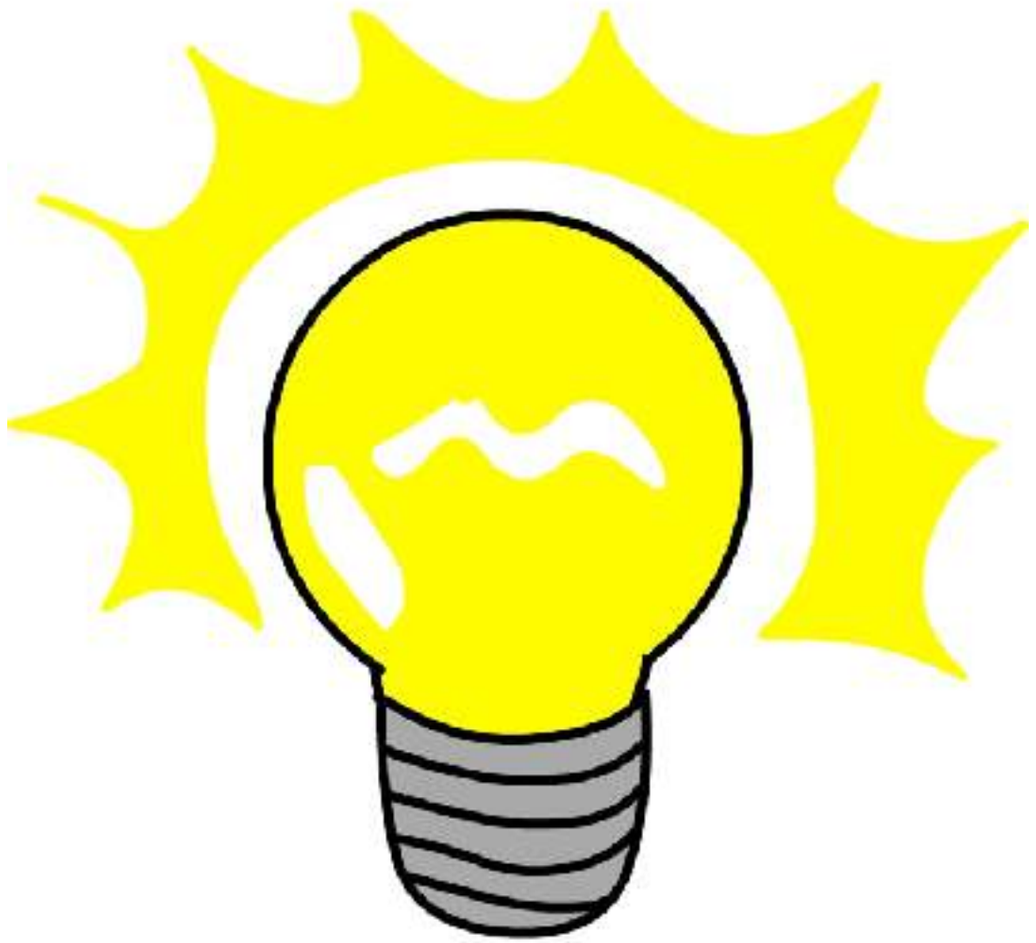

Energy of primary particle

LOFAR

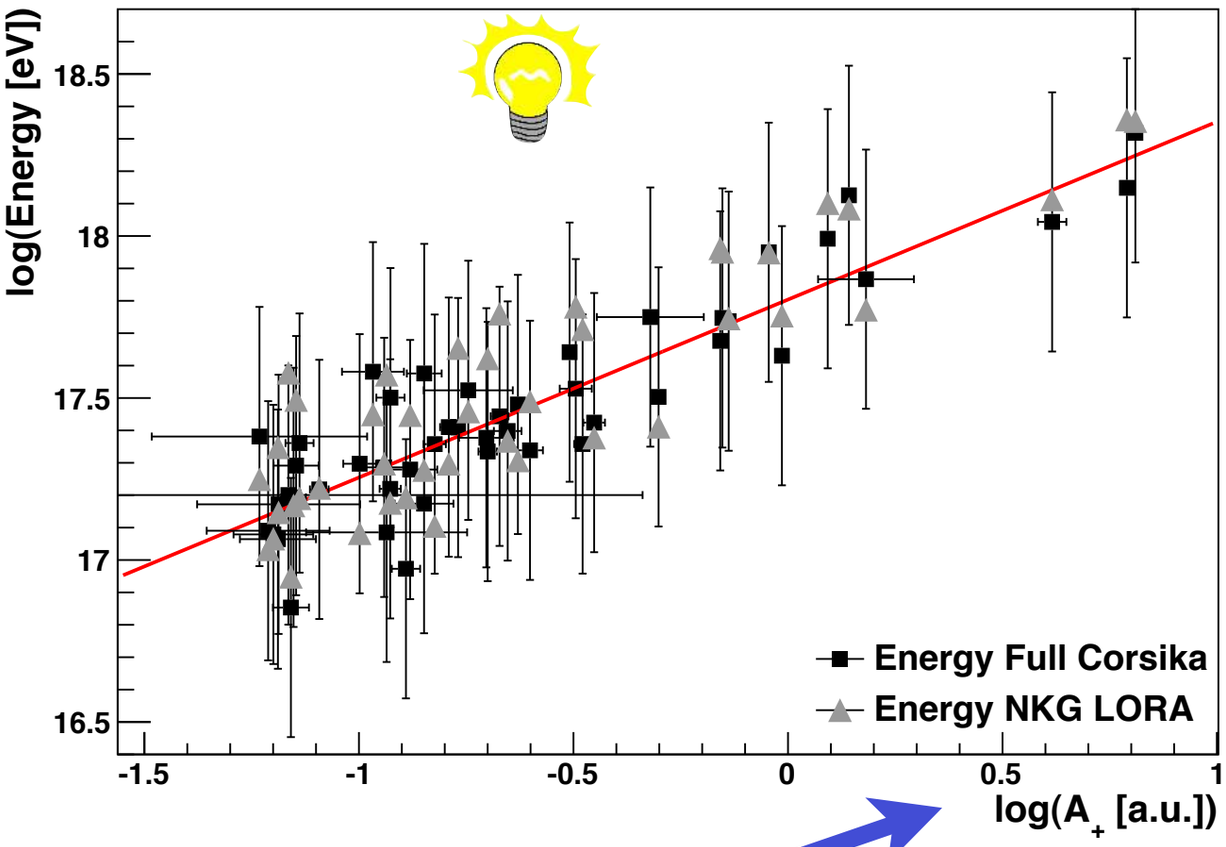

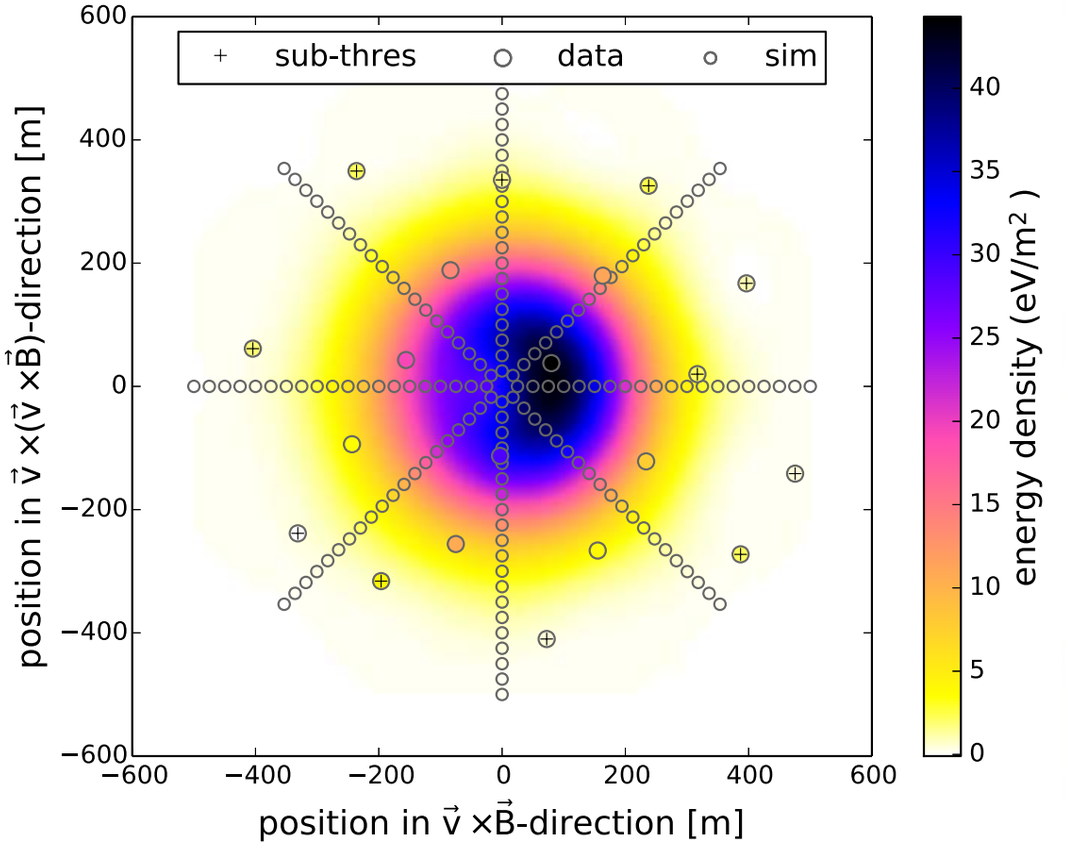

$$P(x',y') = A_+ \cdot \exp\left(\frac{-[(x'-X_+)^2+(y'-Y_+)^2]}{\sigma_+^2}\right) - A_- \cdot \exp\left(\frac{-[(x'-X_-)^2+(y'-Y_-)^2]}{\sigma_-^2}\right) + O$$

A. Nelles et al., JCAP 05 (2015) 018

Measurement of the Radiation Energy in the Radio Signal of Extensive Air Showers as a Universal Estimator of Cosmic-Ray Energy

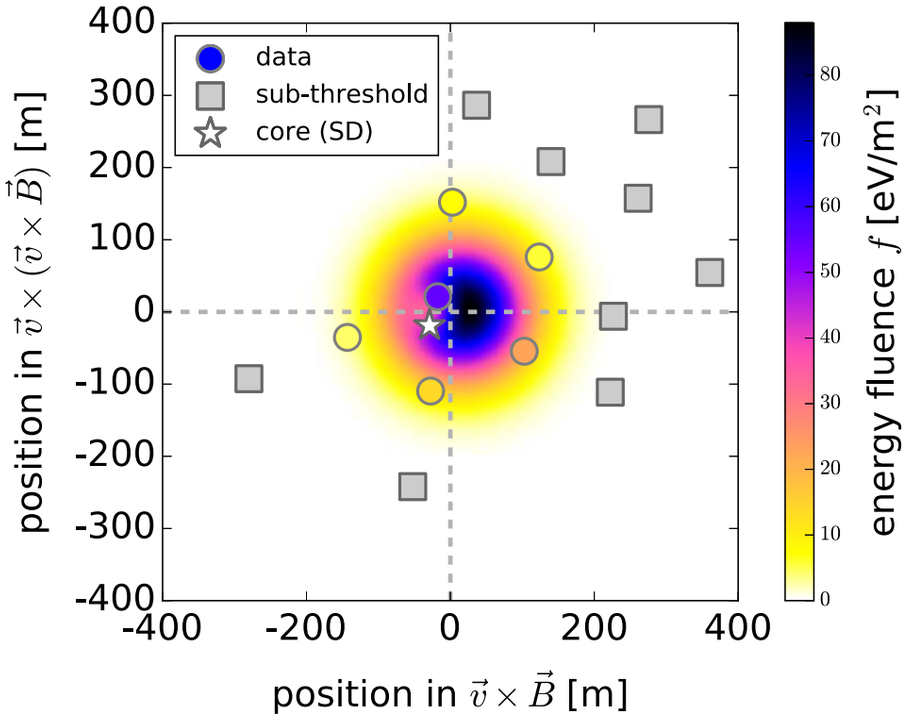

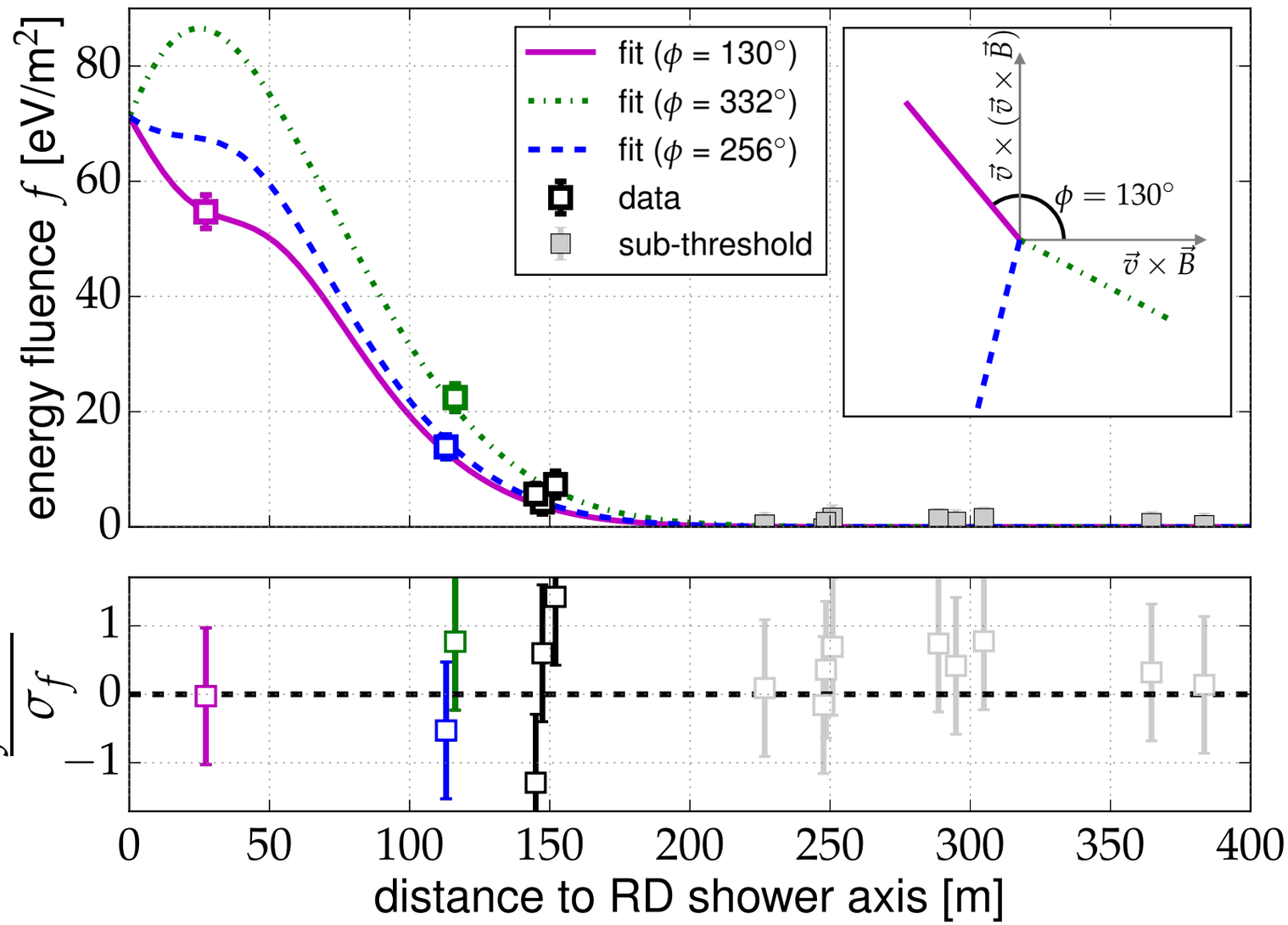

A. Aab et al., PRL 116 (2016) no.24, 241101

Measurement of the Radiation Energy in the Radio Signal of Extensive Air Showers as a Universal Estimator of Cosmic-Ray Energy

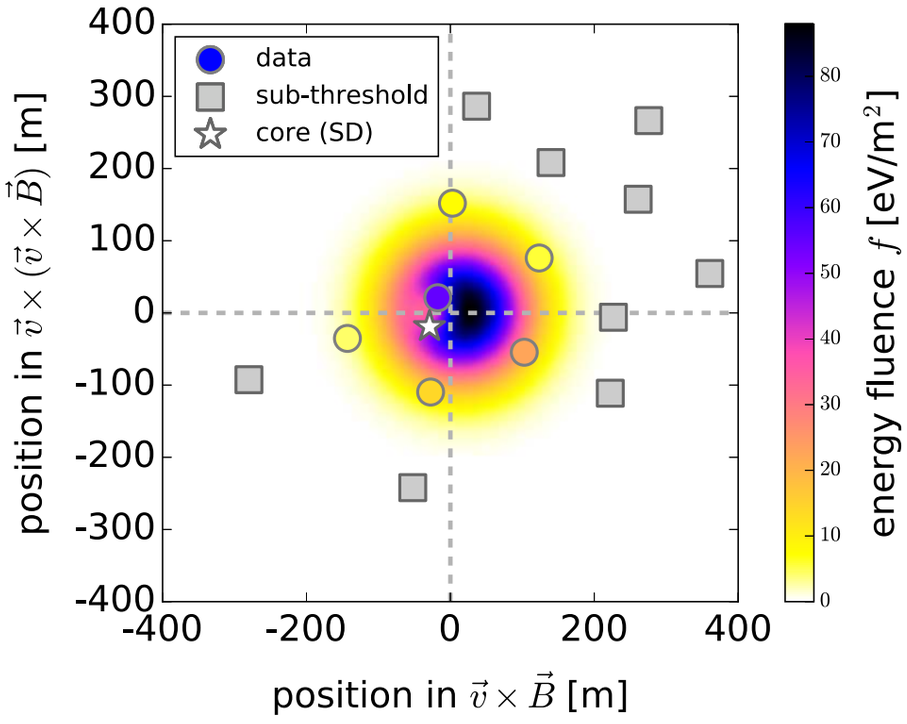

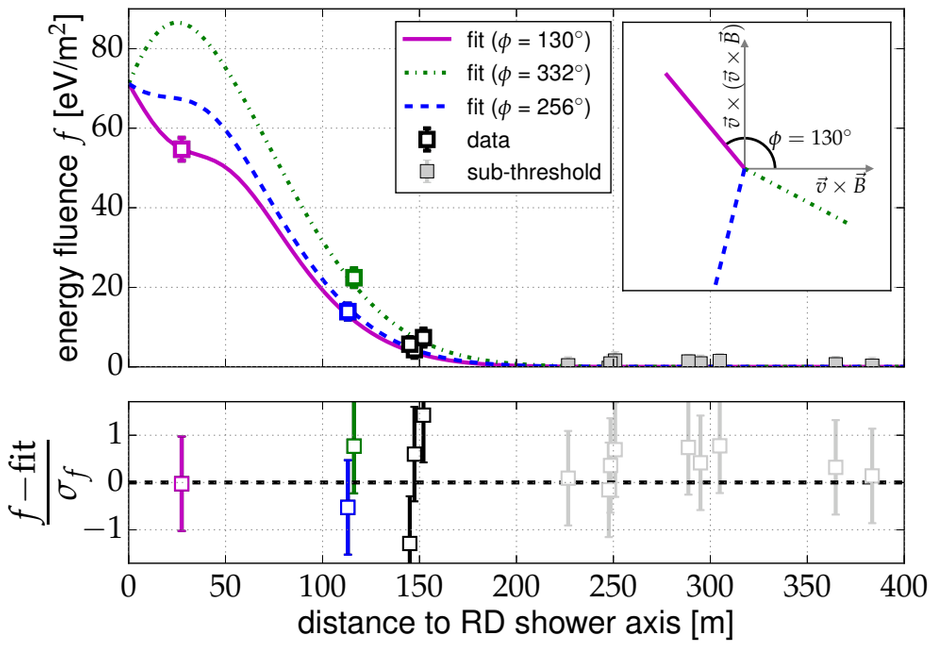

$E_{30\text{-}80\ \mathrm{MHz}} = 15.8\ \mathrm{MeV}\ @\ 10^{18}\ \mathrm{eV}$

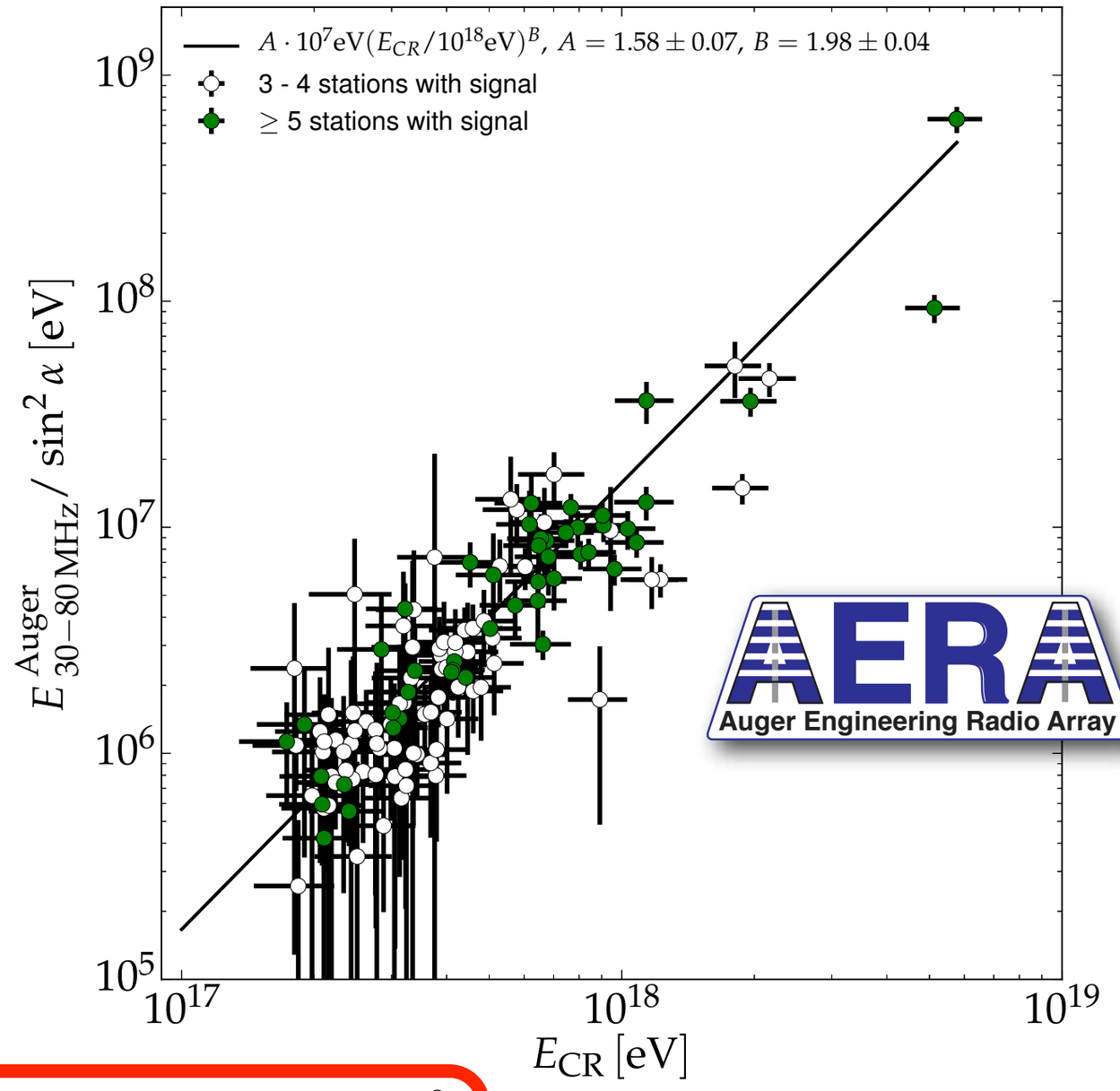

$$E_{30\text{-}80\ \mathrm{MHz}} = (15.8 \pm 0.7(\mathrm{stat}) \pm 6.7(\mathrm{syst})\ \mathrm{MeV}) \times \left(\sin\alpha \frac{E_{CR}}{10^{18}\ \mathrm{eV}} \frac{B_{Earth}}{0.24\ \mathrm{G}}\right)^2$$

A. Aab et al., PRL 116 (2016) no.24, 241101

Energy Estimation of Cosmic Rays with the Engineering Radio Array of the Pierre Auger Observatory

$E_{30\text{-}80}$ MHz = 15.8 MeV @ 10^{18} eV

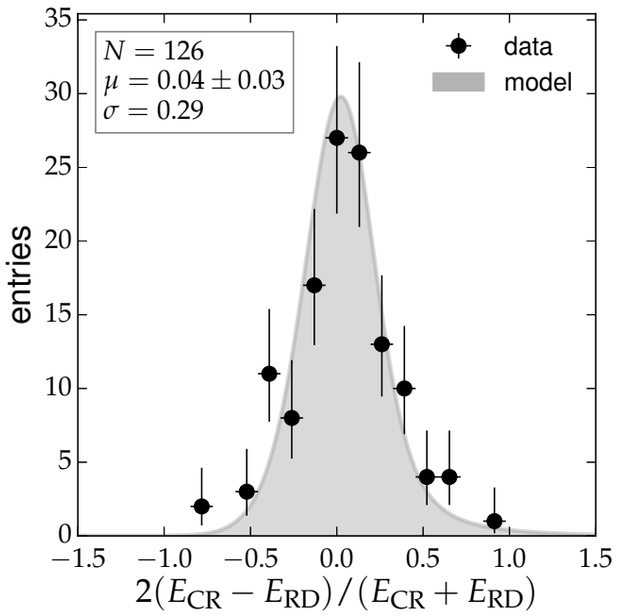

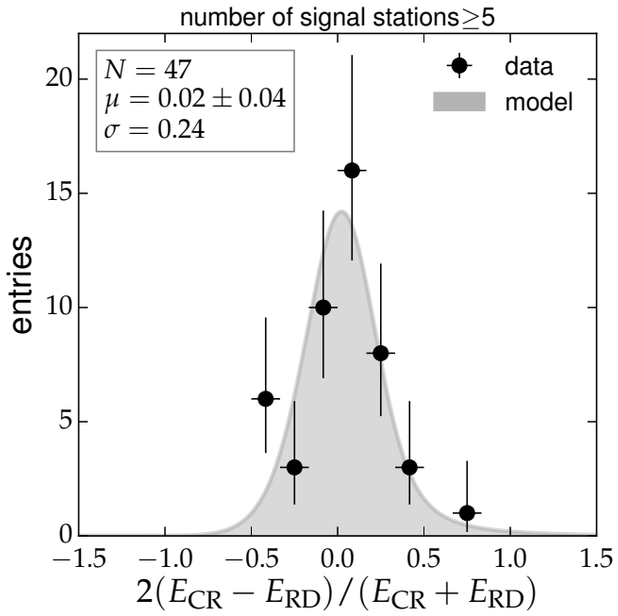

$$\sigma \approx 24\%$$

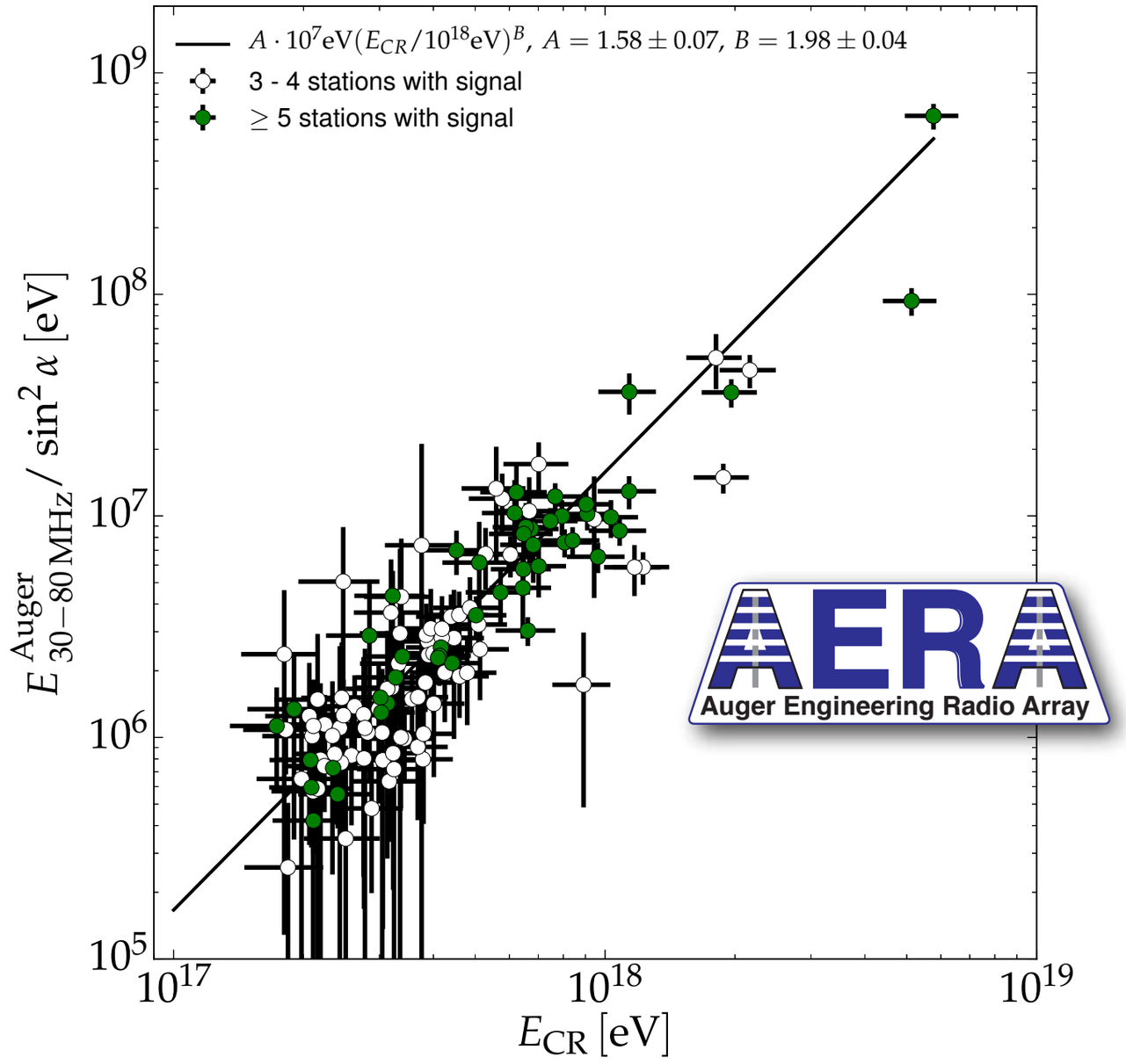

A. Aab et al., PRD 93 (2016) no.12, 122005
A. Aab et al., PRL 116 (2016) no.24, 241101

Cosmic-ray energy (Cherenkov) vs radio signal

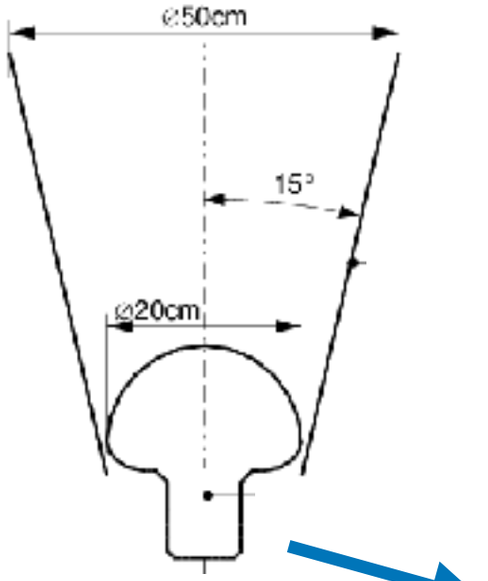

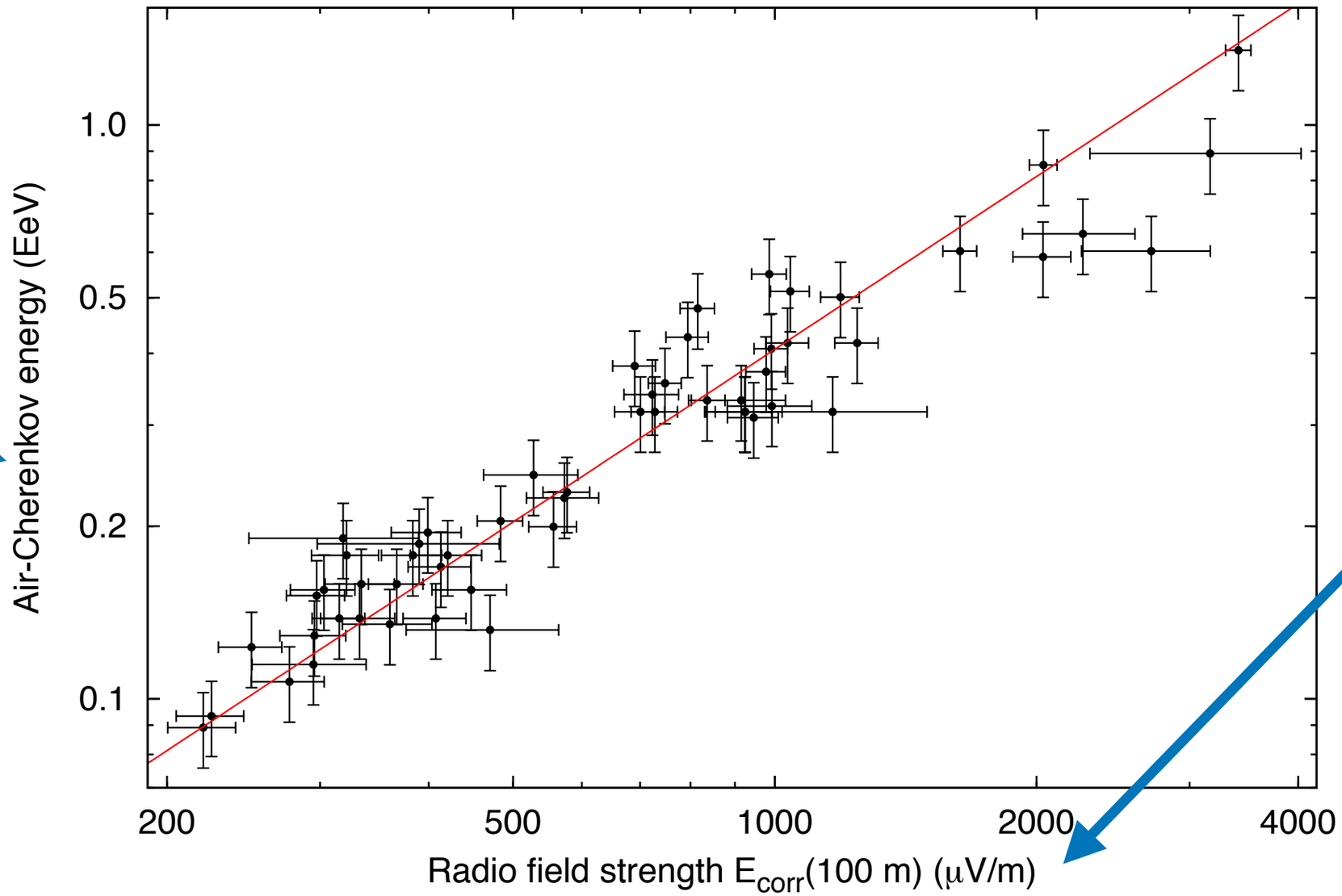

Fig. 3. Correlation of the energy measured with the air-Cherenkov array and an energy estimator based on the radio amplitude at 100 m measured with Tunka-Rex. The line indicates a linear correlation.

F.G. Schröder et al., JPS Conf. Proc. 9 (2016) 010008

Mass

Properties of primary particle

energy

distance to Xmax

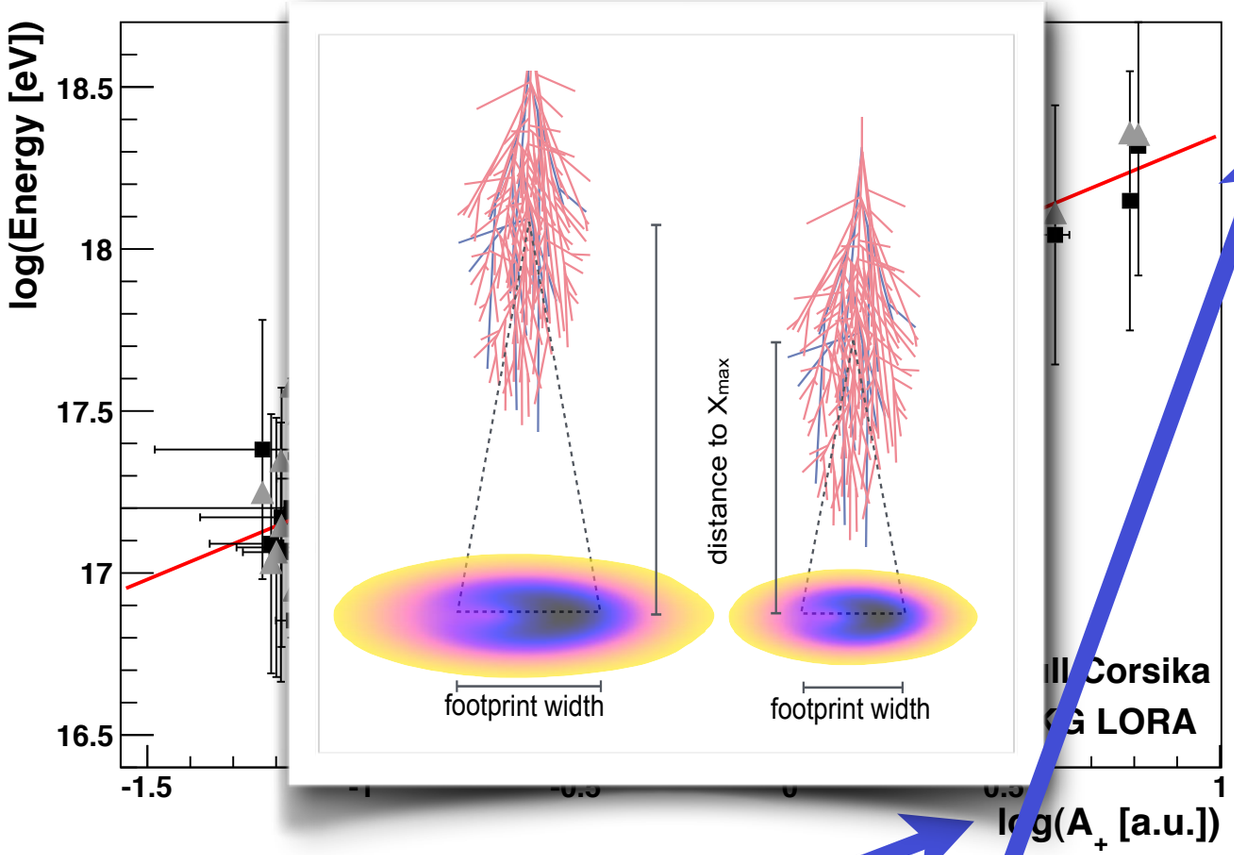

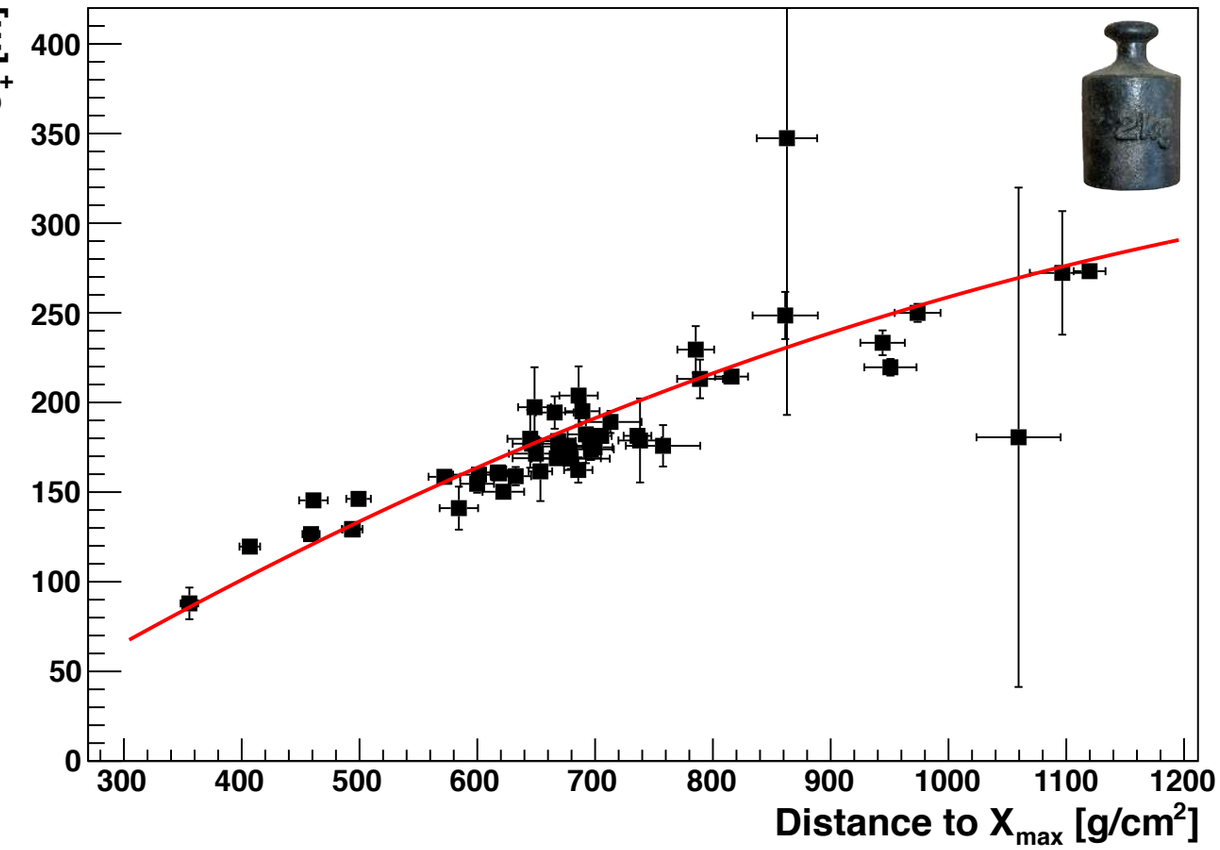

$$P(x',y') = A_+ \cdot \exp\left(\frac{-[(x'-X_+)^2+(y'-Y_+)^2]}{\sigma_+^2}\right) - A_- \cdot \exp\left(\frac{-[(x'-X_-)^2+(y'-Y_-)^2]}{\sigma_-^2}\right) + O$$

LOFAR

A. Nelles et al., JCAP 05 (2015) 018

Measurement of particle mass

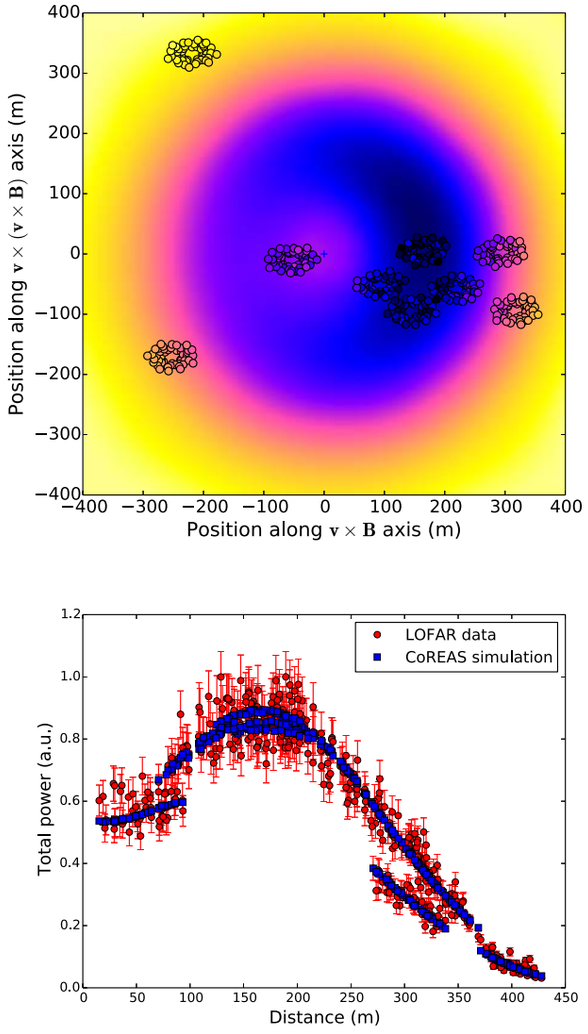

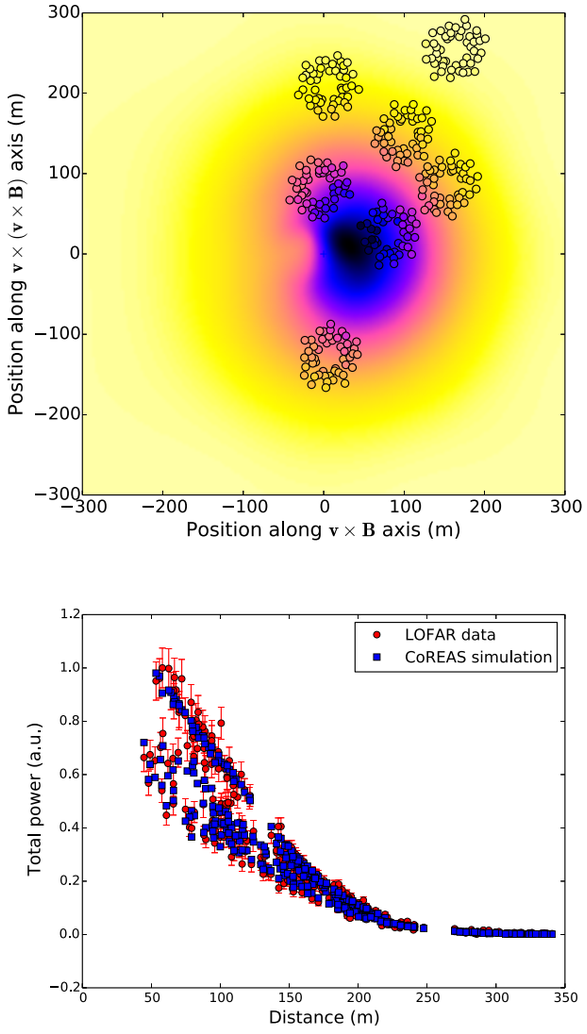

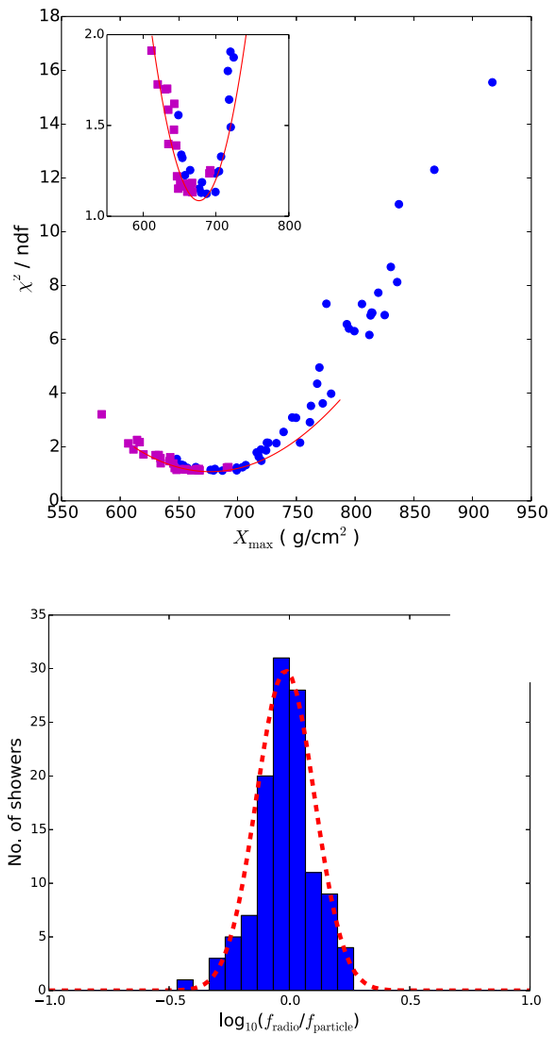

$\sigma_E \approx 32\%$

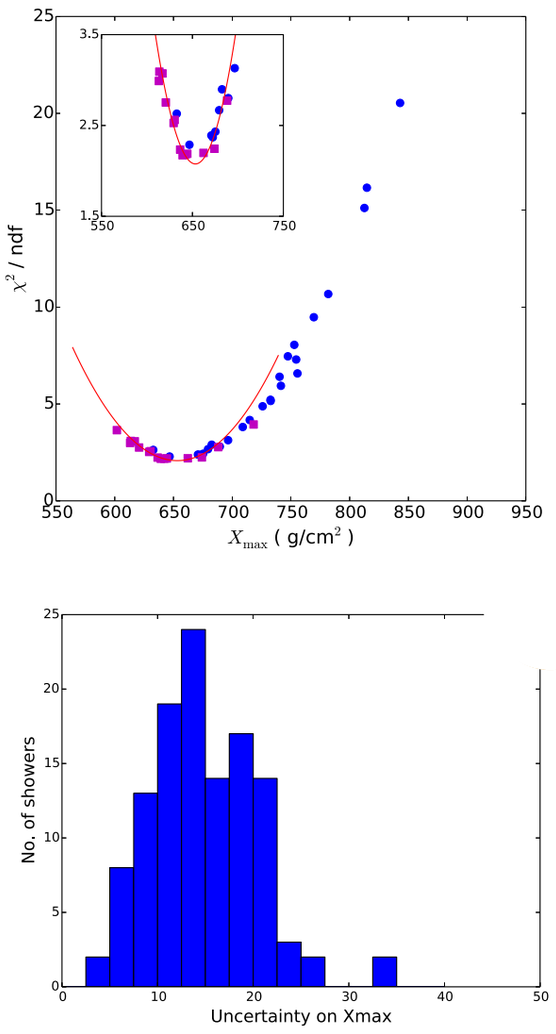

$\sigma_{X_{max}} \approx 17$ g/cm^2

S. Buitink et al., PRD 90 (2014) 082003

Depth of the shower maximum

LETTER nature

doi:10.1038/nature16976

A large light-mass component of cosmic rays at 10^{17}–$10^{17.5}$ electronvolts from radio observations

S. Buitink[1,2], A. Corstanje[2], H. Falcke[2,3,4,5], J. R. Hörandel[2,4], T. Huege[6], A. Nelles[2,7], J. P. Rachen[2], L. Rossetto[2], P. Schellart[2], O. Scholten[8,9], S. ter Veen[3], S. Thoudam[2], T. N. G. Trinh[8], J. Anderson[10], A. Asgekar[3,11], I. M. Avruch[12,13], M. E. Bell[14], M. J. Bentum[3,15], G. Bernardi[16,17], P. Best[18], A. Bonafede[19], F. Breitling[20], J. W. Broderick[21], W. N. Brouw[3,13], M. Brüggen[19], H. R. Butcher[22], D. Carbone[23], B. Ciardi[24], J. E. Conway[25], F. de Gasperin[19], E. de Geus[3,26], A. Deller[3], R.-J. Dettmar[27], G. van Diepen[3], S. Duscha[3], J. Eislöffel[28], D. Engels[29], J. E. Enriquez[3], R. A. Fallows[3], R. Fender[30], C. Ferrari[31], W. Frieswijk[3], M. A. Garrett[3,32], J. M. Grießmeier[33,34], A. W. Gunst[3], M. P. van Haarlem[3], T. E. Hassall[21], G. Heald[3,13], J. W. T. Hessels[3,23], M. Hoeft[28], A. Horneffer[5], M. Iacobelli[3], H. Intema[32,35], E. Juette[27], A. Karastergiou[30], V. I. Kondratiev[3,36], M. Kramer[5,37], M. Kuniyoshi[38], G. Kuper[3], J. van Leeuwen[3,23], G. M. Loose[3], P. Maat[3], G. Mann[20], S. Markoff[23], R. McFadden[3], D. McKay-Bukowski[39,40], J. P. McKean[3,13], M. Mevius[3,13], D. D. Mulcahy[21], H. Munk[3], M. J. Norden[3], E. Orru[3], H. Paas[41], M. Pandey-Pommier[42], V. N. Pandey[3], M. Pietka[30], R. Pizzo[3], A. G. Polatidis[3], W. Reich[5], H. J. A. Röttgering[32], A. M. M. Scaife[21], D. J. Schwarz[43], M. Serylak[30], J. Sluman[3], O. Smirnov[17,44], B. W. Stappers[37], M. Steinmetz[20], A. Stewart[30], J. Swinbank[23,45], M. Tagger[33], Y. Tang[3], C. Tasse[44,46], M. C. Toribio[3,32], R. Vermeulen[3], C. Vocks[20], C. Vogt[3], R. J. van Weeren[16], R. A. M. J. Wijers[23], S. J. Wijnholds[3], M. W. Wise[3,23], O. Wucknitz[5], S. Yatawatta[3], P. Zarka[47] & J. A. Zensus[5]

Cosmic rays are the highest-energy particles found in nature. Measurements of the mass composition of cosmic rays with energies of 10^{17}–10^{18} electronvolts are essential to understanding whether they have galactic or extragalactic sources. It has also been proposed that the astrophysical neutrino signal[1] comes from accelerators capable of producing cosmic rays of these energies[2]. Cosmic rays initiate air showers—cascades of secondary particles in the atmosphere—and their masses can be inferred from measurements of the atmospheric depth of the shower maximum[3] (X_{max}; the depth of the air shower when it contains the most particles) or of the composition of shower particles reaching the ground[4]. Current measurements[5] have either high uncertainty, or a low duty cycle and a high energy threshold. Radio detection of cosmic rays[6–8] is a rapidly developing technique[9] for determining X_{max} (refs 10, 11) with a duty cycle of, in principle, nearly 100 per cent. The radiation is generated by the separation of relativistic electrons and positrons in the geomagnetic field and a negative charge excess in the shower front[6,12]. Here we report radio measurements of X_{max} with a mean uncertainty of 16 grams per square centimetre for air showers initiated by cosmic rays with energies of 10^{17}–$10^{17.5}$ electronvolts. This high resolution in X_{max} enables us to determine the mass spectrum of the cosmic rays: we find a mixed composition, with a light-mass fraction (protons and helium nuclei) of about 80 per cent. Unless, contrary to current expectations, the extragalactic component of cosmic rays contributes substantially to the total flux below $10^{17.5}$ electronvolts, our measurements indicate the existence of an additional galactic component, to account for the light composition that we measured in the 10^{17}–$10^{17.5}$ electronvolt range.

Observations were made with the Low Frequency Array (LOFAR[13]), a radio telescope consisting of thousands of crossed dipoles with built-in air-shower-detection capability[14]. LOFAR continuously records the radio signals from air showers, while simultaneously running astronomical observations. It comprises a scintillator array (LORA) that triggers the read-out of buffers, storing the full waveforms received by all antennas.

We selected air showers from the period June 2011 to January 2015 with radio pulses detected in at least 192 antennas. The total uptime was about 150 days, limited by construction and commissioning of the

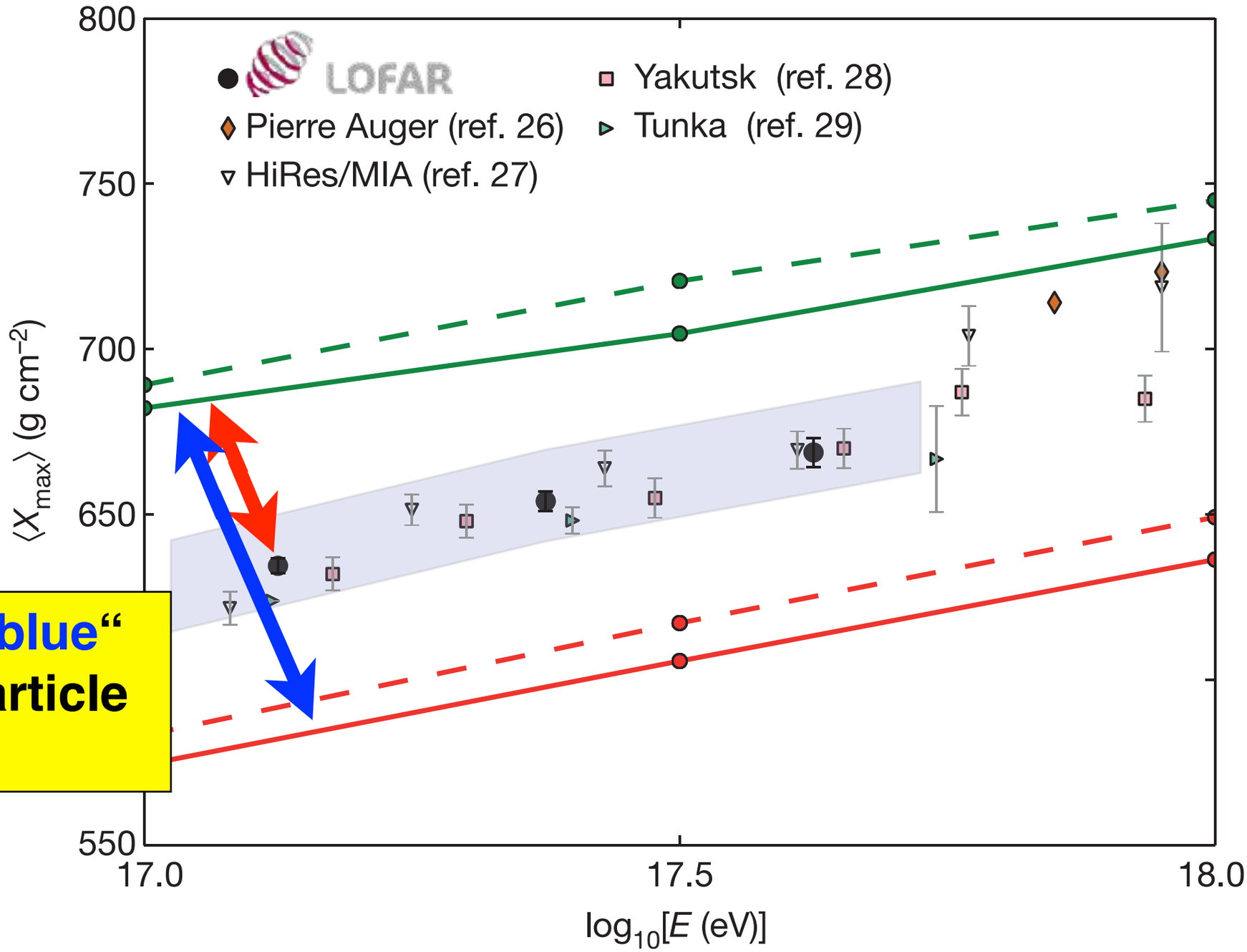

relative distance "red/blue" is measure for ln A (particle type)

S. Buitink et al., Nature 531 (2016) 70

Mean logarithmic mass

$$\ln A = \sum k_i \ln A_i$$

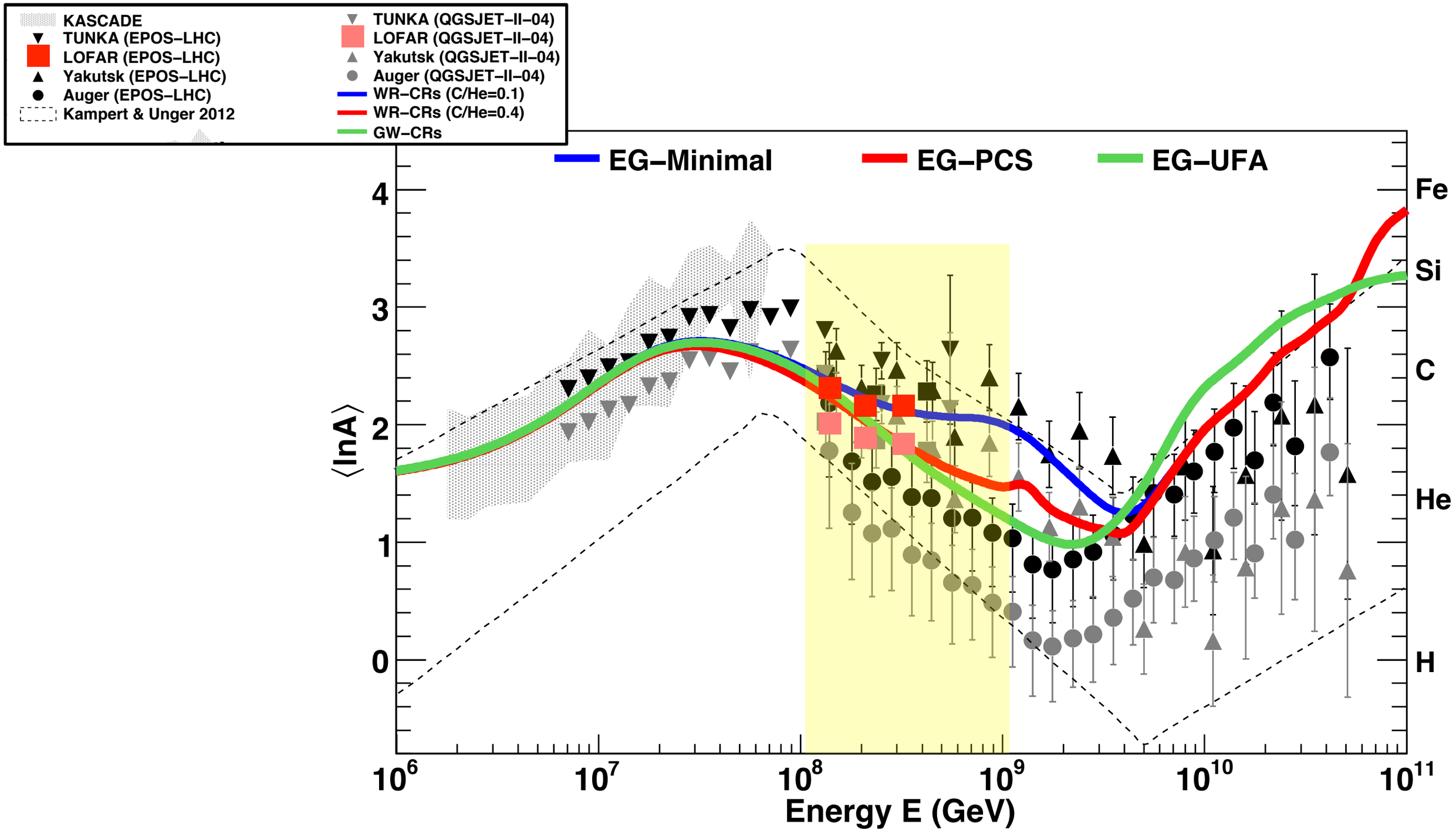

S. Thoudam et al., A&A 595 (2016) A33

Xmax RD vs FD

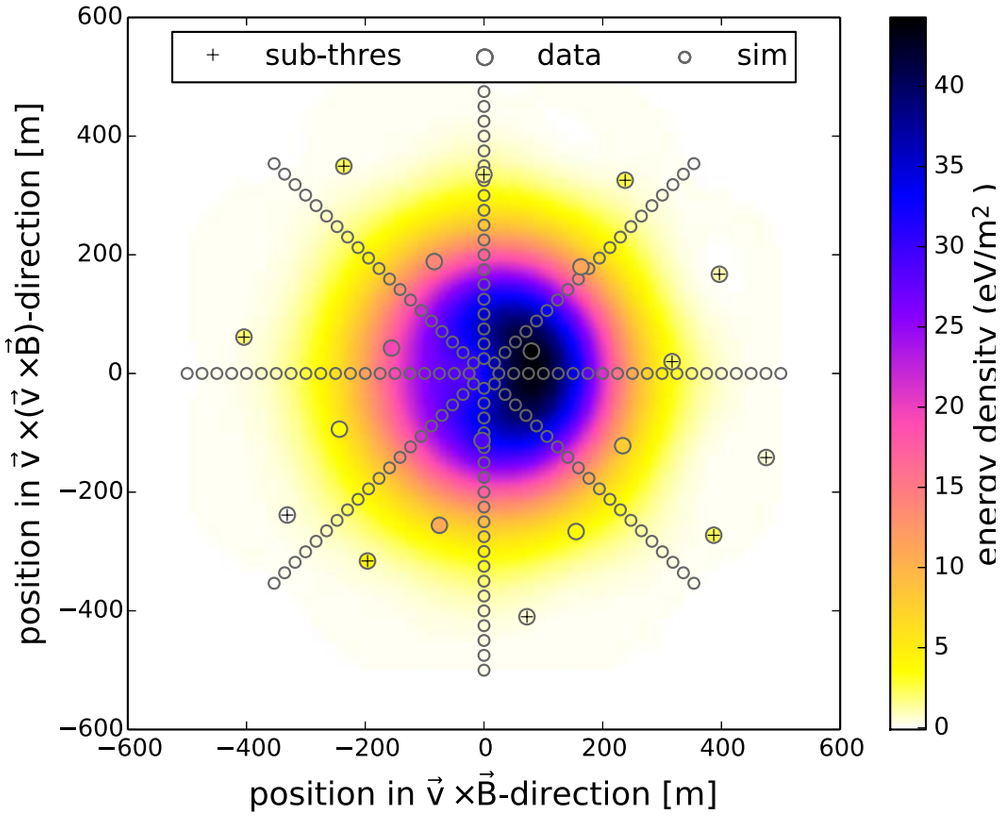

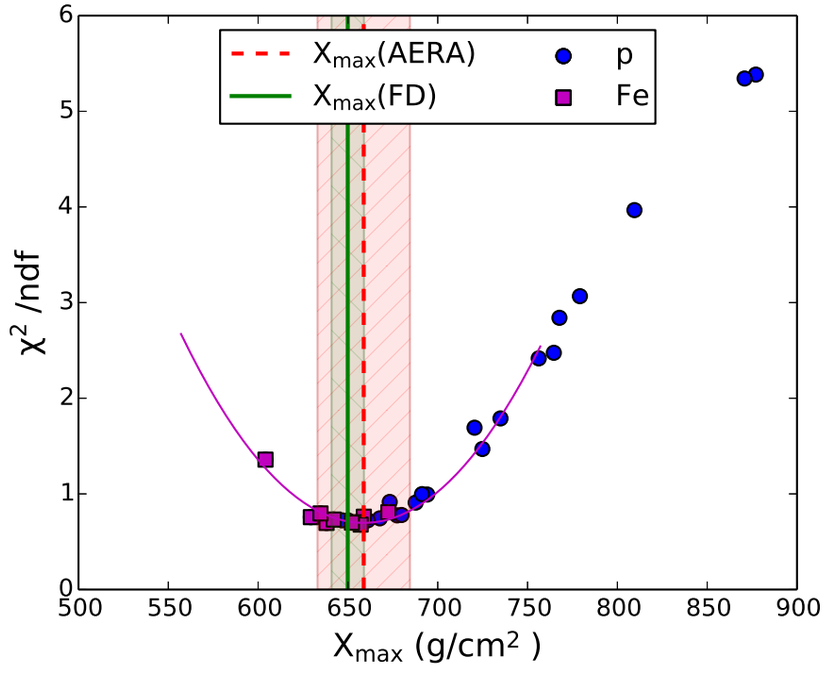

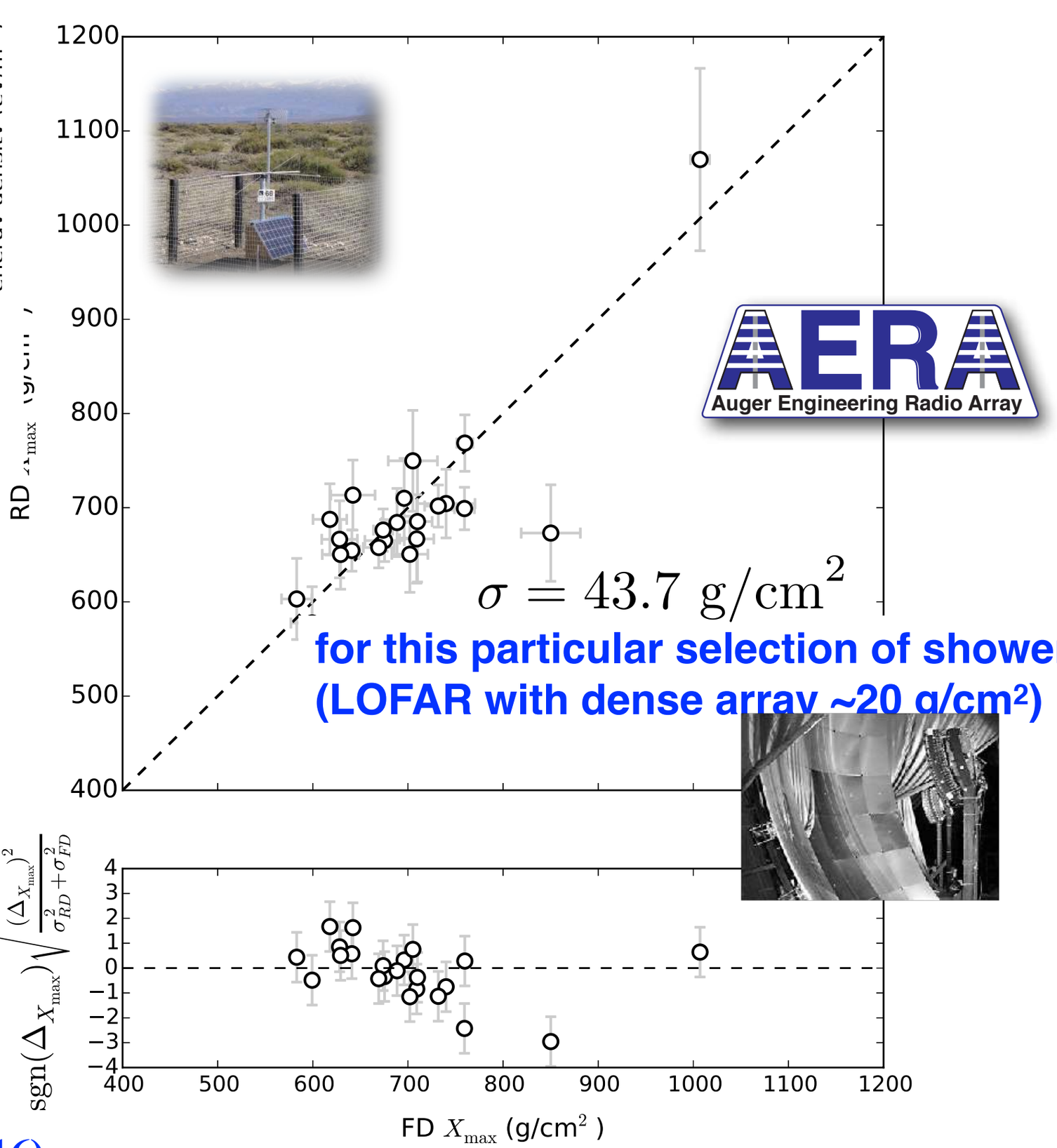

Auger Engineering Radio Array

for this particular selection of showers (LOFAR with dense array ~20 g/cm²)

J. Schulz, PhD thesis RU Nijmegen (2016)

Shower maximum: proof by Tunka-Rex

- One of several methods: slope of lateral distribution

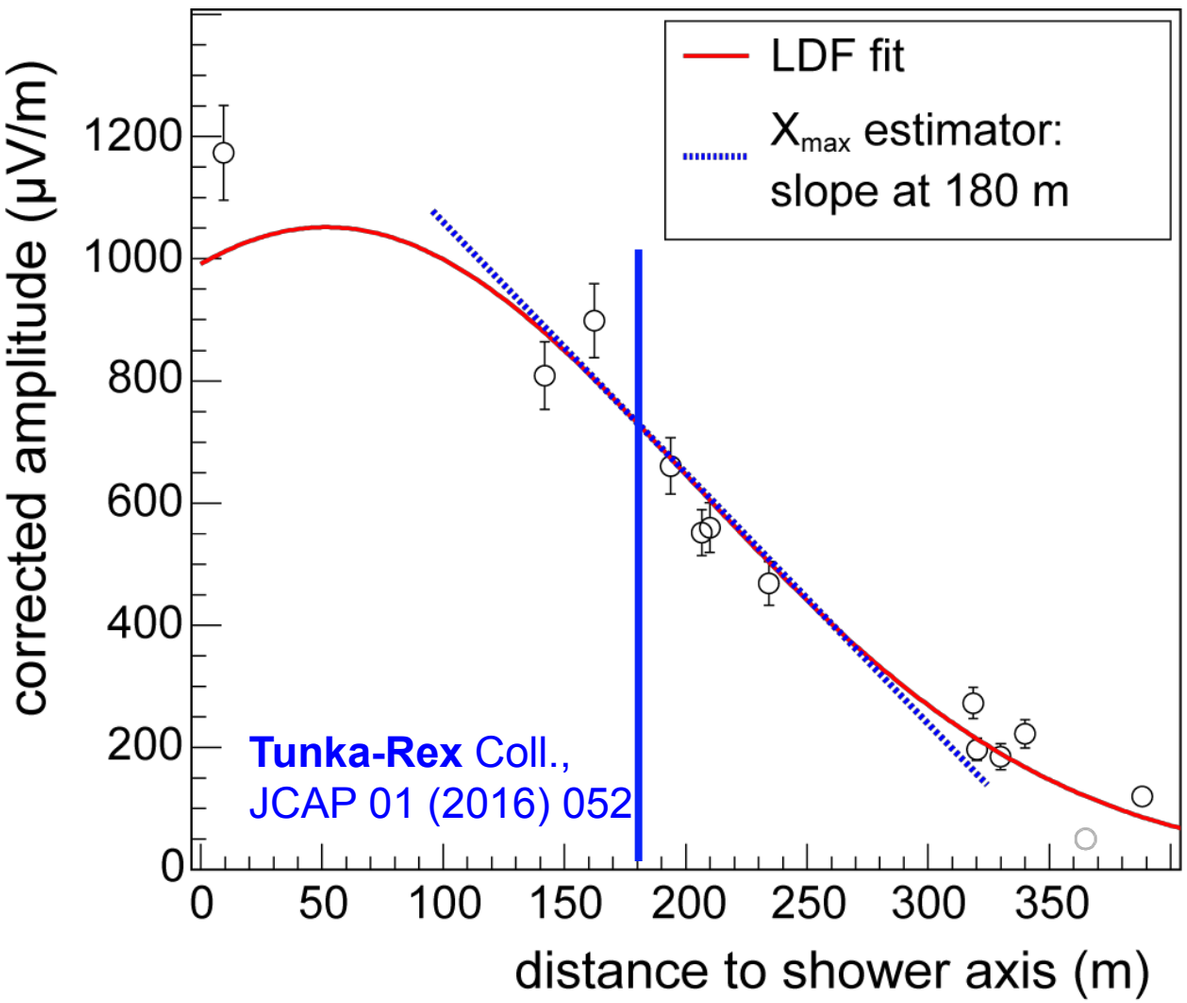

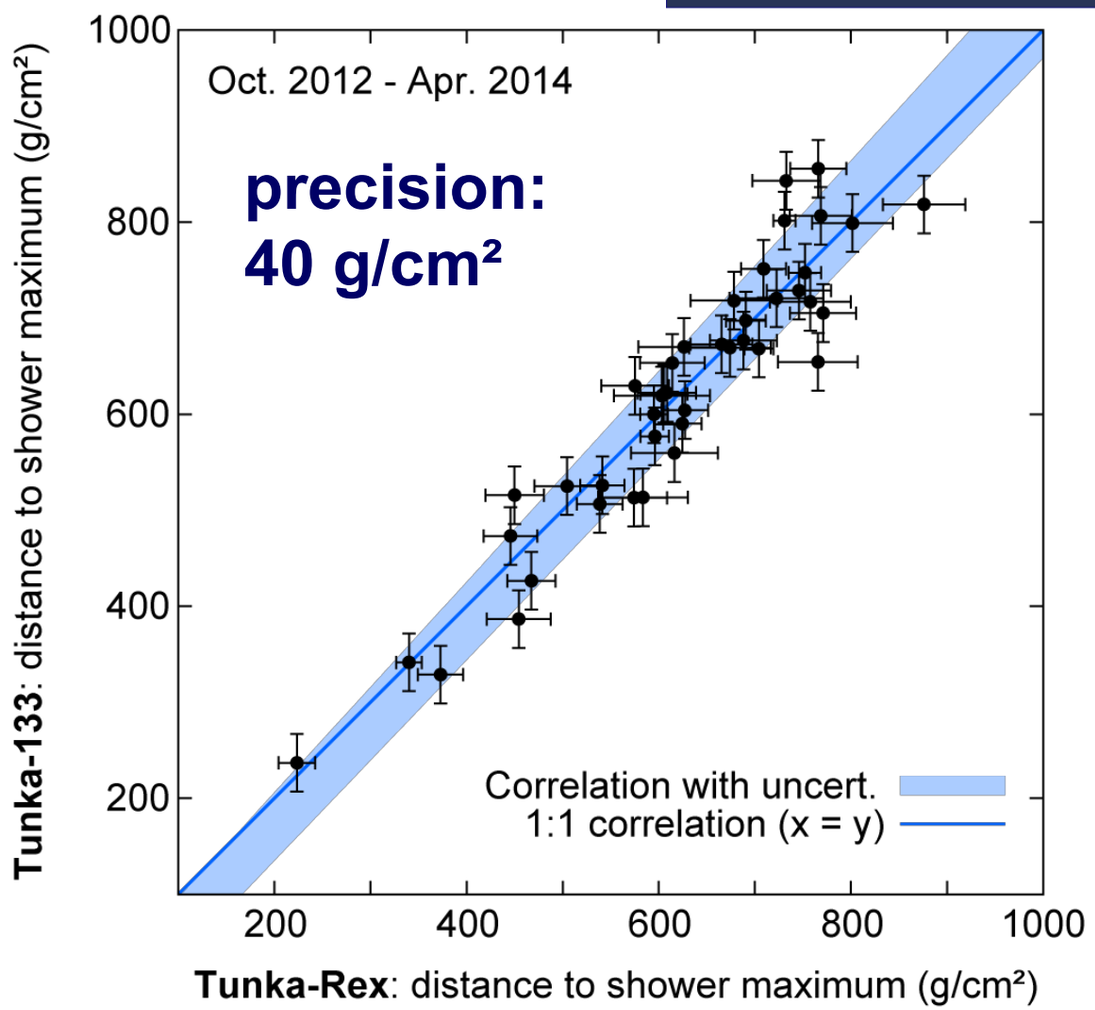

Determine the properties of the incoming particle with the radio technique

- direction ~ 0.1° - 0.5°
- energy ~ 20% - 30%
- type (X_{max}) ~ 20 - 40 g/cm^2

(depending on detector spacing)

—> radio technique is routinely used to measure properties of cosmic rays

Frequency spectrum analysis

Rationale:

→ Analytical calculations and simulation studies indicate a dependence of the **radio frequency spectrum** on cosmic-ray air **shower characteristics**

→ the goal is to **improve** the reconstruction of the shower parameters

Method:

→ characterization of the pattern of radio signals in the **frequency–domain**

→ the analysis has been applied to data collected by LOFAR since 2011 and to CORSIKA/CoREAS simulated showers

→ the following method has been applied to each antenna for each simulated/real event

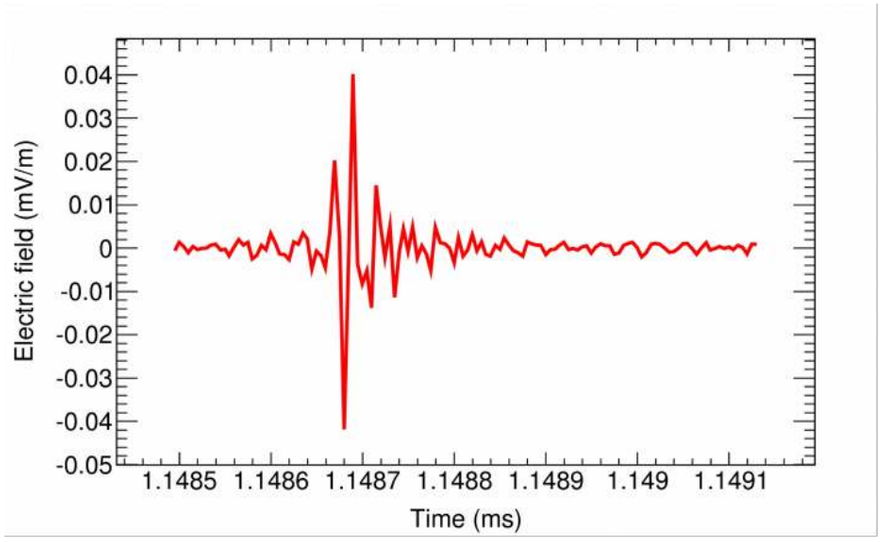

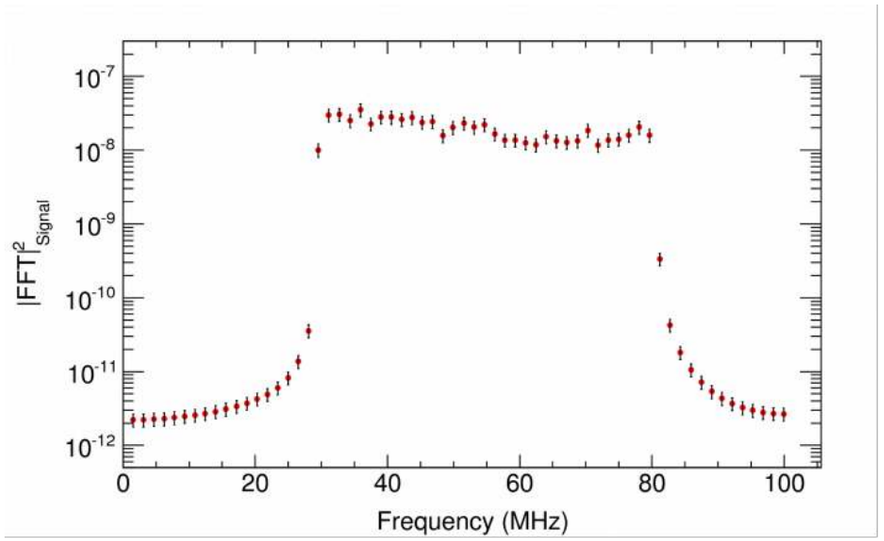

Frequency spectrum analysis: the method

1. Signal in the time–domain has been converted to the frequency–domain by applying a Fast Fourier Transform on Δt = 128 samples = 640 ns (1 sample = 5 ns)
2. $|\mathbf{FFT}|^2_{\mathbf{Signal}}$ → evaluated on $\Delta t = [\ t_0 - 240\ \text{ns}\ ,\ t_0 + 400\ \text{ns}\ ]$ where t_0 = time of the pulse–peak
3. $|\mathbf{FFT}|^2_{\mathbf{Background}}$ → evaluated on 400 sub-windows outside the pulse region
4. $|\mathbf{FFT}|^2 = |\mathbf{FFT}|^2_{\mathbf{Signal}} - |\mathbf{FFT}|^2_{\mathbf{Background}}$
5. linear fit applied to $\log_{10}|\text{FFT}|^2$ in the range ν = 33 – 70 MHz

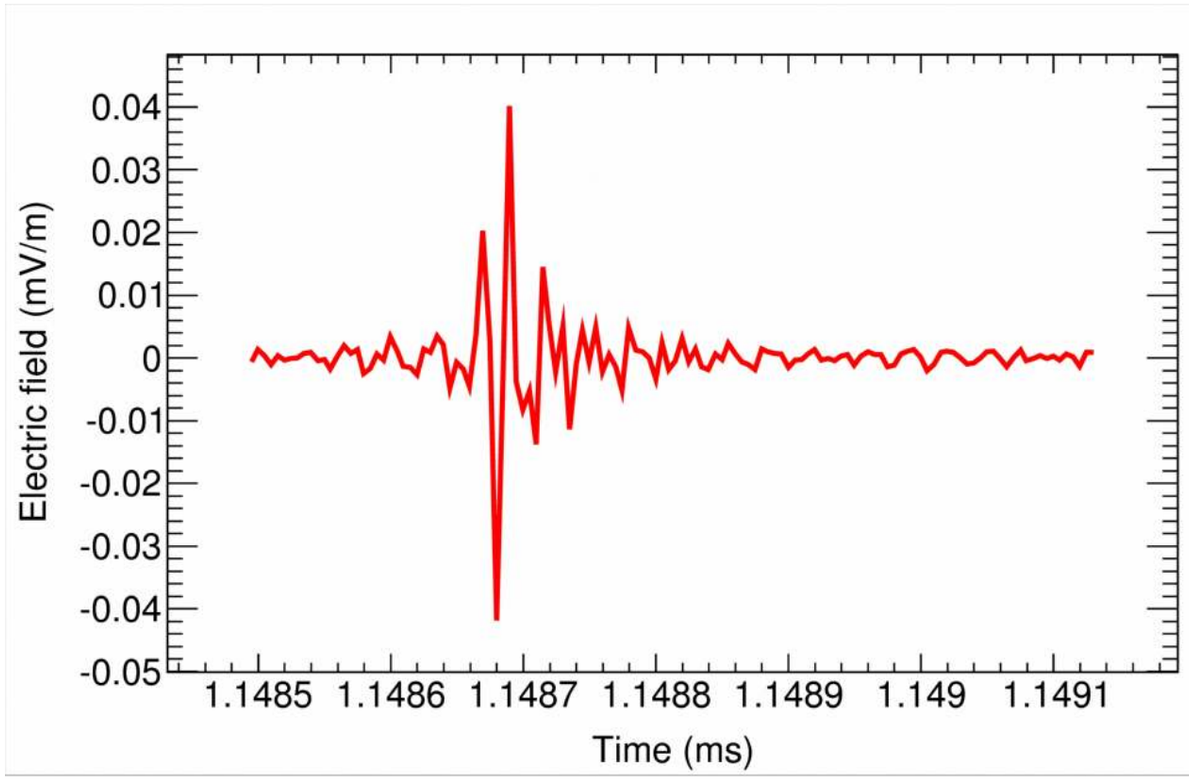

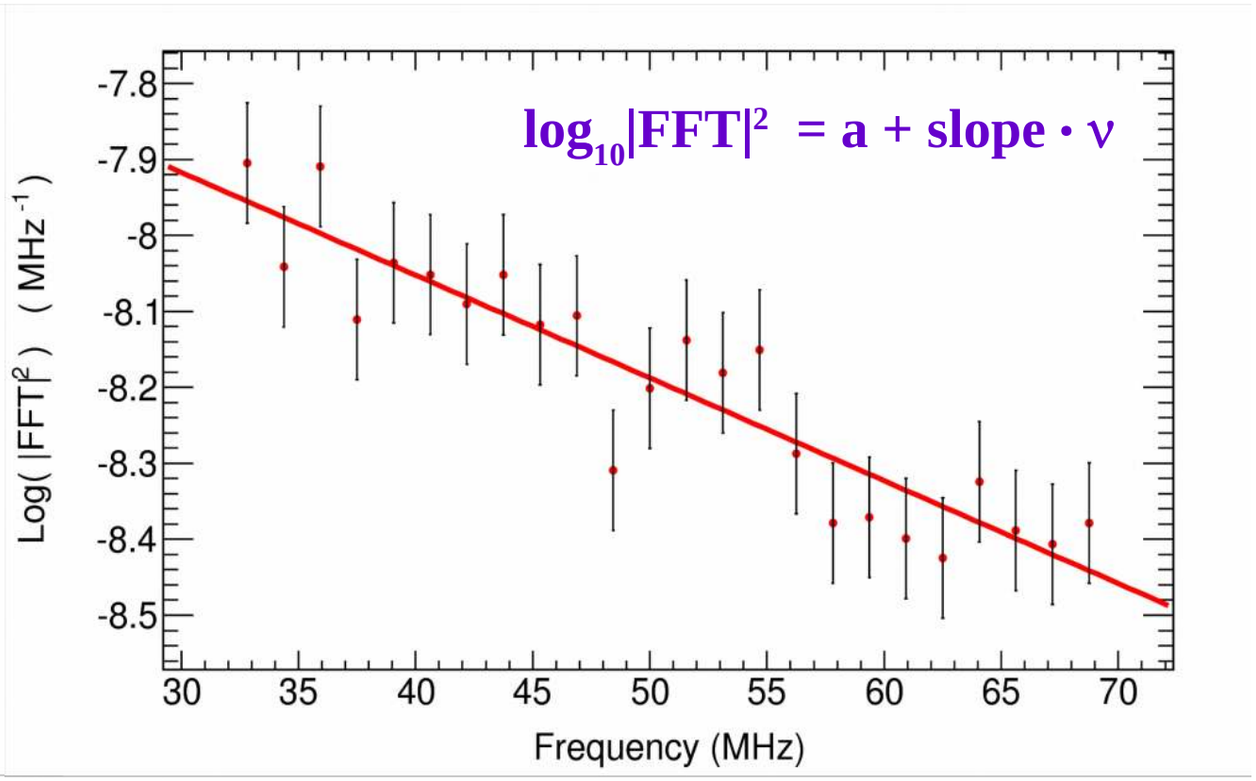

Frequency spectrum analysis: simulations

The **slope** of the frequency spectrum depends on

→ the **distance to the shower axis**

→ the **geometrical distance to X_{max}** (i.e. **D_{max}**)

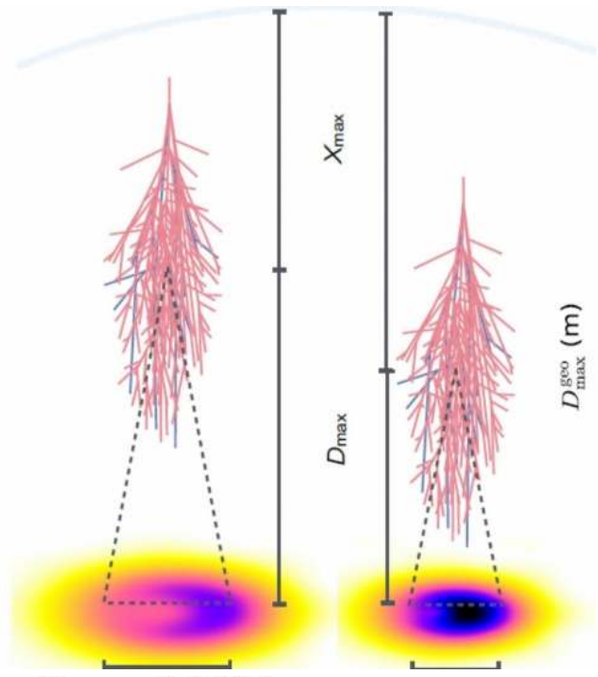

D_{max} = 2.312 km

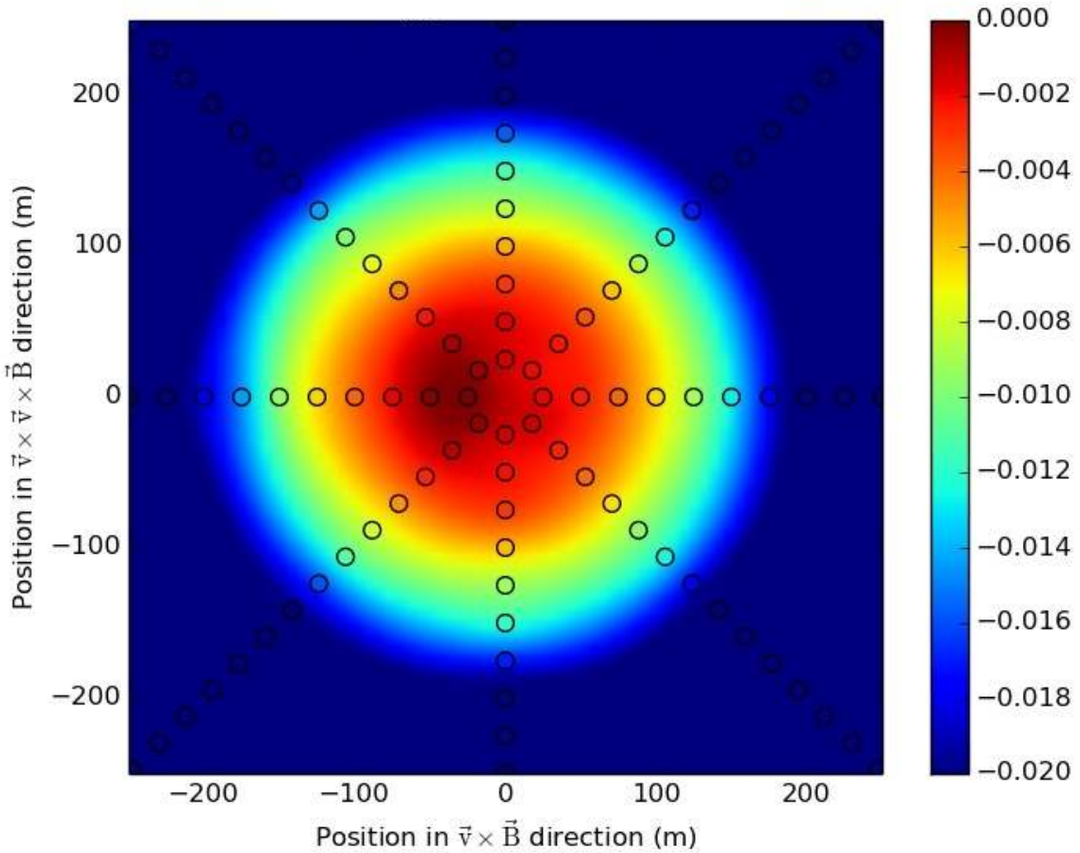

Frequency spectrum analysis: simulations

The **slope** of the frequency spectrum depends on

→ the **distance to the shower axis**

→ the **geometrical distance to X_{max}** (i.e. **D_{max}**)

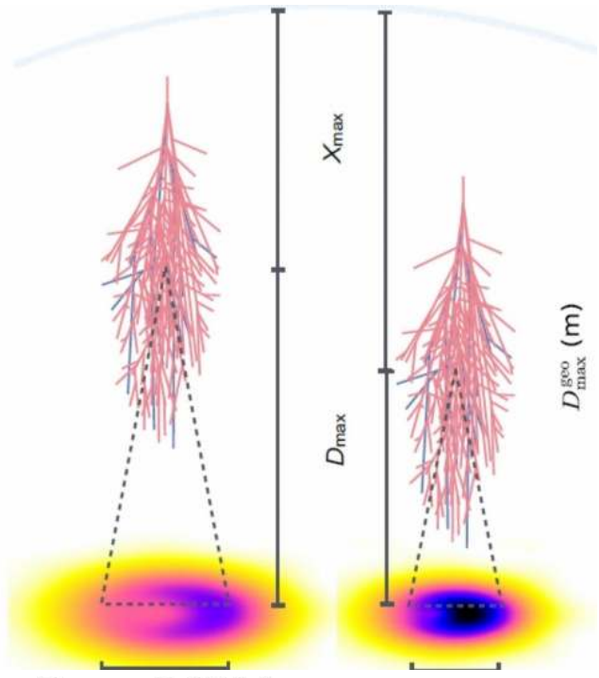

D_{max} = 3.899 km

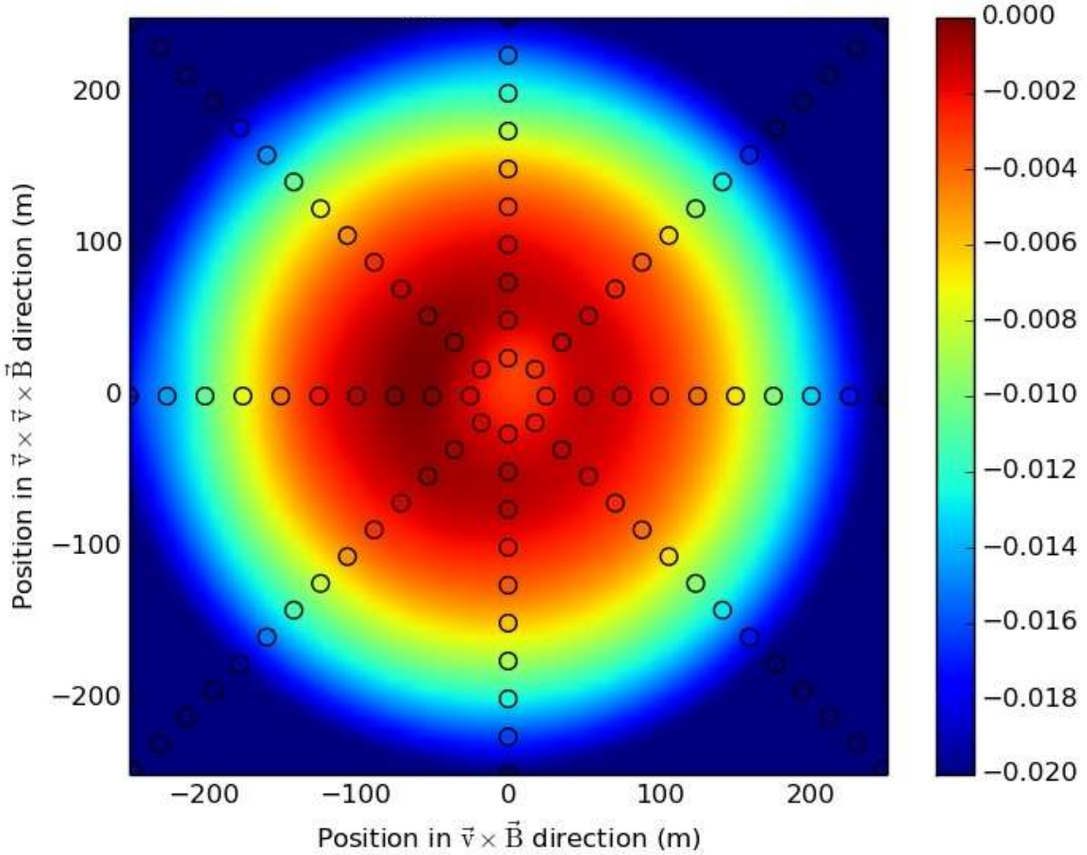

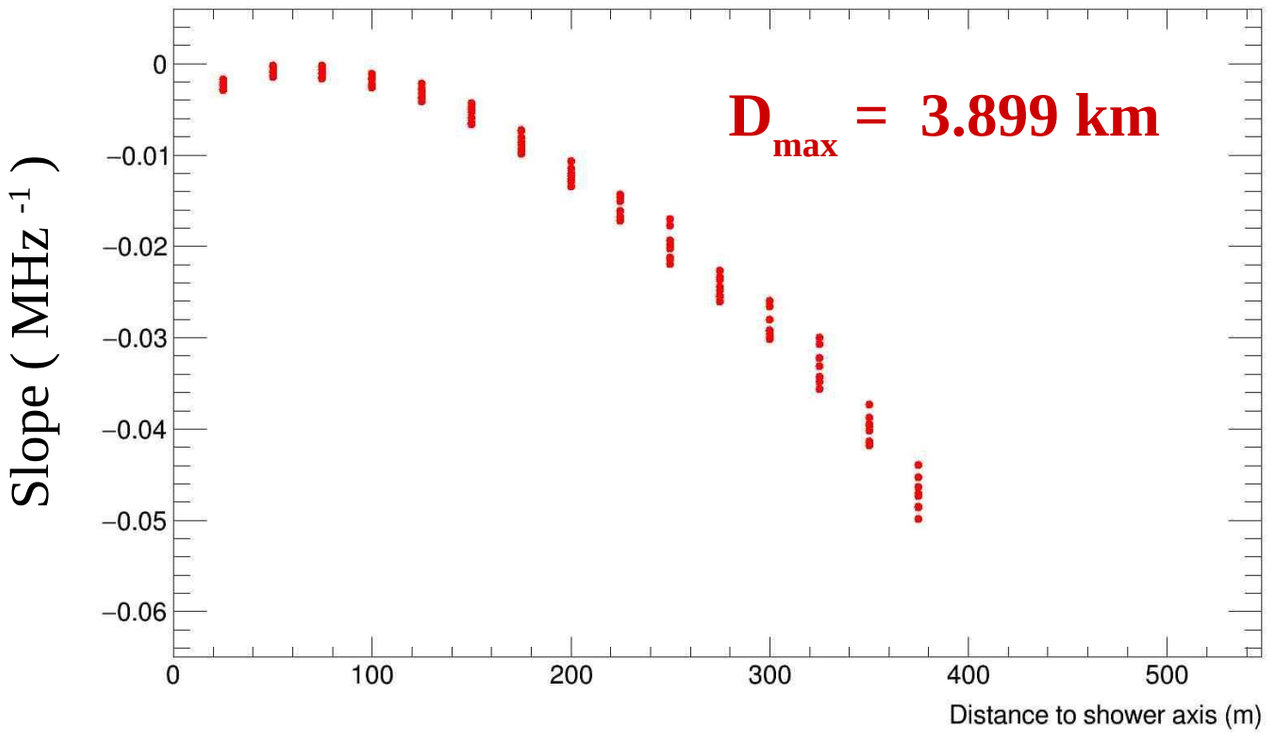

Frequency spectrum analysis: simulations

The **slope** of the frequency spectrum depends on

→ the **distance to the shower axis**

→ the **geometrical distance to X_{max}** (i.e. **D_{max}**)

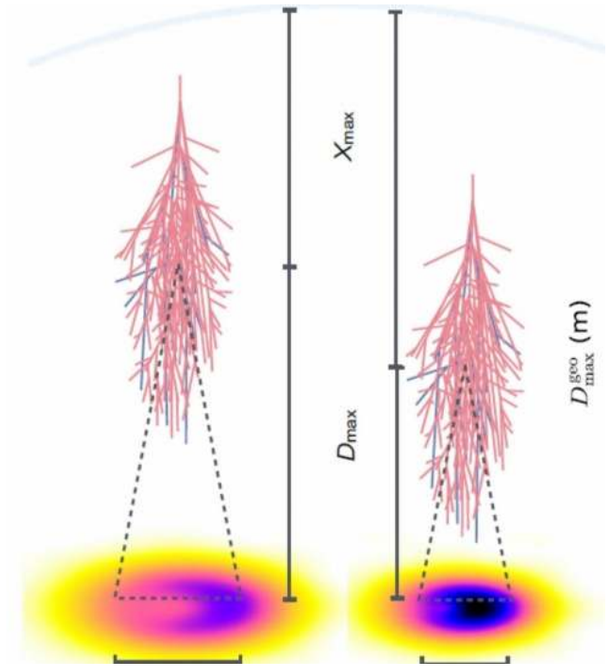

D_{max} = 5.319 km

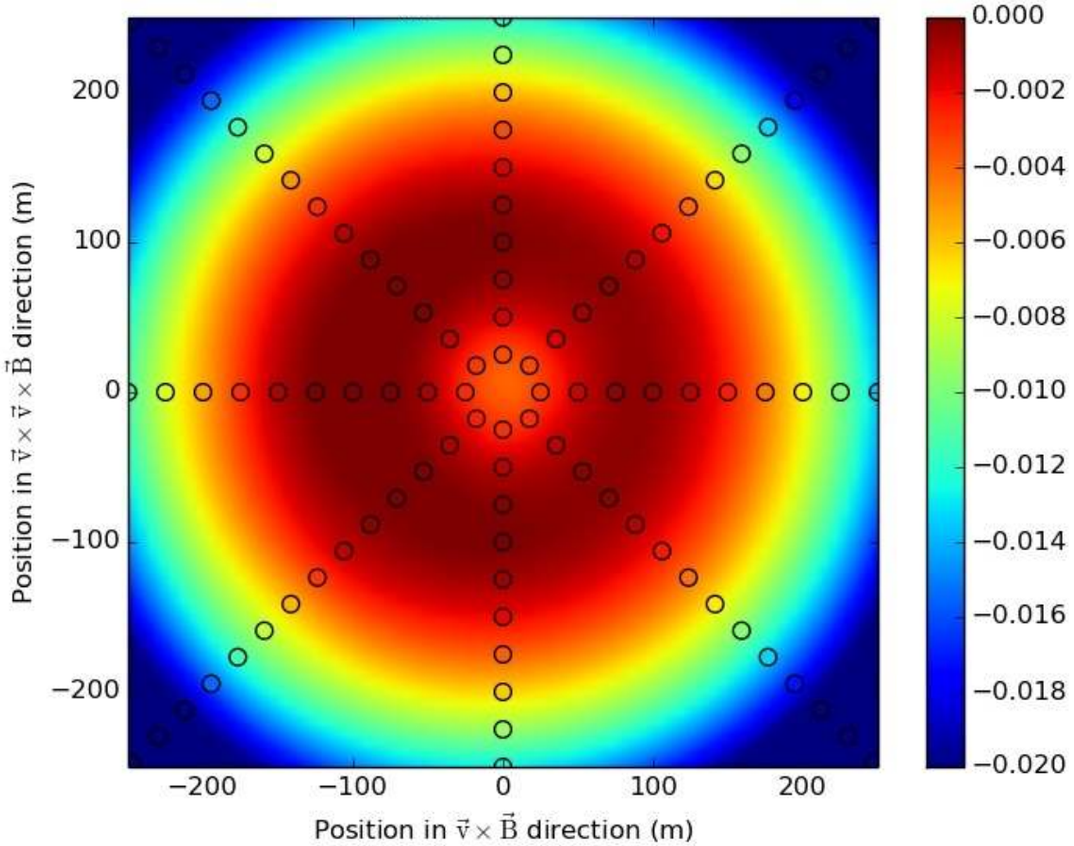

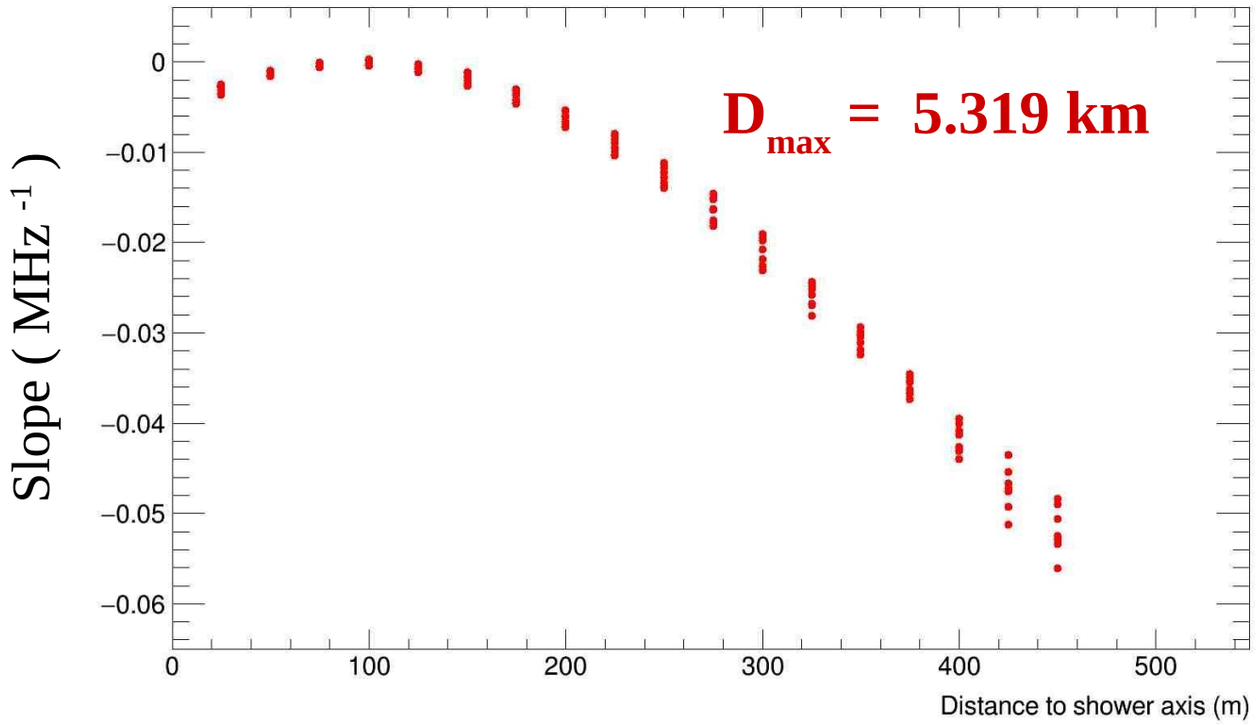

Comparison simulations – real data

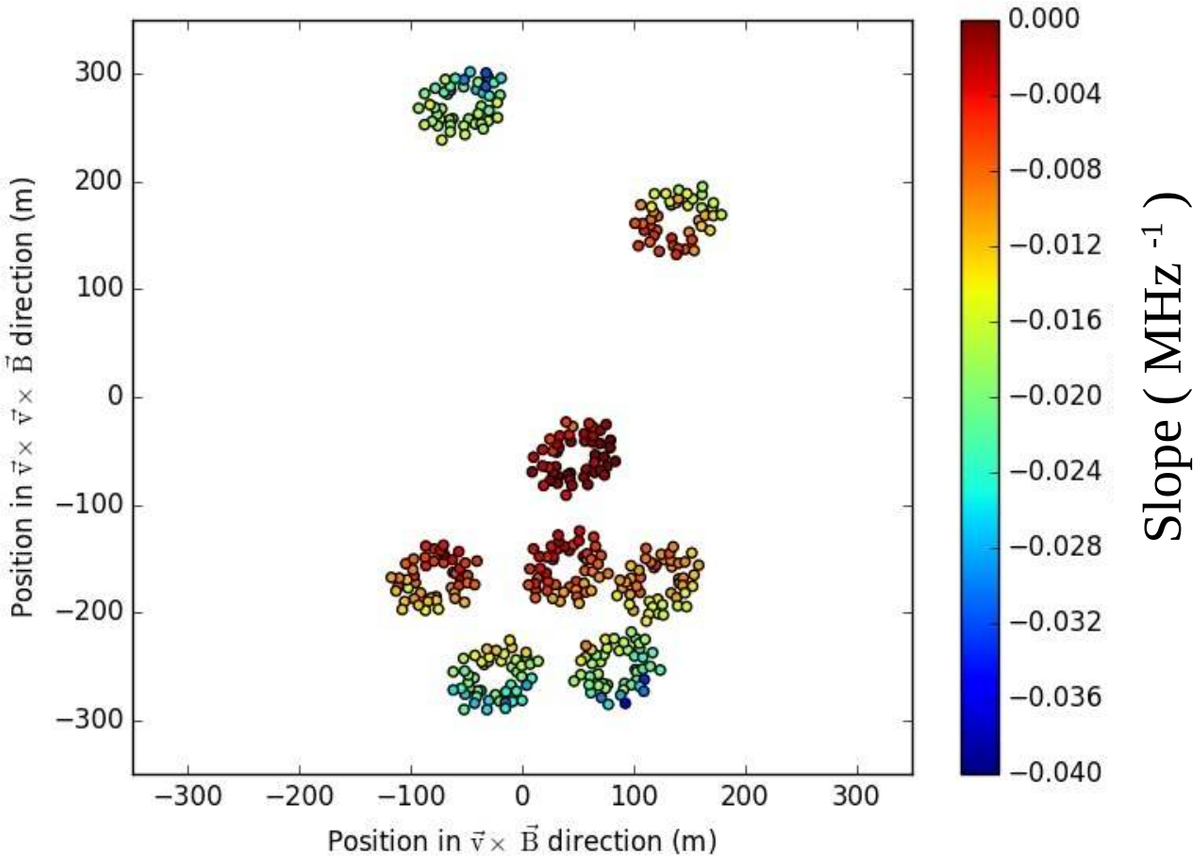

→ Event selection criteria:

1) at least 1 station with half antennas having signal > 10 σ → 142 events

2) events with at least 10 antennas with $|\mathrm{FFT}(\nu_i)|^2 > \mathrm{RMS}(|\mathrm{FFT}(\nu_i)|^2_{\mathrm{Background}})$

→ **103 events**

→ Linear–fit applied to all antennas of each selected event

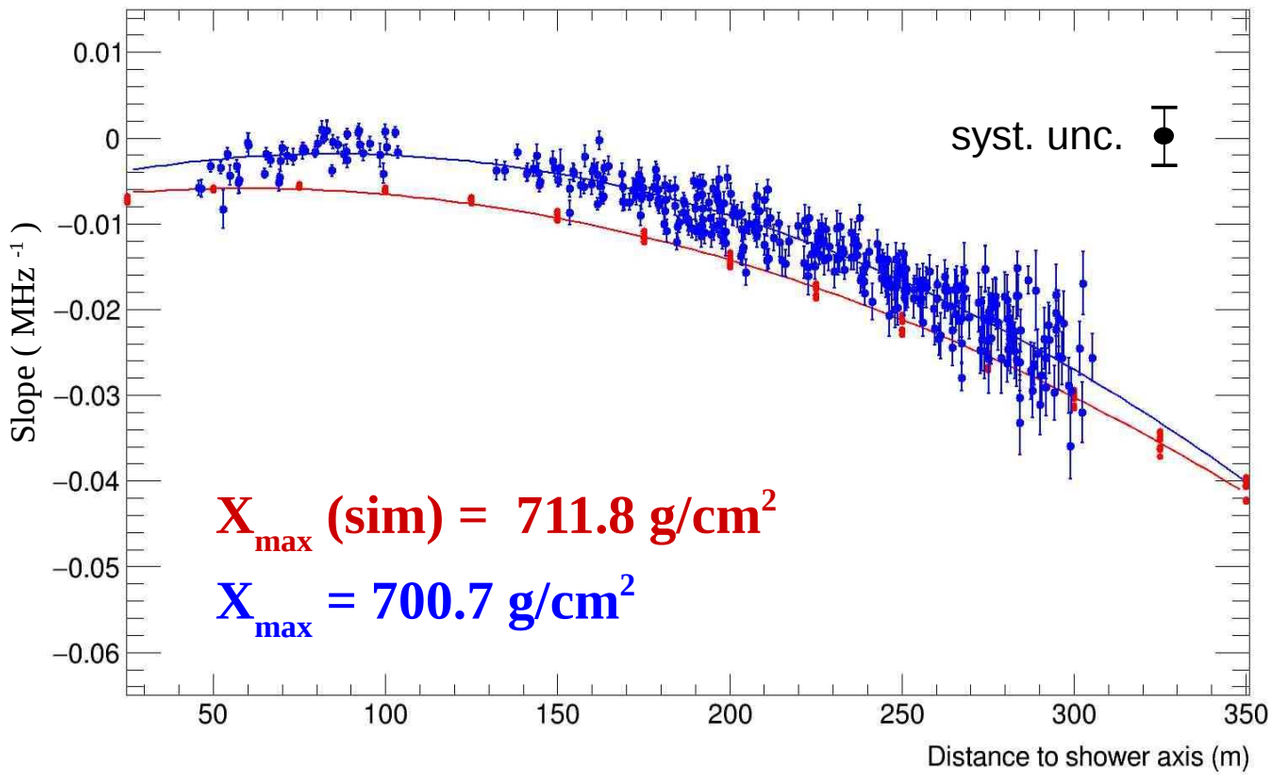

Linear–fit slope as function of distance to shower axis:

→ follows a **parabolic function**

→ **maximum around 100 m** in agreement with the Cherenkov ring region

→ **sensitive to frequency range**

Real data results – D_{max} correlation

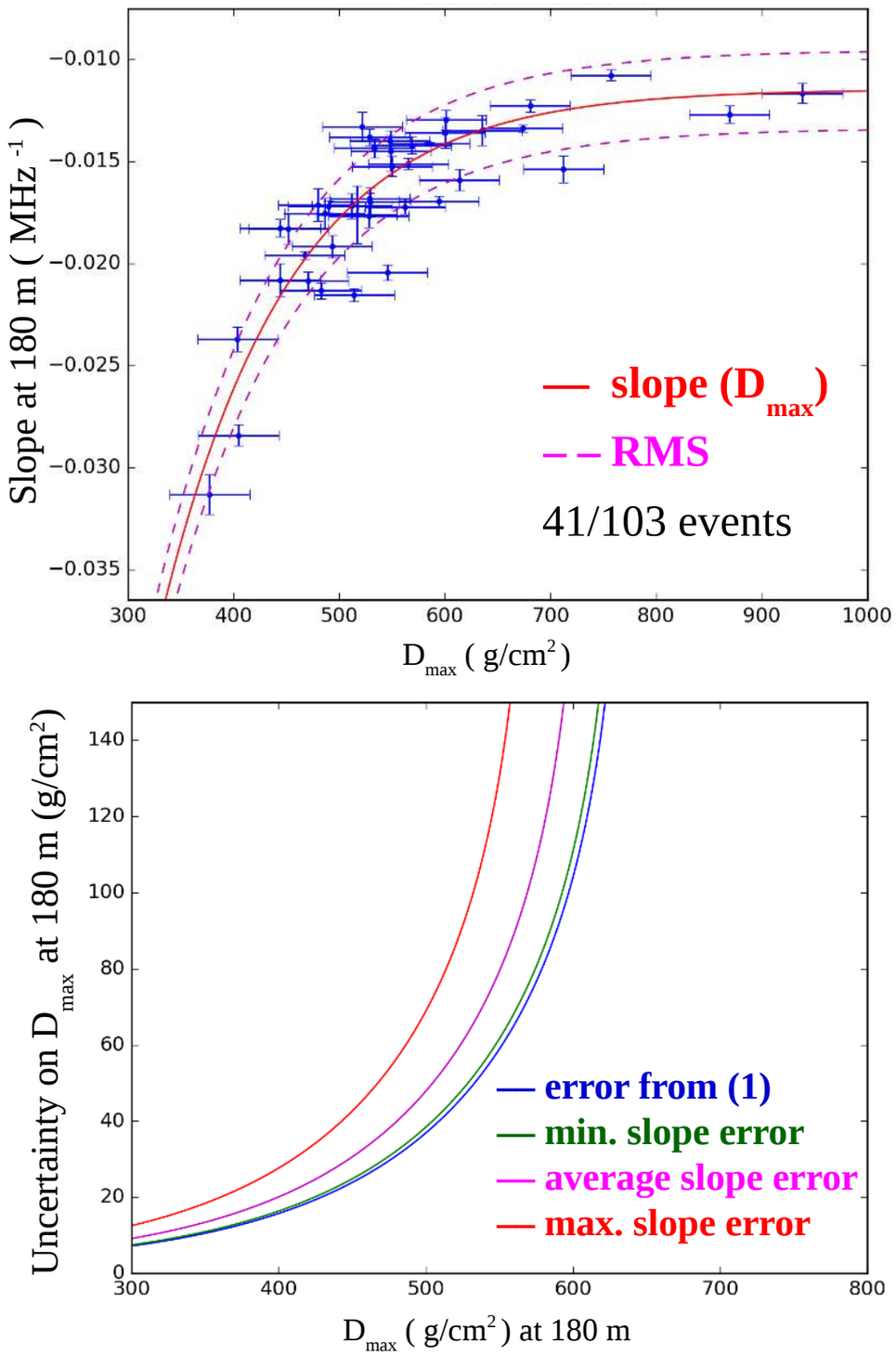

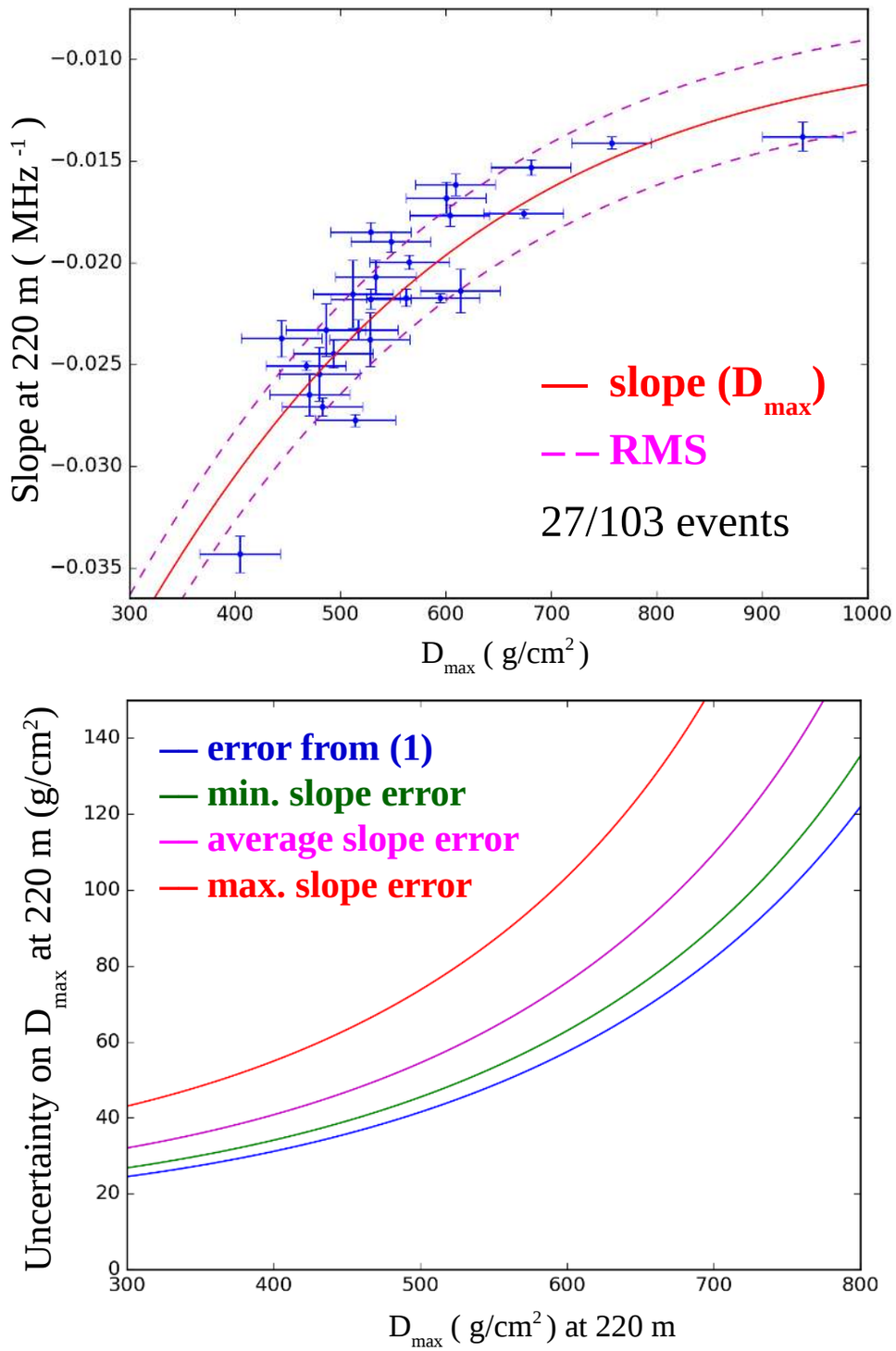


The Future
NEXT EXIT

Extension of scintillator array (LORA)

LOFAR

S. Buitink
K. Mulrey

2.5 km

Existing station

New station

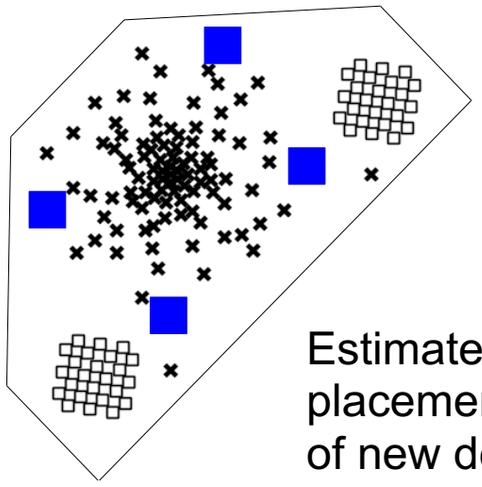

Estimated placement of new detectors

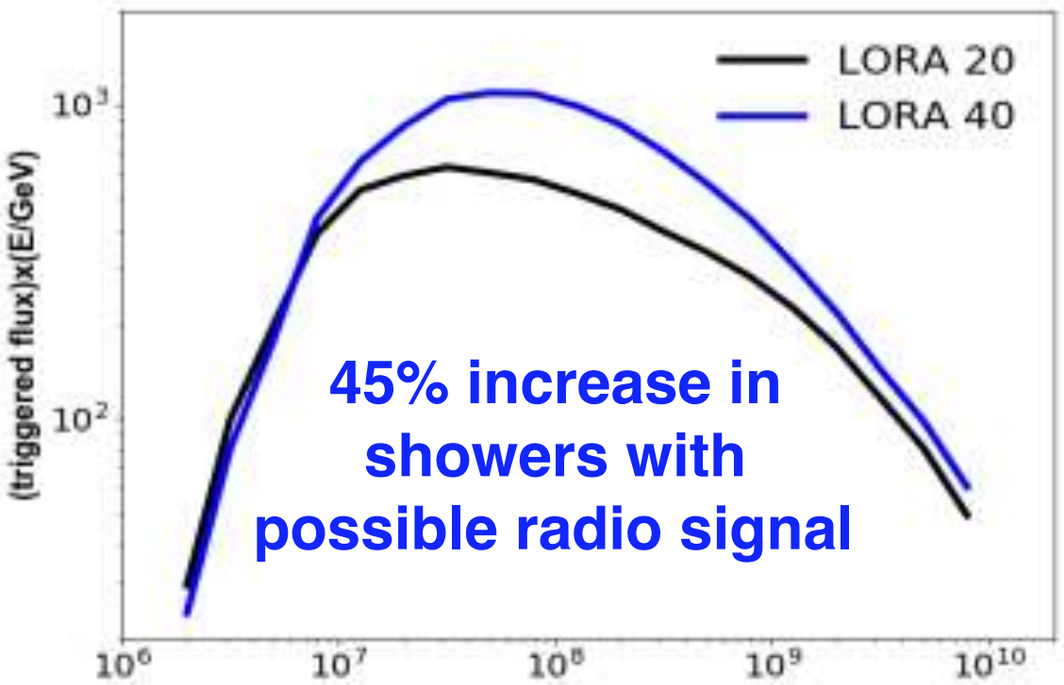

10^{16} eV 10^{18} eV

adding 20 scintillator stations in 2018

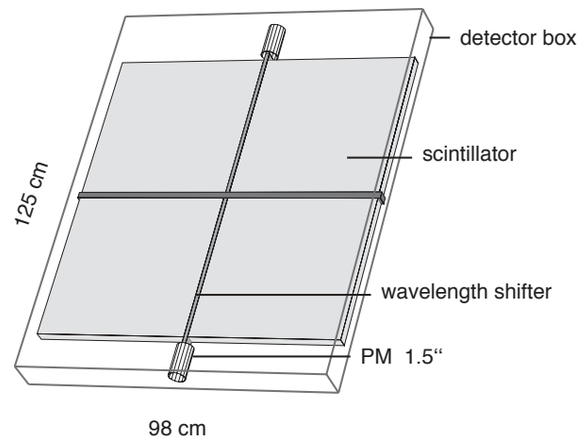

Upgrade of the Pierre Auger Observatory
(astro-)physics of the highest-energy particles in nature

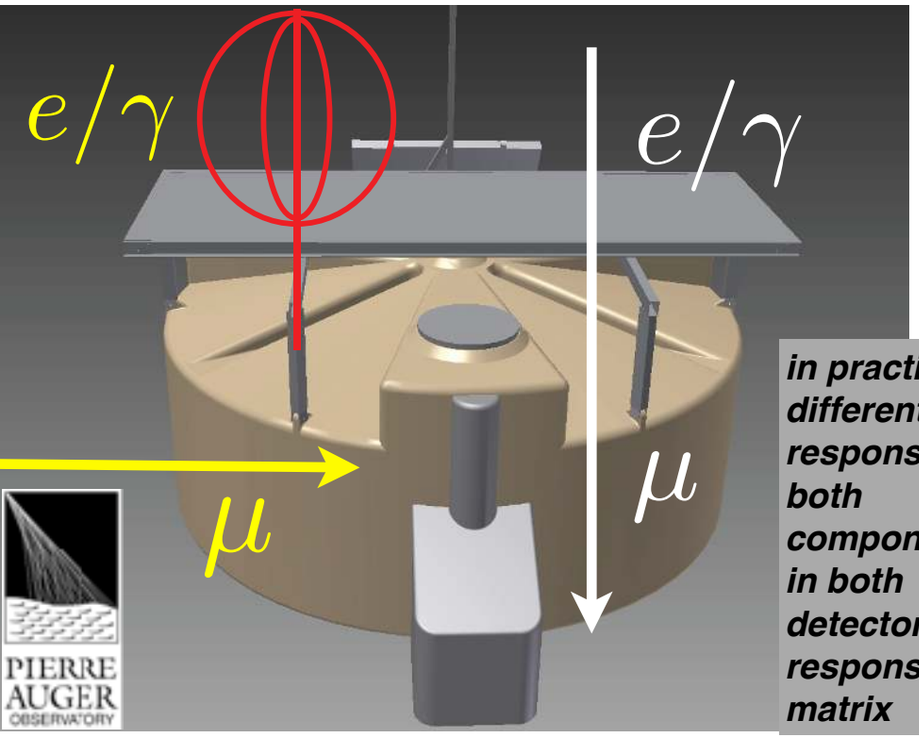

in practice: different response to both components in both detectors: response matrix

upgrade PAO

- electronics
- scintillator layer
- radio detector

Key science questions

- What are the sources and acceleration mechanisms of ultra-high-energy cosmic rays (UHECRs)?
- Do we understand particle acceleration and physics at energies well beyond the LHC (Large Hadron Collider) scale?
- What is the fraction of protons, photons, and neutrinos in cosmic rays at the highest energies?

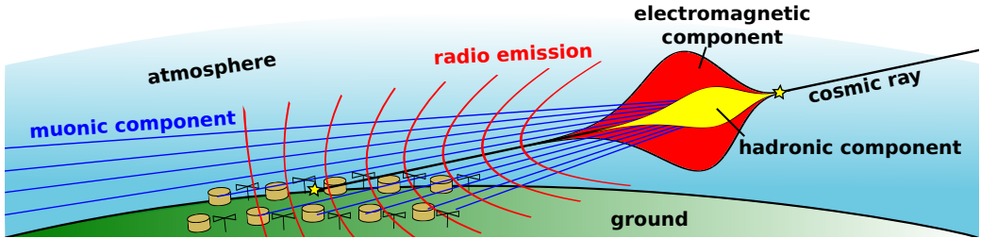

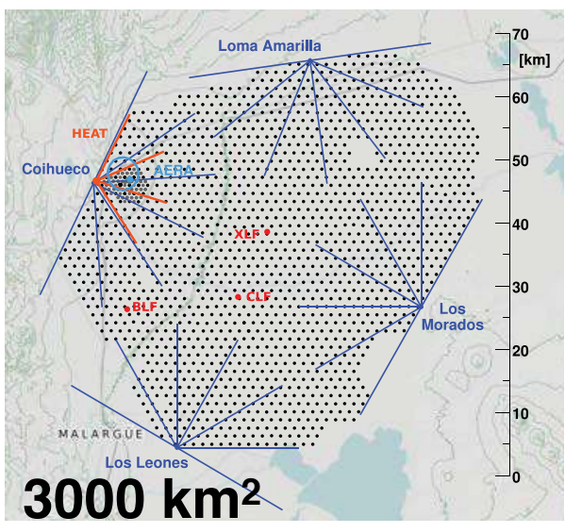

3000 km²

Advanced Grant Hörandel 2018

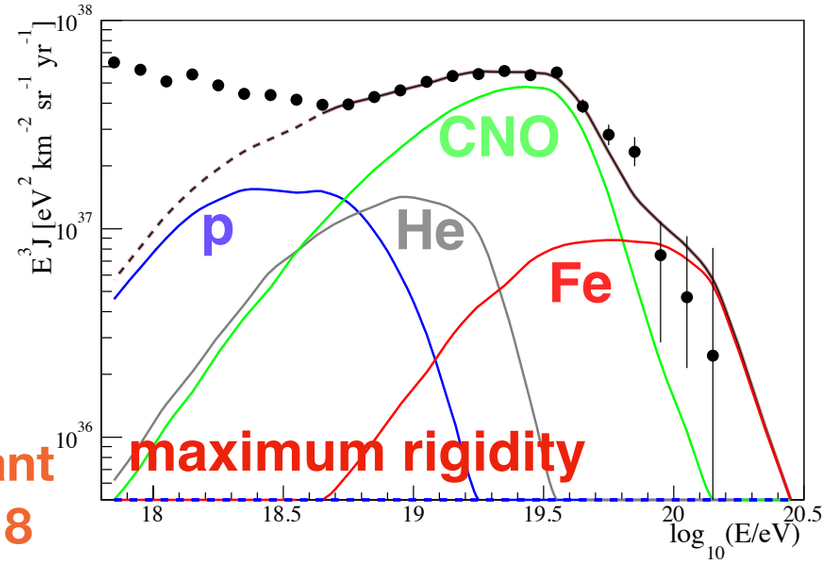

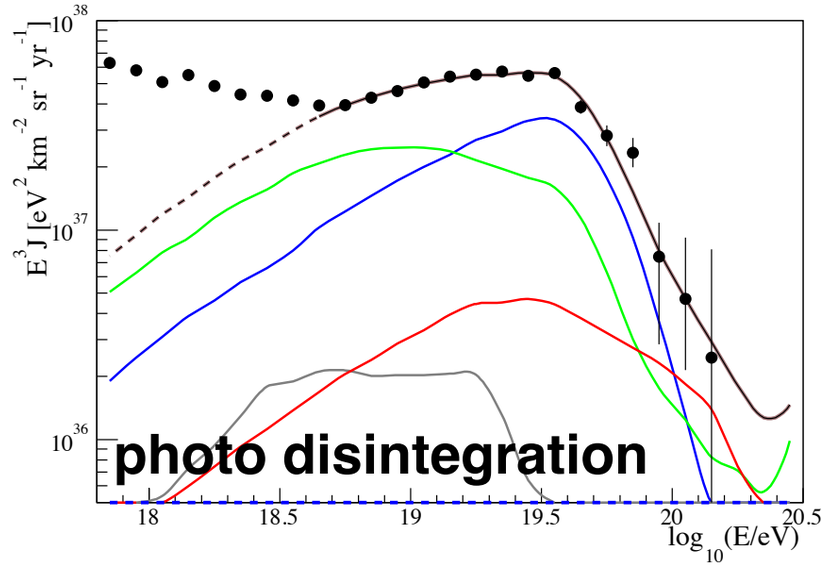

A large radio array the Pierre Auger Observatory

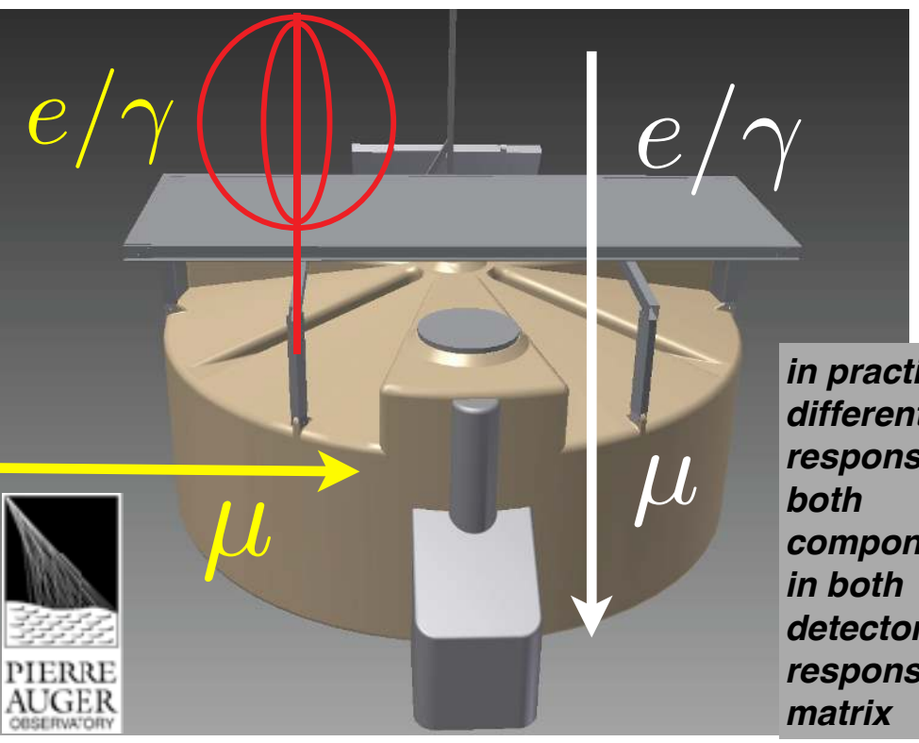

in practice: different response to both components in both detectors: response matrix

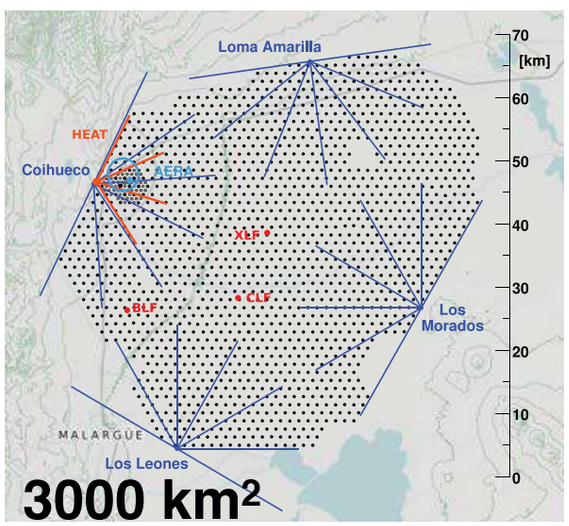

3000 km²

Advanced Grant Hörandel 2018

objective

- origin of cosmic rays
- type of particle up to highest energies
- isolate protons, photons, neutrinos
- extend e/m-muon separation to high zenith angles
  --> horizontal air showers
  (i.e. increase exposure of SSD analyses)
- increase the sky coverage/overlap with TA
- absolute energy calibration from 1st principles
- independent mass scale
- clean e/m measurement
  --> shower physics

A large radio array the Pierre Auger Observatory

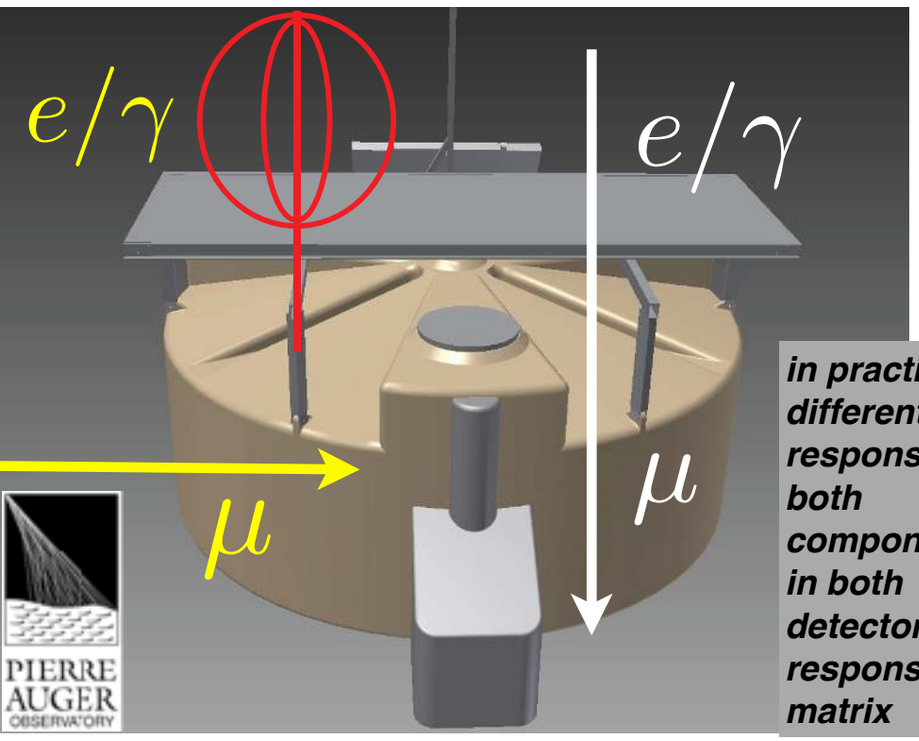

in practice: different response to both components in both detectors: response matrix

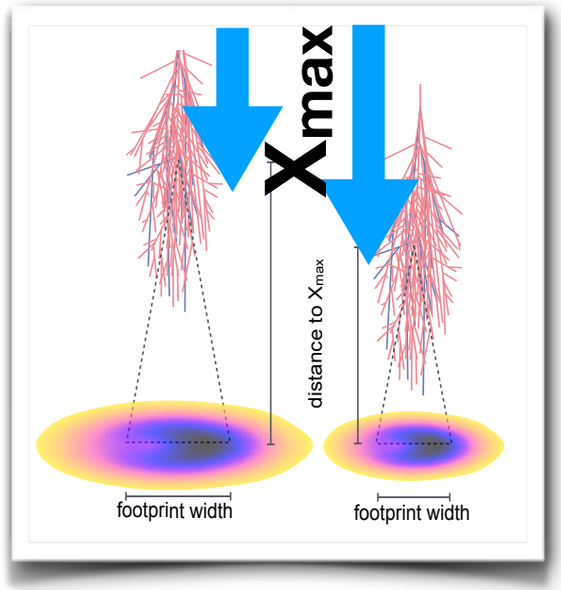

attention:
type of particle determined

for vertical showers:

size of footprint
geometrical measurement

for horizontal showers:

electron/muon ratio
important: radio emission not absorbed in atmosphere

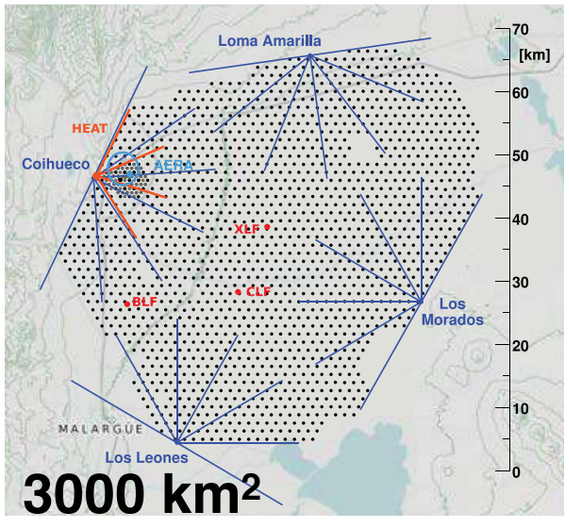

3000 km²

Advanced Grant Hörandel 2018

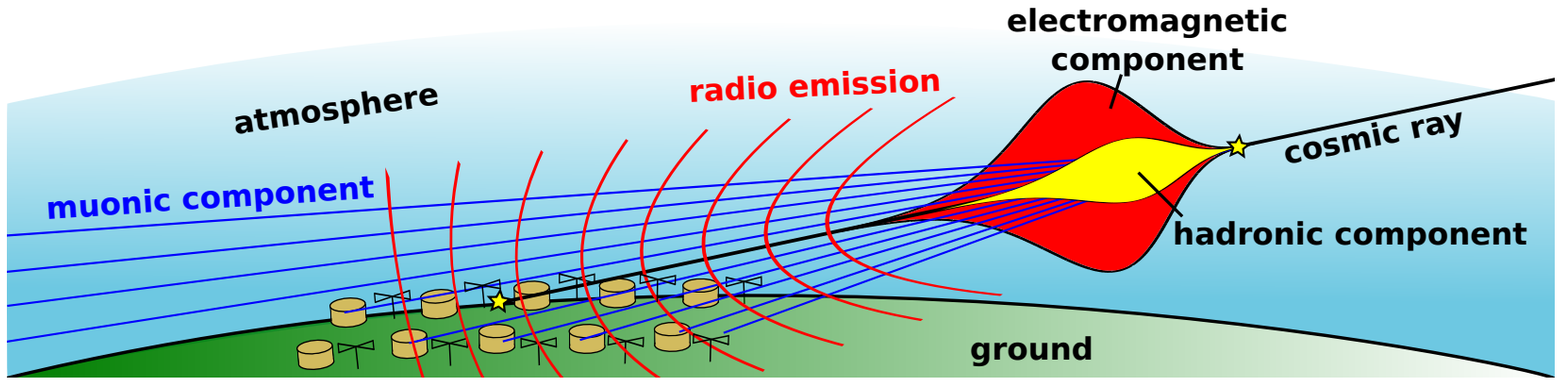

Radio detector provides good mass separation

J.R. Hörandel

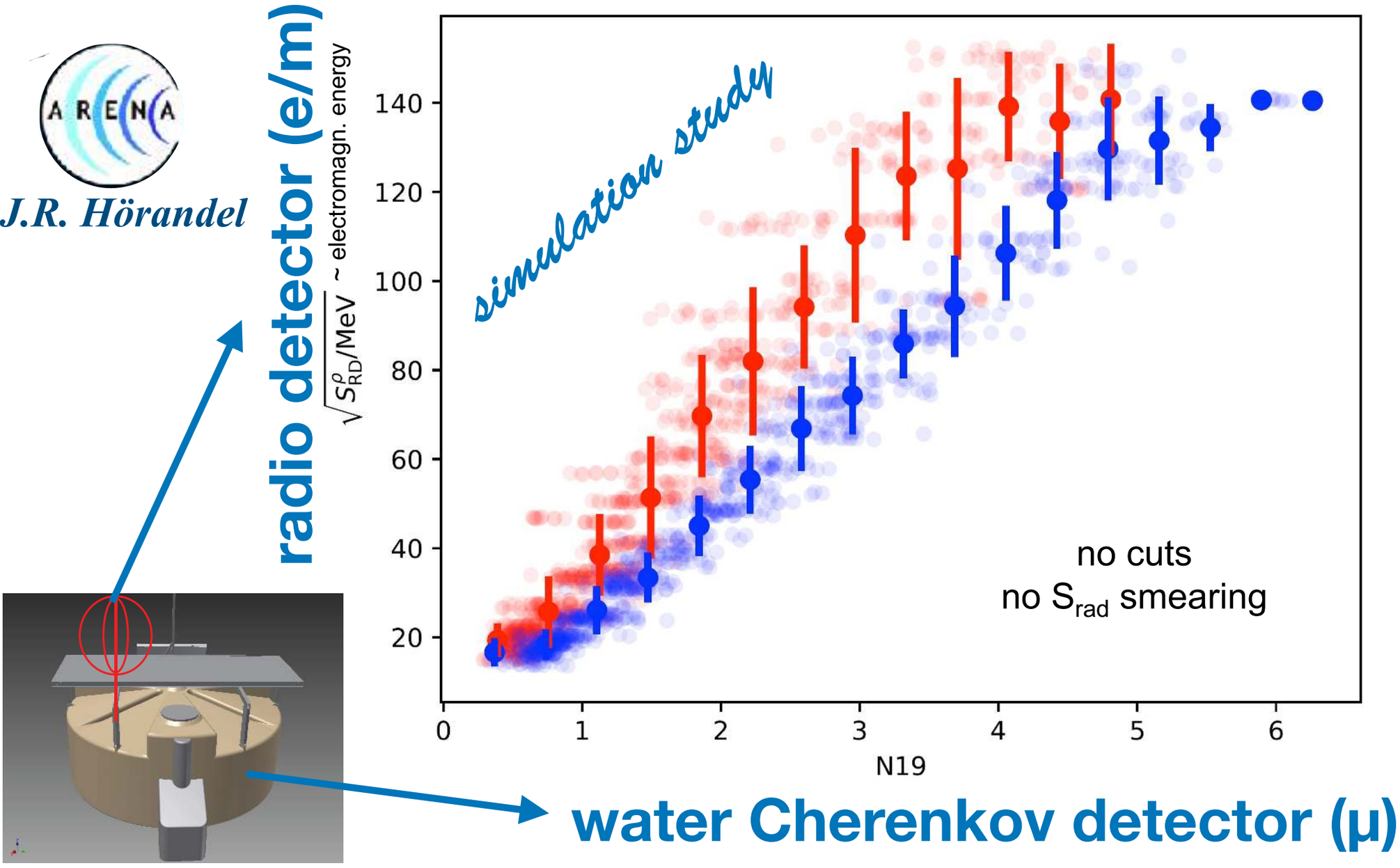

- can separate species with S_{rad} and N19
- separation increases with energy
- scaling at highest energies probably artifact of maximum simulated energy

A large radio array at the Pierre Auger Observatory

preparatory work & feasibility

AERA 17 km²
--> 3000 km²

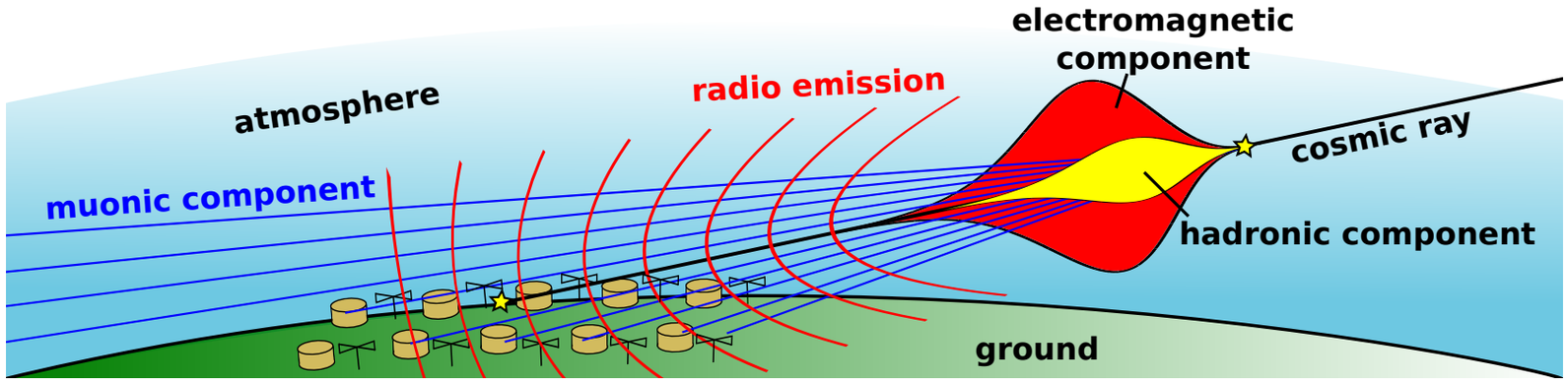

expect large radio footprint from simulations

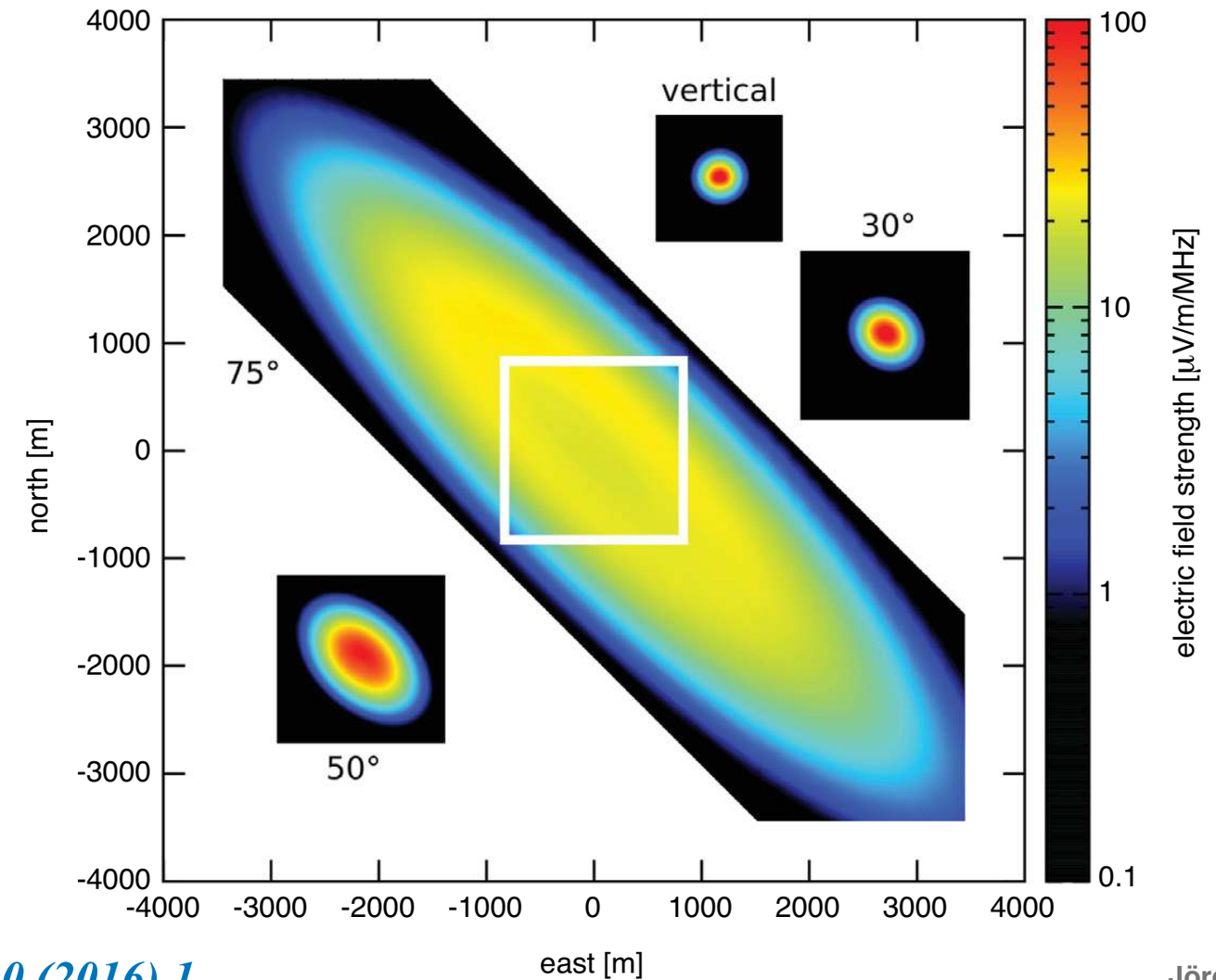

see e.g. T. Huege, Phys. Rep. 620 (2016) 1

A large radio array at the Pierre Auger Observatory

preparatory work & feasibility

AERA 17 km²
--> 3000 km²

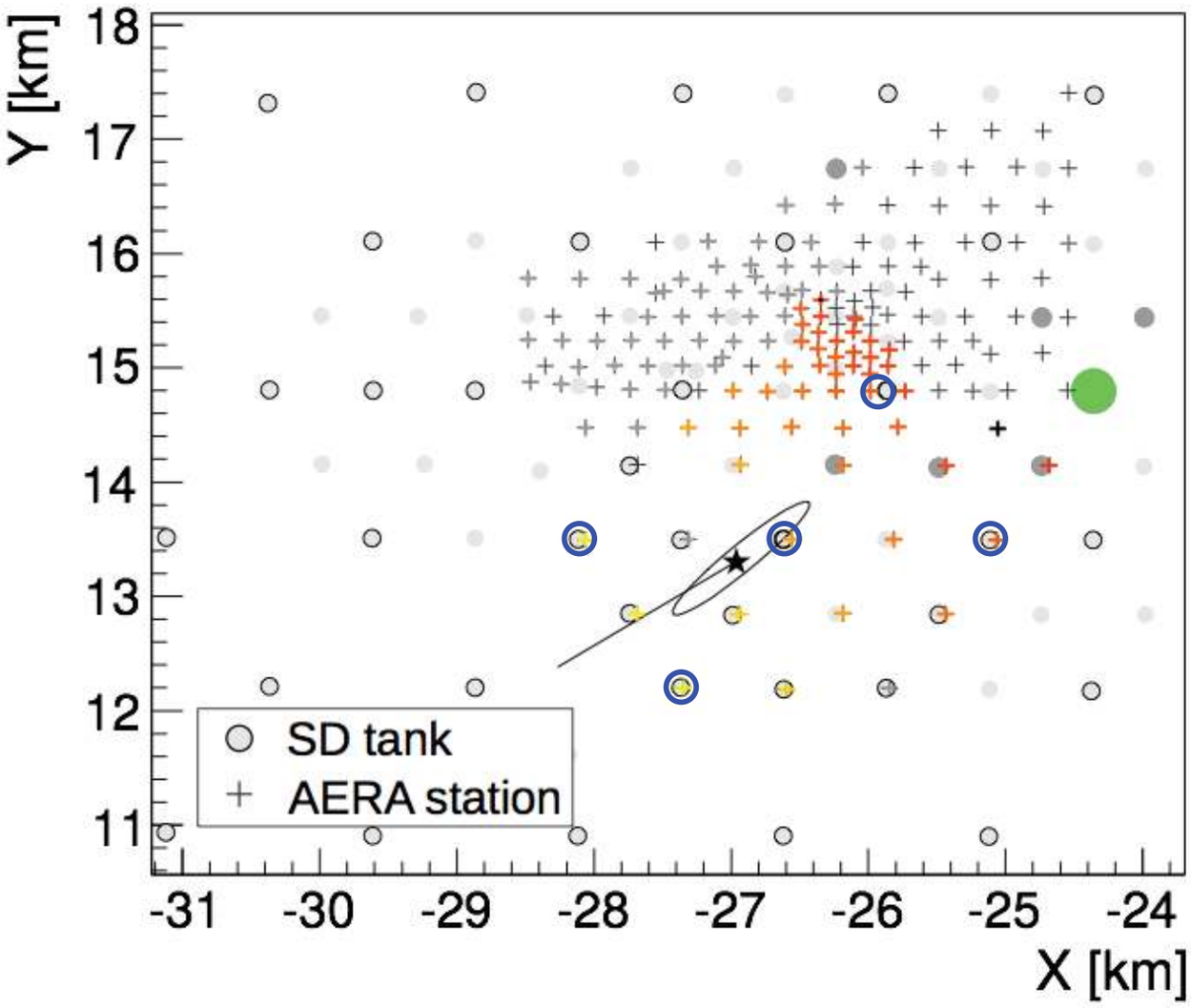

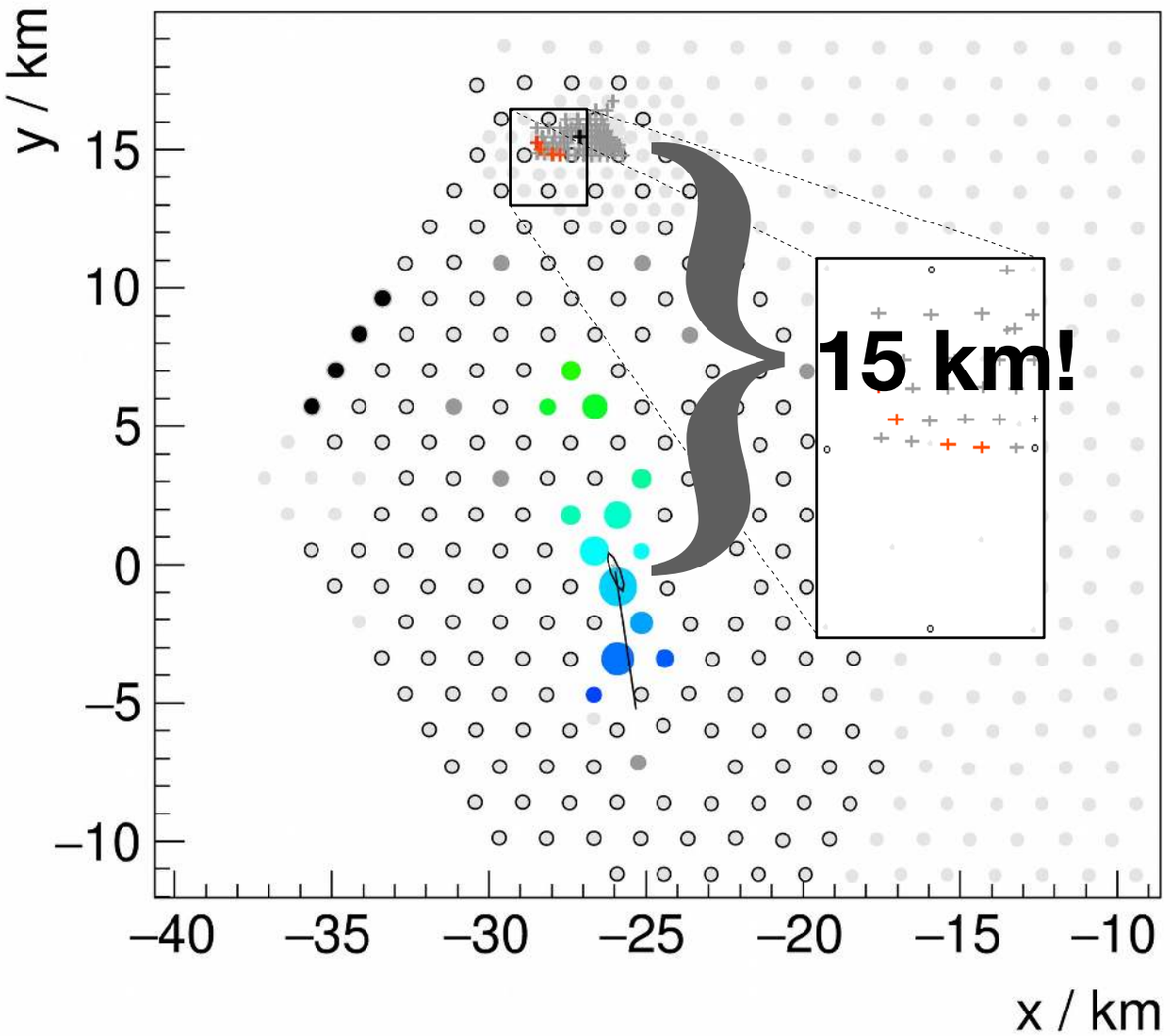

horizontal air showers registered and reconstructed with existing AERA

Pierre Auger coll. submitted (2018) arXiv: 1806.05386

Horizontal air showers have large footprints in radio emission

M. Gottowik

AERA 17 km²
--> 3000 km²

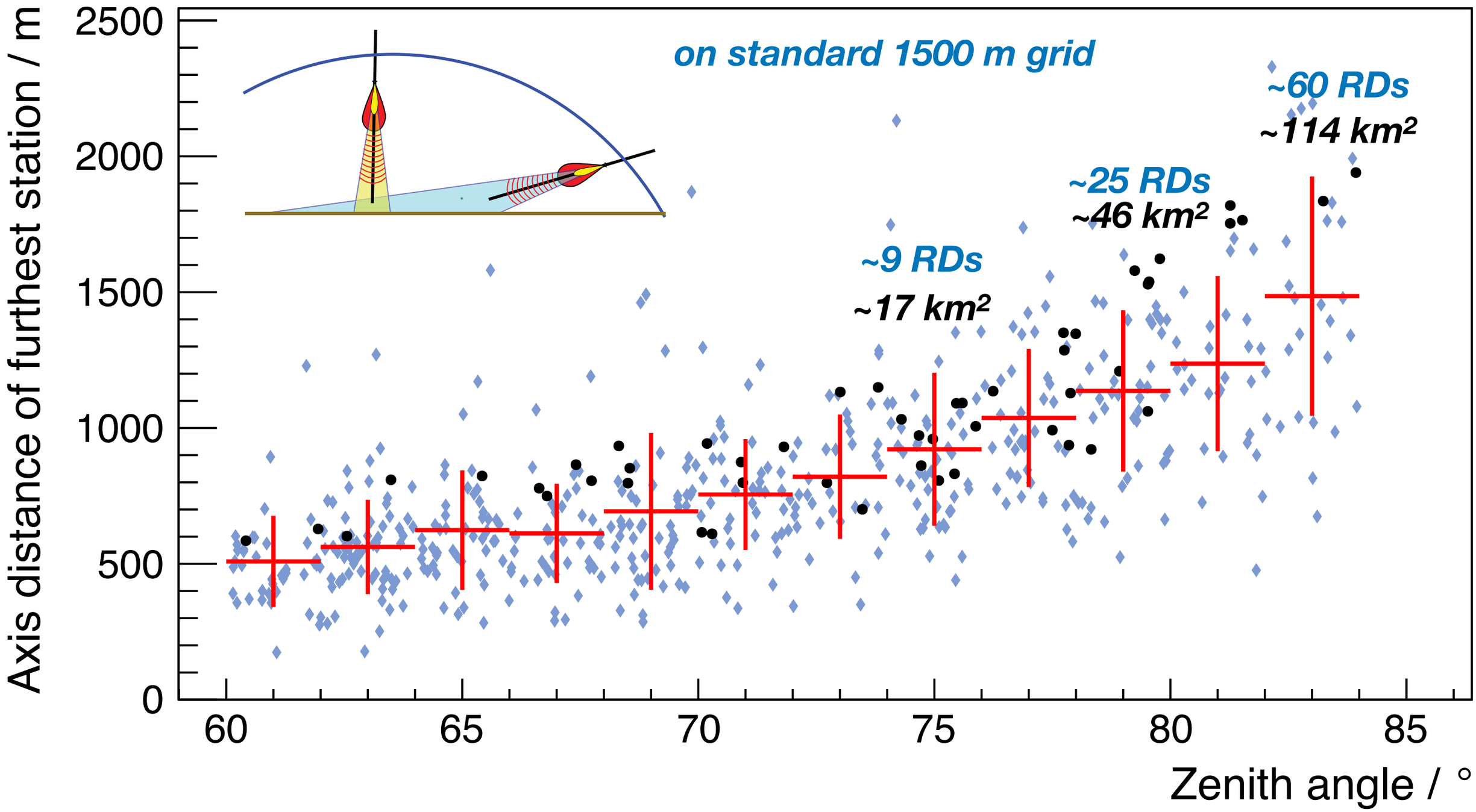

this is MEASURED with the *small* 17km² AERA

Pierre Auger coll. submitted (2018) arXiv: 1806.05386

Radio Antenna - SALLA

Our default antenna is the SALLA antenna.

Well known from Tunka-REX and prototypes at PAO.

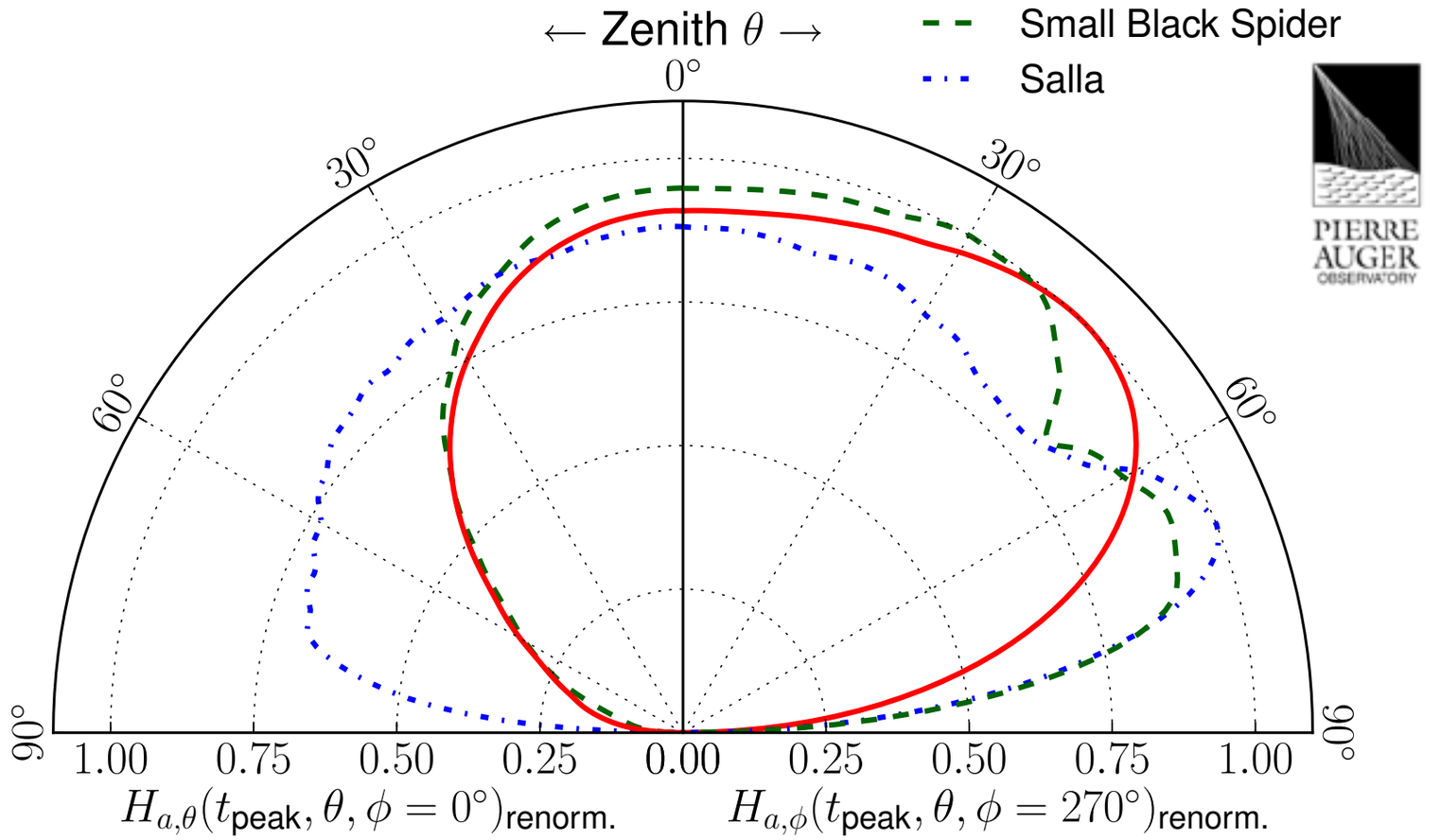

P. Abreu et al., JINST 7 (2012) P10011

measured antenna characteristics

Tunka-REX - 63 stations

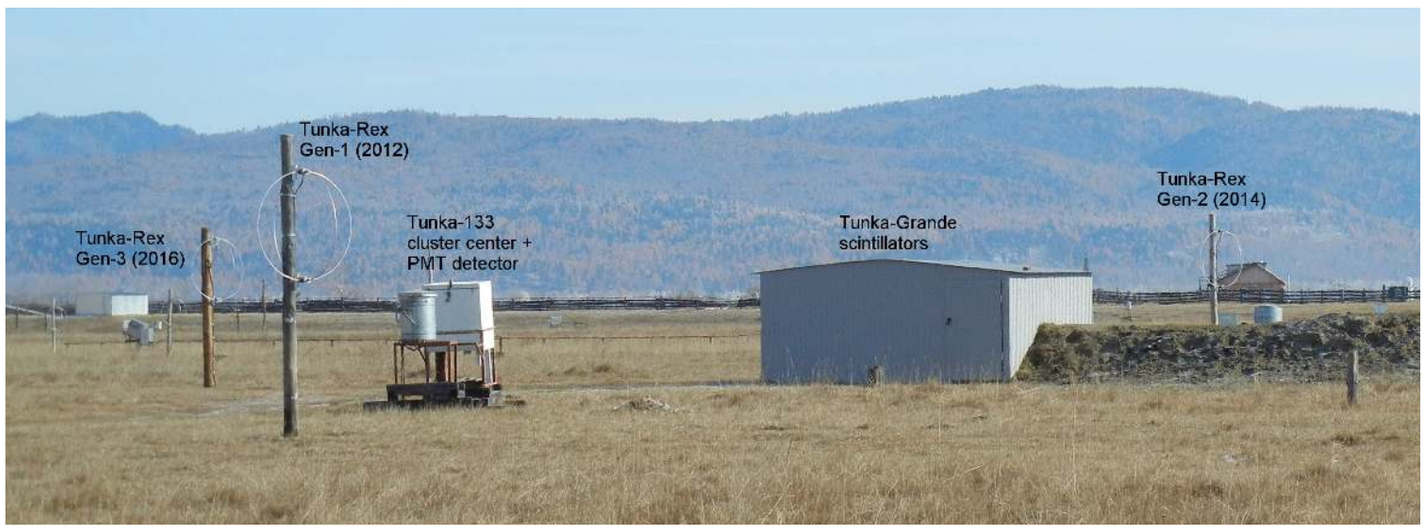

F. Schröder et al, PoS ICRC2017, 459

Antenna mounting

currently studying different scenarios for mechanical mounting

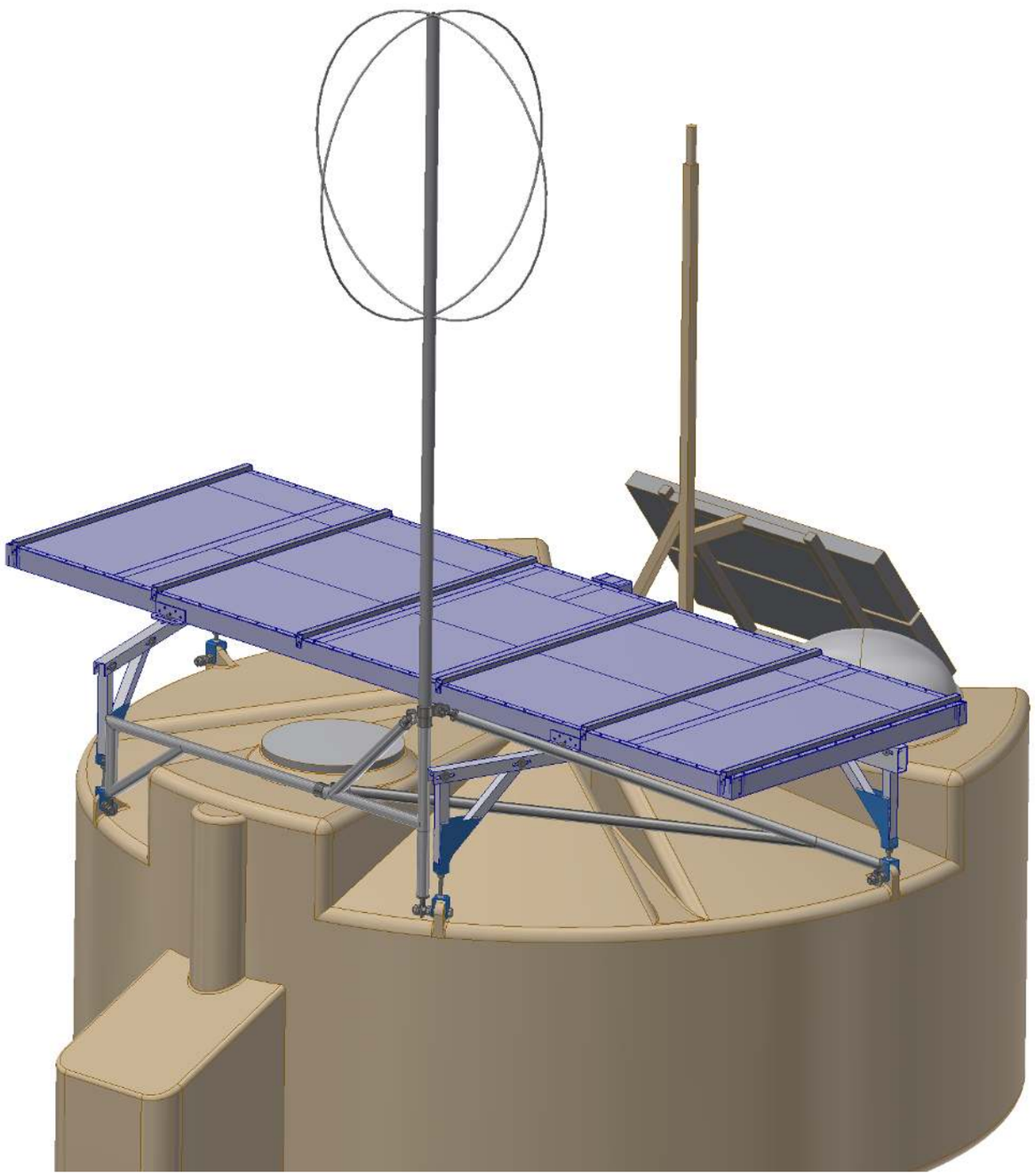

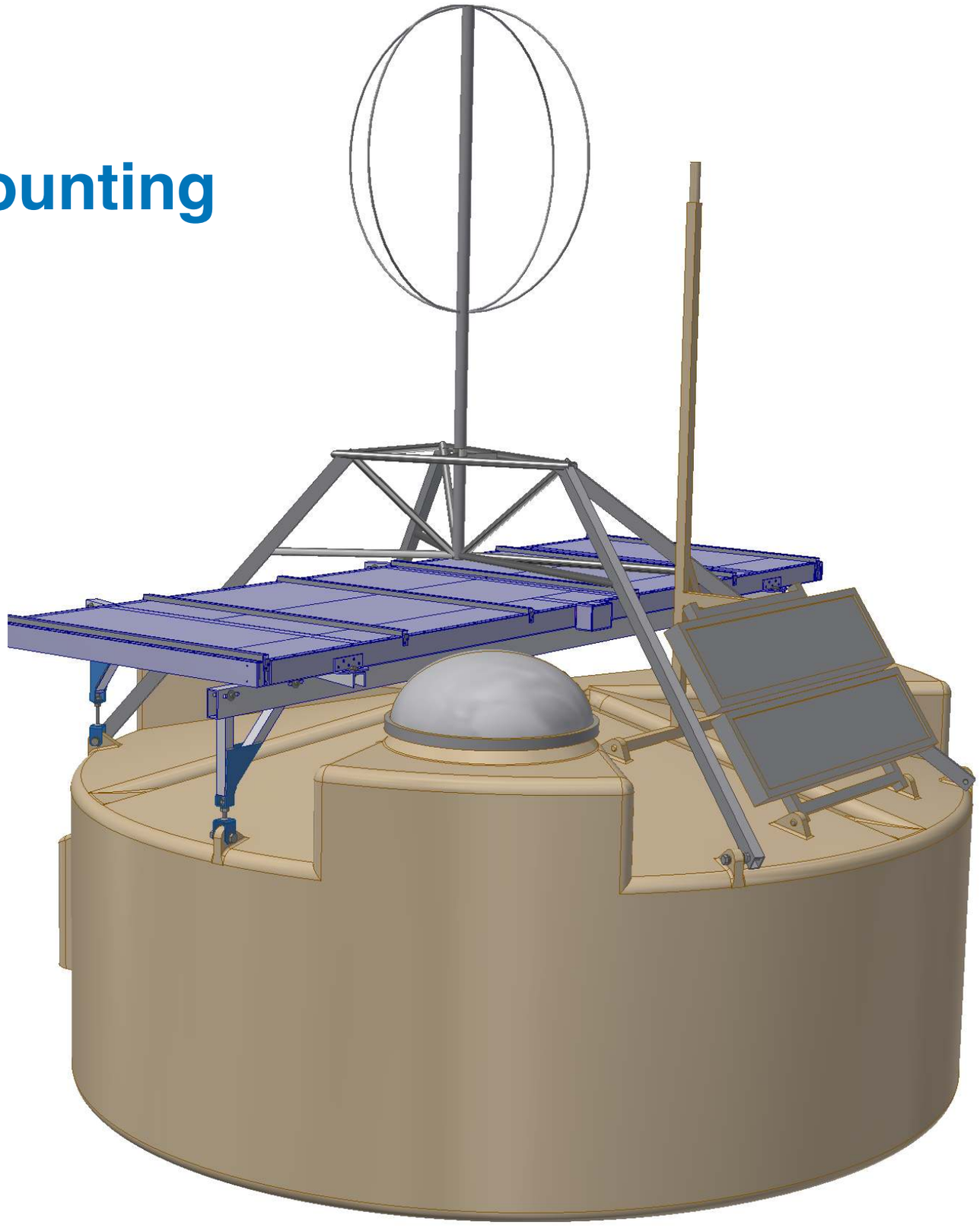

Prototype stations at PAO

since March 2017
R&D stations

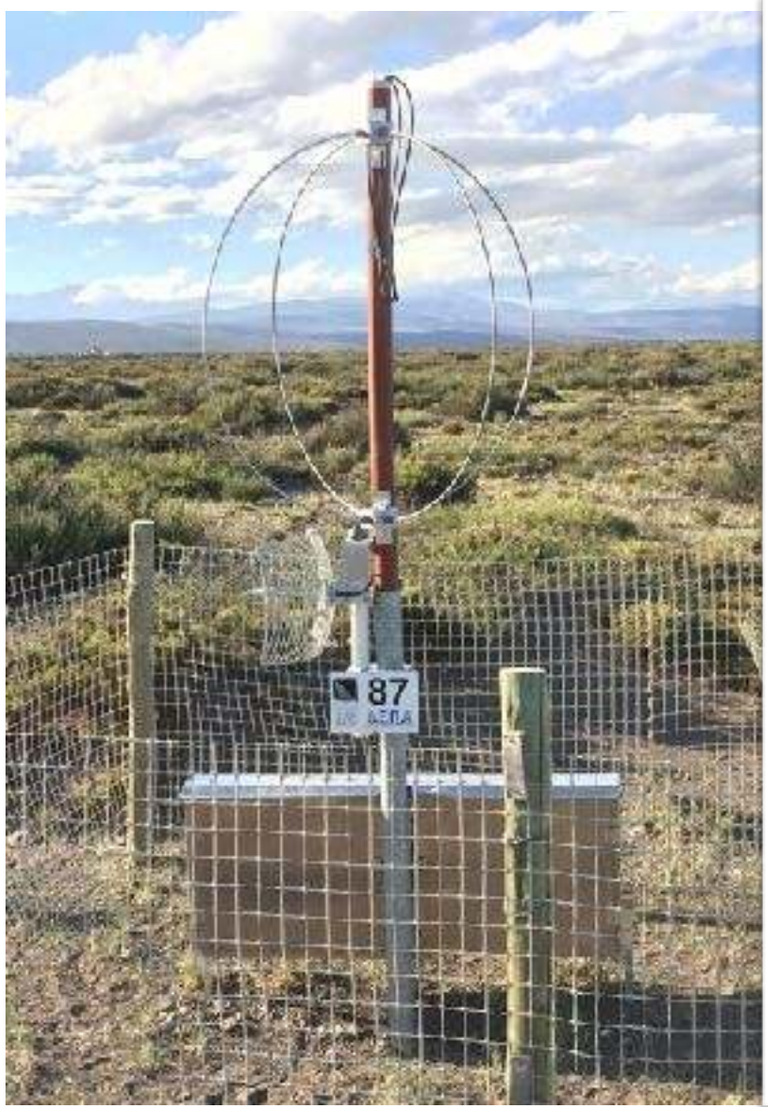

prototype since November 2017

a measured inclined EAS

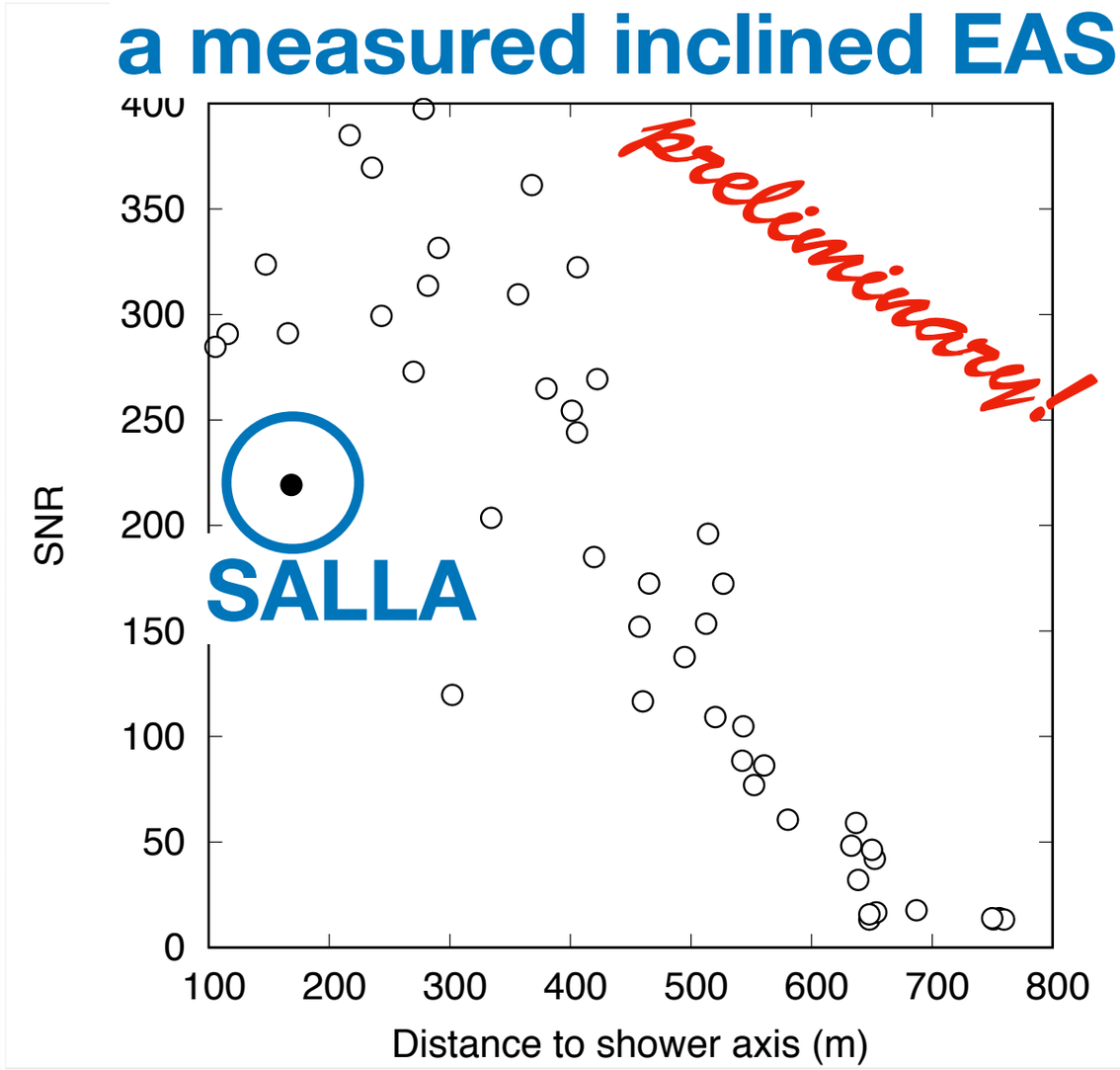

Concept of ARIANNA

- On ice-shelf: **Ice-water boundary** almost perfect reflector for radio emission
- **Independent antenna stations** can be installed at low costs on the surface
- **Real-time data transfer** via satellite
- Solar and wind power possible
- **High gain antennas** (50 - 1000 MHz) can be used to instrument a large volume
- Array of about 1000 antennas needed

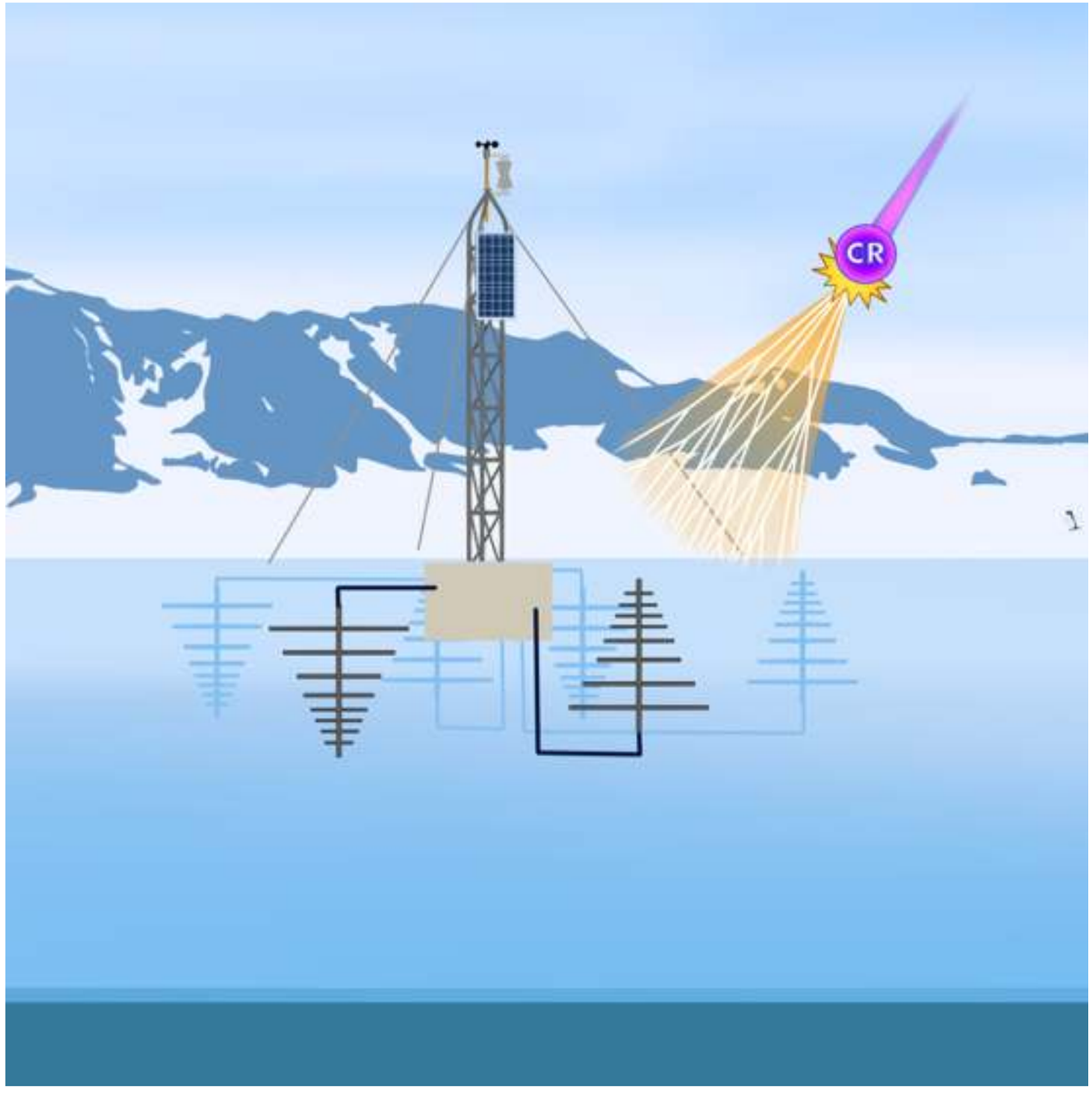

S.W. Barwick et al., Astropart.Phys. 90 (2017) 50

ARIANNA

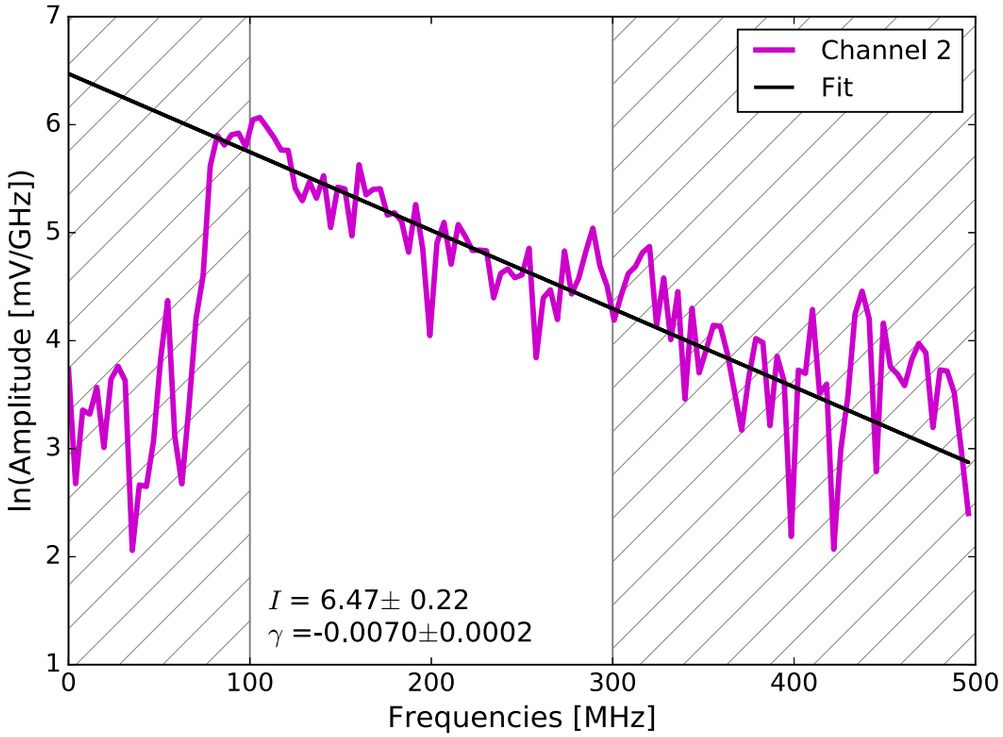

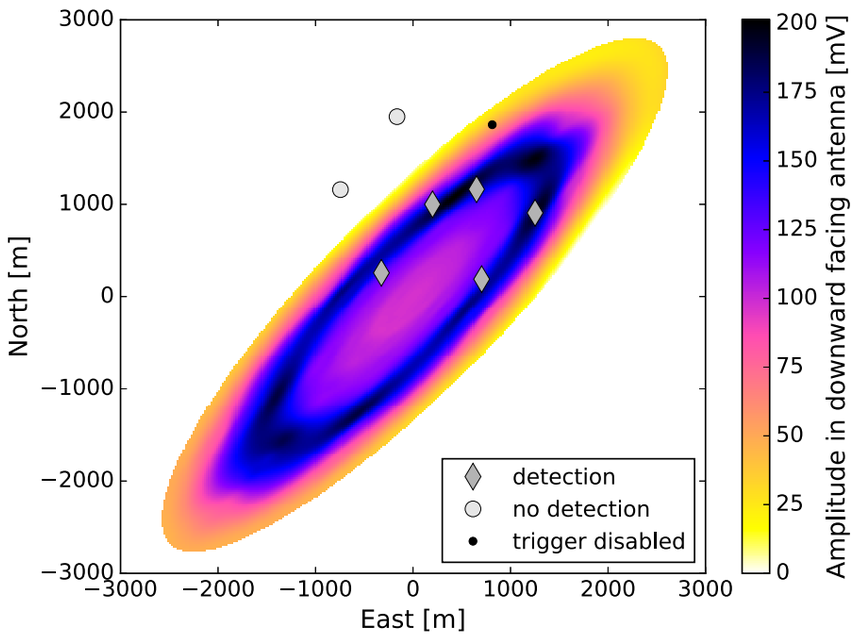

use slope of measured frequency spectrum to derive energy and other shower parameters

full ARIANNA
36 km² x 36 km²
1296 km²

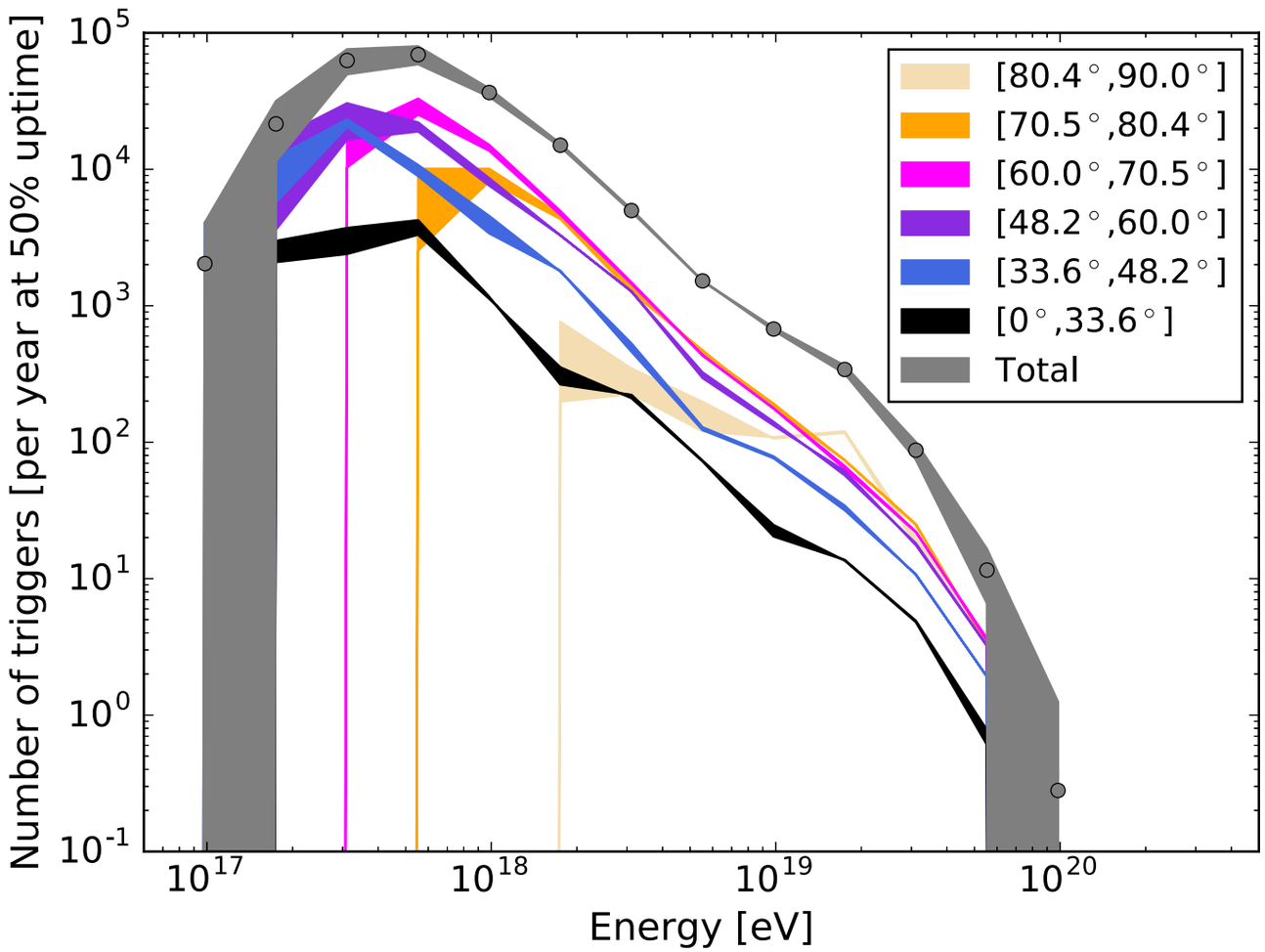

S.W. Barwick et al., Astropart.Phys. 90 (2017) 50

Cosmogenic neutrinos

- GZK neutrinos above $10^{19.5}$eV:

$p + \gamma_{CMB} \longrightarrow \Delta^+ \longrightarrow \pi^+ + n$

$\pi^+ \longrightarrow l + \nu_l$

Guaranteed flux.
Great tool to study UHECRs.

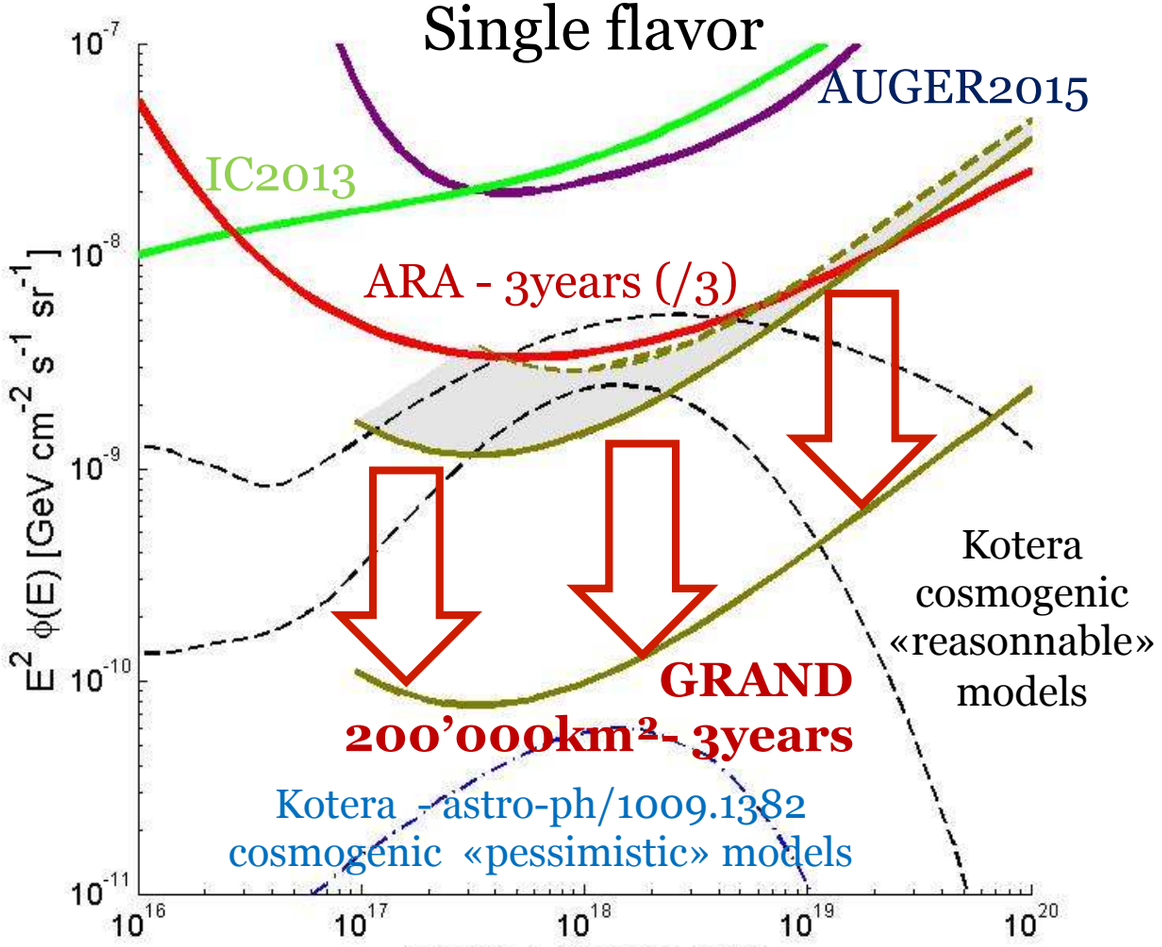

Output of GRAND 1st workshop (LPNHE, Feb. 2015):
GRAND should GUARANTEE detection of cosmogenic neutrinos (and rate of several tens/year for reasonnable models)

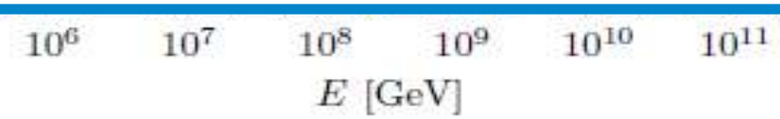

Next-generation cosmic-ray experiment

if upgraded PAO finds p-fraction >10% **--> source hunting**

Key science questions

- isolate protons
- proton astronomy
- identify sources of CRs
- neutrino + photon searches
- particle physics

40000 km² (>10 times PAO)
2 km spacing
--> 10000 detectors
~120 M€

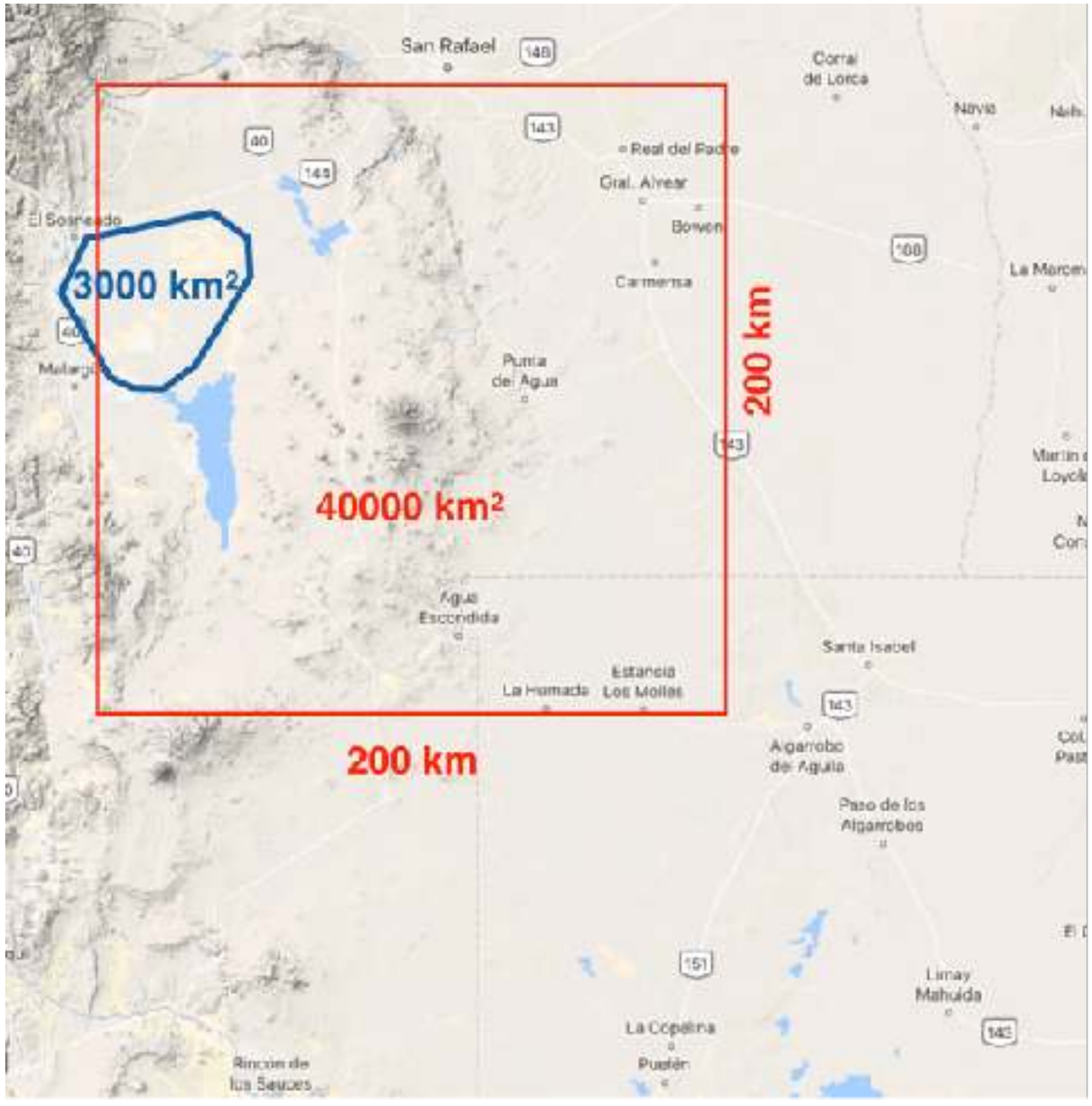

Development of the radio detection of air showers

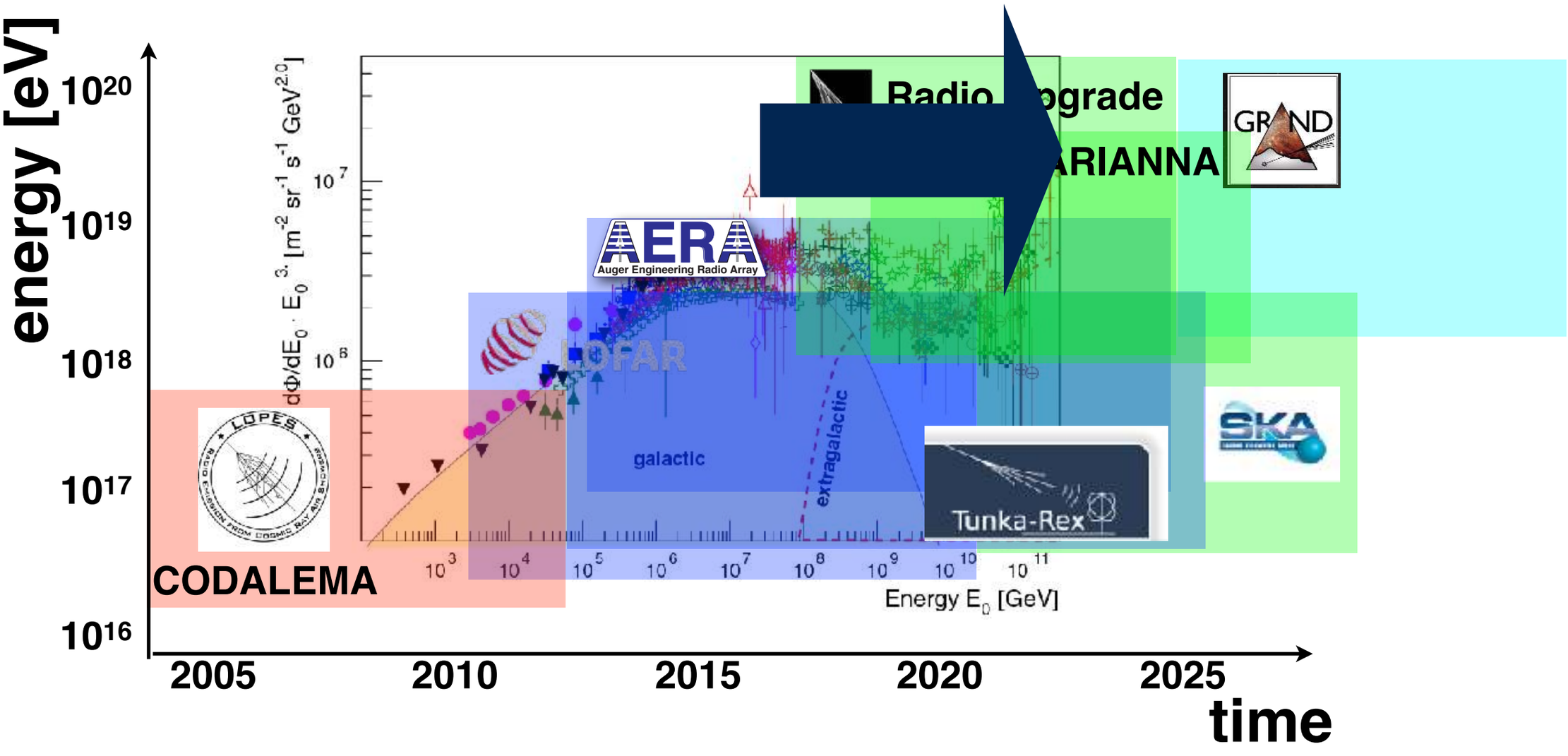

ISAPP-Baikal Summer School 2018

Radio detection of extensive air showers

Precision measurements of the properties of cosmic rays

huge progress in last decade

***2018*: beyond capabilities of standard installations**

***2016*: radio technique mature: properties of cosmic rays**

***2014*: understanding the emission processes**

2013: CoREAS radio simulation in CORSIKA

2011: endpoint formalism

2005: understanding the radio signal

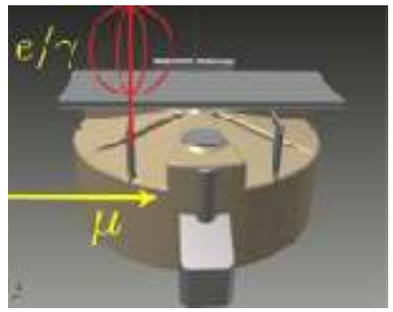

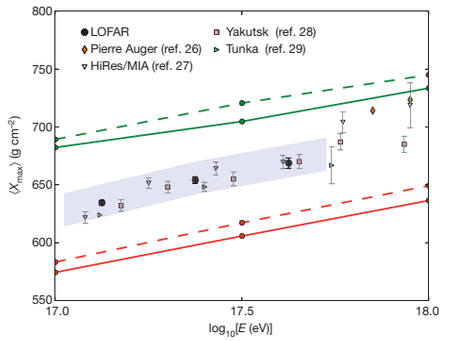

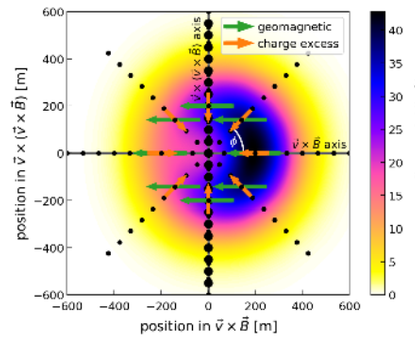

Jörg R. Hörandel RU Nijmegen, Nikhef, VU Brussel http://particle.astro.ru.nl